

Sheffield Hallam University

The response of box-type structures to vibration.

HENG, Raymond Bonn Whee.

Available from the Sheffield Hallam University Research Archive (SHURA) at:

<http://shura.shu.ac.uk/19784/>

A Sheffield Hallam University thesis

This thesis is protected by copyright which belongs to the author.

The content must not be changed in any way or sold commercially in any format or medium without the formal permission of the author.

When referring to this work, full bibliographic details including the author, title, awarding institution and date of the thesis must be given.

Please visit <http://shura.shu.ac.uk/19784/> and <http://shura.shu.ac.uk/information.html> for further details about copyright and re-use permissions.

THE RESPONSE OF BOX-TYPE STRUCTURES TO VIBRATION

by

Raymond Boon Whee Heng
B.Eng.(Hons.)*

A dissertation submitted to the Council of National
Academic Awards for the award of the degree of Doctor
of Philosophy

Sheffield Polytechnic
Department of Mechanical and Production Engineering

* at present
University of Sheffield
Department of Mechanical Engineering

July 1976

ProQuest Number: 10697086

All rights reserved

INFORMATION TO ALL USERS

The quality of this reproduction is dependent upon the quality of the copy submitted.

In the unlikely event that the author did not send a complete manuscript and there are missing pages, these will be noted. Also, if material had to be removed, a note will indicate the deletion.



ProQuest 10697086

Published by ProQuest LLC (2017). Copyright of the Dissertation is held by the Author.

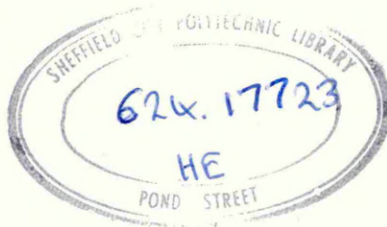
All rights reserved.

This work is protected against unauthorized copying under Title 17, United States Code
Microform Edition © ProQuest LLC.

ProQuest LLC.
789 East Eisenhower Parkway
P.O. Box 1346
Ann Arbor, MI 48106 – 1346



~~77-02659-01~~ 7 THESIS



~~77.02659 017~~

**SHEFFIELD POLYTECHNIC
LIBRARY SERVICE**

MAIN LIBRARY

19. JUN 1978

THE RESPONSE OF BOX-TYPE STRUCTURES TO VIBRATION

by

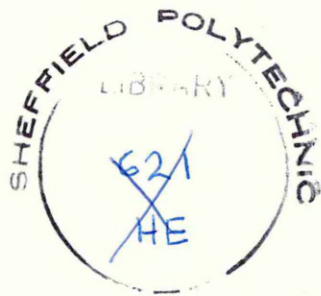
Raymond Boon Whee Heng
B.Eng.(Hons.)*

A dissertation submitted to the Council of National
Academic Awards for the award of the degree of Doctor
of Philosophy

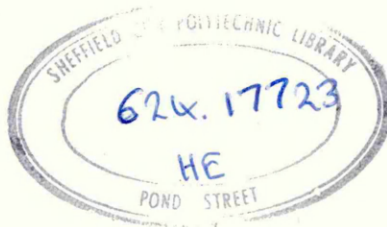
Sheffield Polytechnic
Department of Mechanical and Production Engineering

* at present
University of Sheffield
Department of Mechanical Engineering

July 1976



~~77 02659 -01~~ 7 THESIS



Acknowledgement

I would like to thank Mr. G.J. McNulty of the Sheffield Polytechnic and Dr. J.L. Wearing of the University of Sheffield for their supervision of this project. Thanks are also due to my friends and colleagues in both institutions and in particular Mr. O. Bardsley, Head of Mechanical and Production Engineering Department, Sheffield Polytechnic and Professor D.E. Newland, University of Sheffield, for help and advice rendered me.

I wish to thank my wife Ivy for her encouragement and forebearance throughout the project.

Abstract

The work described in this thesis deals with the vibration study of an open ended folded plate box type structure leading up to the prediction of its response to random excitation. Theoretical and experimental results for the box are presented as one of the main aims of the work is to predict theoretically the response of the structure to random excitation and compare these results with experimentally obtained values using various methods available.

The determination of the response of a structure to random excitation depends on the prediction of the response spectral density. To determine the response spectral density of any point on a structure a knowledge of its natural frequencies and mode shapes and modal damping factors is required. In this work the finite element method of analysis is used to determine the natural frequencies of vibration and the corresponding mode shapes of the box structure and computer programs were developed to perform this analysis. During the project, beam and plate structures have also been investigated to assess the accuracy of the technique and some results for these are included in chapter 7. The natural frequencies and mode shapes obtained are compared with experimental results as well as with those obtained using other theoretical analyses. For the beam the exact method was used and for the plate, the energy method using Warburton's formulae. Computer programs were also developed to calculate the structural receptance from the natural frequencies and mode shapes calculated using the finite element technique and damping factors obtained experimentally. From this the response spectral density of the structure to a known excitation spectrum was obtained.

Experimental work include a) sinusoidal excitation tests to determine natural frequencies, mode shapes and damping factors and b) random excitation using pseudo-random binary sequence signals to determine response to random excitation using narrow band frequency analysis and correlation techniques.

the development of a non-contacting combined exciter pickup probe, are described and discussed. The response to random excitation is obtained experimentally using a pseudo-random binary sequence signal generator and a time domain analyser, giving the cross-correlation function from which the cross spectral density is calculated in a Fourier transform. A Fast Fourier Transform computer program was developed during the work to perform this. The response spectral density is then obtained from a knowledge of the excitation spectral density.

Finally the values of the response spectral density obtained are compared with those obtained using the results of the finite element analysis and using the results of the sine sweep test and narrow band frequency analysis. The technique used in this work has proved satisfactory and the experimental apparatus and computer programs developed, suitable for the investigation.

The work described in this thesis provides the necessary basic requirements for future work in the establishment of suitable experimental apparatus setup and provision of essential computer software. Suggestions as to possible extension of this work are made in the concluding chapter.

CONTENTS

Abstract

Contents

Page

List of Figures

List of Tables

List of Plates

Chapter	1	Introduction	1
Chapter	2	The Finite Element Method	8
		Summary	8
2.1		Introduction	9
2.2		The element stiffness matrices	10
2.2.1		The bending stiffness matrix	11
2.2.2		The membrane stiffness matrix	15
2.3		The element mass matrices	17
2.3.1		The mass matrix in bending	18
2.3.2		The mass matrix in stretching	18
2.4		The combined bend and stretch element matrices	18
2.5		Assembly into the complete structure	19
2.6		The rotational matrix	22
2.7		Method of assembly	27
2.8		Boundary conditions	27
2.9		The solution algorithm	30

Contents	Page
Chapter 3 Random Theory	34
Summary	34
3.1 Introduction	35
3.2 Basic random theory	37
3.2.1 Statistical approach	37
3.2.2 The correlation functions	40
3.2.3 Power spectral densities	41
3.2.4 Fourier analysis of random signals	42
3.3 Response of structures to random excitation	43
3.4 Experimental techniques	46
3.5 The Correlation technique	49
3.6 The Fourier Transform	51
3.7 The pseudo-random binary sequence	56
Chapter 4 The Apparatus	64
Summary	64
4.1 Introduction	65
4.2 The vibration test bed	67
4.3 The non-contacting displacement transducer	69
4.4 Development of the non-contacting exciter	70
4.5 The combined exciter/pickup probe	72

Contents	Page
Chapter 5 Experimental Technique	80
Summary	80
5.1 Introduction	81
5.2 The excitation signal	87
5.3 Experimental technique	91
5.3.1 Determination of natural frequencies & mode shapes	93
5.3.2 Determination of receptance	97
5.3.3 Determination of damping factors	99
5.3.4 Determination of response to random excitation	102
5.4 The Fast Fourier Transform program	105
Chapter 6 The Computer Application	108
Summary	108
6.1 Response prediction	108
6.2 The finite element computer program package	112
Chapter 7 Results	128
Summary	128
7.1 Natural frequencies & mode shapes	128
7.2 Response calculations	143
Chapter 8 Conclusion	164

Contents		Page
Plates		170
References		186
Appendices	1	The stiffness and mass matrices
	2	The solution algorithms
	3	Finite element suite of computer programs
	4	The fast Fourier transform computer program
	5	The experimental apparatus
	6	The Wayne-Kerr probe calibration
	7	The exciter calibration

List of Figures

Figure	Title	Page
2.1	Element configuration (bending)	12
2.2	Element configuration (stretch)	16
2.3	Element node numbering sequence	20
2.4	Element node renumbered	20
2.5	Degree of freedom notation for the element	21
2.6	Coordinate transformation	23
2.7	Plate orientations	25
2.8	Plate in global x'y' plane	26
2.9	Plate in global y'z' plane	26
2.10	Plate in global z'x' plane	26
2.11	Assembly procedure	28
2.12	Node numbers of the open ended box structure analysed	29
3.1	An ensemble of random signals.	38
3.2	A typical Normal probability distribution	39
3.3	Transient testing signals	48
3.4	A pseudo-random binary sequence signal	58
3.5	Autocorrelation function of a PRBS signal	59
3.6	Power spectrum of a PRBS signal	60
3.7	PRBS occurrence distribution	62
3.8	Probability distribution of a multi-level sequence	62
4.1	A cut away view of the combined probe	73
4.2	Calibration of vibration pickup transducer	74
4.3	Frequency response of vibration measurement transducer	75
4.4	Force output of non-contacting exciter	77
4.5	Effect of air-gap on excitation output	78
4.6	Frequency response of non-contacting exciter	79
5.1	Schematic plan of the method	82
5.2	The vibration pickup displacement-volts factor	84
5.3	The non-contacting exciter force-volts factor	86
5.4	Filter characteristics	89
5.5	The open-ended box structure used	92
5.6	Block diagram of instrumentation for discrete excitation of box structure	94
5.7	A typical grid for determining mode shape of plates	96

Figure	Title	Page
5.8	The grid used for determining response spectral density of the box	98
5.9	Determination of damping factors using half power points on the response curve	100
5.10	Block diagram of instrumentation for random excitation of structures	103
5.11	Computer program MOJFTM flowchart	106
6.1	The twenty-four element idealisation of the box structure	110
6.2	Computer program MOJFTM1 flowchart	114
6.3	Computer program MOJFTM2 flowchart	116
6.4	Computer program MOJFTM3 flowchart	118
6.5	Computer program MOJFTM4 flowchart	119
6.6	Computer program MOJFTMD flowchart	120
6.7	Computer program MOJFTM5 flowchart	122
6.8	Computer program MOJFTM6 flowchart	123
6.9	Computer program MOJFTM7 flowchart	124
7.1	1st and 2nd mode shapes of the box	132
7.2	3th and 4th mode shapes of the box	133
7.3	5th and 6th mode shapes of the box	134
7.4	7th and 8th mode shapes of the box	135
7.5	9th and 10th mode shapes of the box	136
7.6	11th and 12th mode shapes of the box	137
7.7	13th and 14th mode shapes of the box	138
7.8	15th and 16th mode shapes of the box	139
7.9	17th and 18th mode shapes of the box	140
7.10	19th and 20th mode shapes of the box	141
7.11	21st mode shape of the box	142
7.12	The excitation power spectral density used	144
7.13	Showing the points for which response measurements are presented	145
7.14	A typical graph plot of the cross correlation / impulse response function	147
7.15	A typical line printer display of the correlation function	148
7.16	Box response to random excitation from the 512 point correlation function (non smoothed)	149
7.17	The 512 point response PSD curve using a three point smoothing	150

Figure	Title	Page
7.18	The 512 point response PSD curve using a five point smoothing	151
7.19	A graph of a nonsmoothed 1024 point response power spectral density computed	152
7.20	The 1024 point response PSD curve using a three point smoothing	153
7.21	The 1024 point response PSD curve using a five point smoothing	154
7.22	A plot of the typical box receptance ² calculated using finite element results	155
7.23	A typical response power spectral density calculated using the finite element results	156
7.24	Response power spectral density - Position A	157
7.25	Response power spectral density - Position B	158
7.26	Response power spectral density - Position C	159
7.27	Response power spectral density - Position D	160
7.28	Response power spectral density - Position E	161
7.29	Response power spectral density - Position F	162
7.30	Response power spectral density - Position G	163

List of Tables

Tables	Page
1 Natural frequencies & mode shapes of a beam with fully fixed and simply supported ends	129
2 Natural frequencies & mode shapes of a plate fully fixed all round	130
3 Natural frequencies of the box structure	131

Plate	Title	Page
1	The original vibration table	171
2	The redesigned vibration table	172
3	The linear fine adjustment mechanism	173
4	The skew fine adjustment mechanism	174
5	The plate with fully fixed edges	175
6	A fixed corner of the box structure	176
7	Close up view of the calibration of the capacitance displacement transducer	177
8	Instrumentation for calibration of the displacement transducer	178
9	Calibration of noncontacting exciter using a simple beam experiment	179
10	The housing for the piezoelectric force transducer used for the calibration of the exciter	180
11	Some of the electromagnetic noncontacting exciters developed	181
12	The combined exciter / pickup in position over the box structure	182
13	Frequency analysis using constant percentage frequency analyser	183
14	Constant bandwidth frequency analyser	184
15	The PRBS instrumentation used for the automatic generation of the cross correlation function on paper tape	185

The trend in recent engineering development is towards the use of light folded-plate boxtype structures as the basic unit of construction in many fields. In buildings and bridges, box girders figure predominantly and in the transport industry, motor cars, buses and trucks have always been basically light folded plate box type structures. This has stimulated interest in the determination of the response to vibration stimuli of these structures, hereafter referred to in this thesis simply as box-structures.. The resulting reduction in the built-in safety factors as well as in the damping because of the use of these lighter structural members can lead to the build up of serious vibration response levels.

Ignorance of the vibration characteristics of such structures is known to account for premature wear and fatigue failings [1]. The more spectacular catastrophes include the breaking up of the Liberty ships and the bridge disaster at Tacoma, in the U.S.A. where, in the latter case, random wind loading had excited one of the natural vibration modes of the bridge.

In the field of transportation, broad band vibrations set up in the vehicle have been shown to affect not only the life expectancy of the vehicle but also to have undesirable effects on the commuter. Once again the excitation here is known to be of a random nature. It is therefore important to study the vibration response of box structures and in particular the response of box structures to random excitation.

This work is an investigation into the vibration characteristics of box structures and ultimately to predict the response of box structures to random excitation. Robson [2] and Crandall [3] provide the necessary background knowledge on random vibration theory and they show that the prediction of the response of a structure at any point d to a single

random input at p depends on the determination of the receptance α_{dp} (Bishop and Johnson [4]) of the structure at the point under consideration. Robson has shown that in this case the output spectral density $S_d(f)$ of the point under consideration is related to the input spectral density $S_p(f)$ of the exciting force by the expression:

$$S_d(f) = |\alpha_{dp}(if)|^2 S_p(f) \quad (1.1)$$

where $\alpha_{dp}(f)$ is the receptance of the system from:

$$\alpha_{dp}(if) = \sum_r \mu_r (X_r - iY_r) \quad (1.2)$$

$$\text{where } \mu_r = \frac{w_r(x_q)w_r(x_p)}{M_r},$$

$$M_r = \int_0^l w_r^2(x) m dx,$$

$$X_r = \frac{f_r^2 - f^2}{4\pi^2 [(f_r^2 - f^2)^2 + \eta_r^2 f_r^4]},$$

$$Y_r = \frac{f_r^2}{4\pi^2 [(f_r^2 - f^2)^2 + \eta_r^2 f_r^4]}$$

$w_r(x_p)$ and $w_r(x_q)$ are deflections of the structure at input and output points p and q respectively when the structure is vibrating in the r th normal mode, f_r is the r th natural frequency, f is the forcing frequency and η_r is the damping loss coefficient for the r th mode.

It is therefore possible to calculate the receptance of any structure given the knowledge of its natural frequencies and mode shapes as well as damping factors.

Any attempt at response work inevitably requires a knowledge of the damping characteristics of the structure. As the mechanism of damping in structures is not yet completely known this work follows a commonly accepted theory for light

structures, that of hysteretic damping (see Crandal [5]). Experimentally derived values of the loss factors η have been used as far as possible for the folded plate box configuration but where this was not possible, extrapolations were used based on results obtained on plate damping measurements or unimodal damping assumptions were made.

In using equation (1.2) the natural frequencies of free vibration and its corresponding mode shapes of the box structure must also be known. These are obtained by solution of the equation of motion of the structure. Vibration analysis of structures can be divided into 'exact' methods and approximate methods.

The exact method solves the exact equation of motion usually using an iterative method. This however is only suitable for beams and plates with simple boundary conditions and becomes far too complicated for complex structures. It has not however prevented a recent attempt by Abrahamson [6] in using the exact method in an analysis of the natural frequencies and normal modes of a four plate box structure. This exact method is well documented in standard dynamics textbooks and will not be gone into here.

Of the approximate methods available the most widely used is the Rayleigh also known as the Energy method used mainly for determination of the lower frequencies of vibration. Here a shape, for example the static deflection curve, is assumed for the true deflected curve. Using this, the maximum potential and kinetic energies are calculated and equated. If the exact shape of the deflected structure happens to be chosen the calculated frequency corresponding to that shape will also be exactly correct but if not a close upper bound approximation will be obtained [4]. This method is also limited to the analysis of the simpler structures.

For plates the exact method of solution is limited to those simply supported around their perimeter. For fully fixed plates Ritz [7] provided probably the earliest analysis using

the Rayleigh method with a series of the various characteristic beam functions. This work was extended by others including Young [8] in 1950. Both the Rayleigh and the Rayleigh-Ritz methods are well documented in standard vibration textbooks e.g. Timoshenko [9] and Bishop & Johnson [4]. Probably one of the best known works in plate vibrations was done by Warburton [10] in which he presented a paper giving approximate formulae for all the twenty one different boundary conditions possible with plates using the Rayleigh method of solution. Recent work on the same subject was done by Leissa [11] who also investigated the effect of changing the values of Poisson's ratio and investigated the accuracy of Warburton's formulae.

A theoretical solution to the vibration of box-type structures using a sine series was presented by Dickinson and Warburton [12]. The analysis is however limited to the case in which deflections at the corners of the structure are assumed to be zero. The use of the Rayleigh and Raleigh-Ritz methods is in general not suitable for box structures because of difficulty in satisfying continuity of slope and bending moments at the common edges. The transfer matrix method (see Uhrig [13]) is also not suitable for the box structure because of the geometric difficulties encountered. The Bolotin edge effect method (Dickinson and Warburton [14]) although able to satisfy these continuity conditions does not solve for all the modes of vibration of box structures particularly at the higher modes when modal patterns are not easily represented by lines parallel to the edges.

Of the remaining approximate methods available the advent of the high speed large capacity computer has seen the emergence of the finite difference and finite element methods of analysis. The former (Heng [15]) was possibly until recently the more popular because of its smaller computer storage requirements but convergence especially in higher order equations was slow (Chang [16]). The latter is possibly more appealing to the engineer and has become one of the most important and powerful of the techniques developed recently.

It also appears to be the most suitable method available for the analysis of the box structure and is therefore the method chosen for this work.

One of the earliest references using this method was reported in a paper by Turner et.al. [17] in 1956. Melosh [18] subsequently applied it to the analysis of thin plates in bending. This was followed by Zienkiewicz and Cheung [19] in which they noticed possible application of the method to include vibration and thermal problems. Dawe [20] presents a solution to plate vibration problems and including non-dimensionalised stiffness and mass matrices using rectangular elements.

The rapid increase in the use of matrix methods in structural mechanics led to one of the first major conferences on the subject [21] being held in 1965 at which the finite element method featured predominantly. Since then several textbooks on the method have been published (Przemieniecki [22] and Zienkiewicz [23]).

Rockey and Evans [24] applied the method to the static analysis of box structures. In dynamic analysis, Handa [25] deals with in-plane vibrations of box structures and Ali, Hedge & Mills [26] approximates the vibrations of an idealised motor car chassis using beam elements only. This project will therefore extend the work to consider the finite element analysis of both in plane and transverse vibration of box structures and to use the results for the determination of the response power spectral density to random excitation. The full potential of the finite element method of analysis is still being constantly increased with new literature on the work being published at the moment in many research establishments.

Use of the finite element method necessitates the availability of some finite element computer package. However, in general, such computer program packages are not always available and it is up to the individual establishments to develop their own.

It is therefore one of the aims of the work undertaken in this project to produce such a computer program package to solve for the natural frequencies and mode shapes of the box structure. These results are then used in the calculation of the receptance of the box structure from equation (1.2). The receptance is used in the prediction of the response power spectral density to any known input from equation (1.1) and its calculation incorporated in the finite element package developed.

Little work, analytical or experimental, appears in the literature on the vibration study of box structures. As a result an extensive experimental as well as analytical program is pursued to obtain:

- (a) natural frequencies and mode shapes, with which the accuracy of the finite element prediction of the natural frequencies and mode shapes of the box structure can be assessed, and
- (b) the experimental response power spectral density, with which the predicted response power spectral density can be compared.

Although it is not expected that experimentally obtained and analytically predicted results correspond exactly, it is hoped that some degree of collaboration will be achieved.

The experimental work entailed the design and development of suitable experimental apparatus from which the necessary response measurements can be obtained. Because of the lightness of the box structure a non-contacting exciter-pickup had to be developed. The natural frequencies and mode shapes of the box structure were obtained. The response power spectral density was however not obtained by a narrow band frequency analysis of the response itself because of the inaccuracy involved. Instead an alternative method using the cross-correlation of the excitation and response signals is used. Davies [27] and Jones [28] show that if white noise is applied to a linear system, the cross correlation of the input signal to the system with the resulting response of the system gives the systems impulse response function. The pseudo random binary sequence signal is used for determining this impulse response function with considerably less difficulty in

obtaining the delayed signal for correlation and in the operations involving multiplication and integration. Moreover the perfect repeatability otherwise unobtainable with pure random signals is here possible making it suitable for work of this kind.

A Fourier Transform is necessary to evaluate the frequency response function of the structure from its impulse response. The calculation is found to require very long computational times using the usual method of evaluating the terms. A new technique using the Fast Fourier Transform algorithm (Cooley and Tukey [29], Bingham et.al. [30], Cochran et.al. [31]) is found to reduce this time considerably and forms an important part of the correlation technique used in this work. The theory behind this method of calculating the Fourier transform of a series will be looked into in more detail in the appropriate chapter.

Both the experimental as well as the analytical programme for the box structure has been successfully completed. The necessary apparatus has been developed and the natural frequencies and mode shape of the box structure have been obtained. The response power spectral density of the box structure subjected to random excitation has been obtained experimentally. A finite element computer program package has been developed giving the natural frequencies and mode shapes of the box structure. A further computer program has also been developed to predict the response power spectral density of the box structure subjected to random excitation. Agreement between the experimental and predicted results is found to be satisfactory.

Summary

The Finite Element method is used to predict theoretically the mode shapes and frequencies of free vibration of a folded plate box type structure using rectangular isotropic plate elements. Both the stiffness and the mass matrices are derived for the element used and the assembly into the complete structure explained. The use of various standard library routines for the solution of the eigenvalue problem is discussed. A full listing of the complete computer program developed is included in Appendix 3.

2.1 Introduction

The finite element method is one of the most suitable methods for the analysis of complex structures. In the analysis, whether static or dynamic, the original structure is replaced by an assemblage of small but finite elements which interconnect with one another only at a finite number of points known as node points. These are usually found at the corners of the element but are also commonly chosen to be along the sides of the element. At each node a number of degrees of freedom are represented usually the deflections and slopes or their derivatives. The theory then is to assume that the displacements in any part of the element will be defined in terms of these nodal degrees of freedom via a displacement polynomial of the form

$$w = \{P\} [C] \quad (2.1)$$

where $\{P\}$ is a matrix of the coordinates x, y and z ,

$[C]$ is a vector matrix of constants,

and the polynomial $w(x, y, z)$ is chosen to satisfy the following conditions:

- (a) The number of independent terms must equal the number of degrees of freedom in the element
- (b) For convergence to the correct solution it must be complete up to order n where n is the order of the highest derivative appearing in the strain energy integral appropriate to the type of element under consideration.
- (c) conforming or compatible elements further satisfy the condition that the $(n-1)$ th derivatives are continuous across the element boundaries.

From this displacement polynomial an elemental 'stiffness' matrix $[k]$ is obtained via strain energy considerations relating the elemental nodal forces and displacements in the form

$$\{F\}^e = [k] \{d\}^e \quad (2.2)$$

In a static analysis the nodal forces $\{F\}^e$ are due to the applied forces and in a dynamic analysis they represent inertia forces acting on the element. The characteristics of the complete but considerably simplified structure is then represented on the computer by the equation

$$\{F\} = [K] \{d\} \quad (2.3)$$

where $[K]$ is the stiffness matrix for the complete structure, made up of all the elemental stiffness matrices $[k]$. This then relates the applied forces $\{F\}$ and the nodal displacements $\{d\}$ of the complete structure and at the same time satisfies the relevant boundary conditions applied.

2.2 The element stiffness matrices

In folded plate structures the plates are subjected to both bending and stretching effects. This is conveniently considered separately as the plate element purely in bending and then in stretching only. The former has three degrees of freedom, w , θ_x , θ_y at each node and the latter, u and v only. However, depending on the orientation of the element in the complete structure, a θ_z component may present itself so that an allowance must be made for this in retaining a total of six degrees of freedom per node, displacements u, v, w , and rotations, $\theta_x, \theta_y, \theta_z$.

2.2.1 The bending stiffness matrix

Figure 2.1 represents one of the four node rectangular elements which is a component idealising a complete side of the box. At each node during bending there are three degrees of freedom, a displacement w , and rotations θ_x , θ_y to which correspond the three bending forces W , M_x , M_y . Thus for the 4 node element with 12 degrees of freedom, a 12 x 12 matrix is required to express nodal forces in terms of the nodal displacements. Other types of elements may also be used e.g. the 3 node triangular element or even the 8 node rectangular element with midside nodes [23]. However, a pair of the former will be necessary to represent each of the 4 node rectangles. The eight node rectangle is used primarily to represent curved geometries and is therefore unnecessary, for the box column with its straight sides, and also has a higher number of degrees of freedom to contend with.

For the 4 node rectangular element chosen, it is assumed that under load the deflected form of the element can be expressed as

$$w = A_1 + A_2x + A_3y + A_4x^2 + A_5xy + A_6y^2 + A_7x^3 + A_8x^2y + A_9xy^2 + A_{10}y^3 + A_{11}x^3y + A_{12}xy^3 \quad (2.4a)$$

where w is the deflection at the point (x,y)
or in matrix form

$$w = [m]\{A\} \quad (2.4b)$$

where $[m] = 1, x, y, x^2, xy, y^2, x^3, x^2y, xy^2, y^3, x^3y, xy^3$

and $\{A\}$ is a vector of the constants A_1, A_2, \dots, A_{12} . This displacement polynomial fully satisfies the necessary requirements discussed in 2.1. The constants of the expression can be evaluated by satisfying the displacement conditions at each node point, i.e. $w = w_i$, $\partial w / \partial y = \phi_i$, $\partial w / \partial x = -\theta_i$ at node point i ($i = 1, 2, 3, 4$).

The elemental stiffness matrix is then obtained via a strain energy analysis.

$$\frac{NB}{\theta_x} = \frac{\partial w}{\partial y}$$
$$\theta_y = -\frac{\partial w}{\partial x}$$

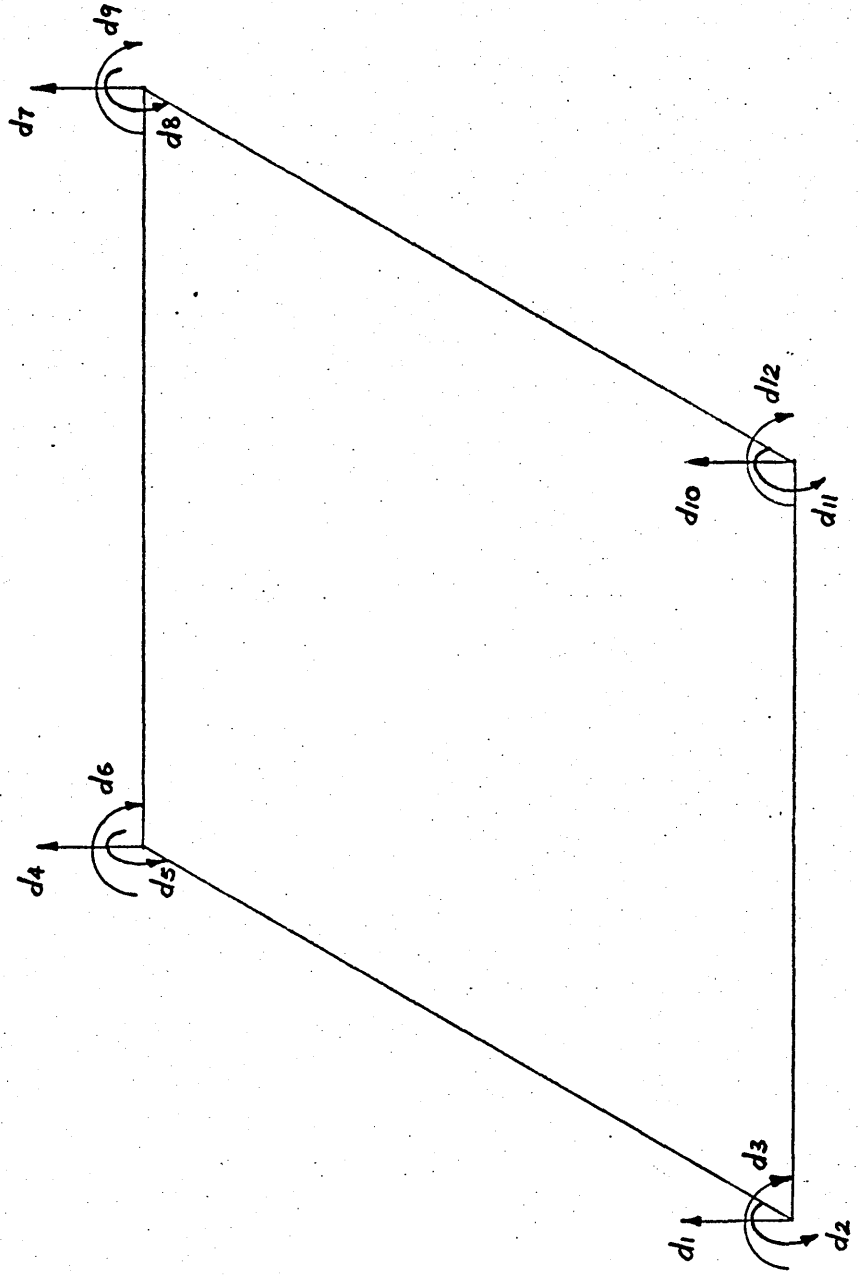


Fig 2.1 Element configuration (Bending)

Now the bending strain energy U of an isotropic plate of uniform flexural rigidity, D , is given by $\frac{1}{2} \int_V \epsilon^T \sigma dV$ where $\sigma = \zeta \epsilon$

$$U = \frac{D}{2} \int_{y=0}^b \int_{x=0}^a \left[\left(\frac{\partial^2 w}{\partial x^2} \right)^2 + \left(\frac{\partial^2 w}{\partial y^2} \right)^2 + 2 \left(\frac{\partial^2 w}{\partial x^2} \right) \nu \left(\frac{\partial^2 w}{\partial y^2} \right) + 2(1-\nu) \left(\frac{\partial^2 w}{\partial x \partial y} \right)^2 \right] dx dy$$

$$= \frac{D}{2} \int_{y=0}^b \int_{x=0}^a \{C\}^T [\zeta] \{C\} dx dy \quad (2.5)$$

where $\{C\} = \left\{ \frac{\partial^2 w}{\partial x^2}, \frac{\partial^2 w}{\partial y^2}, \frac{\partial^2 w}{\partial x \partial y} \right\}$

and $[\zeta] = \begin{bmatrix} 1 & \nu & 0 \\ \nu & 1 & 0 \\ 0 & 0 & 2(1-\nu) \end{bmatrix}$ (2.6)

The curvatures can easily be obtained by differentiating equation (2.4a):

$$\{C\} = \begin{cases} \frac{d^2 w}{dx^2} \\ \frac{d^2 w}{dy^2} \\ \frac{d^2 w}{dx dy} \end{cases} = \begin{cases} 2A_4 + 6A_7 x + 2A_8 y + 6A_{11} xy \\ 2A_6 + 2A_9 x + 6A_{10} y + 6A_{12} xy \\ A_5 + 2A_8 x + 2A_9 y + 3A_{11} x^2 + 3A_{12} y^2 \end{cases}$$

i.e. $\{C\} = [E] \{A\}$ (2.7)

where $[E] = \begin{bmatrix} 0 & 0 & 0 & 2 & 0 & 0 & 6x & 2y & 0 & 0 & 6xy & 0 \\ 0 & 0 & 0 & 0 & 0 & 2 & 0 & 0 & 2x & 6y & 0 & 6xy \\ 0 & 0 & 0 & 0 & 1 & 0 & 0 & 2x & 2y & 0 & 3x^2 & 3y^2 \end{bmatrix}$ (2.8)

In order to find the matrix of constants $\{A\}$ we return to figure 2.1 considering each node of the element in turn and using equation (2.4a) to determine the deflections at the nodes of the element to obtain

$$\begin{aligned}
d_1 &= w_1 = A_1 \\
d_2 &= \phi_1 = A_3 \\
d_3 &= \theta_1 = -A_2 \\
d_4 &= w_2 = A_1 + A_3 + A_6 + A_{10} \\
d_5 &= \phi_2 = A_3 + 2A_6 + 3A_{10} \\
d_6 &= \theta_2 = -[A_2 + A_5 + A_9 + A_{12}] \\
d_7 &= w_3 = A_1 + A_2 + A_3 + A_4 + A_5 + A_6 + A_7 + A_8 + A_9 \\
&\quad + A_{10} + A_{11} + A_{12} \\
d_8 &= \phi_3 = A_3 + A_5 + 2A_6 + A_8 + 2A_9 + 3A_{10} + A_{11} + 3A_{12} \\
d_9 &= \theta_3 = -[A_2 + 2A_4 + A_5 + 3A_7 + 2A_8 + A_9 + 3A_{11} + A_{12}] \\
d_{10} &= w_4 = A_1 + A_2 + A_4 + A_7 \\
d_{11} &= \phi_4 = A_3 + A_5 + A_8 + A_{11} \\
d_{12} &= \theta_4 = -[A_2 + 2A_4 + 3A_7] \tag{2.9a}
\end{aligned}$$

where the subscripts refer to the nodal members.

In matrix notation

$$\{d\} = [B]\{A\} \tag{2.9b}$$

$$\text{so that } \{A\} = [B^{-1}]\{d\} \tag{2.10}$$

Substitution of equations (2.7) and (2.10) back into (2.5) and noting that only $[E]$ is a function of x and y gives the strain energy

$$U = \frac{D}{2} \{d\} \left\{ [B^{-1}]^T \left(\int_{y=0}^b \int_{x=0}^a [E]^T \left[\frac{\partial}{\partial x} \right] [E] dx dy \right) [B^{-1}] \right\} \{d\}$$

$$\text{or } U = \frac{1}{2} \{d\}^T [K] \{d\} \tag{2.11}$$

Applying the theorem of virtual work $\frac{\partial U}{\partial d_i} = F_i$ gives

$$\{F\} = [K]\{d\}$$

where $\{F\}$ is the column matrix of nodal forces

$$\text{i.e. } \{F\} = \{W_1, M\phi, M\theta_1, W_2, \dots, M\theta_4\}$$

$[K]$ is thus the required stiffness matrix and from (2.11)

$$[K] = [B^{-1}]^T \left(\int_{y=0}^b \int_{x=0}^a [E]^T [\zeta] [E] dx dy \right) [B^{-1}] \quad (2.12)$$

where the component matrices $[\zeta]$, $[E]$ and $[B^{-1}]$ are given in (2.6), (2.8) and the inversion of (2.9a) respectively.

In order to retain the element dimension parameters a and b , the matrix manipulation are carried out by hand giving the matrix $[K]$ (Appendix 1a).

2.2.2 The Membrane stiffness matrix

Figure 2.2 represents the configuration and notation used for the 4 node rectangular element in stretching. The displacements in the x and the y directions, u and v , are independent of each other and so can be considered separately and the analysis is identical in both cases. The displacement polynomial chosen for the displacements in the x direction is

$$u = A_1x + A_2xy + A_3y + A_4$$

and that in the y direction is

$$v = B_1x + B_2xy + B_3y + B_4$$

The assumption for a plane stress distribution is made where $\sigma_{zz} = \sigma_{zx} = \sigma_{zy} = 0$; this being valid for thin plates.

By following the same steps as illustrated previously for bending, equations (2.5) to (2.12), the stiffness matrix for the element in stretching is obtained (Appendix 1a).

We now have the stiffness matrices for the separate bending and stretching modes of the element which can be used for the solution of problems involving plate structures bending and stretching respectively under static loading.

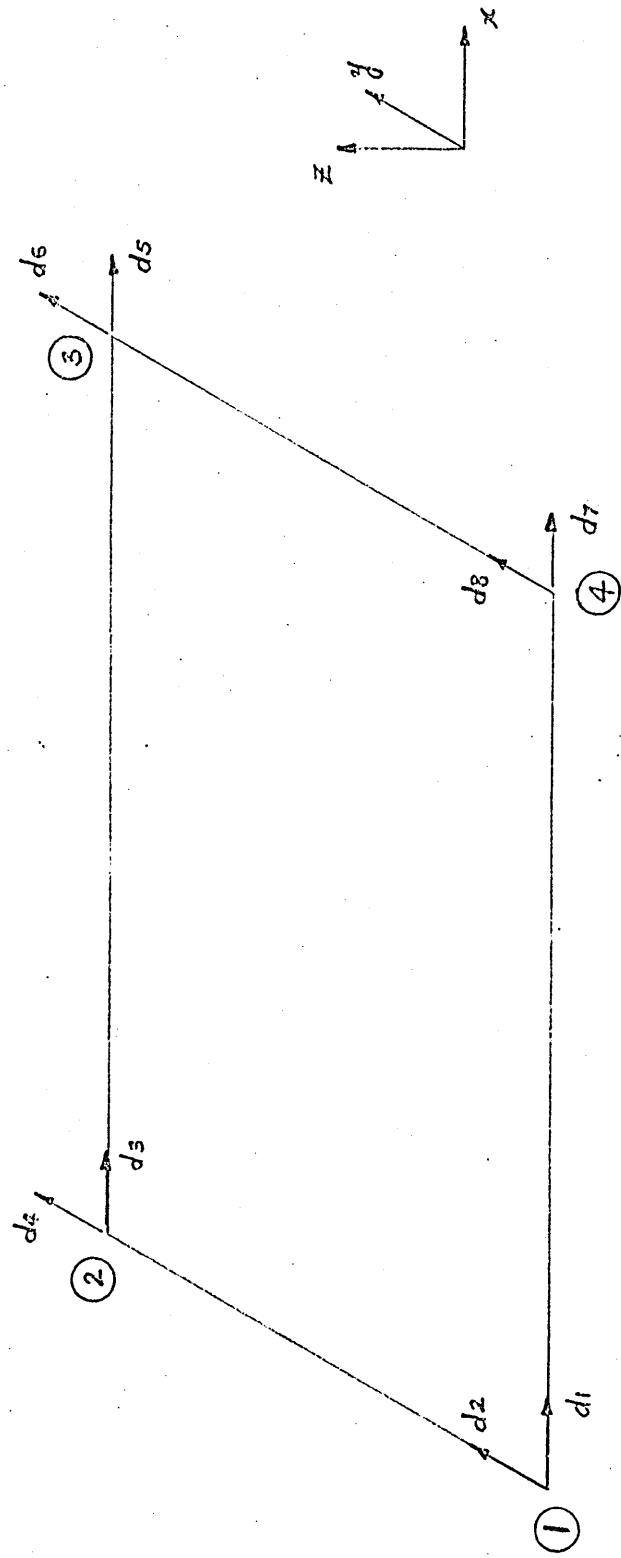


Fig 2.2 Element configuration (Stretch)

In dynamic analysis the nodal forces are induced by inertia loading of the displaced structure. The inertia loading distributed over an element during vibration is here replaced by a system of equivalent nodal forces by means of the formation of a 'mass' matrix. The criterion adopted for such replacement is that the work done by the equivalent nodal inertia forces U_e is equal to that done by the actual inertia forces of the element U_a . The former is given by the equivalent nodal forces $\{F_m\}$ in moving through virtual nodal displacements $\{d_v\}$.

$$\text{i.e. } U_e = \{F_m\} \{d_v\} \quad (2.13)$$

The latter is given by the actual distributed inertia loading, $\{f\}$, in moving through a virtual deflection $\{w_v\}$

$$\text{i.e. } U_a = \{f\} \{w_v\} \quad (2.14)$$

$$\text{where from (2.4) and (2.10) } \{w_v\} = [m][B^{-1}]\{d_v\} \quad (2.15)$$

The inertia force per unit area when the plate is vibrating sinusoidally with circular frequency p is

$$\{f\} = \rho p^2 w = \rho p^2 [m][B^{-1}]\{d\} \quad (2.16)$$

where ρ is the density per unit area of the element.

Thus, equating the work done in both cases, from equations (2.13) and (2.14)

$$\{d_v\}^T \{F_m\} = \int_{y=0}^b \int_{x=0}^a \{w_v\} \{f\} dx dy$$

which from equations (2.15) and (2.16)

$$= \rho p^2 \{d_v\}^T [B^{-1}]^T \left(\int_{y=0}^b \int_{x=0}^a [m]^T [m] dx dy \right) [B^{-1}]\{d\} \quad (2.17)$$

If each virtual nodal displacement is given the value unity in turn while the remaining displacements are held zero, equation (2.17) becomes

$$\begin{aligned} \{F_m\} &= \rho p^2 [B^{-1}]^T \left(\int_{y=0}^b \int_{x=0}^a [m]^T [m] dx dy \right) [B^{-1}]\{d\} \\ &= \lambda [M]\{d\} \end{aligned} \quad (2.18)$$

$$\text{where } [M] = [B^{-1}]^T \left(\int_{y=0}^b \int_{x=0}^a [m]^T [m] dx dy \right) [B^{-1}] \quad (2.19)$$

is the required mass matrix of the element as $\{F_m\}$ is the column matrix of nodal forces representing the inertia loading on the element. Once again this is derived separately for the element in bending and in stretching.

2.3.1 Bending mass matrix

From the previous section we have that the mass matrix of the element is given by

$$[M] = [B^{-1}]^T \iint [m]^T [m] dx dy [B^{-1}] \quad (2.20)$$

For the element in bending $[m]$ is given by equation (2.4) and $[B^{-1}]$ by equation (2.9a) so that $[M]$ is easily found (Appendix 1b).

2.3.2 Stretch mass matrix

Again the element mass matrix considering the stretching case is given by equation (2.20) above. In this case the mass matrix can be divided into two separate submatrices, one for each direction as they are mutually independent of each other (Appendix 1b).

2.4 The combined element stretching and bending matrices

We now have the four bending and stretching rectangular plate element stiffness and inertia matrices, $[K_B]$, $[K_S]$, $[M_B]$ and $[M_S]$ of the element. These are combined to form the combined bending and stretching stiffness and mass matrices $[K]$ and $[M]$ of the element. These are full 24 x 24 matrices with the complete set of six rotational and linear displacements $u, v, w, \theta_x, \theta_y, \theta_z$ at each of the four nodes. The matrices available so far only form a 20 x 20 matrix as the plane rotation θ_z had not been taken into account in the derivation of the mass and stiffness matrices but must be included for rotation into the three dimensional structure. The method used to overcome this is simply to include rows and columns of zeros for the appropriate degree of freedom θ_z . This method makes the

idealised structure more flexible than the actual but has been successfully used (Rockey and Evans [24], and Clough and Johnson [32]).

The notation (fig. 2.3) used previously was chosen quite arbitrarily and was sufficiently suitable for the purposes of determining the stiffness and inertia matrices of the element. However, it was found that for ease in analysing large and complex structures, a more suitable system of numbering for the element had to be followed so that programming for the computer is simpler. The following system (fig. 2.4) was chosen. This gives a smooth flow in the numbering system, considering first the x axis and then the y axis. In the program this is accomplished by first interchanging rows and columns 2 and 4 in the stiffness and inertia matrices and then doing the same for rows and columns 3 and 4. This procedure is carried out in subroutine REORDER (Appendix 3).

The complete nodal and degree of freedom notation for an element lying in the xy plane is given in figure 2.5 where, considering node 1,

degree of freedom:

- 1 = u = displacement in x direction
- 2 = v = displacement in y direction
- 3 = w = displacement in z direction
- 4 = θ_x = rotation along vector in x direction
- 5 = θ_y = rotation along vector in y direction
- 6 = θ_z = rotation along vector in z direction

2.5 Assembly into the complete structure

The basic element obtained by the previous analysis is a four node plate element which has combined bending and stretching capabilities.

If we inspect the stiffness matrices obtained we see that a column of either matrix is in fact a list of the forces acting at each node when the displacement corresponding to that column is given a unit displacement and all other degrees of

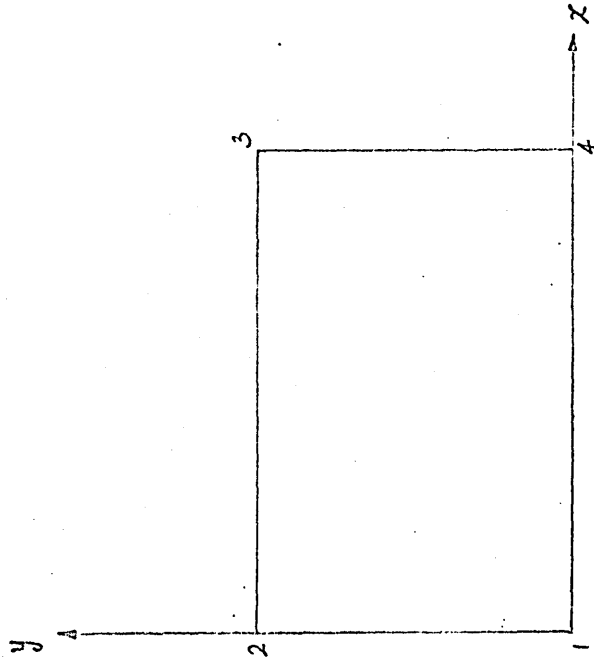


Fig 2.3 Element node numbering sequence

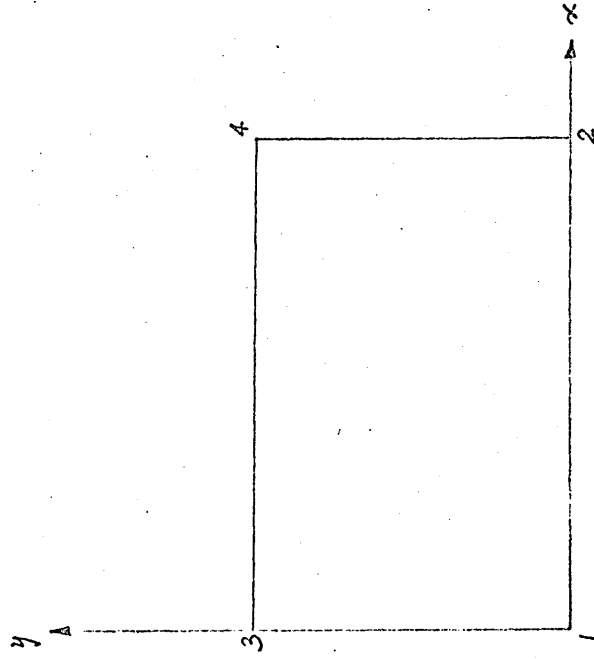


Fig 2.4 Element node renumbered

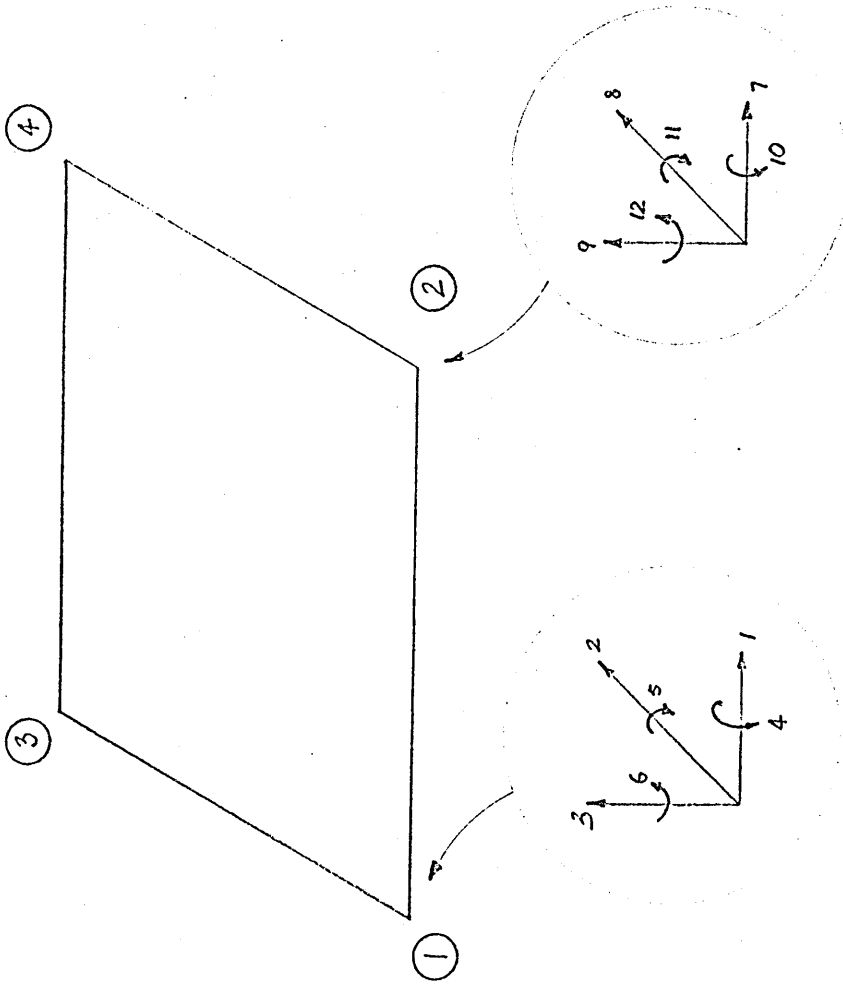


Fig 2.5 Degree of freedom notation for the element.

freedom given the value zero. Thus if two or more elements have a common node point then the total force acting at that node point is obtained by addition of forces. The assembly into the complete structure is then accomplished by the merging of all the element matrices into that of the complete structure by a simple point by point addition. The degree of freedom notation as illustrated in figure 2.5 has been chosen to facilitate easy assembly into the complete structure.

This merging of the basic element matrices into that of the complete structure also requires the following

- a) rotation of the element into the correct plane before assembly.
- b) a systematic assembly of the various elements into the complete structure.
- c) a systematic numbering sequence of the nodes of the complete structure to facilitate easy refinement of mesh size.
- d) incorporation of the boundary conditions of the complete structure.

2.6 The rotational matrix

So far the stiffness and mass matrices have been found for a plate element in its local coordinate system (i.e. the stiffness and mass matrices have been calculated for the element lying in the xy plane). As an element can also lie in the xz or yz planes or in any inclined plane, its inclination to the global axis of the whole structure has to be taken into consideration before it can be assembled into its proper place in the actual structure (see for example Gere and Weaver [33]).

To illustrate the procedure, consider a rod of length L lying on the x axis in the local coordinate system as shown in fig. 2.6. Any point of the rod has components of deflection $u, v,$ and w relative to the local axes x, y and z . It also has components of deflection u', v' and w' relative to the global axes x', y' and z' . These two sets of deflections are related

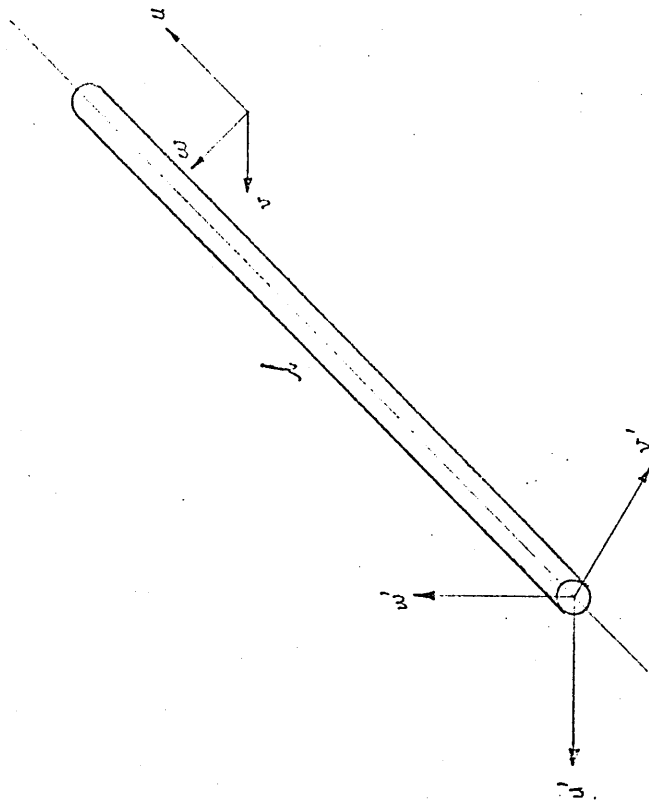


Fig 2.6 Co-ordinates transformation

by the expression

$$\begin{Bmatrix} u \\ v \\ w \end{Bmatrix} = \lambda \begin{Bmatrix} u' \\ v' \\ w' \end{Bmatrix} \quad (2.21)$$

From fig. 2.6,

$$l(u) = u' \cos u'u + v' \cos v'u + w' \cos w'u$$

where $u'u$ etc., refer to the angle turned through from the u' axis to the u axis.

Similarly,

$$l(v) = u' \cos u'v + v' \cos v'v + w' \cos w'v$$

$$l(w) = u' \cos u'w + v' \cos v'w + w' \cos w'w \quad (2.22)$$

For the purposes of this investigation the directional cosines involved are either 1, 0, or -1 since the sides of the box structure investigated are all at right angles to one another (fig. 2.7).

- i) Consider the case of a plate lying in the $x'y'$ plane (fig. 2.8). The matrix is simply:

$$\begin{bmatrix} 1 & 0 & 0 \\ 0 & 1 & 0 \\ 0 & 0 & 1 \end{bmatrix}$$

- ii) For a plate lying in the $y'z'$ plane, (fig. 2.9) it is:

$$\begin{bmatrix} 0 & 1 & 0 \\ 0 & 0 & 1 \\ 1 & 0 & 0 \end{bmatrix}$$

- and iii) For a plate in the $z'x'$ plane (fig. 2.10):

$$\begin{bmatrix} 1 & 0 & 0 \\ 0 & 0 & 1 \\ 0 & -1 & 0 \end{bmatrix}$$

Using these rotation transformation matrices, the stiffness and mass matrices of the plate element in its local coordinate system can be transformed into that of the global coordinate system using the equations

$$[K_G] = [R]^T [K_L] [R] \quad (2.23)$$

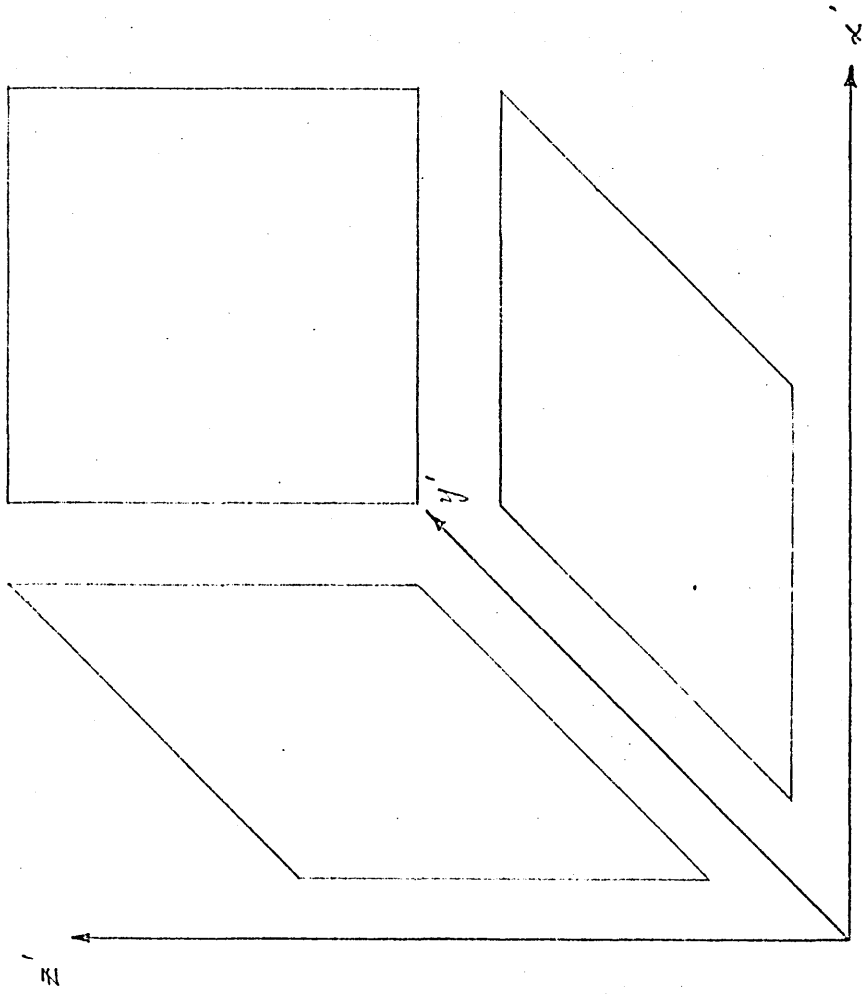


Fig. 2.7 Plate Orientations.

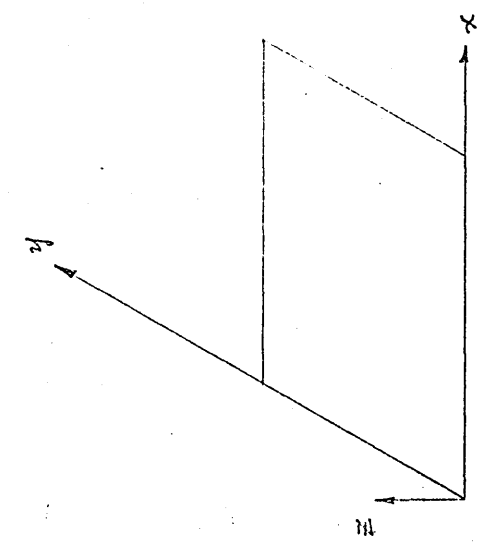


Fig 2.8 Plate in global $x'y'$ plane

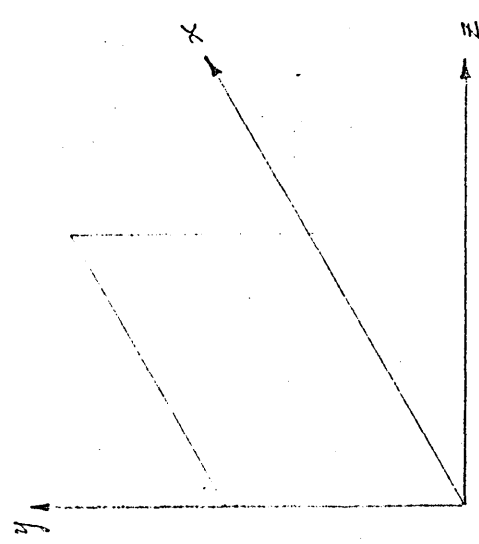


Fig 2.9 Plate in global $y'z'$ plane

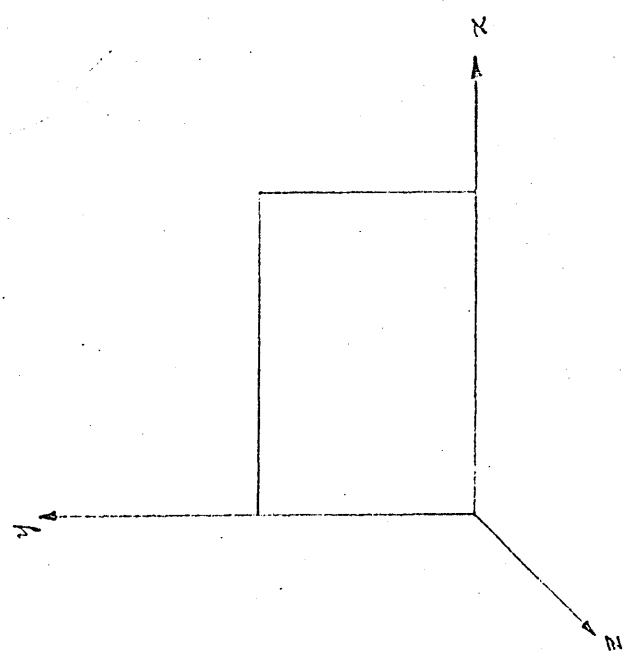


Fig 2.10 Plate in global $x'z'$ plane

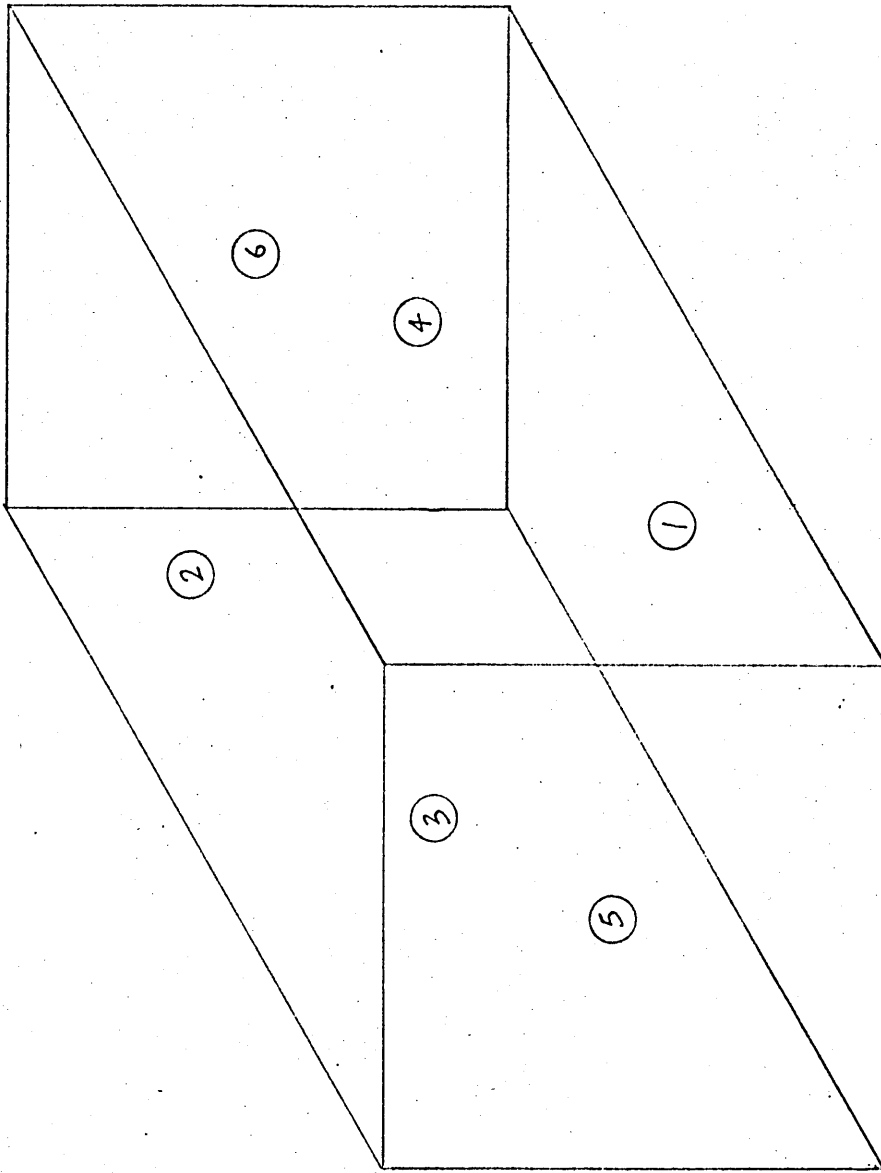
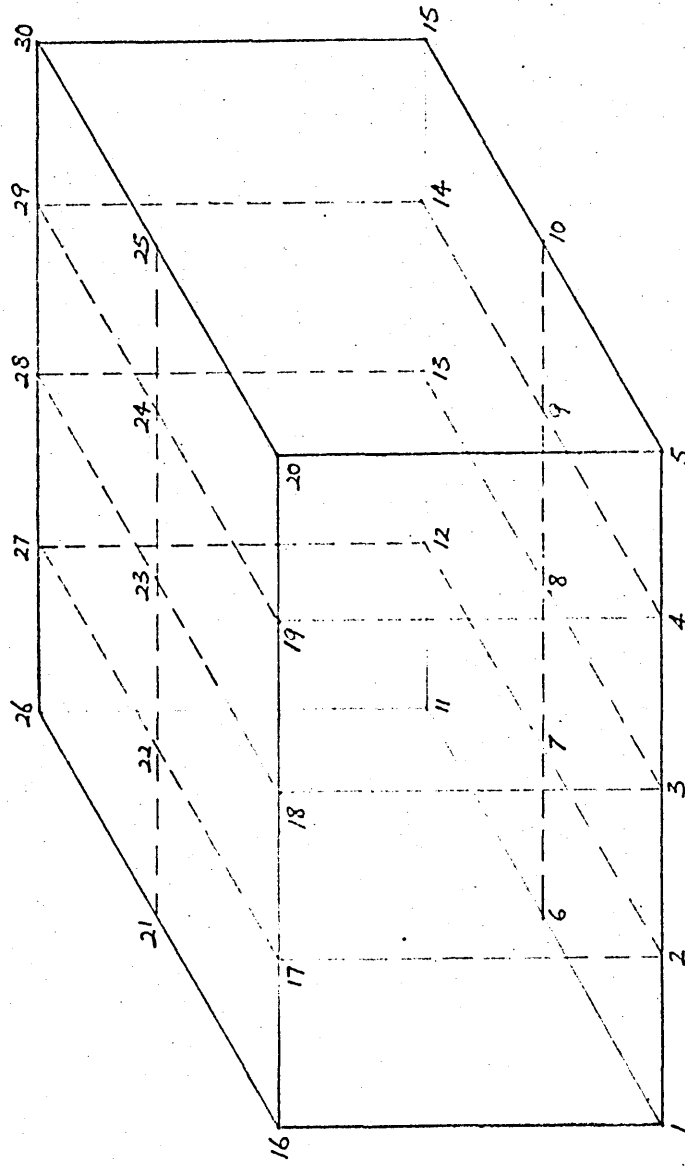


Fig 2.11. Assembly procedure



Node numbers of the open ended
box structure analysed.

Fig 2.12 Sketch showing assembled structure

corresponding to that particular degree of freedom. This is because the inertia forces produced in such a case is non-existent since no displacement is allowed at that point. In this way a fully fixed node at the boundary of the structure may have all its degrees of freedom $u, v, w, \theta_x, \theta_y, \theta_z$ eliminated from the system matrices. Similarly a node along a simply supported boundary along the x axis may have rows and columns corresponding to its w and θ_x displacements removed. Other degrees of freedom that are also reduced out are those of dummy nodes and the dummy degree of freedom θ_z which had been assigned for ease of assembly. Where there are no contributions to the assembled stiffness and mass matrices the relevant rows and columns (which are all zeros) are removed from these matrices as they would otherwise become singular. The removal of these rows and columns is achieved using a control matrix in which a list is maintained of all the degrees of freedom of the structure, those to be removed represented by zeros and those to be retained by ones.

The subroutine BOUNDARY removes all rows and columns corresponding to the degree of freedom having the value zero, leaving n by n stiffness and mass matrices where n is the total number of degrees of freedom remaining in the structure.

2.9 The solution algorithm

The structural vibration problem (section 2.3) is now reduced to one of solving the generalized symmetric eigenproblem

$$[K] x = \lambda [M] x \quad (2.25)$$

for its eigenvalues and eigenvectors. From these are obtained the natural frequencies and mode shapes of the vibrating box structure. A short summary of the method used is given here and the reader requiring more detailed information is referred to the computer subroutine manual used [34] and Wilkinson [35].

For the generalised symmetric eigenvalue problem where $[K]$ is a real symmetric matrix and $[M]$ is a real symmetric positive definite matrix i.e. one whose eigenvalues are all greater

than zero, the solution is straightforward. $[M]$ is factorised by Cholesky's method into $[M] = [L][L]^T$ where $[L]$ is a lower triangular matrix. Hence $[K]\{x\} = \lambda[M]\{x\}$ can be written in the form

$$([L]^{-1}[K][L]^{-T})[L]^T x = \lambda[L]^T x \quad (2.26)$$

which is the standard symmetric problem

$$[A]y = \lambda y \quad (2.27)$$

where $[A] = [L]^{-1}[K][L]^{-T}$

and $y = [L]^T x$

The eigenvalues of $[K]\{x\} = \lambda[M]\{x\}$ are the same as those of $[A]$ and if y is an eigenvector of $[A]$ then x , the corresponding eigenvector of the original problem, is obtained by back substitution in the set of linear equations

$$[L]^T x = y \quad (2.28)$$

Householder's method is then used to tridiagonalise the matrix $[A]$ and the eigenvalues are found using the QL algorithm [35]. The eigenvectors $\{y\}$ of the derived problem are then determined using the QL algorithm and normalised so that $\{y\}^T \{y\} = 1$ and the eigenvectors $\{x\}$ of the original problem are found from $[L]^T \{x\} = \{y\}$ and normalised so that $\{x\}^T [M] \{x\} = 1$. This method can however only be used if $[K]$ is real and symmetric and $[M]$ is positive definite. $[K]$ is checked to be real and symmetric by inspection and in the computer program. The program also has built-in facilities to check the eligibility of $[M]$ using the criterion that its determinant is positive since the determinant is equal to the product of its eigenvalues (which must all be greater than zero).

In some instances due to rounding errors $[M]$ may not be found to be positive definite so that an alternative method has to be used. The procedure commences with the generalised symmetric eigenproblem being manipulated into the standard symmetric form

$$[B]z = \lambda z \quad (2.29)$$

where $[B] = [K]^{-1} [M]$

and $\lambda'_n = 1/\lambda_n$

The $[K]$ and $[M]$ matrices are both symmetrical but since $[K]^{-1}$ is not, so neither is the product $[B]$. The problem then becomes one of solving for the eigenvalues and eigenvectors of equation (2.29) where $[B]$ is an unsymmetric matrix. An iterative method applied to this $[B]$ matrix then proceeds to find the lowest natural frequency first directly.

Because the elements of the matrix $[B]$ often varies considerably in size, the process of balancing is used. This is the name given to the rearrangement performed, necessary to obtain maximum accuracy in the subsequent solution for the eigenvalues and eigenvectors. The object of balancing is to make the norm (the sum of the absolute values of the matrix elements in each row or column) the same order of magnitude in the corresponding rows and columns. Error in the calculation of the eigenvalues of the problem is reduced since the eigensolution program used produces results with errors found to be proportional to the norm of the matrix.

The solution then follows with similarity transformation on the balanced matrix $[A]$ so that $[A]$ is transformed into the real upper Hessenberg matrix $[H]$ where $[H] = [S]^{-1}[A][S]$. An upper Hessenberg matrix is one whose elements h_{ij} are such that $h_{ij} = 0$ when $i - j > 1$. The transformation matrix $[S]$ is built up as the product of $n-2$ stabilised elementary transformation matrices, chosen so that the eigenvalues and eigenvectors of $[H]$ can be more readily determined than those of $[A]$. The eigenvalues of $[H]$ are the same as those of $[A]$ and if y is an eigenvector of $[H]$ then $[S]y$ is the corresponding eigenvector of $[A]$. The transformation process is however considerably simplified because of the balancing already carried out and only part of the matrix is operated upon. There is no simple method for easily calculating selected eigenvalues of an upper Hessenberg matrix and all eigenvalues of $[H]$ are always calculated. A slight saving in computing

time and storage may be made if only at most 25 percent of the eigenvectors are required. Since more than this is required it is actually more efficient, both in time and storage, to use back substitution subroutines which calculate all the eigenvectors and then to discard those that are not needed. The QR algorithm [36] is used in the eigensolution subroutine. This is a very stable method but accuracy is dependant on the eigenvalues being well spaced out.

A detailed description of all the algorithms and the actual subroutines used is included in Appendix 2. More details of the computer program written is given in Chapter 6.

Summary

This chapter describes the basic terms and concepts of random theory. The significance of the correlation function of the excitation and the response signals for the case of white noise excitation is discussed. The Pseudo random binary sequence signal is a convenient white noise signal suitable for use in obtaining the cross correlation function easily and giving the system impulse response function. The receptance of the system is obtained by a Fourier transform of the system impulse response and calculation of the discrete Fourier transform using a new and faster technique is used. It is also shown that the frequency analysis of any response to random excitation is not accurate and an alternative method of determining the response in form of its power spectral density from a knowledge of the excitation PSD as well as the receptance of the system is described.

3.1 Introduction

Knowledge of the response of structures to random excitation of any given type of spectrum is important. This chapter deals with the background theory relating to random excitation of a folded plate box type structure which may represent a car travelling along an uneven road surface, an aircraft subjected to high speed air turbulence or buildings and bridges to wind gusts. A brief description of basic random signal theory is given. The reader requiring a more detailed knowledge of random vibration theory is referred to standard text-books e.g. Robson [2].

A truly random process is by definition unpredictable. In order to make possible any analysis at all a statistical type solution of the response of structures to random excitation must be relied upon. Moreover it is difficult experimentally to generate a true random signal and to be able to reproduce it again when required. The use of a special type of random signal overcomes these difficulties. This is known as the pseudo random binary sequence and will be discussed later in this chapter.

The response of structures to random excitation is discussed and the theoretical basis for its experimental as well as analytical derivation is examined. The method used in this work to determine this response experimentally is based on the time domain correlation of the input and response signals. For the special case of a flat excitation spectrum the cross spectral density obtained on performing a Fourier transformation on the cross correlation function also gives the frequency response function or receptance of the structure. The advantage resulting in the elimination of interference signals greatly enhances this method of systems evaluation. It also gives an accurate method whereby the response power spectral density to the white noise excitation is easily obtained.

Robson also shows (eqn. 1.2) that the receptance of a structure can be calculated from a knowledge of its natural frequencies and mode shapes. He provides the theoretical basis for the prediction of the response spectral density from this receptance as well as the knowledge of the excitation power spectral density.

The finite element method of analysis described in the previous chapter enables the calculation of natural frequencies and mode shapes of the box structure. From these the receptance and hence the response power spectral density is predicted.

3.2 Basic Theory

Before going into the realm of random vibration some of the basic theory and concepts of random processes as given in [2] are here reviewed, and basic terms peculiar to random theory are defined.

3.2.1 Statistical approach

Because random signals are by definition unpredictable they can only be described in statistical terms. The basic requirement of such a description is an 'ensemble' of time series records of the signal (fig 3.1) which may represent force, acceleration, displacement etc.

One common way of describing the signal statistically is by means of its probability density distribution $p(x)$ which is defined so that

$$\text{Prob} [x \leq x(t_0) \leq x + dt] = p(x)dx \quad (3.1)$$

where the total area under the $p(x)$ curve is equal to one, and indicates that the probability of the signal lying between extreme limits of the curve is 100 %. Many naturally occurring random signals have a bell shaped probability density function (fig 3.2) given by

$$p(x) = \frac{1}{\sigma\sqrt{2\pi}} \exp\left[-\frac{(x-m)^2}{2\sigma^2}\right] \quad (3.2)$$

where σ^2 is the mean square value, also called the variance of the signal and m is its mean.

The process is then said to have a normal or Gaussian probability distribution.

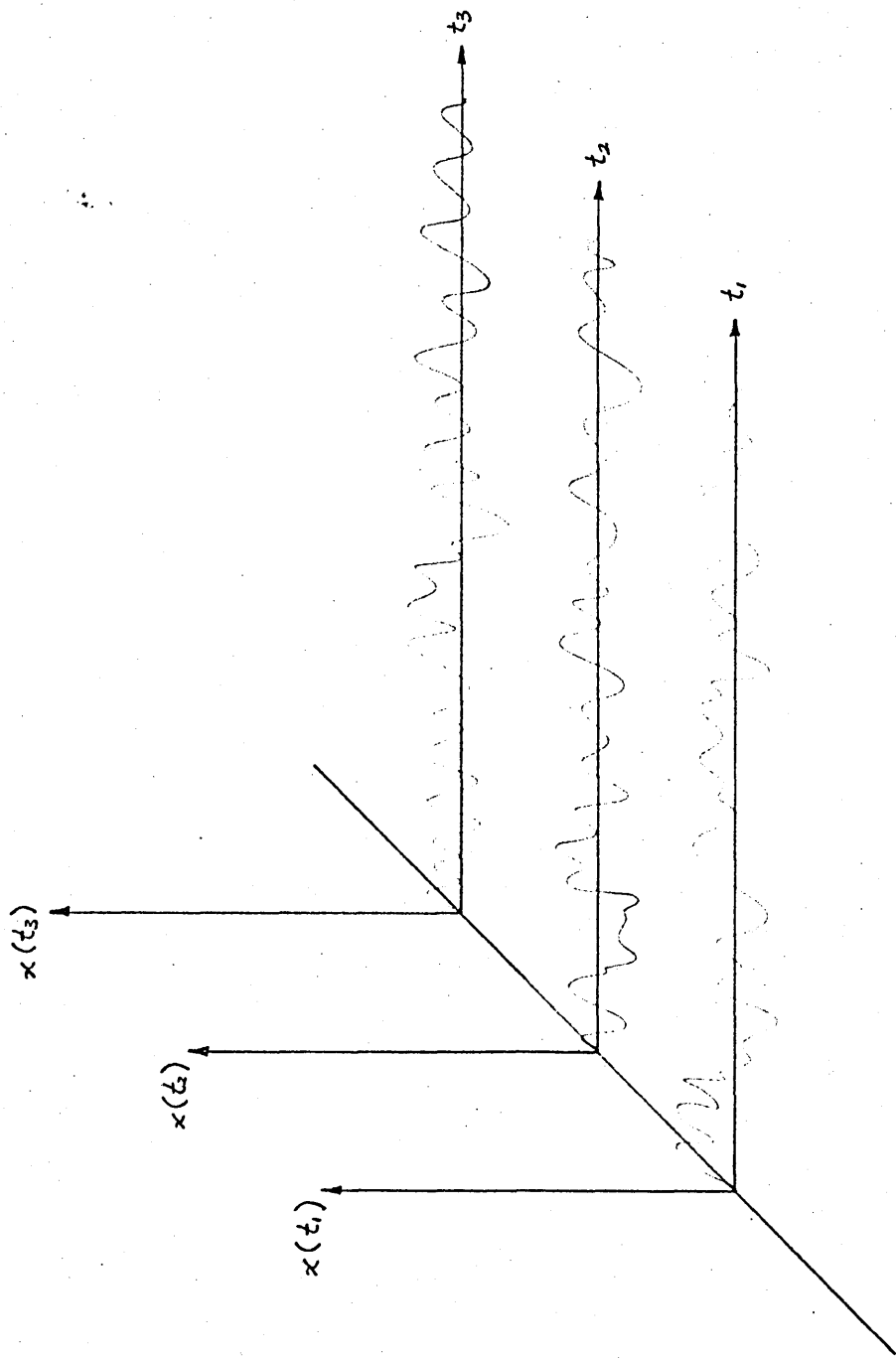


Fig. 3.1 An ensemble of random signals.

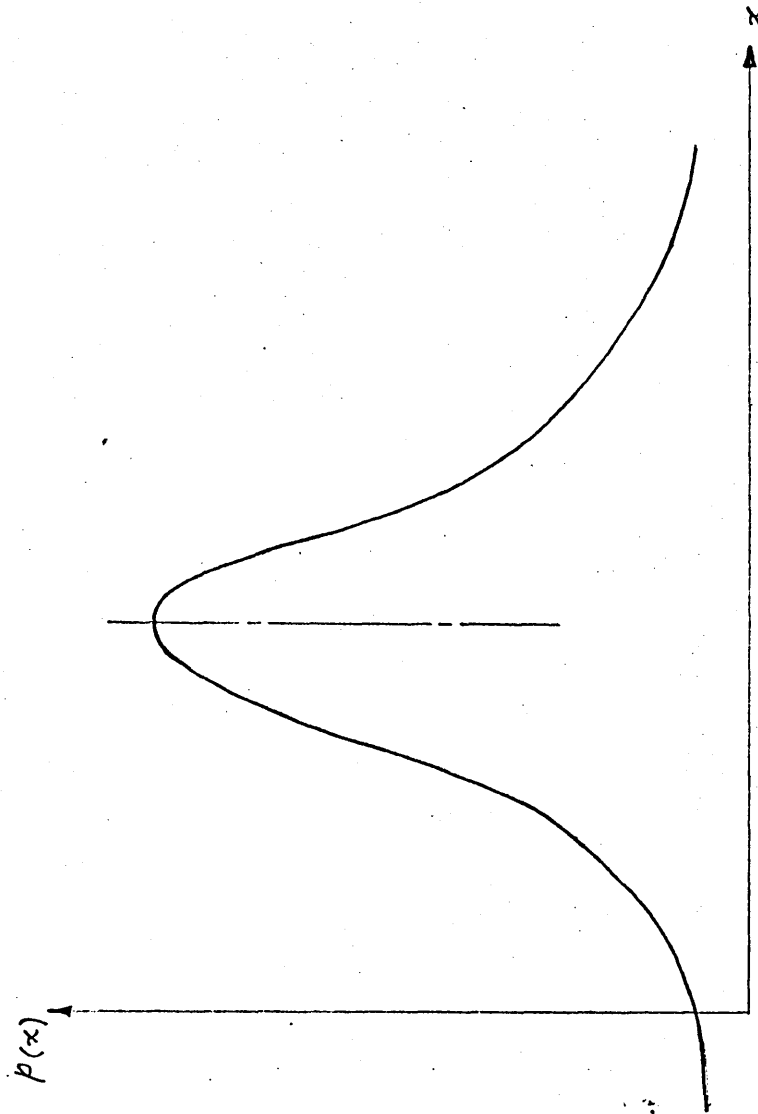


Fig. 3.2 A typical Normal probability distribution.

In practice analysis is simplified by the introduction of the concept of the 'stationary' random process. This is one in which a probability distribution obtained for a particular record is identical to those obtained for all the other records and is therefore independent of the time at which the record is taken. All the statistical characteristics of a stationary random process e.g. its mean, mean square etc. are therefore time invariant. This concept is taken a step further by the introduction of the ergodic process which is defined as not only being stationary but also has its probability distribution taken across the ensemble identical with that taken along any particular record.

3.2.2 The correlation functions

The correlation of the excitation and response signals of the structure will be used in later calculations and provides an important means of signal analysis.

The auto-correlation function $R_{xx}(t,z)$ is defined as the average over several records of the product of $x(t)$ and its delayed version $x(t+z)$ which for a stationary signal is

$$R_{xx}(z) = E[x(t)x(t+z)] \quad (3.3)$$

where E represents the averaging process.

Similarly the cross correlation function $R_{xy}(t,z)$ of two stationary signals $x(t)$ and $y(t)$ is

$$R_{xy}(z) = E[x(t)y(t+z)] \quad (3.4)$$

so that in the limit as $z \rightarrow \infty$, $R_{xy}(z) \rightarrow 0$

This is because there is no correlation between two different signals at that period of delay and this important property makes it suitable for Fourier transformation as will be seen later.

3.2.3 Power spectral densities

Another term commonly used in random signal analysis is power spectral density $S(f)$ or $S(\omega)$, spectral density for short. The spectral density $S_x(\omega)$ can be defined in terms of the auto-correlation function $R_x(z)$ of the signal and was first clearly stated by Wiener [37] as

$$S_x(\omega) = \frac{1}{2\pi} \int_{-\infty}^{\infty} R_x(z) e^{-i\omega z} dz \quad (3.5)$$

This is an important concept in random vibration analysis since $\int S_x(\omega) d\omega$ is in fact the mean square $E[x^2]$ of the process i.e.

$$E[x^2] = \int_{-\infty}^{\infty} S_x(\omega) d\omega \quad (3.6)$$

For Gaussian processes whose mean is zero, eqn (3.2) becomes

$$p(x) = \frac{1}{\sigma\sqrt{2\pi}} e^{-\frac{x^2}{2\sigma^2}} \quad (3.7)$$

Knowledge of $E[x^2]$ would define the process completely since for a process with a mean about zero

$$E[x^2] = \sigma^2 \quad (3.8)$$

Hence since $E[x^2]$ can be obtained from eqn 3.6, the determination of the power spectral density is extremely useful in all calculations involving random signals. It should be noted here that $S_x(f)$ is expressed as a function of frequency and 2π times larger than $S_x(\omega)$. From equation (3.6) the mean square value of $x(t)$ in any given band of frequencies Δf is simply $S_x(f) \Delta f$ or $S_x(\omega) \Delta \omega$. As an example, if $x(t)$ is a varying force expressed in newtons, then $S_x(f)$ would be in newtons²/Hz and $S_x(\omega)$ in newtons²sec.

3.2.4 Fourier analysis of random signals

In many cases it may be desirable to express a random signal in a Fourier series type expansion. However because the signal is not periodic this is not possible. Moreover since the signal must be assumed to extend over an infinite period of time to have stationary properties it cannot be expressed as a Fourier integral either. A method of measurement is therefore adopted to overcome the difficulties, using the Fourier transform $A_T(if)$ of a signal $x_T(t)$ which is identical to the signal to be analysed over the period $-\frac{T}{2} < t < \frac{T}{2}$ and zero elsewhere. The spectral density of the original signal has been shown by Jenkins & Watts [38] to be approximated by

$$S_x(f) = E \left[\lim_{T \rightarrow \infty} \left\{ \frac{2}{T} |A_T(if)|^2 \right\} \right] \quad (3.9)$$

From this it can be seen that the direct Fourier transform of the response of the structure required, measured within any finite length of time will at best give only an approximation to the true power spectral density of the response. A different approach is therefore adopted in this work to attempt at obtaining a better estimate and the method is described in section 3.5

The classical method of determining the response of a structure to excitation requires the solution of the differential equation (Newland [39]) relating the excitation $x(t)$ and the response $y(t)$ in

$$\sum_{n=0}^r A_n \frac{d^n y}{dt^n} = \sum_{n=0}^s B_n \frac{d^n x}{dt^n} + \sum_{n=0}^t C_n \frac{d^n x_2}{dt^n} \quad (3.10)$$

This relationship however cannot be used in random vibration work because

- (i) inadequate data is available to determine the coefficients A, B & C so that the complete differential equation is not available.
- (ii) even if the equation is known, a complete time history of $x(t)$ is not obtainable because of its random nature.

Analysis of the response of any structure to random excitation is therefore best carried out using the form of its response power spectral density, described in the previous chapter. This requires the determination of the structural frequency response curve commonly called the receptance (Bishop & Johnson [4]) of the structure.

The receptance of the structure is defined as the response d of the structure to a unit applied sinusoidal force p of frequency f . It should be noted that the receptance is different at different points of the structure and relates only two specific points on the structure, A the point at which the force is applied and B the point at which the response is measured i.e.

$$d_B = \alpha_{AB}(if)p_A \quad (3.11)$$

Determination of $\alpha(if)$ will therefore give the response of the structure to any given force p . The receptance and hence the response is complex, with a real and an imaginary part, the physical significance being that there is a time lag between the application of the force p and the occurrence of

the response d . For a single degree of freedom structure with a hysteretic damping factor η the equation of motion may be written as

$$m\ddot{x} + k(1 + i\eta)x = p \sin \omega t \quad (3.12)$$

from which the receptance is found to be

$$\alpha(i\omega) = \frac{1}{k - 4\pi^2 m\omega^2 + i\eta k} \quad (3.13)$$

Robson [2] shows that the receptance of a multi-degree of freedom structure can be expressed in terms of its natural frequencies and mode shapes (equation 1.2). For a structure with light damping and hence pronounced resonance peaks the receptance becomes

$$|\alpha(i\omega)|^2 = \sum_r \frac{[w_r(x_A)]^2 [w_r(x_B)]^2}{M_r^2 [16\pi^4 \{(f_r^2 - \omega^2)^2 + \eta_r^2 f_r^4\}]} \quad (3.14)$$

where $w_r(x)$ is the r th mode shape

f_r is the r th natural frequency

and M_r is the generalised mass at mode r

given by $\int_0^L w_r^2(x) m dx$

Here structural damping is taken to be hysteretic only (applicable to light structures) and any coupling between the structure and a medium such as air is assumed to be negligible. η the hysteretic damping factor for the structure is calculated from its response curves and is discussed in more detail later.

The natural frequencies and mode shapes of a simple structure can be determined using the exact method of solving differential equations or by approximations using various energy methods. For more complicated structures however the finite element method which is basically an energy method, described in chapter 2, is increasingly used because of difficulties encountered with other methods. In this work therefore the natural frequencies and mode shapes of the box structure are predicted using a finite element computer program package developed by the author and given in Appendix 3. Once the receptance of the structure is known a prediction

of the response spectral density is possible using the relationship given previously in equation (1.1) provided the input spectral density is also known.

$$S_d(f) = |\alpha_{dp}(if)|^2 S_p(f) \quad (1.1)$$

Therefore once the receptance of the structure is known, the response spectral density can be obtained for any given excitation spectral density, from which other parameters describing the response such as the mean square value and probability distribution are obtained using equations (3.7) and (3.8).

3.4 Experimental Techniques

There are basically two ways of obtaining experimentally the response of structures to random excitation. The first is the direct approach, measuring the frequency content of the response using a frequency analyser. This method however is not accurate in any finite sampling time because of the random nature of the signal and also because of the low signal to noise ratio generally encountered. The alternative method is the synthesis of the response power spectral density from experimentally derived values of both the structural receptance as well as the excitation power spectral density using the equation given previously.

$$S_d(f) = |\alpha(if)|^2 S_p(f) \quad (1.1)$$

This method is found to be more accurate than the first since the excitation power spectral density is often known or can be obtained accurately.

There are three main ways of determining experimentally the frequency response or receptance of structures to vibrations. They are (a) sinusoidal frequency testing (b) transient testing using a ramp or impulse input and (c) tests using correlation methods.

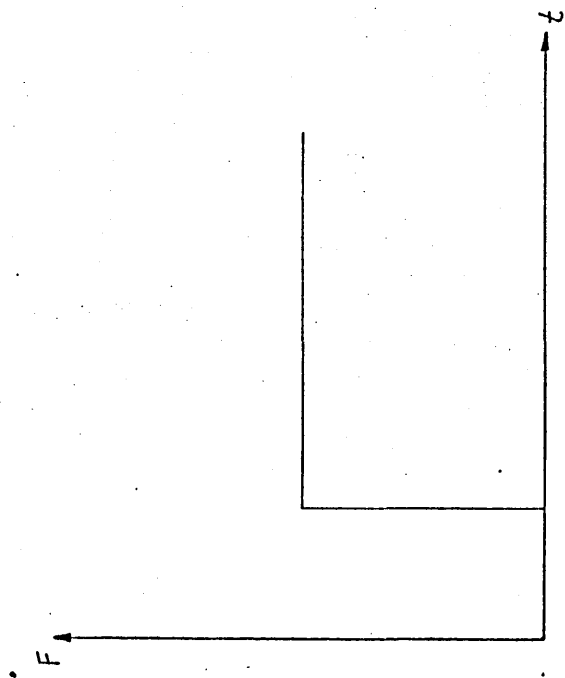
The simplest and most commonly used method is sine wave excitation, measuring the amplitude and phase angle of the response over a range of frequencies giving the frequency response curve directly. Disadvantages encountered with this method include inaccuracy as often the response is contaminated with extraneous noise. The excitation cannot be increased since the system will lose its linear behaviour so that an averaging process is often incorporated. It is also very time consuming to excite each frequency separately and to sweep sufficient frequencies for a complete frequency response curve.

Transient testing involves either step (ramp) response (fig. 3.3a) or impulse response measurements (fig. 3.3b). The former is quick and contains all frequencies in the step and it is therefore possible to obtain the structural frequency response using curve fitting techniques. It is however limited to simple systems and involves a drastic change of initial conditions. The latter retains the steady state initial conditions but is impossible to generate in practice. Both are also susceptible to inaccuracies due to noise interference at low levels of excitation and non linear behaviour at higher levels.

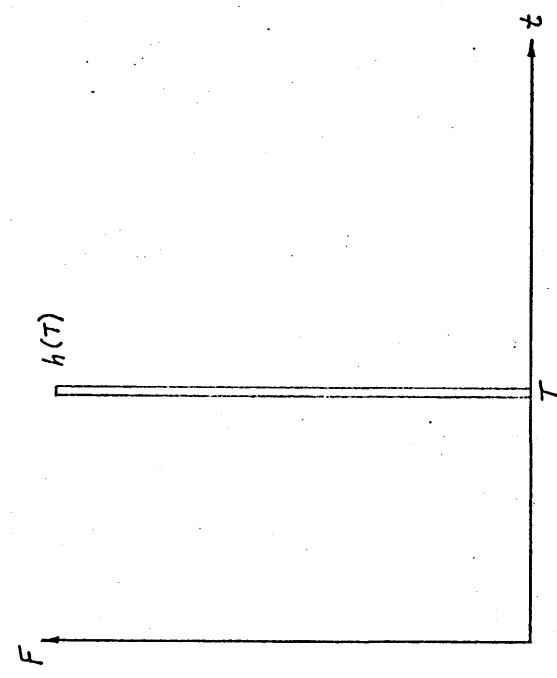
The third method and one of the most important time domain techniques available is the correlation of two signals, giving a measure of the similarity between the two. The input $x(t)$ and output $y(t)$ of a system are related through a finite integral known as the convolution integral described in Robson [2] and elsewhere as

$$y(t) = \int_{-\infty}^{\infty} h(\tau)x(t-\tau)d\tau \quad (3.15) \quad X$$

where $h(t)$ is the impulse response of the structure and τ is the time delay between the application of the impulse and time t at which the impulse was applied. This convolution integral provides a direct method of obtaining the output signal from a knowledge of the input signal and the impulse response of the structure. As it stands this does not mean very much since the impulse response of the structure is unknown but the application of the correlation method opens up an entirely different approach to the problem.



(a) A step function



(b) An impulse function

Fig. 3.3 Transient testing signals

The theory behind the technique lies in the definition of the correlation functions themselves (see section 3.1). The auto correlation function of the excitation $x(t)$ may be expressed as

$$R_{xx}(\tau) = \lim_{T \rightarrow \infty} \frac{1}{2T} \int_{-T}^T x(t)x(t + \tau) dt \quad (3.16)$$

and the cross correlation function of the excitation $x(t)$ and the response $y(t)$ as

$$R_{xy}(\tau) = \lim_{T \rightarrow \infty} \frac{1}{2T} \int_{-T}^T x(t)y(t + \tau) dt \quad (3.17)$$

Since the impulse response must be zero before its application $h(t) = 0$ for $t < 0$ and hence (3.15) becomes

$$y(t) = \int_{-\infty}^{\infty} h(s)x(t - s) ds$$

and substituting into eqn. 3.17 ,

$$\begin{aligned} R_{xy}(\tau) &= \lim_{T \rightarrow \infty} \frac{1}{2T} \int_{-T}^T x(t) \left[\int_{-\infty}^{\infty} h(s)x(t+\tau-s) ds \right] dt \\ &= \int_{-\infty}^{\infty} h(s) \left[\lim_{T \rightarrow \infty} \frac{1}{2T} \int_{-T}^T x(t)x(t+\tau-s) dt \right] ds \end{aligned}$$

which from 3.16 becomes

$$R_{xy}(\tau) = \int_{-\infty}^{\infty} h(s) R_{xx}(\tau - s) ds \quad (3.18)$$

It is immediately apparent that if we choose an excitation signal with a autocorrelation function in the form of a spike or impulse, the impulse response function can be obtained quite simply from the cross-correlation function between the excitation and response signals.

A white noise signal satisfies this requirement. The autocorrelation function of a white noise signal with a flat power density spectrum of K/f is an impulse of magnitude K .

Thus for white noise equation 3.18 becomes

$$R_{xy}(\tau) = Kh(\tau) \quad (3.19)$$

White noise excitation therefore gives a particularly important aspect to correlation techniques as the cross correlation between the excitation and the response of the structure under consideration gives the impulse response function of

the structure multiplied by a constant K. It is therefore no longer necessary to physically hit the structure with an impulse of force in order to obtain its impulse response. The frequency response function or receptance is then quite simply the Fourier transform of the impulse response function.

$$H(\omega) = \mathcal{F}[h(\tau)] \quad (3.20)$$

The impulse response function of any structure can therefore be obtained without the problems associated with sinusoidal and transient testing and has with it the advantage that noise originating within the system does not correlate with the excitation signal and is hence effectively eliminated. Thus a signal of low amplitude can be used even in a noisy environment. This is the basis of the so called method of random systems testing. The method however has several drawbacks. Firstly the truly random signal is difficult to generate artificially and impossible to reproduce exactly. The delayed signal required for calculation of the correlation function is therefore not available. Furthermore the correlation also requires multiplication and integration over a theoretically infinite period, and it would be difficult to obtain a satisfactory correlation over a finite period of an essentially unpredictable process. The use of the pseudo random binary sequence signal, described later overcomes this difficulty.

3.6 The Fourier Transform

The concept of the frequency analysis of a signal of period T by splitting it into its component frequencies using the Fourier Series is well known (see Newland [39])

Thus

$$x(t) = \sum_{n=0}^{\infty} A_n \cos \frac{2\pi nt}{T} + B_n \sin \frac{2\pi nt}{T} \quad (3.21)$$

where

$$A_0 = \frac{1}{T} \int_{-\frac{T}{2}}^{\frac{T}{2}} x(t) dt$$

$$A_n = \frac{2}{T} \int_{-\frac{T}{2}}^{\frac{T}{2}} x(t) \cos \frac{2\pi nt}{T} dt$$

and

$$B_n = \frac{2}{T} \int_{-\frac{T}{2}}^{\frac{T}{2}} x(t) \sin \frac{2\pi nt}{T} dt$$

or also expressed as

$$X_n = \frac{1}{T} \int_0^T x(t) e^{-\frac{i2\pi nt}{T}} dt \quad \text{where } X_n = A_n - iB_n \quad (3.22)$$

The limit when T tends to infinity is reached in non-periodic signals so that the Fourier series becomes a Fourier integral whose coefficients are the corresponding Fourier transforms.

i.e.

$$x(t) = 2 \int_0^{\infty} [A(\omega) \cos \omega t d\omega + B(\omega) \sin \omega t d\omega] \quad (3.23)$$

and

$$A(\omega) = \frac{1}{2\pi} \int_{-\infty}^{\infty} x(t) \cos \omega t dt$$

$$B(\omega) = \frac{1}{2\pi} \int_{-\infty}^{\infty} x(t) \sin \omega t dt \quad (3.24)$$

with the limitation that $\int_{-\infty}^{\infty} x(t) dt < \infty$

This thus provides an indispensable tool which facilitates signal analysis in transforming a signal from the time to the frequency domain or vice versa. However, because of the limitation on the signal $x(t)$ itself, unless special precautions are taken only a process which in the limit is finite can be analysed.

In the work a time series which satisfies this requirement of being finite in the limit is used. This is the cross correlation function of the white noise excitation and the resulting response of the structure. The direct frequency analysis of the response itself is not used as it does not satisfy this requirement however long the record taken may be.

From the previous section (eqn. 3.19), we have seen that for white noise the cross correlation function $R_{xy}(\tau)$ is in fact $K h(\tau)$ where $h(\tau)$ is the impulse response of the system and K is a constant, given by the power spectral density of the excitation. The Fourier transform of this gives its equivalent in the frequency domain, the frequency response function of the structure, (eqn. 3.20), multiplied by the same constant K . Because the excitation is white noise, this function when multiplied by the constant 2π gives the output power spectral density of the structure as well.

Here a continuous function is to be analysed by taking discrete samples of it at equally spaced intervals of time. Such a series completely represents the continuous waveform providing the waveform is band limited and the samples are taken at a rate of at least twice the highest frequency present in the original waveform [39]. The samples are then called Nyquist samples and the highest frequency present, the Nyquist frequency. The discrete Fourier transform or DFT of such a time series is then closely related to the Fourier transform of the original continuous waveform and has mathematical properties analogous with it. If however frequencies in the original signal exist which are higher than half the sampling frequency the Nyquist frequency, a corruption of the graph known as aliasing occurs. In this case, to obtain a true DFT either a higher sampling frequency is required or the existing high frequencies contravening the Nyquist criteria must be filtered out of the signal. In this work the latter method is used.

Thus from eqn. 3.2 the DFT of N equally spaced samples taken at intervals of time can be obtained using the formula

$$X_n = \frac{1}{T} \sum_{r=0}^{N-1} x_r e^{-\frac{i2\pi nr\Delta}{T}} \Delta \quad (3.25)$$

where n ranges from 0 to $N - 1$ corresponding to harmonics of $\frac{2\pi}{N\Delta}$.

The use of eqn. 3.24 to obtain the DFT is perfectly satisfactory for processing small amounts of data and a computer routine to carry out the algorithm is included in Appendix 4. For large quantities of data however, this conventional method quickly takes up a large amount of computer core and the computing time required becomes prohibitive.

The Fast Fourier Transform or FFT is an algorithm that was developed recently to calculate the Discrete Fourier Transform (DFT) and takes advantage of the fact that the calculation of the coefficients of the DFT can be carried out iteratively resulting in a considerable saving of computing time and increased accuracy. The algorithm used is that reported by Cooley and Tukey [29]. The FFT method is perhaps not as obvious as the DFT and the steps are briefly outlined here.

A time series X_k of N points is divided into two functions Y_k and Z_k where Y_k consists of all the even numbered points and Z_k the odd.

$$\left. \begin{aligned} Y_k &= X_{2k} \\ Z_k &= X_{2k+1} \end{aligned} \right\} k = 0, 1, 2, \dots, \left(\frac{N}{2} - 1\right)$$

Therefore the DFT of Y_k and Z_k will be given by

$$\left. \begin{aligned} B_r &= \sum_{k=0}^{\frac{N}{2}-1} Y_k \exp\left(-\frac{4\pi irk}{N}\right) \\ C_r &= \sum_{k=0}^{\frac{N}{2}-1} Z_k \exp\left(-\frac{4\pi irk}{N}\right) \end{aligned} \right\} \text{where } r = 0, 1, 2, \dots, \left(\frac{N}{2} - 1\right)$$

The DFT of the original series X_k is then

$$A_r = \sum_{k=0}^{\frac{N}{2}-1} \left\{ Y_k \exp\left(-\frac{4\pi irk}{N}\right) + Z_k \exp\left(-\frac{2\pi ir}{N}(2k+1)\right) \right\}$$

$$= \sum_{k=0}^{\frac{N}{2}-1} Y_k \exp\left(-\frac{4\pi irk}{N}\right) + \exp\left(-\frac{2\pi ir}{N}\right) \left[\sum_{k=0}^{\frac{N}{2}-1} Z_k \exp\left(-\frac{4\pi irk}{N}\right) \right]$$

where $r = 0, 1, \dots, N-1$.

which may be written as

$$A_r = B_r + \exp\left(-\frac{2\pi ir}{N}\right) C_r \quad \text{for } r = 0, 1, 2, \dots, \left(\frac{N}{2} - 1\right)$$

The DFTs, B_r and C_r repeat themselves outside this interval so that

$$A_{\left(r + \frac{N}{2}\right)} = B_{\left(r + \frac{N}{2}\right)} + \exp\left[-\frac{2\pi i}{N} \left(r + \frac{N}{2}\right)\right] C_{\left(r + \frac{N}{2}\right)}$$

$$= B_r - \exp\left(-\frac{2\pi ir}{N}\right) C_r$$

$$\text{since } \exp\left(-\frac{2\pi iN}{2N}\right) = -1$$

Therefore

$$A_r = B_r + W^r C_r \quad \text{for } r = 0, 1, 2, \dots, \frac{N}{2}$$

$$A_{\left(r + \frac{N}{2}\right)} = B_r - W^r C_r \quad \text{where } W = e^{-\frac{2\pi i}{N}}$$

Thus the two halves of the DFT of the N point X_k , A_r and $A_{r + \frac{N}{2}}$ can be obtained from the B_r and C_r , DFT's of Y_k and Z_k each of $\frac{N}{2}$ points. By successively dividing the series into further subseries as long as they are divisible by two, we end up with the DFT of a small series from which the DFT of the original series can be built up. Variations on the method allow the series to be broken up into series of multiples other than two but we shall not look into these here.

In this work, series containing 512 and 1024 points are finally reduced to the single term, the DFT of the single term being the term itself, and the DFT of the series built up from it, and simply divided by the factor 512 or 1024 respectively. Thus it will be seen that a considerable saving in the number of complex multiplications and complex

additions is made using this algorithm. The resulting saving in the time taken enables this method of calculating Fourier transforms to be run more economically than the normal method especially on the slower computers.

Random-type signals used in the laboratory can be classified into being naturally or artificially generated. Commonly used natural sources of random signals include (a) a tape recordings of a naturally occurring random signal such as wind noise, road noise etc. (b) the emission of electrons by a thyratron or zener diode. These have several disadvantages. The former requires an infinitely long record to be statistically accurate, the latter is difficult to control particularly in the low frequency ranges and moreover is not reproducible whenever required. To overcome these drawbacks other sources of random signals have to be used.

Pseudorandom binary sequence signals (referred to as PRBS signal hereafter) provide artificially generated signals that are completely random within any specified period of time but repeat themselves thereafter. Since the signal is completely random within this interval it meets all the requirements and has all the properties of random signals discussed in the previous section. The use of a PRBS signal as an excitation signal has several advantages over the use of true random signals.

These include

- (a) repeatability - it is possible to obtain exact signals for repeated tests and these tests do not have to be infinitely long. Statistical type results do not have to be relied on as in the case with true random signals.
- (b) spectrum can be tailored to requirements - the frequency of interest, resolution, length of time available for each test etc. can be allowed for in each case.
- (c) correlation of excitation and response can be easily obtained over a discrete number of signal points.
- (d) for the particular equipment used a time domain correlator is available as standard equipment so that automatic recording of the usually lengthy correlation function is possible.

A brief description of the signal (fig. 3.4) is now given. For a more detailed account, the reader is referred to the handbook [40].

The PRBS signal is generated using a shift register, the length n of which can be changed at will and which gives it the name of the maximum length sequence of simply m sequence. The outputs from two stages of the shift register are connected to a modulo two adder (exclusive OR gate) whose output controls the state of the first shift register stage. These connections are chosen so that a maximum length sequence is generated of $N = (2^n - 1)$ bits. The necessary delayed signal is obtained simply by dividing the full shift register into two equal parts to form master and slave PRBS generators. The main control logic then arranges for the slave shift to begin its sequence the required number of clock pulses after the master.

It is completely controllable, a considerable advantage over true random signals but unlike random binary signals has the number of positive and negative bits differing by one since the total number of bits in the sequence is given by $(2^n - 1)$. Being a binary signal it has only 2 levels, $+1$ and -1 , which change at intervals of Δ sec given by the clock pulse. Multi-level sequences may however be chosen to assume particular types of probability distributions if necessary.

As mentioned previously the PRBS signal is completely random within the period

$$T = N\Delta$$

where $1/\Delta$ = clock frequency

$$N = \text{no. of bits in the sequence} = (2^n - 1)$$

A comparison of its autocorrelation function (fig. 3.5) reveals that (a) it is a spike which repeats itself at intervals of N (see Newland [39]). (b) a small negative correlation $-a^2/N$ persists. However it approaches that of true white noise when the sequence length N is made large and the clock time Δ small. Within the time interval $N\Delta$ therefore it has all the properties necessary for the random systems testing described in the previous chapter.

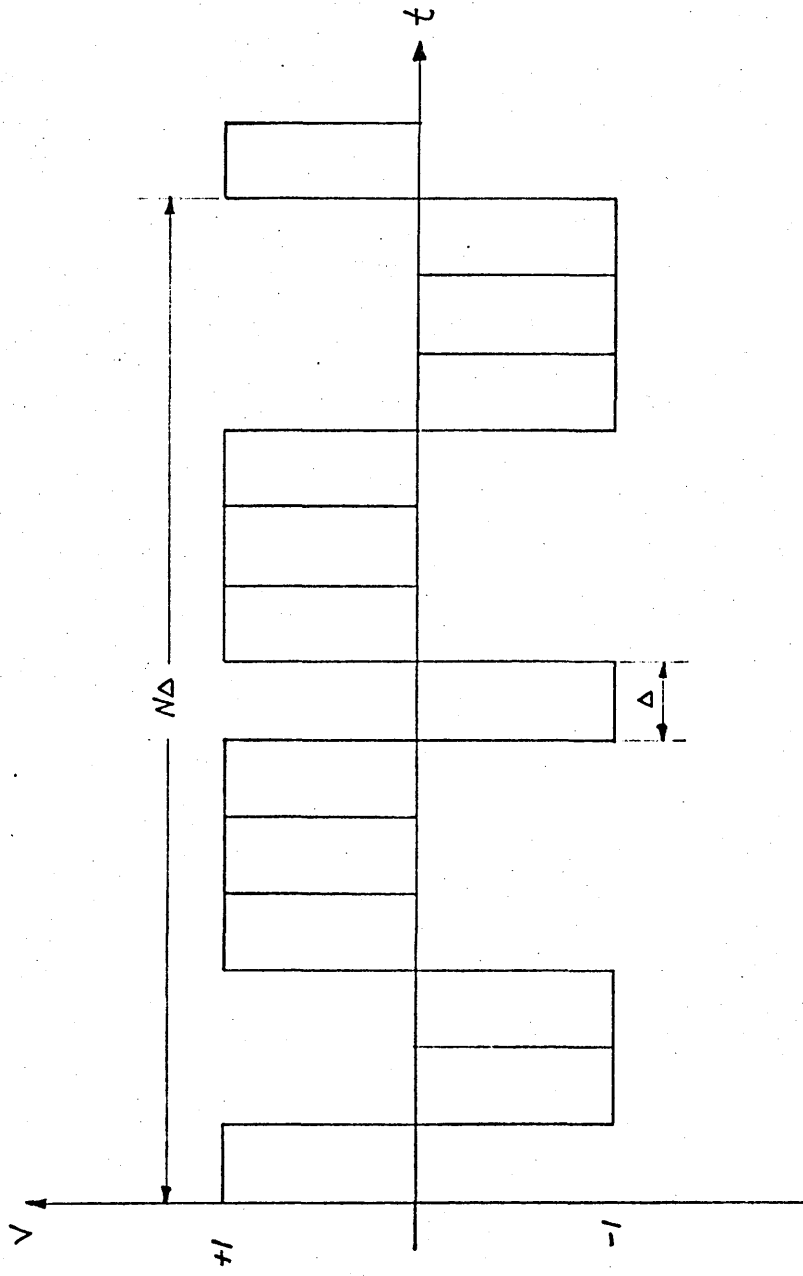


Fig. 3.4 A PRBS signal.

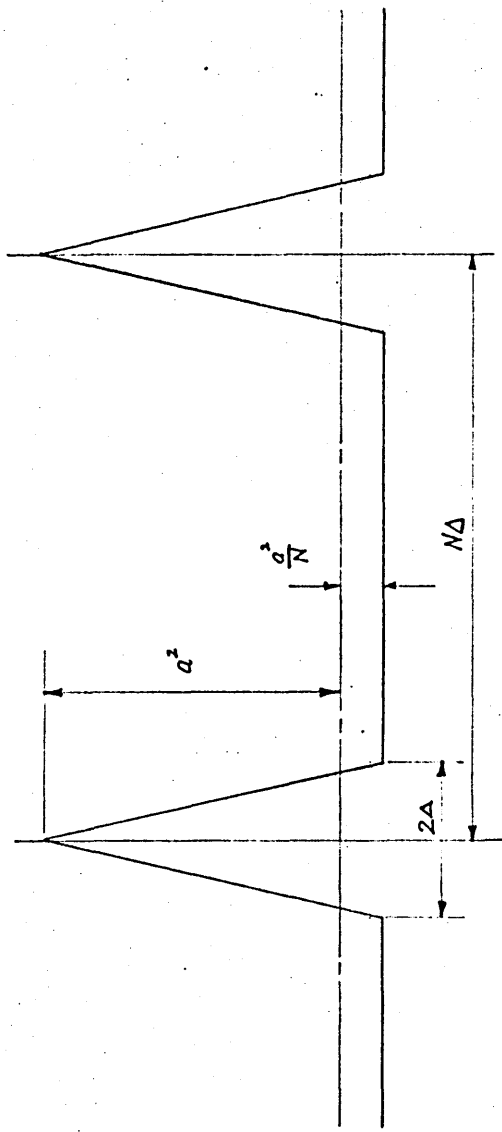


Fig 3.5 Autocorrelation function of a PRBS signal.

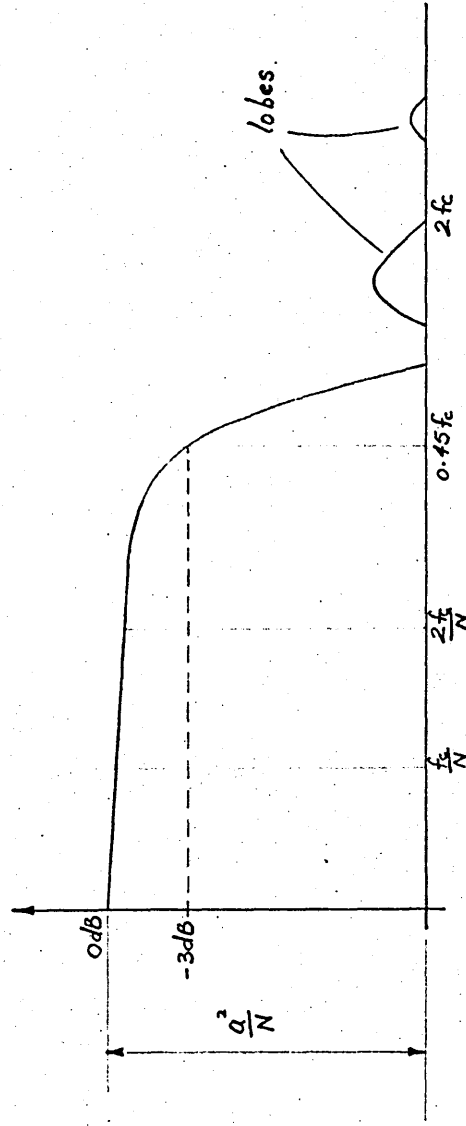


Fig 3.6 Power spectrum of the PRBS signal.

The Fourier transform of the autocorrelation function gives the graph of relative power plotted against frequency (fig. 3.6). Referring to the figure, because the signal changes only at discrete intervals of time it will be seen that this is a line spectrum i.e. one made up of individual lines instead of the continuous spectrum of true white noise.

These are spaced out at a distance of $\frac{f_c}{N}$ Hz apart where $f_c = \text{clock frequency} = \frac{1}{\Delta}$ and are constant to -3 dB at $0.45 f_c$ Hz as shown. The shape of the envelope is given in the manufacturers' specification as being described by the function $(\frac{\sin x}{x})^2$ where $x = \frac{\pi f}{f_c}$ with a d.c. component of power = a^2/N since N is an odd number. A closer approximation to a continuous spectrum is obtained by increasing the sequence length but reducing the clock frequency. This is achieved at the expense of amplitude in the former and the upper frequency in the latter.

The PRBS signal has a probability distribution shown in fig 3.7. This reveals that the signal occurs only at 2 levels, $\pm aV$ (see fig 3.4) and, of the $2^n - 1$ bits of signal in a sequence, has one more + a bit than - a bit. This can however be tailored to approximate the Gaussian distribution of commonly occurring random signals in a binomial type distribution (fig 3.8) using multi-level sequences. This is achieved however at the expense of (a) reducing the amplitude of the output signal from a^2 to $a^2/(M-1)$, (b) widening the impulse type spike of its autocorrelation function (fig 3.5) from 2Δ to $2(M-1)\Delta$ and (c) reducing the highest frequency (fig 3.6) from f_c to $f_c/(M-1)$ Hz.

It is possible therefore either to approximate a given random signal or to generate a suitable excitation signal for any given system and at the same time to be able to repeat it exactly both for correlation calculations as well as to repeat a test subsequently. A suitable signal with which to excite any given structure is governed by the choice of upper frequency limit, shape of excitation power spectrum, resolution of component frequencies, probability distribution

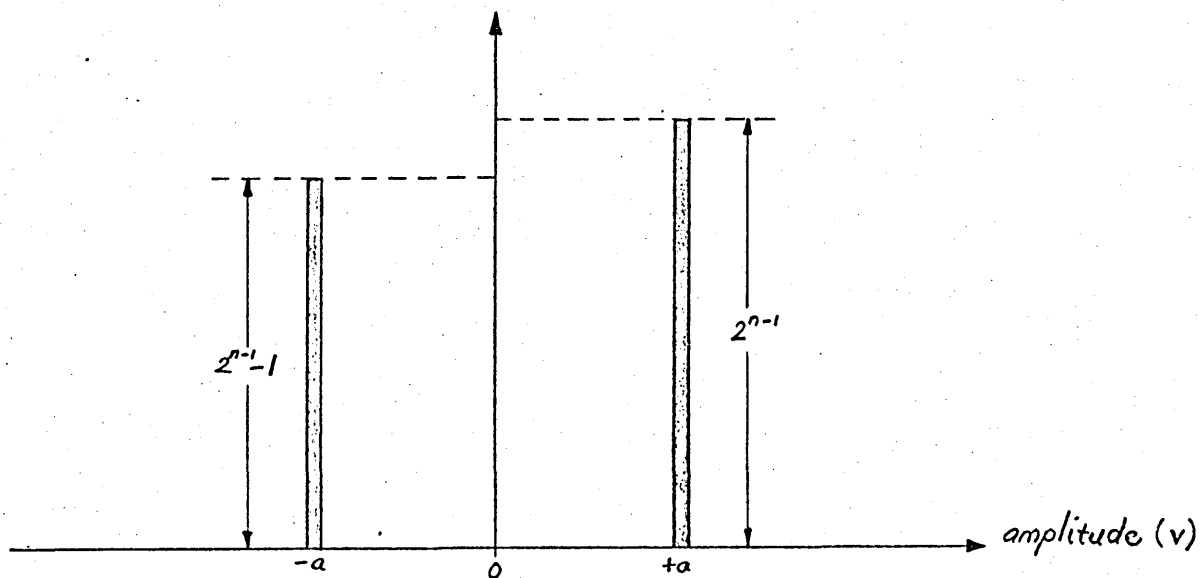


Fig. 3.7 PRBS occurrence distribution.

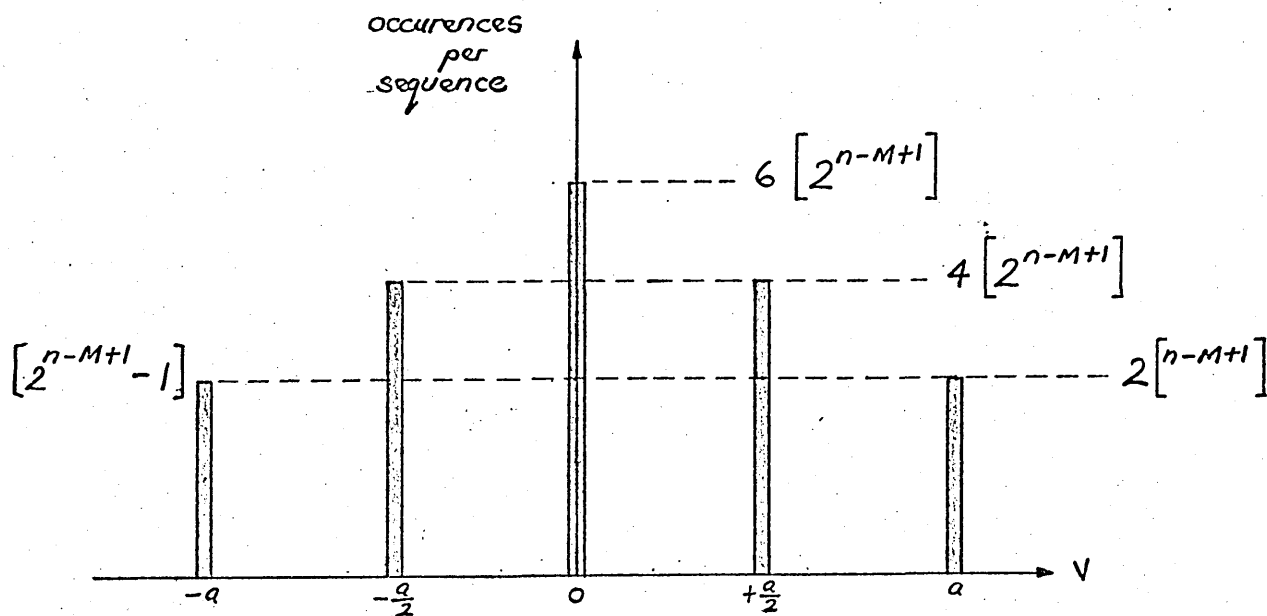


Fig 3.8 Probability distribution of a multi-level sequence.

and so on. All these are easily obtained with a PRBS signal. The upper frequency limit is given by the clock frequency of the PRBS generator and is determined by the requirement to stimulate the structure up to a given frequency. In many structures the most important frequencies are the lowest few as the response at higher frequencies tends to be attenuated. In practice most structures also tend to have the higher frequencies occurring close together and with the line spectrum of the PRBS signal there is a danger that a natural frequency of the structure may not be stimulated.

To summarise therefore the PRBS signal is within its sequence length completely satisfactory for random testing purposes. It is easy to generate, reproduce and multiply and is therefore particularly suitable for correlation measurements. Since the correlation is performed over a finite period however, some degree of correlation with unrelated noise may lead to a variance in the measurements obtained. By correlating over a number of complete sequences this effect is nevertheless considerably reduced.

Summary

This chapter describes how the necessary experimental apparatus was designed, calibrated and used. A vibration table was built having the necessary characteristics for a good vibration testing mounting and incorporating an accurate two way traverse mechanism over the horizontal plane. A novel non-contacting exciter/pickup probe incorporating an electromagnetic exciter and a capacitance pickup is described. A brief description of the investigation into variations in both material and design leading up to the final probe configuration is included. A fine adjustment mechanism, linear as well as angular, is incorporated for accurate adjustment of the air gap between the probe and the structure. For random vibration work a pseudorandom binary sequence generator and time domain correlator is used from which a completely automatic system has been built up.

Since the aim of this investigation is ultimately to be able to predict the response of box-type structures to vibration stimuli, a large part of the work necessarily involves response measurements obtained experimentally to complement the equally important theoretical analysis. This basically requires a firm vibration testing table on which the structure and all the necessary transducers can be mounted. These exciters and vibration pickup transducers must be suitable for the structure to be tested.

As light structures are to be tested, in order to reduce inaccuracies due to the added masses of exciters or pickups, non-contacting transducers are necessary. Furthermore it is known that the ideal point at which to excite a particular mode is its antinode (Plunkett [41] and Dunn [42]). Exciting the structure at any point other than at a antinode requires a higher force per unit displacement response. This is because it can give rise to (a) displacement of a point which would otherwise be a node (b) rigid body displacement (c) excitation of adjacent nodes or (d) local distortion of the structure at the point of excitation (Pandered and Bishop [43]). The inherent drawback of a contacting exciter is immediately apparent since multiple holes must be made in the structure for excitation of more than one mode.

Non contacting vibration pickups are fairly widely used and capacitance displacement transducers are well known and available commercially. In general contacting exciters are still relied upon and work on non contacting electromagnetic exciters are fairly poorly documented. Recent work by Shapiro [44] to produce suitable apparatus for similar experimental investigations relied on contacting exciters although non-contacting capacitance displacement transducers were used. This may be due to difficulties such as a frequency doubling effect of the original signal in the force output of an electromagnetic exciter.

This frequency doubling effect and the heat generated in the exciter during operation were noted in the course of this work and is discussed later in this chapter. The development of an efficient non-contacting exciter pickup is therefore necessary and will be one of the tasks of this investigation.

4.2 The Vibration testing table

The importance of the vibration testing table is that it provides a good vibration mounting for the test structure isolated from interference which is mainly structural borne. It also provides a stable support for the mounting of the exciters and vibration pickup transducers with fine adjustment available between these and the structure. An accurate traverse mechanism is necessary on which the vibration pickup probe and the exciter can be suspended to scan the surface area of the structure locating the required points.

The work commenced using an existing vibration table (plate 1). Structural borne interference (the laboratory was next to a busy main road) was found to be transmitted straight through the table and picked up at the measuring transducers. The traverse mechanism holding these transducers were independent of the table and some floating relative to the table was detected. A means of fine adjustment of the transducer-plate gap was found to be necessary because the plates were not absolutely flat and the exciter-plate gap size was found to be critical. A new and larger table was made with these requirements in mind.

This is fairly large and heavy and supported on wide base plates resting on $\frac{1}{4}$ " vibration isolation pads to reduce vibration transmitted through it (plate 2). Structures measuring up to 1,500 x 900 x 430 mm can be accommodated. An accurate traverse mechanism is built on to the table and a screw-type winding, at the ends of which are hand wheels, drive the exciter-pickup probe in the two perpendicular horizontal directions. The winding mechanism is supported on special end ball races and phosphor bronze sliders to reduce friction at the slideways. When the point to be measured is arrived at, the end clamps are tightened thus eliminating extraneous vibrations from the traverse mechanism.

The fine adjustment mechanism is a double screwed device

(plate 3) which allows for accurate changes in linear displacements in the probe-structure gap size. This is necessary since both the exciter as well as the pickup have characteristics which depend on this gap size. The mechanism screws down clockwise at 0.24 mm per turn with a maximum travel of 20 mm. Coarse adjustment is by loosening allen screws holding the whole mechanism in its holder in a vertical sliding arrangement. For angular adjustment three knurled screws on a swivelling ball joint allow for tilt of the transducer relative to the structure (plate 4).

The structures to be tested are held with supports made which would approximate required boundary conditions, e.g. a fully fixed flat plate (plate 5), clamped to the table using large 'G' clamps. A close-up view of the method of fastening of the box structure is shown in plate 6.

4.3 The Vibration Pickup Transducer

Since the box-type structure to be investigated was light, a non-contacting vibration pickup transducer was used. Contacting transducers e.g. accelerometers, invariably implies additional masses attached to the test structures affecting the frequency characteristics of the structure.

Capacitance probes are part of a large family of non-contacting transducers which are used in vibration studies to eliminate the possibility of the transducer interfering with the vibration characteristics of the structure to be investigated.

The Wayne Kerr capacitance probe was chosen because of its good characteristics and already widespread use amongst research workers. It works on the principle that when placed near to a conducting surface, a capacitance effect exists between this surface and the face of the probe. The capacitance so formed is connected to the feedback loop of a high gain amplifier hence changing its impedance and causing a voltage output to be formed which is proportional to the gap distance between the probe and the surface.

The type 'E' probe is most suitable for the purposes of this investigation, measuring amplitudes of up to 2.5 mm with a frequency response flat up to 1000 Hz. This is calibrated together with the associated distance meter, the 2 channel Wayne Kerr TE 2000 (plate 7 & 8). A full description of the calibration procedure is given in Appendix 6.

4.4 The non-contacting exciter

A non-contacting exciter was chosen as being necessary since the response to excitation at various points of the structure is required. Contacting exciters would have contributed additional weight and required holes to be made in the structure which would have altered the mode shapes and natural frequencies and hence the overall response of the structure. This is especially so since light folded plate structures were investigated.

At the outset of this project a literature survey of current research work revealed little information on the use of non-contacting exciters. As a result it was decided to design a suitable electromagnetic exciter, modifying it from experience gained as the project progressed. Investigations were carried out and calibrated using a simple beam experiment (Plate 9) as well as using a sensitive piezoelectric force transducer in a housing made for the purpose (plate 10). The complete calibration procedure is described in Appendix 7. The electromagnetic exciter is basically made up of enamelled copper wire wound on a central core. The number of coils used is limited by a corresponding increase in the heat generated and so this was fixed at between 200 and 300 turns for the investigation. Increasing the gauge thickness of the windings also resulted in increased heat generation with the increased current flow.

A search for an optimum exciter design was made into the effect of changing the material of which the core is made (plate 11). The first exciter tested was made with a permanent magnet core. Tests revealed that hysteresis losses were present in the core and as a result of the considerable heat generated, further investigation of this particular exciter configuration was abandoned. In an attempt to eliminate hysteresis losses and to consider the effect of omitting the permanent magnet core, a perspex former was used as the exciter core. The result was a much lower force output than obtained using the permanent magnet core and moreover was found to be at a frequency of 60 Hz,

twice that of the 30 Hz input signal. This was attributed to the absence of the permanent magnet core which provided a net positive or negative field onto which the exciter output would be superimposed. Thus in the absence of the polarising field, a sinusoidal signal produces an attraction when the signal is positive and yet another attraction even though the signal goes negative the next time.

To create a substitute for the effect of the permanent magnet a second layer of coils was wound on top of the existing and a d.c. voltage applied to it. This produced a considerable increase in force output and also eliminated the frequency doubling effect. However a marked temperature rise for the higher d.c. voltage ranges in the inner coil caused over-heating and melting of the enamel coating insulating the copper coils.

A final investigation was made using a hollow iron bobbin core. To prevent over-heating due to eddy currents in the circuit formed by the ferrous bobbin, a slot was machined completely through it and filled with araldite. This greatly reduced the heat produced and whatever was produced was quickly dissipated through the bobbin. Hysteresis losses were much less than that of the permanent magnet exciter and force output much improved over the perspex core exciter. This split core design is incorporated into the combined exciter/pickup (plate 12) described in the next section.

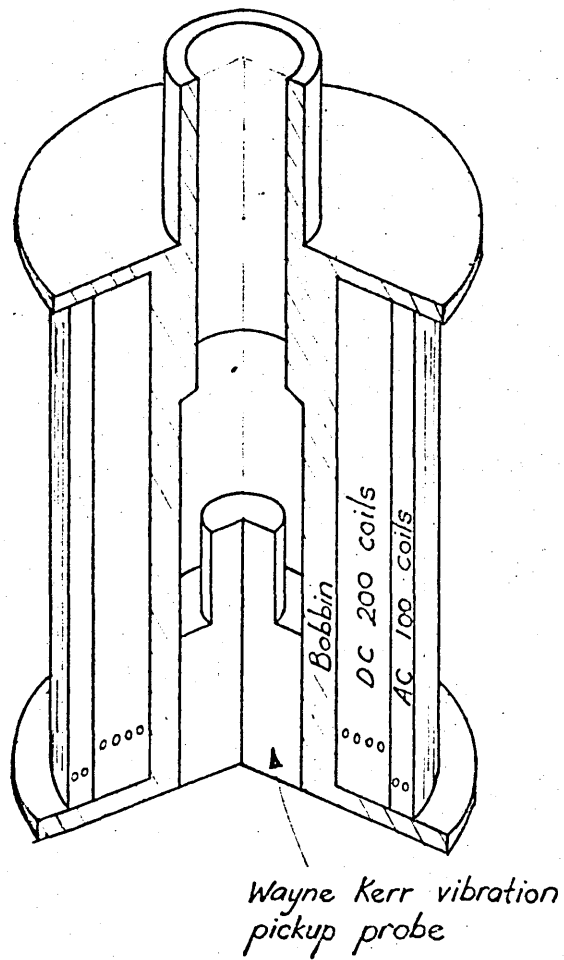
4.5 The combined exciter/pickup probe

In order to obtain a compact transducer as well as to alleviate the necessity of having separate traverse mechanisms for both the exciter as well as the vibration pickup transducer, it was decided to combine the two into a single exciter/pickup probe. Excitation and response are thus measured at the same point on the structure. This has the added advantage of effectively reducing the impedance to vibration hence increasing the measurement accuracy. Furthermore, for excitation at the antinodes there is less tendency to rigid body motion and minimal excitation of adjacent nodes (section 4.1).

The pickup transducer was easily incorporated into the final exciter design in the hollow core of the former on which the exciter windings were wound. This was made a good fit and held in place with a grub screw. A cut away view of the combined probe is shown in fig 4.1. The calibration procedure followed is as carried out previously for the separate exciter and pickup components and described in Appendices 6 & 7.

From tests made of the separate as well as the combined transducers it was found that no interaction occurred between the capacitance type vibration pickup probe and the inductance type electro-magnetic exciter in the combined probe. The result of the calibration of the combined probe in its vibration measurement capacity is as follows:

1. The output of the probe in distance measurement is 1.85 mm per volt displayed on the distance meter.
2. The output of the probe measuring amplitude of vibration is 2.25 mm/volt output (fig 4.2).
3. The effect of the gap distance between the probe and the vibrating surface measured is negligible. This is true provided the total distance (i.e. the amplitude of vibration + the mean distance between the probe and the measured surface) is less than 2.72 mm.
4. The frequency response of the probe (fig 4.3) is flat and independent of frequency in the range tested from 30 Hz to 300 Hz.



Wayne Kerr vibration
pickup probe

Fig. 4.1 A cut away view of the combined probe.

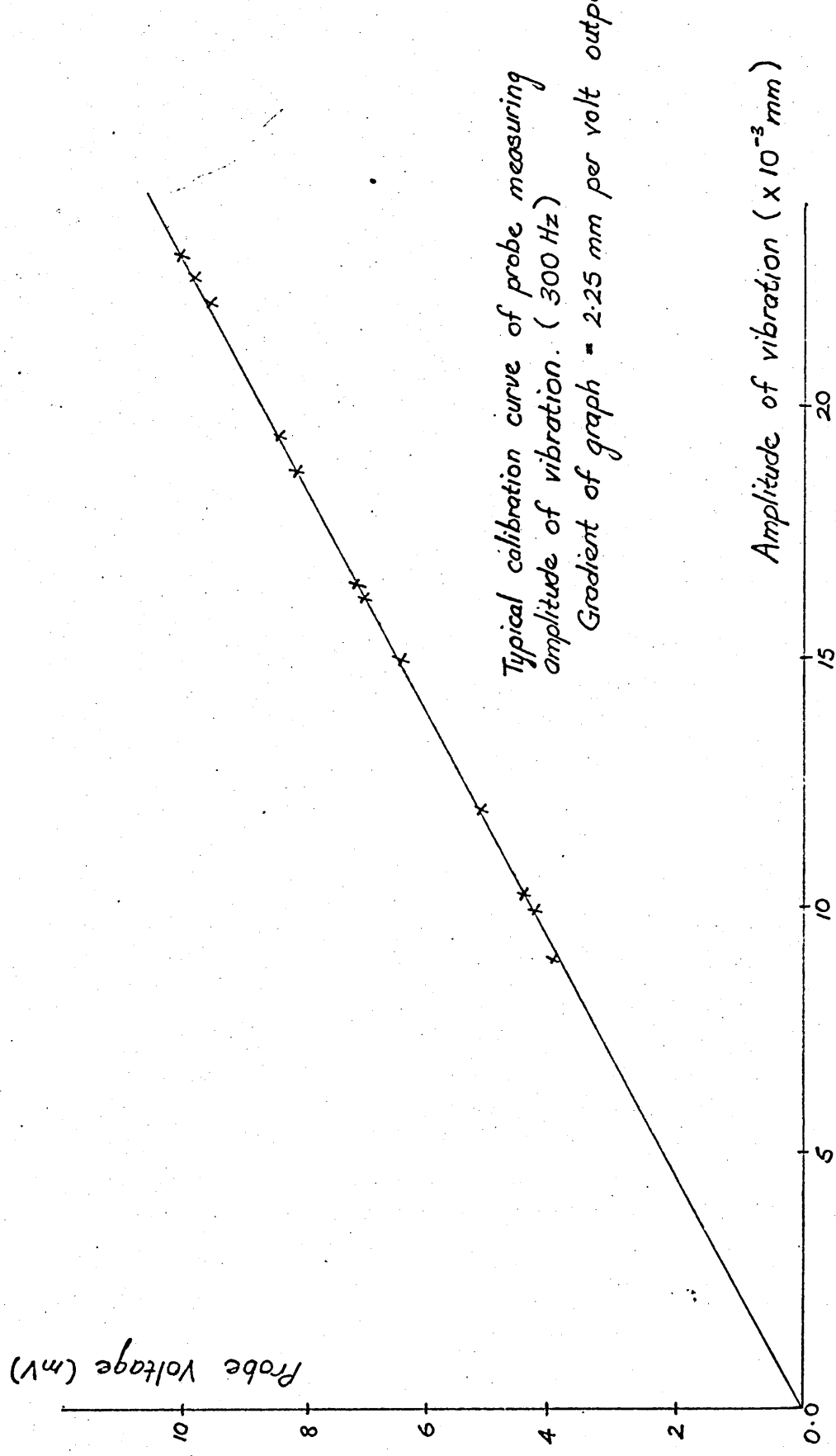


Fig 4.2 Calibration of vibration pickup transducer.

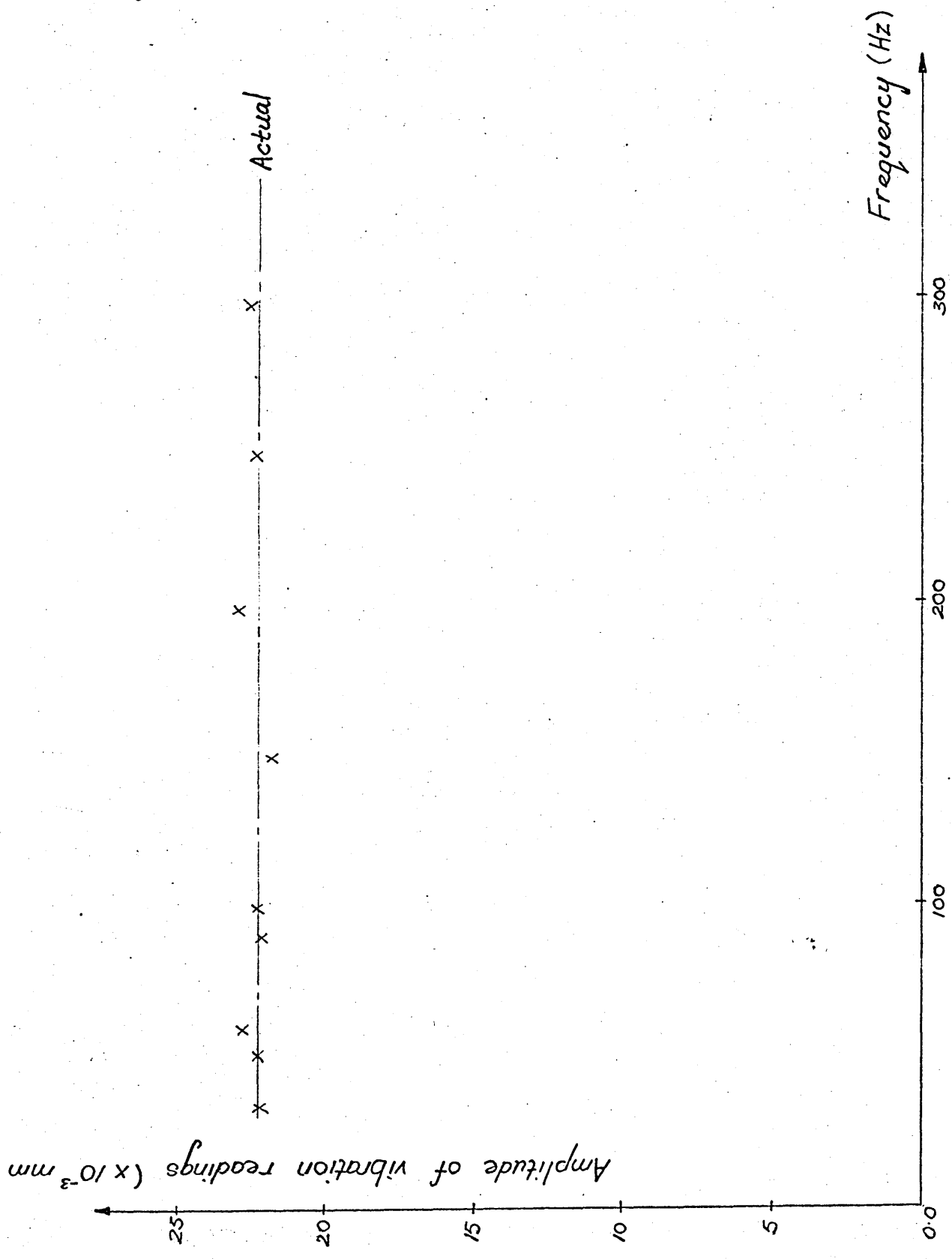


Fig 4.3 Frequency response of vibration measurement transducer.

The calibration of the combined probe in its excitation capacity is as follows:

1. The force output per input volt at a frequency of 100 Hz and probe-to-structure gap of 1 mm is shown in fig 4.4.
2. The change in force output with probe-to-structure gap at a frequency of 100 Hz and excitation voltage of $3 V_{\text{rms}}$ is shown in fig 4.5.
3. The frequency response at a constant excitation voltage and gap size is shown in fig 4.6.

In all these curves the d.c. polarisation voltage/excitation voltage is taken as unity. The effects of variation of this factor is given in McNulty [45]. The output excitation power spectral density to a PRBS signal input was also checked using the correlation method previously described in chapter 3.

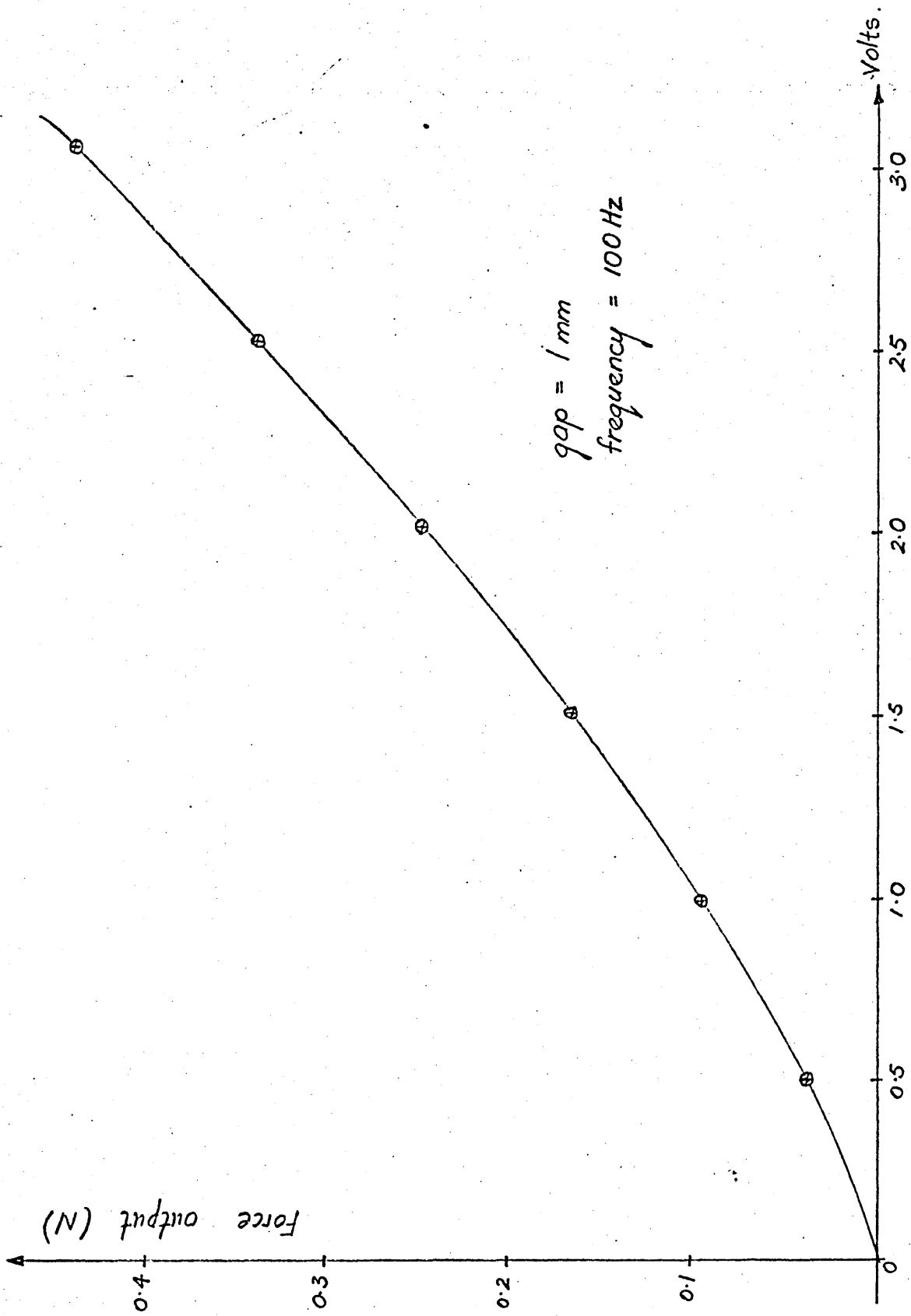


Fig 4.4 Force output of non-contacting exciter

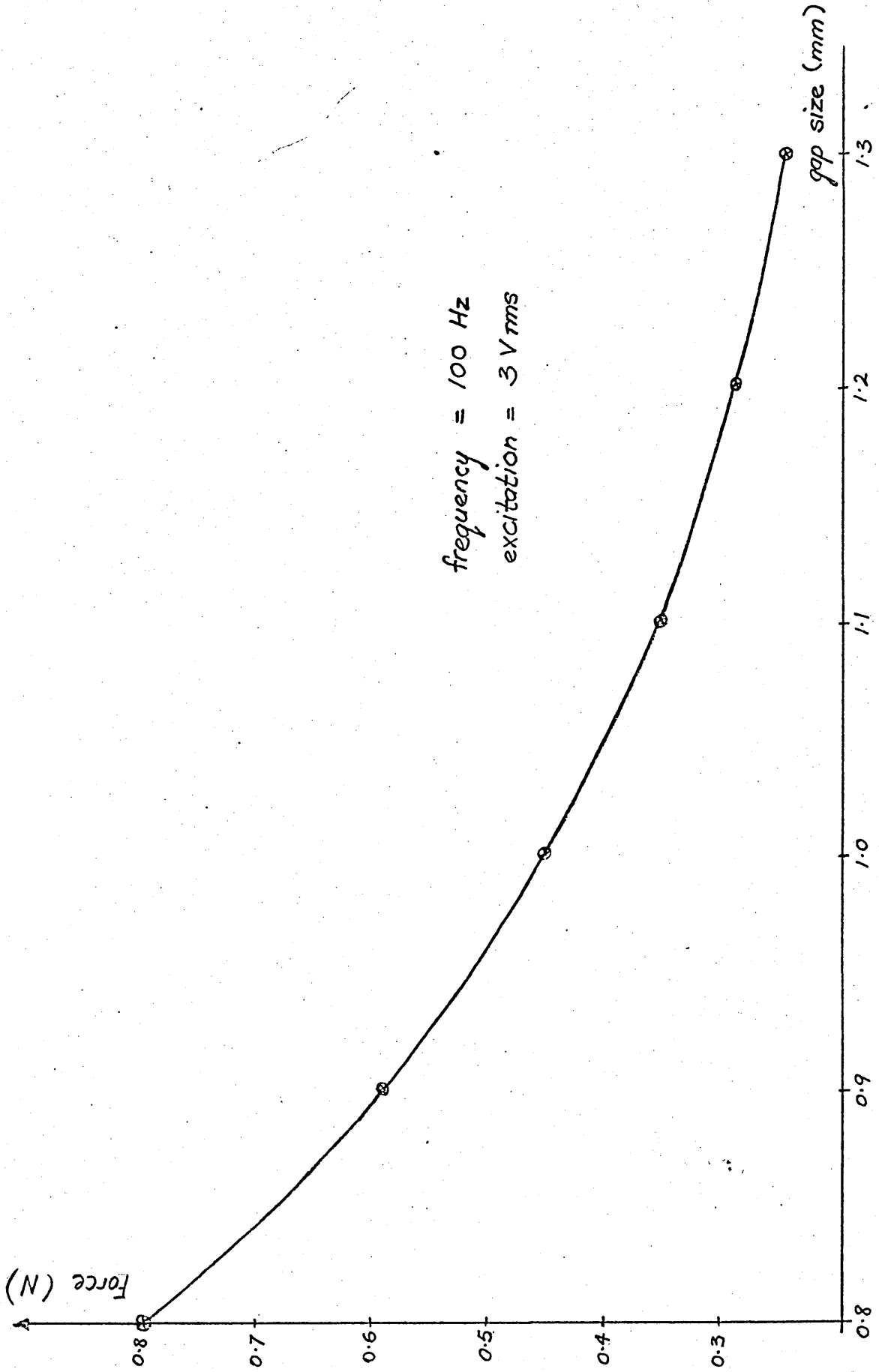


Fig 4.5 Effect of air-gap on excitation output.

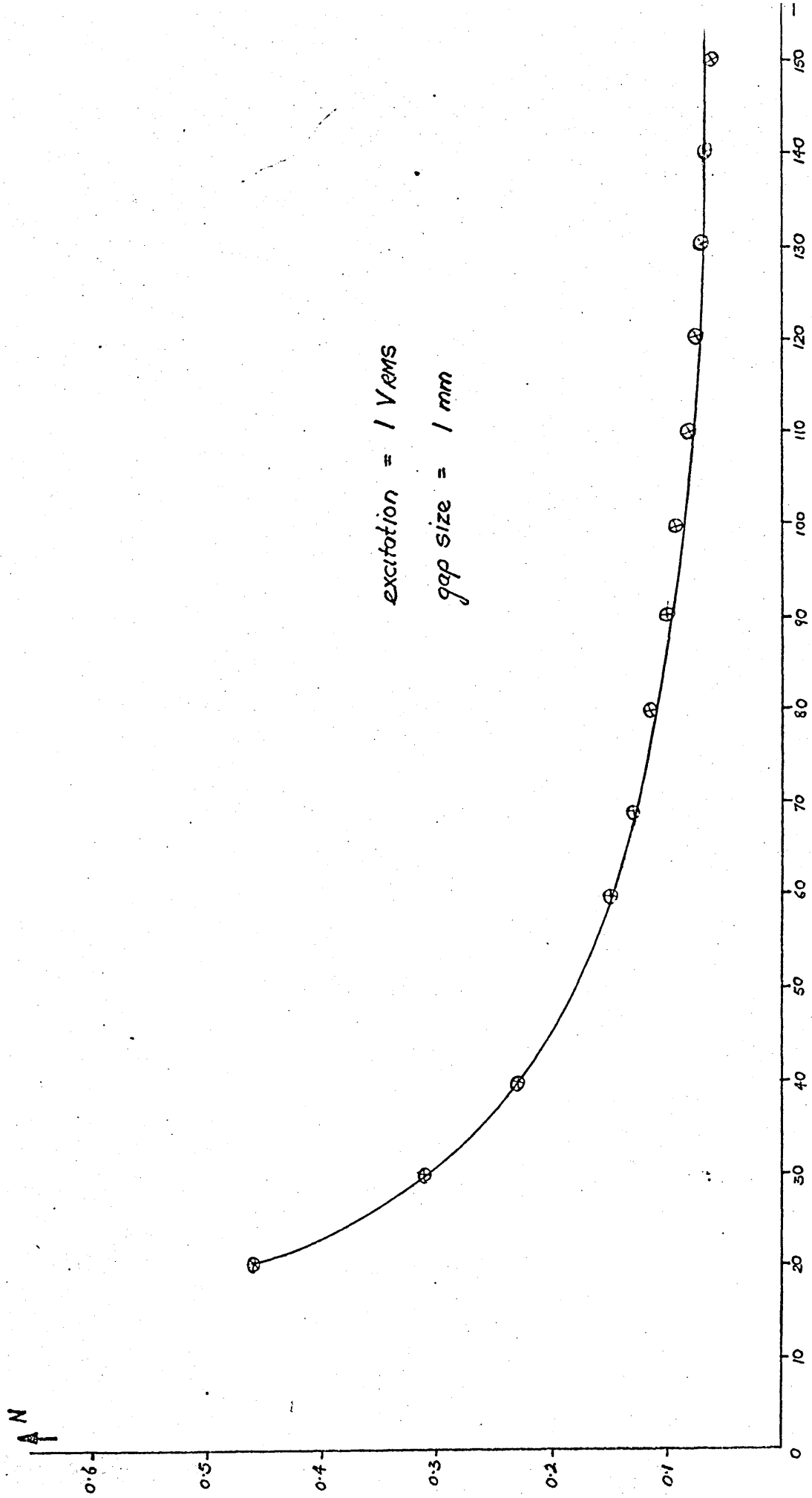


Fig. 4.6 Frequency response of non-contacting exciter.

Summary

This chapter describes how the correlation technique (section 3.5) was applied to obtain the receptance of the box structure despite the excitation being non-white noise. It shows how the natural frequencies and mode shapes of beams, plates and boxes were obtained experimentally using the apparatus developed and discusses the choice of the various parameters governing the pseudo random binary sequence signal used for response measurements of the box structure. It also describes how natural frequencies and mode shapes obtained for a finite element analysis of the box structure were used to predict the response power spectral density using an excitation power spectral density and damping factors obtained experimentally. The Fourier transform computer program developed is presented with flowcharts and descriptions and the advantages using an optional faster algorithm is illustrated.

5.1 Introduction to the problem

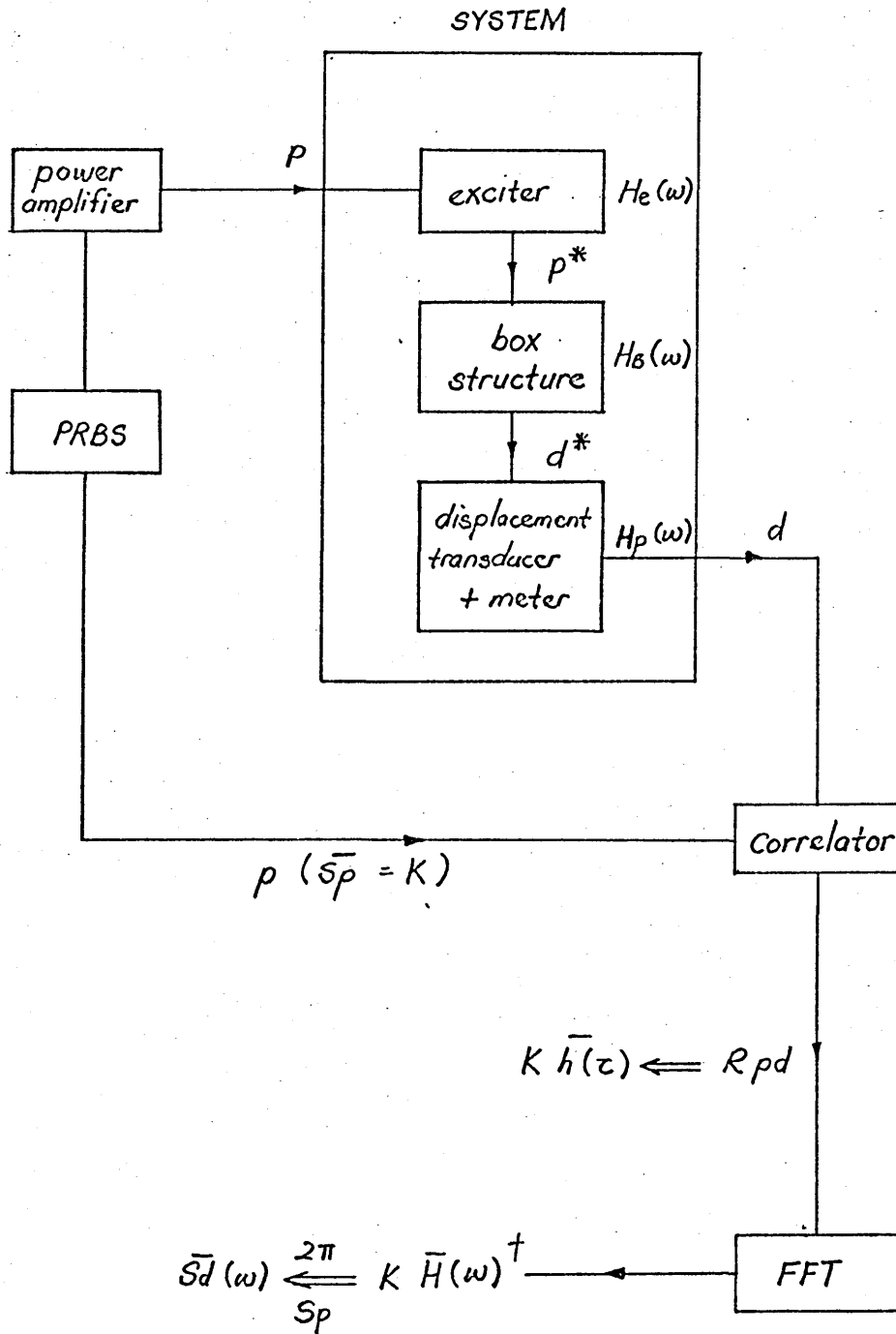
Chapter 3 describes the general theory applicable to random excitations and how the theory is applied to the special case when the excitation has a flat spectrum. It is shown that in this case the impulse response function of the structure can be easily obtained directly from the cross correlation between the input and response. (eqn 3.18 & 3.19)

This impulse response function can then be Fourier transformed to give the receptance of the structure at the point of excitation (eqn 3.20). Having used this technique to determine the receptance, the response power spectral density of the structure at the point of interest can be determined from eqn (1.1) when the input power spectral density is known.

In general engineering environments the excitation experienced rarely has a completely uniform force spectrum and often has one which tapers off at higher frequencies. Also the advantages of a non-contacting exciter pickup entailed the development of an electromagnetic exciter which, unless sophisticated circuitry was provided, has this same tapering force spectrum. Although an excitation signal having a white power spectral density (the PRBS signal) is applied to the system shown in fig 5.1 the actual excitation of the structure is no longer white due to the characteristics of the associated exciter pickup equipment and the response spectral density at the point of interest is difficult to obtain.

In this chapter therefore some approximations are made to take such experimental factors into account by introducing intermediate stages of analysis which basically depend on the assumption of linearity in each stage. This is considered to be valid because of the generally low signal levels used in all the tests.

Referring to fig 5.1 let $p(t)$ and $d(t)$ be the input and the response of the system respectively. Within the system itself let $p^*(t)$ and $d^*(t)$ be the actual input and



† where $\bar{H}(\omega)$ is the impulse response function of the system shown above.

Fig 5.1 Schematic plan of the method.

response of the box itself. Application of the correlation method using the correlation of $p^*(t)$ and $d^*(t)$ would not give the required impulse response function of the box since p^* is not white noise. However by considering the system as a whole it will be seen that as far as the system is concerned, a white PRBS spectrum is being applied to it so that the necessary requirement for the correlation technique to be applied to the system is satisfied. Therefore, using a PRBS signal $p(t)$ with a flat frequency spectrum of mean square value K , the cross correlation function of the input and output to the system, R_{pd} , gives the impulse response of the system $h(\tau)$ multiplied by the factor K . The Fourier transform of $h(\tau)K$ gives $H(\omega)K$ the frequency response function of the system multiplied by K which from above is the mean square value of the PRBS input. From $H(\omega)$ the system response power spectral density can be obtained according to

$$S_d(\omega) = |H(\omega)|^2 S_p \quad (5.1)$$

where S_p is a constant for the PRBS signal and given by

$$\int S_p(\omega) d\omega = K \quad (5.2)$$

We have therefore obtained experimentally the power spectral density of system response d . Now in order to obtain the power spectral density of the response d^* of the box itself we have to go back a stage and consider the characteristics of the displacement transducer which produces d from d^* (see fig 5.2) The displacement transducer converts displacement d^* into voltage d and with its associated equipment provides the relationship

$$S_d(\omega) = |H_p(\omega)|^2 S_{d^*}(\omega) \quad (5.3)$$

where $H_p(\omega)$ is obtained from calibration of the displacement transducer described in the previous chapter (fig 4.2 & 4.3). This as we have seen is independent of frequency and therefore a constant, H_p , which is given in units of volts/mm so that

$$S_{d^*}(\omega) = \frac{1}{H_p^2} S_d(\omega) \quad (5.4)$$

The response power spectral density of the box itself is therefore obtained.

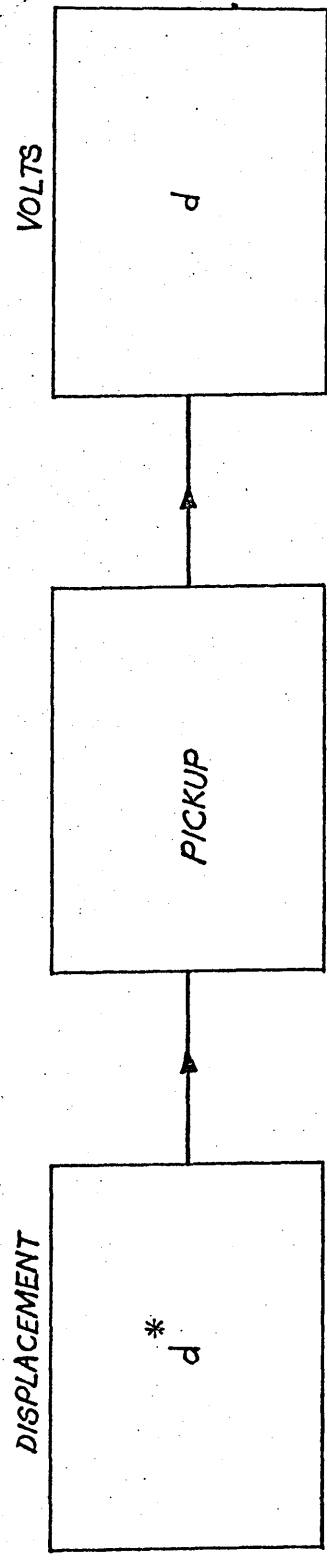


Fig. 5.2 The vibration pickup displacement-volts factor.

The aim of this work is to predict this response from knowledge of the characteristics of the box from its receptance $\alpha(i\omega)$ (see chapter 3). In order to do this the excitation power spectral density to the box must be known. From fig 5.1 we see that although p has a white spectrum p^* the actual box excitation does not have the same type of spectrum. In fact $S_p(\omega)$ to the system is modified on passing through the force transducer to become $S_p^*(\omega)$ to the box (fig 5.3). Looking therefore at the stage where the signal is converted into force we see that

$$S_p^*(\omega) = |H_e(\omega)|^2 S_p \quad (5.5)$$

where S_p is again a constant given by eqn (5.2) and $H_e(\omega)$ represents the output characteristics of the non-contacting exciter at a particular amplifier setting. This is again obtained from the calibration curves given in the previous chapter (fig 4.6) but unlike the displacement transducer is frequency dependant to a considerable extent. Since we now know the power spectral density of the actual excitation to the box we can now attempt to predict the box response using the equation

$$S_d^*(\omega) = |H_B(\omega)|^2 S_p^*(\omega) \quad (5.6)$$

where

$$|H_B(\omega)|^2 = |\alpha(i\omega)|^2$$

To summarise therefore we have (a) a method using the correlation technique of obtaining the response power spectral density of the ^{structure} experimentally and (b) an analytical method of predicting this using the natural frequencies and mode shapes of the box obtained using the finite element program developed. The next sections will discuss the experimental details which arose as work proceeded to determine an experimental response power density as well as a predicted one for comparison.

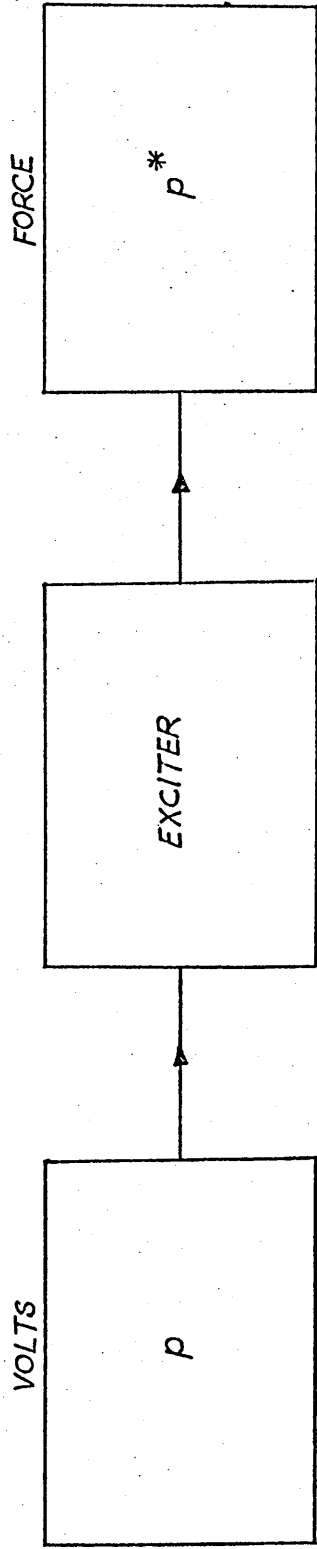


Fig. 5.3 The non-contacting exciter force-volts factor.

5.2 The excitation signal

For the random excitation of the box structure considered in this work, the PRBS signal discussed in section 3.6 is used. The range of frequencies of interest of the box chosen is from 20 Hz to 100 Hz which contained over 20 natural frequencies. Also it was found that at higher frequencies the response becomes attenuated and natural frequencies bunched together, making discrimination between individual peaks difficult.

The PRBS excitation signal is controlled by several parameters. The most important being the clock frequency, the sequence length and the filter cut off frequency. The choice of these depend on the following considerations. The clock frequency chosen is not simply that of the highest of the range of response frequencies required even though from section 3.6 it could give the highest frequency in the excitation signal. This is because in the equipment used, the clock frequency is also the sampling frequency. The sampling frequency is determined by considering the spectrum using the Fourier transformation

$$X_k = \frac{1}{N} \sum_{r=0}^{N-1} x_r e^{-i2\pi kr\Delta} \quad (5.7)$$

The properties of the transformation are briefly summed up as follows. X_n is limited to the range $n = 0$ to $n = N - 1$ and repeats itself thereafter. This corresponds to the frequency range 0 to $\frac{N-1}{N} f_c$. Moreover of this the unique part of the series lies in the range 0 to $\frac{N-1}{2N} f_c$ only, and higher terms are mirror images of these. This can be expected since the N bits of information can only give the $N/2$ real and $N/2$ imaginary A and B components of the first $N/2$ complete Fourier Transform terms. The frequency $\frac{N-1}{2N} f_c$ is known as the Nyquist frequency or the 'folding' frequency.

The result of the Nyquist frequency is that for a maximum

frequency of say 150 Hz to be realised in a signal, a sampling frequency of at least 300 Hz is necessary. Since the sampling frequency on the PRBS signal generator used is also the clock frequency, f_c is therefore set at 300 Hz. Now if frequencies above the Nyquist frequency of 150 Hz are present in the signal a distortion of the Fourier transform graph called aliasing is introduced. Setting the clock frequency at 300 Hz however means that frequencies up to 300 Hz will be present in the excitation signal which will inevitably distort the results. Consequently, to enable the use of a high clock frequency for accurate sampling purposes and yet retain only those frequencies in the range of interest, a low pass filter (fig 5.4) is included. Known as a third order Butterworth filter, it is flat to -3dB at f_b the upper bound frequency chosen, then falling off at 18dB/octave , whereas the normal PRBS spectrum has an envelope given by $(\frac{\sin x}{x})^2$ where $x = \frac{\pi f}{f_c}$ with -3dB at $0.45 f_c$ (section 3.6). Using this filter, clock frequencies of 300 and 1000 Hz were used. The bulk of the results were however taken from the former as they contain the main response frequencies and also the latter gave an inaccurate disperse spectrum.

The accuracy of a spectral measurement depends on the effective bandwidth B_e Hz of the measurement and the record length T sec. If σ is the standard deviation of a measurement of spectral density of mean value m , then Blackman and Tukey [46] shows that

$$\frac{\sigma}{m} \approx \frac{1}{B_e T} \quad (5.8)$$

Thus for a required accuracy of $\frac{\sigma}{m} = 1$ with a frequency resolution of 1 Hz using a clock frequency of 300 Hz, a record of 1 second in length is required. i.e. N the number of samples must be at least 300. For a required accuracy of $\frac{\sigma}{m} = \frac{1}{2}$ with a resolution of 2 Hz requires a 2 second sample i.e. 600 samples using the same clock frequency as before. Thus N is chosen to be at least $2^9 = 512$ in the tests.

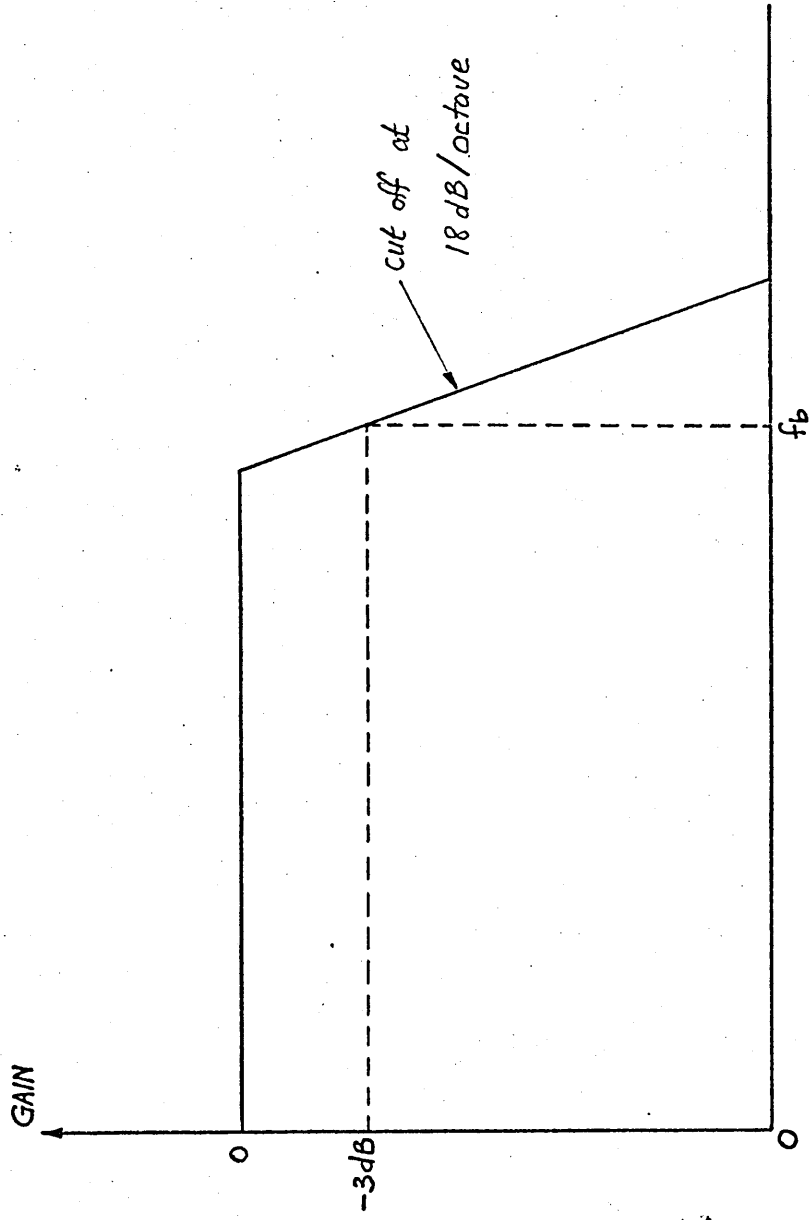


Fig. 5.4 Filter characteristics.

In practice, in order to ensure adequate stimulation at the resonances, the spectral line interval must be such that two spectral lines occur within the half power bandwidth of the resonance

$$\text{i.e. } \frac{f_c}{N} \leq f_h \quad \text{where } (f_h) = \text{half power bandwidth} = (\eta f_n)$$

$$\text{so that } N \geq \frac{f_c}{\eta f_n} \quad (5.9)$$

Taking typical values used for the structure

$$f_c = 300 \text{ Hz}, \quad \eta = 0.018, \quad f_1 = 24.6 \text{ Hz}$$

$$N \geq \frac{300}{0.45} = 666$$

It is evident from (5.9) that only the first natural frequency is critical in determining the minimum number of data N required in the sequence. N is limited physically by the equipment available and on the Solartron equipment used the largest number available with correlation in one sequence is 1023. However, run times increase rapidly as N is increased and a typical time required for a test was approximately $3\frac{1}{2}$ hours using $N = 511$ and 11 hours using $N = 1023$ in correlation $\times 10$ mode using fifteen sequences per trigger.

Using the apparatus which was described in the previous sections, the experimental investigation was carried out to determine the response of folded plate structures to random excitation.

An open ended box structure as shown in fig 5.5 was tested. This was made from four thin plates each of thickness twenty thousandths of an inch and soldered together along their edges at right angles. This formed a simple structure which had a low fundamental frequency and was easy to vibrate. The box was fastened to supports at the corners of its lower surface (Plate 6) to approximate simply supported boundary conditions at the corners. These supports were themselves attached to the vibration table with large G clamps. In the preliminary stages of the investigation, work was also done to determine the natural frequencies, mode shapes and damping factors of a fully fixed beam, a beam simply supported at both ends and a flat plate with fully fixed edges all round (Plate 5). Results for these are included in chapter 7.

In the course of the experimental investigation the natural frequencies and mode shapes of the box were obtained. Difficulty in obtaining the damping factors from the response curves was experienced (see section 5.3.3). The cross correlation function of the input and response signals were also obtained experimentally for the box structure when excited by white noise generated using a P.R.B.S. signal generator. This gave the impulse response function of the box system which, when Fourier transformed, gave the receptance of the box at the point under consideration. The experimental procedure is discussed in detail in the following sections.

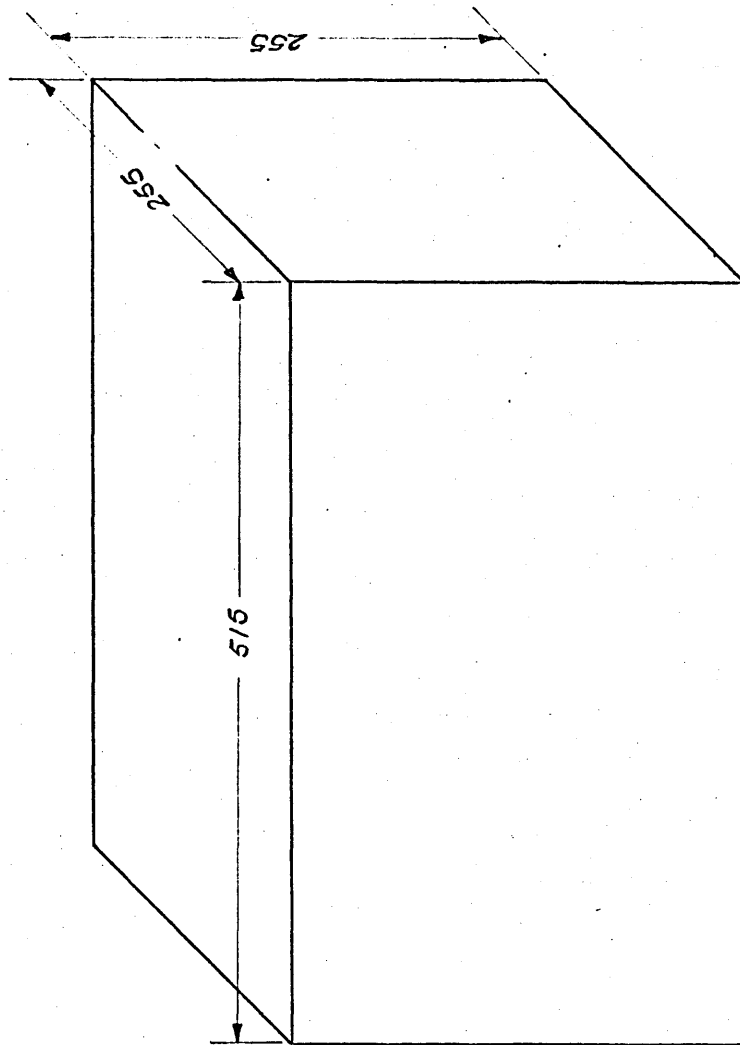


Fig. 5.5 The open-ended box structure used.

5.3.1 Determination of natural frequencies and mode shapes

The natural frequencies and mode shapes were determined using sine wave excitation. The sine wave was generated by a Muirhead decade oscillator which was connected through a power amplifier as shown in figure 5.6 to the combined exciter pickup and a d.c. bias applied as described in section 4.5.

To obtain the natural frequencies, the pickup is positioned at a suitable point (antinode) on the structure and resonant frequencies located by adjusting the excitation frequency from the decade oscillator until the amplitude of vibration is at a maximum (resonance). The excitation frequencies when the vibration amplitudes are greatest are measured using the narrow band frequency analyser and correspond to the natural frequencies of the structure under consideration. Natural frequencies in the range 20 to 100 Hz were obtained for the box structure. The natural frequencies of the beam, plate and box structure analysed are given in tables 7.1, 7.2 and 7.3 in section 7.1.

The mode shape corresponding to each natural frequency was obtained by measuring the amplitude of vibration at a sufficiently large number of points on the structure to define it, keeping the excitation force and frequency fixed. An approximate idea of the mode shape is first obtained using an acoustical method by traversing a hand held microphone across the surface. This was then followed-up using the probe and traverse mechanism using the following technique to give the accurate mode shape.

The combined exciter probe is positioned at the required point using the traverse mechanism and the probe-to-structure airgap checked using the displacement calibration curves for the probe (section 4.5). This is necessary as the force output by the probe is affected by the size of this gap (figure 4.5). The air gap between the probe and

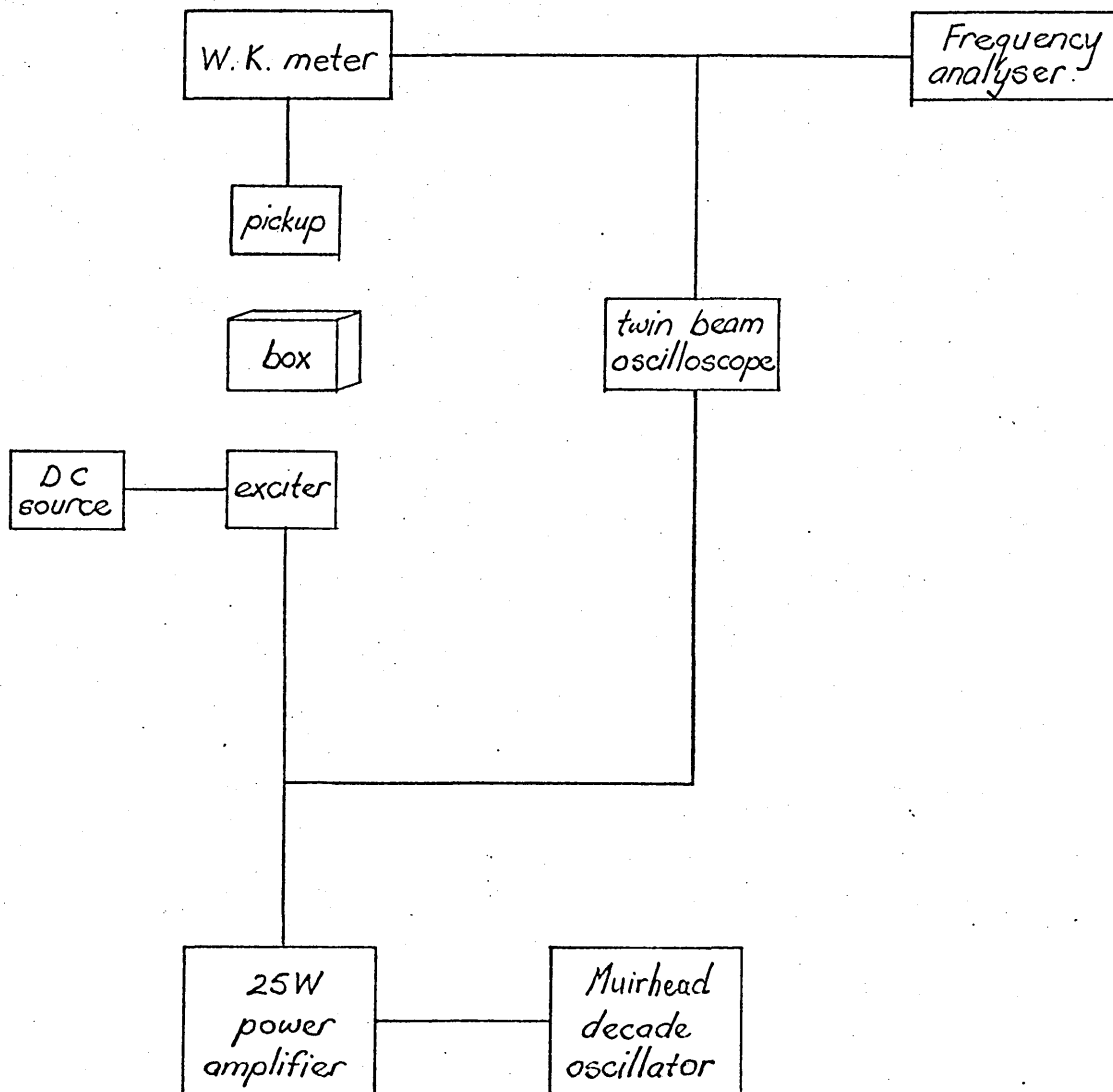


Fig.5.6 Block diagram of instrumentation for discrete excitation of box structure.

the structure is adjusted to an approximately parallel position with the fine adjustment mechanism. A block diagram of the necessary instrumentation used is shown in figure 5.6. The actual force input to the box is given by the current into the probe and is read off the appropriate calibration curves corresponding to that frequency and probe-to-structure air gap. In determining the mode shape at each natural frequency the amplitude of the response signal is measured using a constant percentage frequency analyser at the low frequency ranges, shown in Plate 13, and a constant bandwidth frequency analyser (Plate 14) at the higher frequencies. The actual response amplitude is then given off the probe vibration measurement calibration curves. The response at each of the points chosen were then obtained by traversing the probe to each of the points in turn keeping the excitation force and frequency constant, giving the required mode shape. To plot any particular mode shape the knowledge of the relative values of the various amplitudes is sufficient although the receptance described in the next section requires the absolute amplitudes to be ascertained.

For the beam structure the exciter probe is simply traversed along its length and keeping the excitation force constant, measuring its response at a number of points sufficient to describe the particular mode shape. Again for the mode shape only relative values of response are required. These are illustrated in Table 7.1. The mode shape of the plate is obtained by dividing the plate into a grid (figure 5.7) and determining the response at each of the grid points. The fineness of the grid required depends on the mode shape to be measured. Some of the lower natural frequencies and mode shapes of the plate analysed are also indicated in Table 7.2, described in terms of the number of half wavelengths along and across the plate. The same procedure is followed for the determination of the mode shapes of the box structure since only the top plate of the box structure was measured using the traverse mechanism. Figures 7.1 to 7.11 show the vibration modes of the box existing between 20 Hz and 100 Hz.

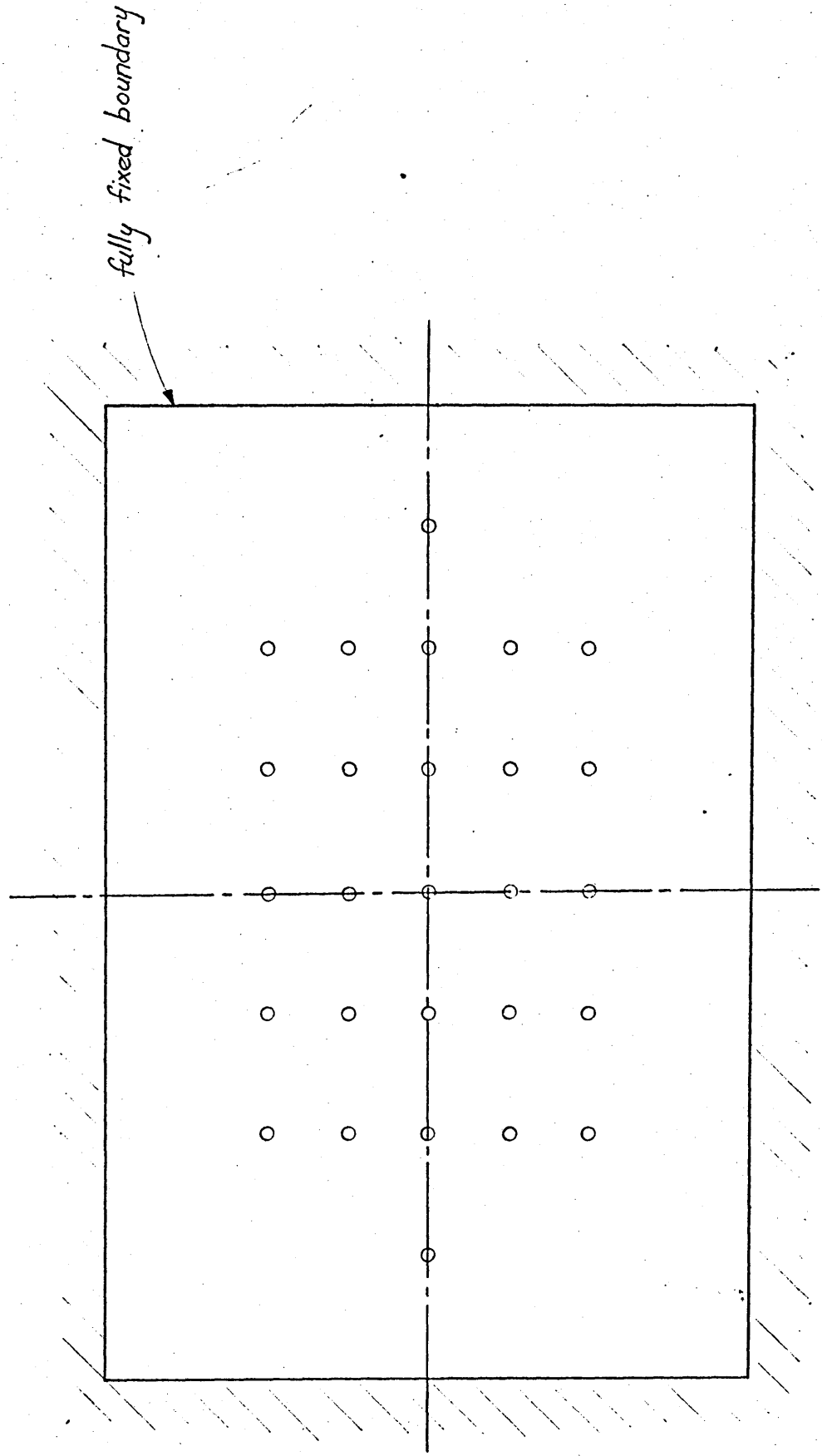


Fig. 5.7 A typical grid for determining mode shape of a fully fixed plate.

Because of the tapering shape of the force spectrum created by the exciter probe the response to a sweep test and hence the 'receptance' obtained of the box tested was not that of the generally accepted response to a unit force spectrum. A correction to the results obtained by the sweep test was therefore necessary. This factor was given by the conversion of the tapering force spectrum to that of a constant force spectrum of unit magnitude.

The receptances of the box were determined experimentally at various points using sine wave excitation from the Muirhead decade oscillator which was connected as before through the power amplifier to the combined exciter-pick-up. The probe was positioned in turn at each point of interest and the gap between probe and structure was measured and adjusted to give a suitable force output, the magnitude of which is obtained from the probe calibration curves (figure 4.4). Having adjusted the probe-structure gap, the structure was excited at discrete frequency intervals of 1 Hz in the range 20 Hz to 100 Hz. In the region of a resonant, the frequency interval was reduced to 0.5 Hz. At each of these frequencies the magnitude of the displacement of the structure was measured using a frequency analyser as described previously. From the probe calibration curves the force corresponding to that excitation signal amplitude, frequency and gap size was determined. The response amplitude corresponding to a unit force can then be obtained. This procedure is repeated over the range of frequencies selected and the receptance of the box at the chosen points obtained. The receptance of the box using this technique was obtained at the points which are indicated in figure 5.8 and from it the response power spectral density was obtained.

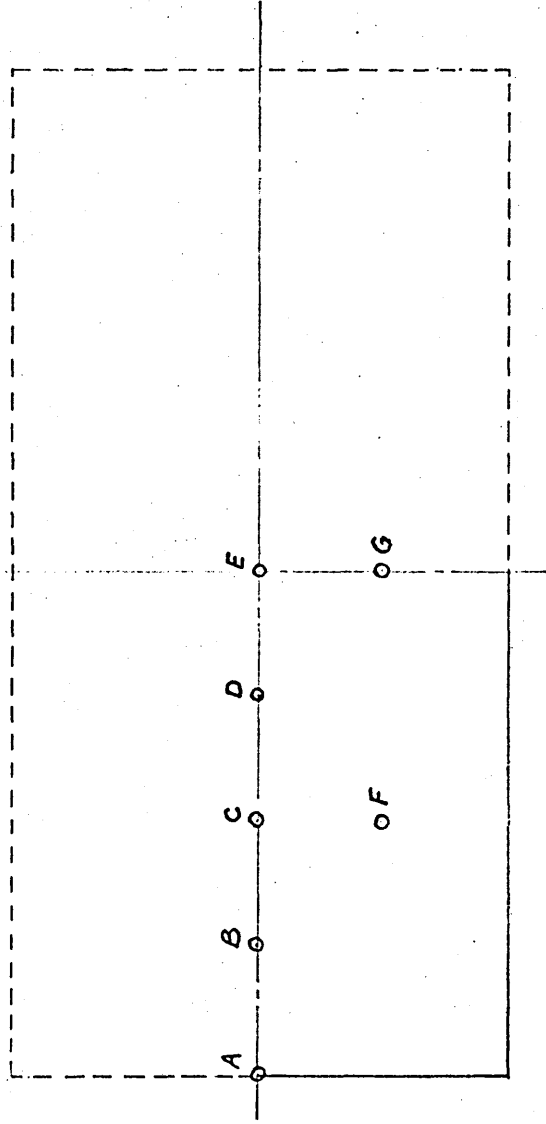


Fig. 5.8 The grid used for determining receptance and response spectral density of the box.

5.3.3 Determination of damping factors.

In this investigation the response of the box structures to vibration stimuli is required. In the ideal case all the excitation energy put into the system is converted into response motion. In practice this is not so.

When the structural material is cyclically stressed, energy is lost either through radiation to the surrounding medium or is dissipated in the material. There are various commonly accepted theories [5] & [47]. In structural damping the assumption of hysteretic damping has been found to be a realistic concept where damping is proportional to displacement rather than velocity as in viscous damping. The equation of motion

$$m\ddot{x} + c\dot{x} + kx = F_0 \sin \omega t$$

then becomes

$$m\ddot{x} + (1 + i\eta)kx = F_0 \sin \omega t \quad (5.10)$$

where η the non dimensional damping loss factor is defined as the ratio of the energy loss per cycle to 2π times the energy stored during that cycle. For linear systems for small amplitudes, η is usually taken as a constant, η_r , at the natural frequency ω_r . Although this is not strictly correct at other frequencies it is acceptable because the response in a lightly damped structure is dependant on η_r only at its natural frequency ω_r and would be virtually insignificant elsewhere. This holds for multi-degrees of freedom systems if any possible coupling of modes due to damping is neglected.

From chapter one eqn 1.2 the calculation of the receptance of the box structure requires the knowledge of this damping loss factor. This is calculated experimentally using its frequency response curve (fig. 5.9)

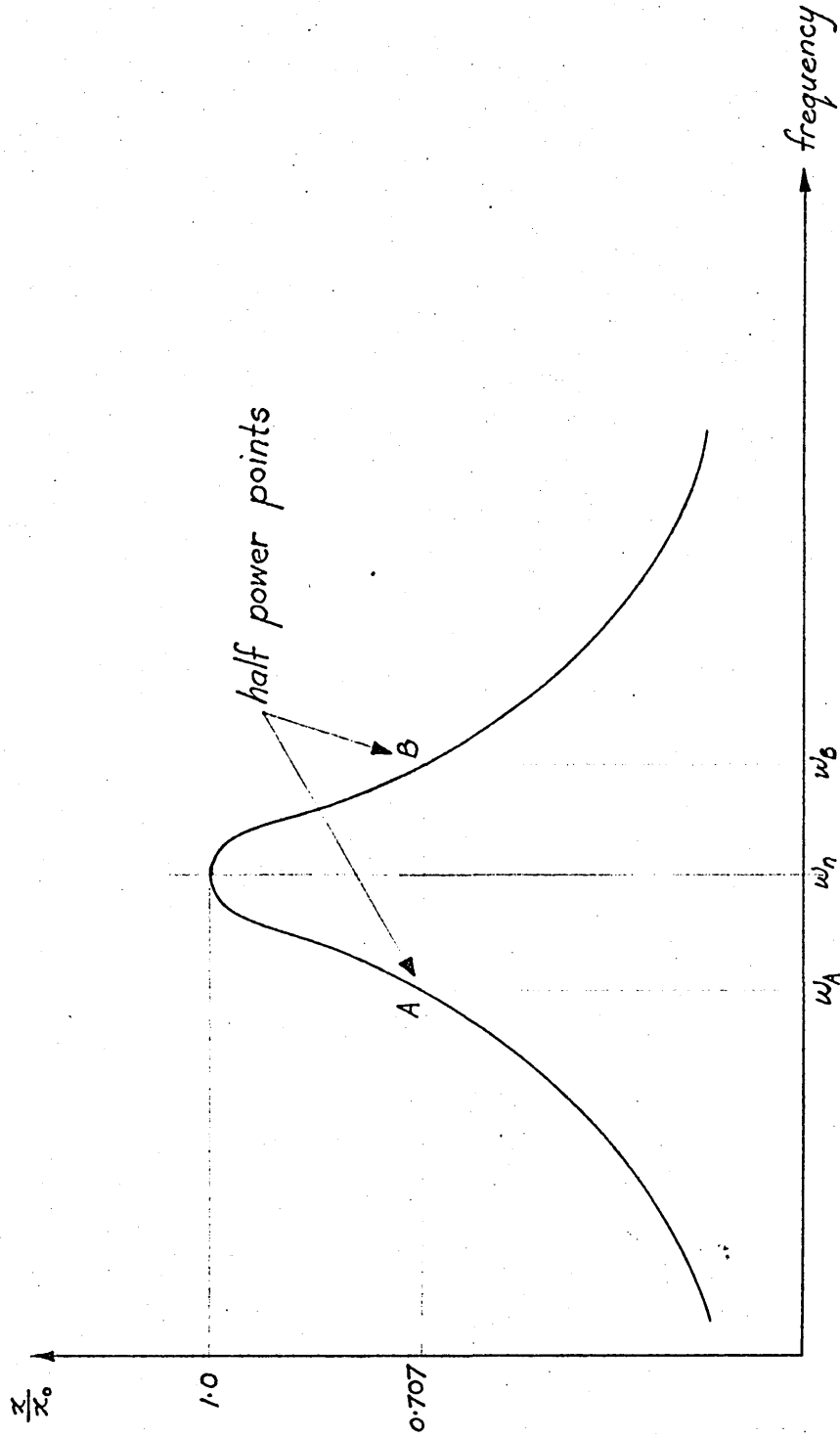


Fig. 5.9 Determination of damping factors using half power points on the response curve.

The separation ($\omega_B - \omega_A$) between the frequencies associated with the points A and B, where $x/x_0 = 1/\sqrt{2}$, increases with damping. The non-dimensional ratio ($\frac{\omega_B - \omega_A}{\omega_n}$) is therefore a basis for determination of the damping loss factor ζ .

The method used, of determining the damping loss factor of a structure from its resonance curve is known as the half power point method. The name originates in the relevant points A and B which are known as half power points since the power during steady state conditions in a linear system is proportional to the square of its amplitude. These points for each mode of vibration of the structure are therefore experimentally obtained and the corresponding frequencies used to calculate the damping loss factor for that particular mode.

This method worked satisfactorily for the preliminary work, where simple beams and plates were used, having their individual resonance peaks well defined and separate. However for the box structure itself, apart from the lowest natural frequencies, some overlapping and coupling of modes occur. As a result approximate values were used, based upon experience gained on the simpler structures and assumption of unimodal damping at the higher frequencies.

Unfortunately in the event it was found that the method used was not completely satisfactory and possibly an oversimplification and gave rise to inaccuracies in the calculated response values in the higher frequency regions. Other methods of experimentally measuring the damping of structures exist (Kennedy and Panu [48] , Pendered and Bishop [43] and Bert [49]) which may therefore be more profitably used.

5.3.4 Determination of response to random excitation

The PRBS signal described in section 3.6 was chosen as a suitable excitation signal to simulate random excitation of the box structure. The parameters of the particular PRBS signal chosen to excite the box was described previously in section 5.2. In order to ensure adequate stimulation of close adjacent resonance peaks, sufficient numbers of spectral lines must be chosen. Thus sequences containing 512 and 1024 samples were used.

Since response frequencies of up to 100 Hz were required the sampling rate necessary to satisfy the Nyquist criterion, as described in section 5.2, is at least twice this. On the equipment available, the sampling rate is determined by the clock frequency f_c and the nearest frequency available was 300 Hz. Two complete sets of values were obtained, using first^a clock frequency of 300 Hz and after that the next higher clock frequency of 1000 Hz. Since the clock frequency is also the highest frequency of the signal, a low pass filter was necessary to prevent aliasing (section 5.2).

The points chosen at which the cross correlation measurements were obtained are shown in fig. 5.8. The exciter probe was first positioned at one of the points required. The air gap was then checked using the appropriate calibration curves and adjusted if necessary to a predetermined value. The PRBS signal was then applied to the main coils of the exciter via a power amplifier (and a d.c. bias to the secondary coil) and displayed on the oscilloscope is shown in the block diagram (fig. 5.10). A true RMS random noise voltmeter was used to measure the excitation signal. The response signal picked up by the displacement transducer is also displayed on the oscilloscope and fed into the time domain analyser and a narrow band analyser. Care is taken to record the position at which measurements were made as well as all the amplification factors of both the excitation and response signals for converting back into the original units later.

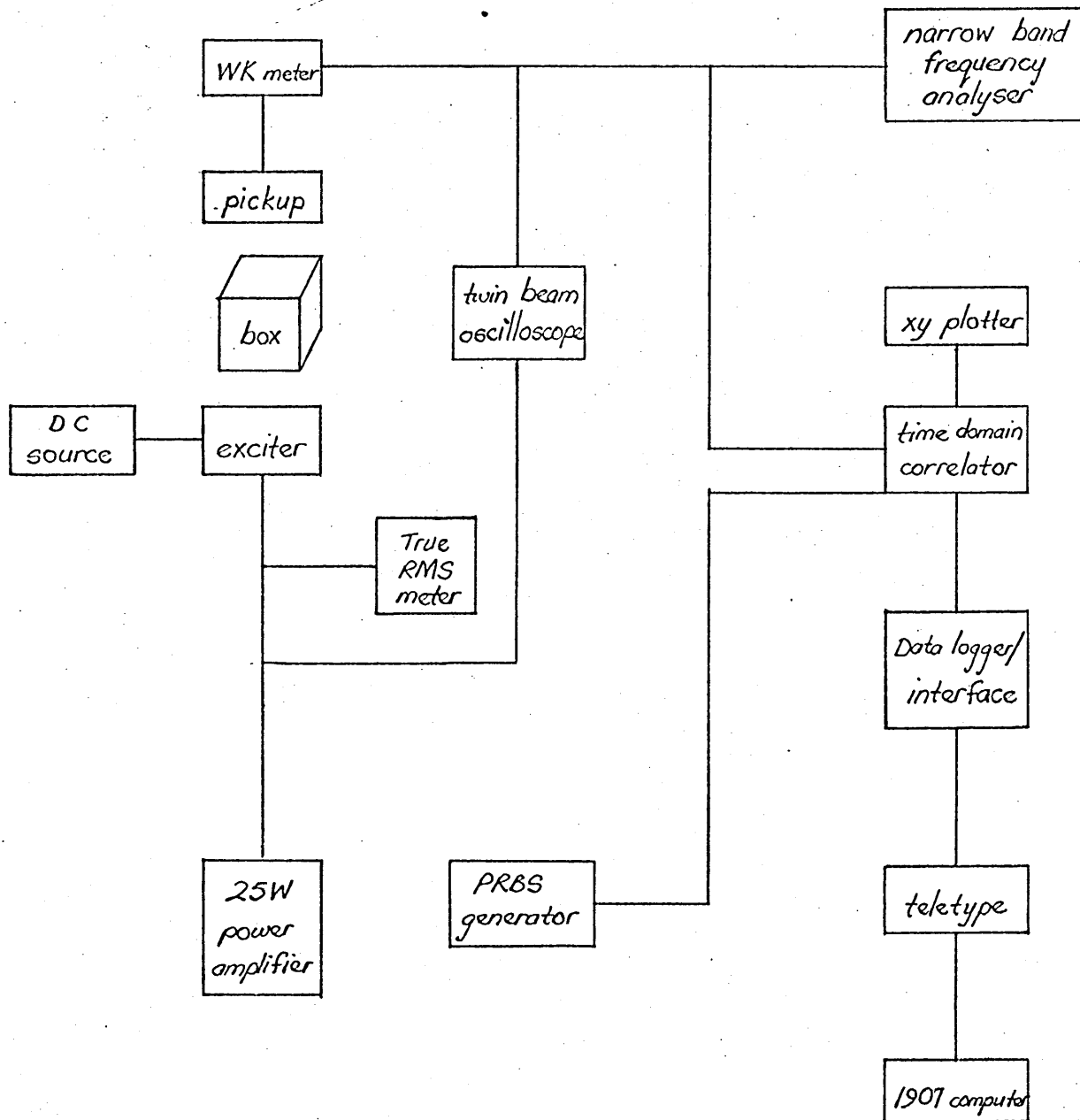


Fig. 5.10 Block diagram of instrumentation for determination of response of box structures to random excitation.

The time domain analyser calculates the cross correlation function of the excitation and the response signals and produces it on paper tape via an interface with a teletype. The paper tape produced is compatible with the paper tape reader in the ICL 1907 computer where it is to be processed using the FFT program described in the next section. The procedure is then repeated at each of the points shown in fig. 5.8, a different point receptance being obtained at each respective point as it is position dependant as discussed in section 3.3. The instrumentation used is shown in Plate 15.

In this work the response spectral density of the box structure is calculated from the receptance of the box structure system (section 5.1) as obtained experimentally by the Fourier Transformation of the cross correlation function of the PRBS excitation to the box and the resultant response of the box.

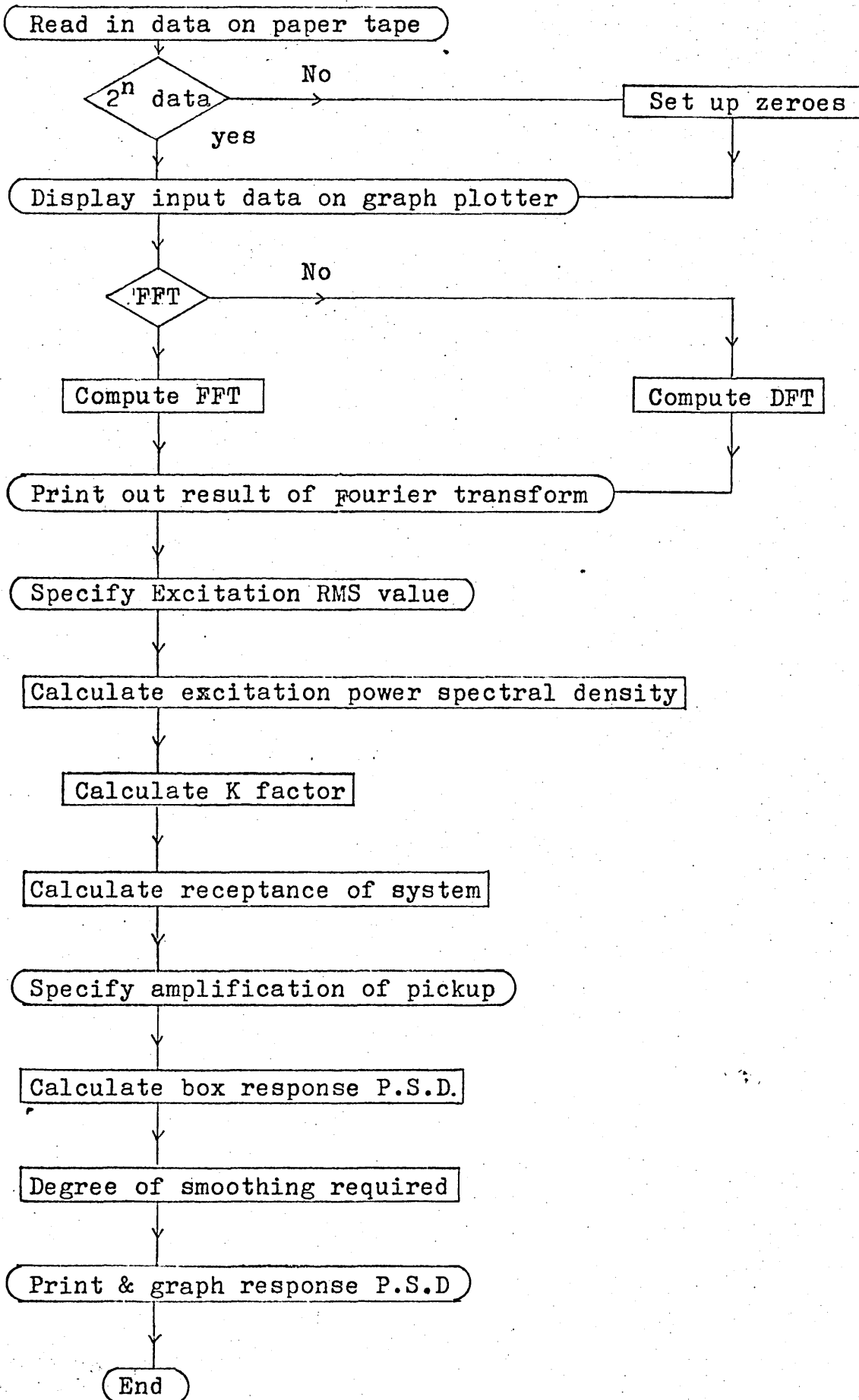
In chapter 3 it was seen that a considerable saving in the number of complex multiplications and additions is made using the Fast Fourier Transform algorithm. The resulting time saving achieved also enables the Fourier transform to be obtained much more economically than by the normal straightforward operation.

The Fourier transform computer programs developed, MOJFTM1 and MOJFTM2 (fig. 5.11), contains both the FFT and the DFT algorithms in separate subroutines either of which can be called up. MOJFTM1 is used for transformation of correlation functions containing up to 512 points and can be run as a small express job on the University ^{computer} whereas MOJFTM2 has to be run as a medium priority job and is used for the transformation involving more than 1024 points.

The cross correlation function of the excitation and the response of the structure is obtained from the time domain analyser in the form of a paper tape via an interface with a teletype in a code compatible with the computer. This program is written to read this data directly off the paper tape displaying the cross correlation function on a graphical output (see chapter 7, fig. 7.14) as well as on a lineprinter output with the exact values obtained, for an immediate and more accurate output (fig. 7.15). The results of the Fourier transformation (the receptance) may also be graphically displayed as well as printed out on the computer lineprinter output. Finally the response spectral density is calculated (section 3.2) and displayed in the same manner. This program also has the facility for producing a linear

Figure 5.11

Computer program MOJFTM flowchart.



or a logarithmic graph as chosen.

Also incorporated into the computer program package developed are subroutines using which smoothing of the coarse peaky results could be obtained. Figures 7.16-7.21 are typical traces of the response power spectral density obtained at the same point but using a pair of PRBS signals of different sequence lengths and with various degrees of smoothing. This is done by averaging $(2N + 1)$ adjacent values to give smoother graphs as N is increased. This, as discussed in Newland [39], also has the effect of improving the statistical accuracy of the result (at the expense of frequency resolution) which now becomes

$$\left(\frac{\sigma}{m}\right)_{\text{new}} = \left(\sqrt{\frac{1}{2N + 1}}\right) \left(\frac{\sigma}{m}\right)_{\text{old}}$$

so that from eqn (5.8)

$$(Be)_{\text{new}} = (2N + 1) (Be)_{\text{old}} \quad (5.11)$$

The superiority of the FFT algorithm is clearly demonstrated in the following requirements for two jobs one using the FFT and the other the DFT algorithm on a sample of 512 points. The former required less than $2 \times 512 \times \log_2(512)$ computer manipulations compared with 512^2 , and took 80 sec and 971 sec respectively. The saving achieved on a sample of 1024 points would be even greater.

The results obtained using these computer programs are given in chapter 7.

Summary

The previous chapter describes the experimental derivation of the response of the box structure. Here a computer prediction of the same is described.

6.1 Response prediction

From chapter 3 (equation 3.14) it was shown that the natural frequencies and mode shapes could be used to calculate the receptance of a structure from which the response power spectral density to any known excitation can be predicted. This section deals with the application of this method to the prediction of the response power spectral density of the box structure to the PRBS excitation used. The natural frequencies and mode shapes of the box in free vibrations were calculated using the finite element method (chapter 2). The hysteretic damping loss coefficients were found experimentally (section 5.3.3). The excitation power spectral density to the box itself was found experimentally (chapter 4).

The receptance of a structure, given in terms of its natural frequencies and mode shapes, is given by equation 6.1

$$|\alpha_{dp}(if)|^2 = \sum_r \frac{w_r^2(x_d)w_r^2(x_p)}{16\pi^4 M_r^2 [(f_r^2 - f^2)^2 + \eta_r^2 f_r^4]} \quad (6.1)$$

In the equation only mode shapes, in relative units, such as that given by a finite element analysis are required. The actual units of the calculated receptance are given by the generalised mass M_r used, by specifying the units in which the mass of the structure is chosen and will be discussed later in this section. In this work using the S.I. units of measurement in M_r the predicted receptance squared will be in m^2/N^2 .

In the experimental work both the excitation and response measurements were concerned with transverse displacements of the top surface of the box. In the computation of the receptance of the structure, therefore only the transverse displacement degrees of freedom are required. In the finite element idealisation, the open ended box structure is divided into twenty-four elements as shown in fig. 6.1. This gives a total of 50 transverse degrees of freedom which describe the deflected shape of the structure in each vibration mode. This will also be required in the calculation of M_r , the generalised mass for the r - th mode of vibration of the structure. (eqn 6.2)

In the choice of the number of natural frequencies and mode shapes required to adequately determine the receptance, by considering its magnitude it will be seen that only frequencies in the immediate vicinity of the natural frequencies are important. The frequencies of interest are taken to range up to 100 Hz, covering some twenty natural frequencies of the box structure. The computation requires that sufficient natural frequencies be taken for convergence to the true value at the upper frequency limit. However, frequencies much above this becomes redundant as their contribution is negligible. Also since comparison with experimental results is one of the main aims of this work, the range of the range of the instrumentation must also be considered. In this case only the lower frequency limit of 20 Hz is important as the upper limit is well above the 100 Hz limit chosen. Therefore in the computation only the 21 natural frequencies and their corresponding mode shapes occurring within this band of frequencies are required.

In the calculation of the generalised mass of the structure when vibrating in mode r

$$M_r = \int w_r^2(x) m dx \quad (6.2)$$

where x represents the points at which a transverse degree of freedom occurs and m is the mass of the structure assumed to be evenly distributed amongst these points. A summation is then taken of the product of the square of the mode shape and the distributed mass over the points on the structure.

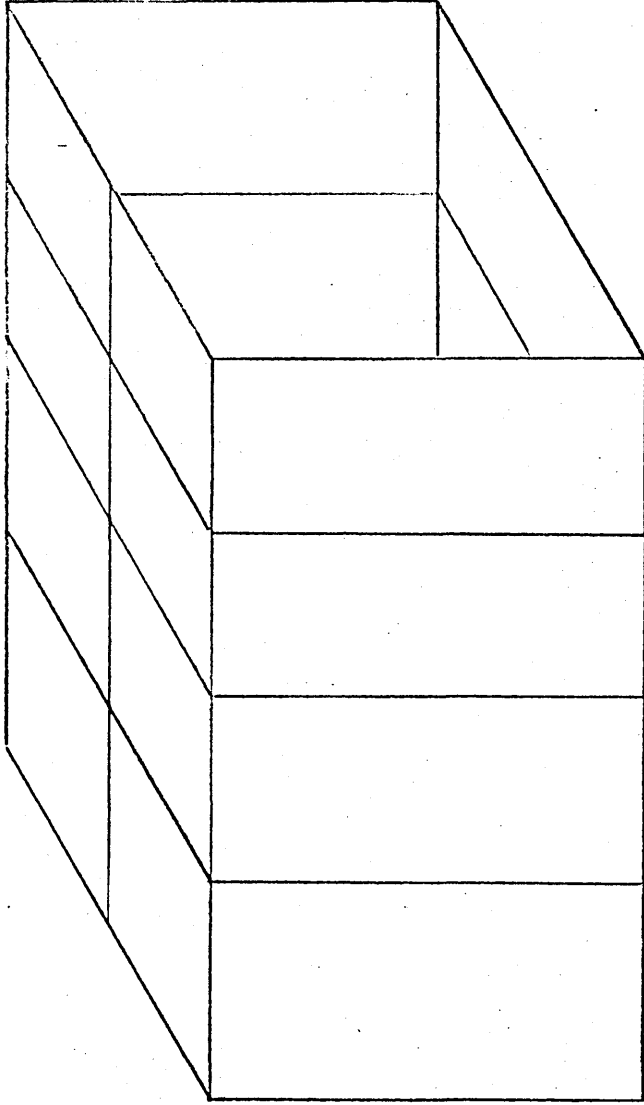


Fig 6.1 The 24 element idealisation of the box structure.

The receptance is then calculated according to equation 6.1 summing over the number of nodes required. Once the receptance is obtained, the response spectral density is calculated according to equation 6.3.

$$S_d(f) = |\alpha(if)|^2 S_p(f) \quad (6.3)$$

where now both the excitation power spectral density $S_p(f)$ and the receptance $\alpha(if)$ is known.

From chapter 2 it was shown how the finite element method of analysis was applied to the prediction of the natural frequencies and mode shapes of a box structure in free vibration. In the previous section it was further shown that the natural frequencies and mode shapes could be used to calculate the receptance of the box and from it to predict the response power spectral density if the damping and excitation power spectral density were known. In chapter 5 the experimental derivation of both the damping and the excitation power spectral density has been described. A computer based prediction of the response power spectral density of the box is therefore possible and was carried out.

The suite of computer programs is given in full in Appendix 3 but a brief description of their development and details of their operation will be discussed here. Because of the size of the problem the computation was divided into 7 programs each communicating with the following program via a magnetic tape or disc peripheral. This strategy also enabled each program to be developed independantly of the others and in fact each program was developed and run on different computers.

The various programs were written and tested on the Sheffield Polytechnic's IBM 1130 computer, a small machine now gradually being replaced by a new IBM 360. The IBM 1130 has a core store of only 10K so that from the start it was realised that the actual computations would have to be done on that of the collaborating institution in this project, the University of Sheffield. This was a ICL 1907 computer, a medium sized computer with up to 70K of core storage. The programs were therefore written in a Fortran language subset that was common to both computers.

In 1974 the University acquired a share of the use of the CDC 7600 of the University of Manchester Regional Computing Centre with the installation of a satellite terminal. This is a large and fast machine with up to 124K of storage available

for any job. The programs were therefore modified to run on this computer to take advantage of the much faster computing times.

The first program MOJFEM1 fig. 6.2 calculates the stiffness matrix for the element for the specified element geometry and the material properties. It then assembles all the element matrices into their proper places in the system stiffness matrix for the box structure as shown previously in fig. 6.1. This is then written to a file for storage. The same procedure is then followed for the mass matrices re-using matrices previously used for the stiffness matrices.

MOJFEM2 fig. 6.3 then retrieves the stiffness matrix for the complete box and reduces out the redundant degrees of freedom caused by the boundary conditions specified. A check is then made for the preservation of symmetry in the matrix after which it is written back to the storage file. This is repeated for the mass matrix.

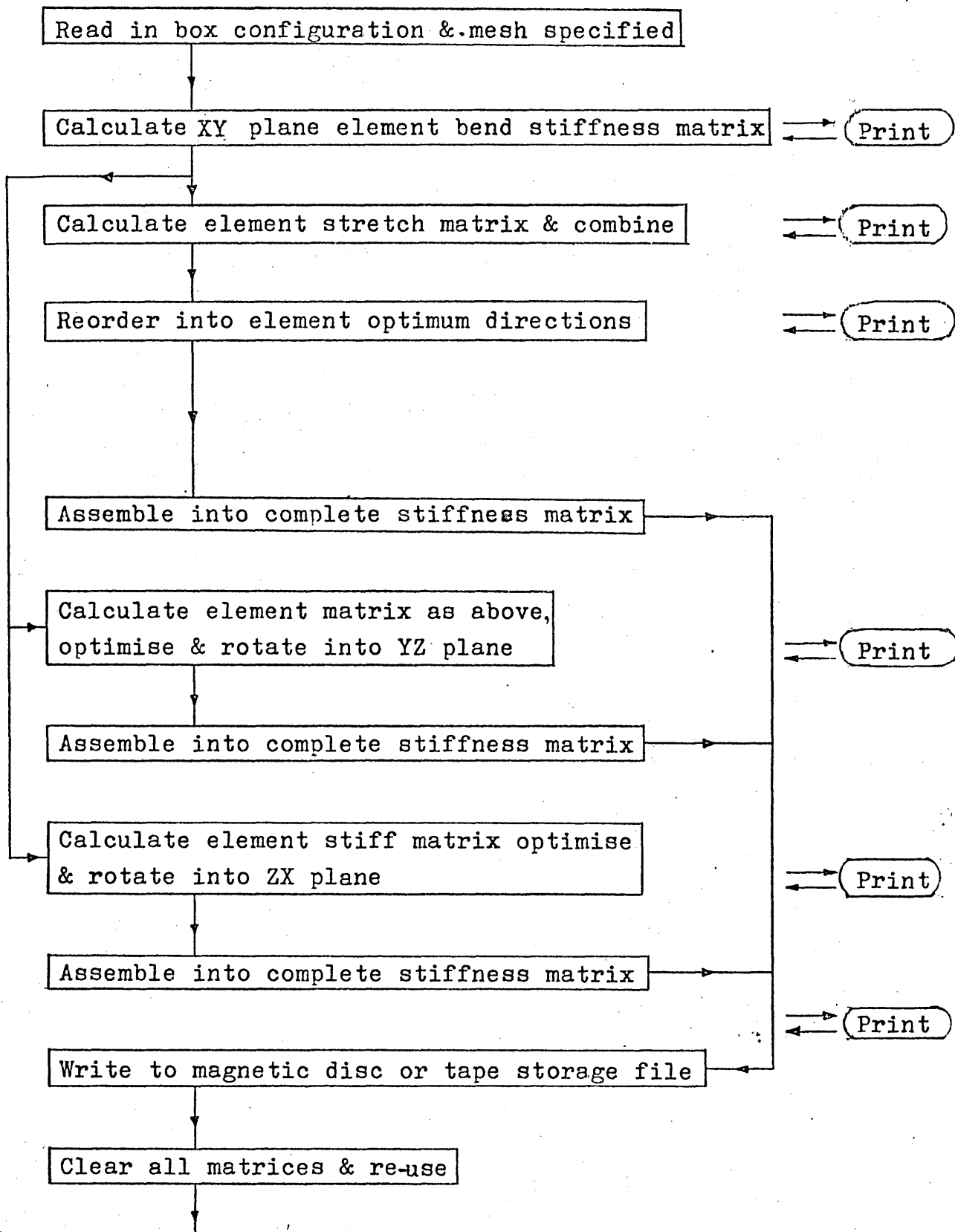
MOJFEM3 fig. 6.4 checks that the final reduced mass matrix is 'positive definite' a necessary condition for the physical system (see section 2.9).

The problem has by this stage been fully set up and MOJFEM4 fig. 6.5 is the solution program solving the resulting eigenproblem. The alternative program MOJFEMD fig. 6.6 is used if the mass matrix is found to be non-positive definite. As may be expected this phase demands the most core and also takes the bulk of the total computing time of the whole suite of programs. Standard library subroutines are used which perform the various operations described in section 2.9 and are outlined in Appendix 2. From the solution of the eigenvalue problem the natural frequencies mode shapes of the box are calculated and written to file storage.

MOJFEM5 fig 6.7 selects the required number of natural frequencies and the degrees of freedom to give the normal modes as prescribed in the previous section and creates a storage file from which a paper tape can be obtained.

MOJFEM6 fig. 6.8 then creates another file from this paper tape for the final program which is run locally on the ICL

Figure 6.2 Computer program MOJFEM1 flowchart.



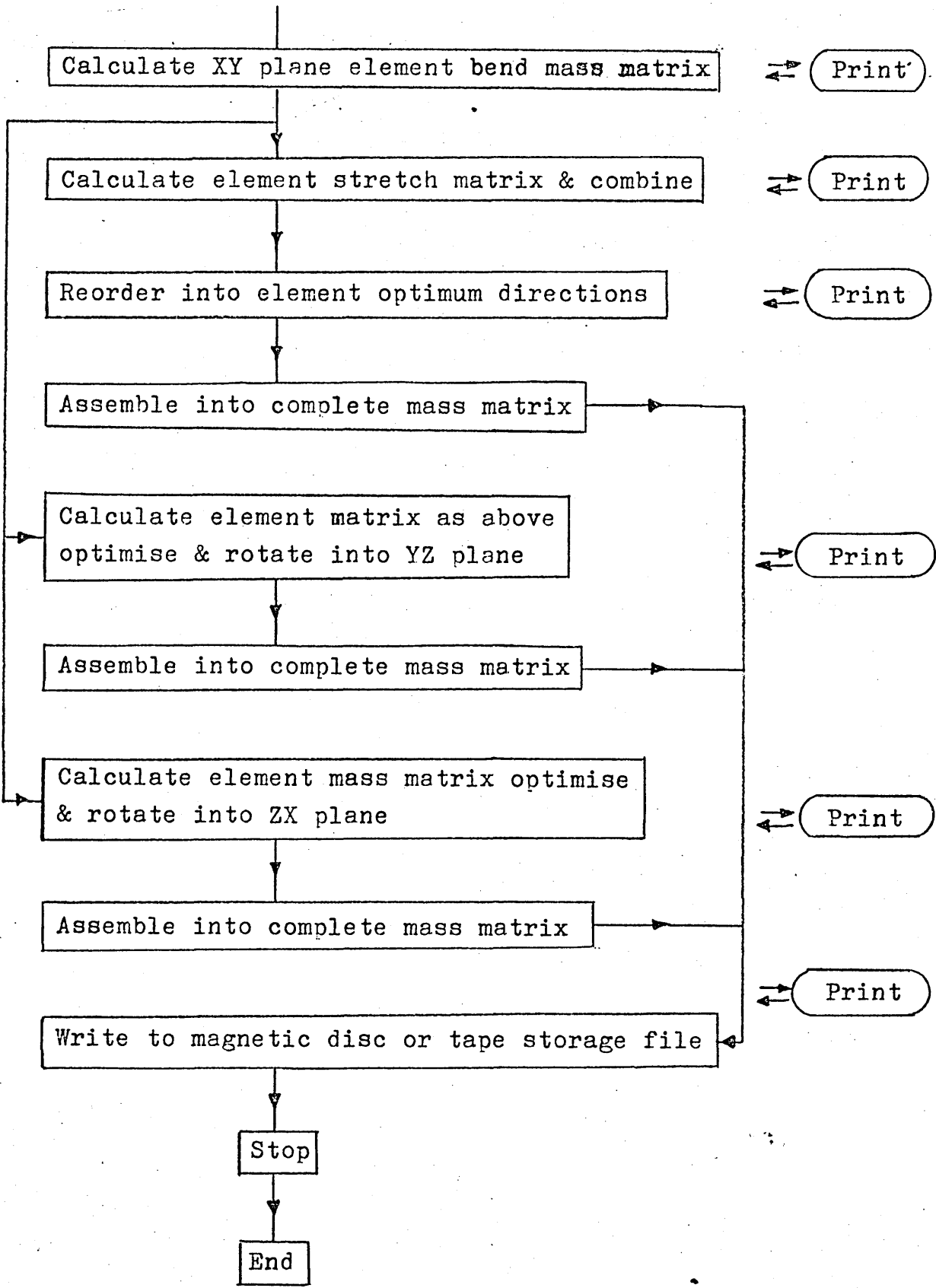
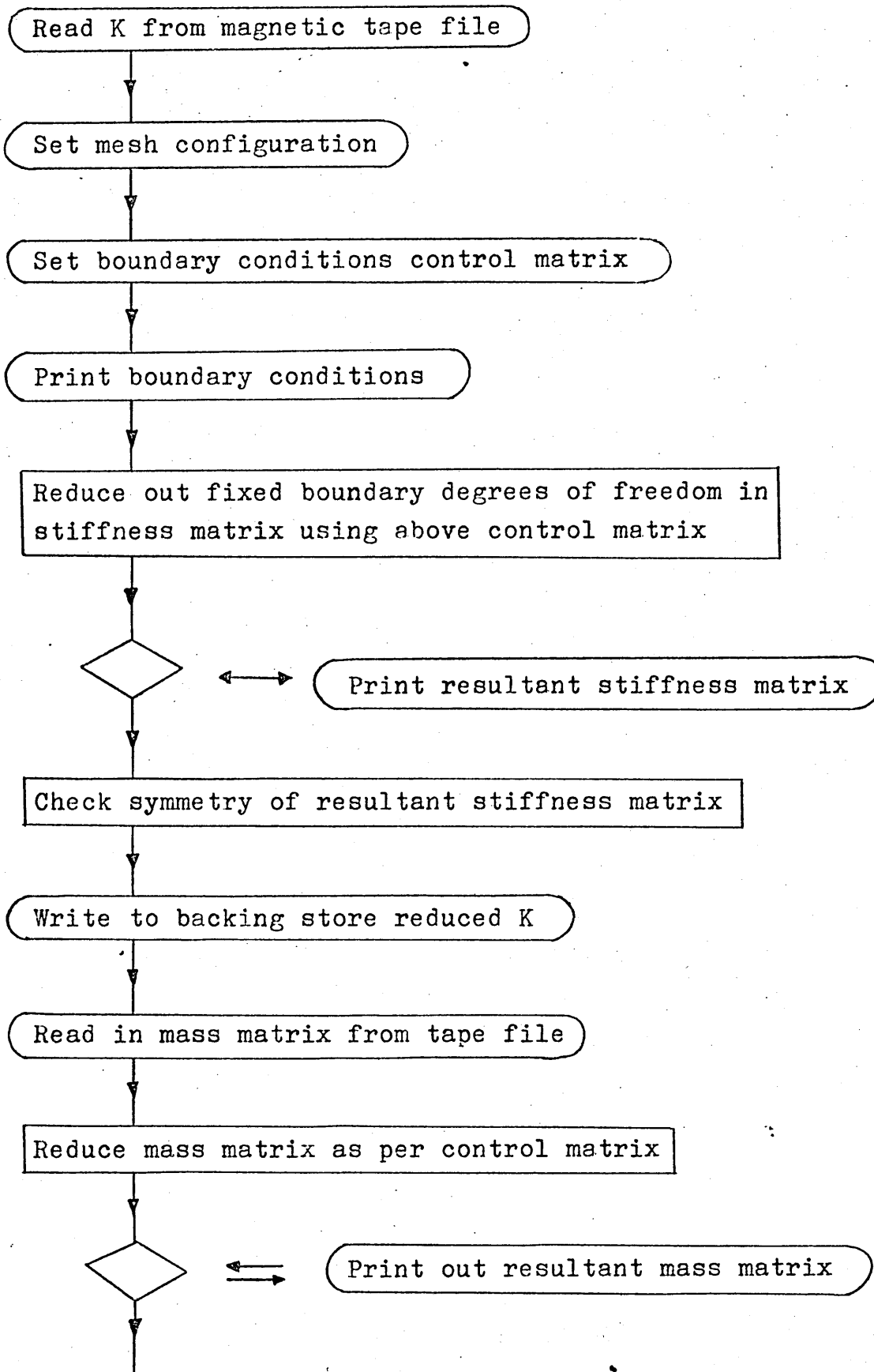


Figure 6.3 Computer program MOJFEM2 flowchart.



Write reduced matrices to magnetic tape file

End

Figure 6.4 Computer program MOJFEM3 flowchart.

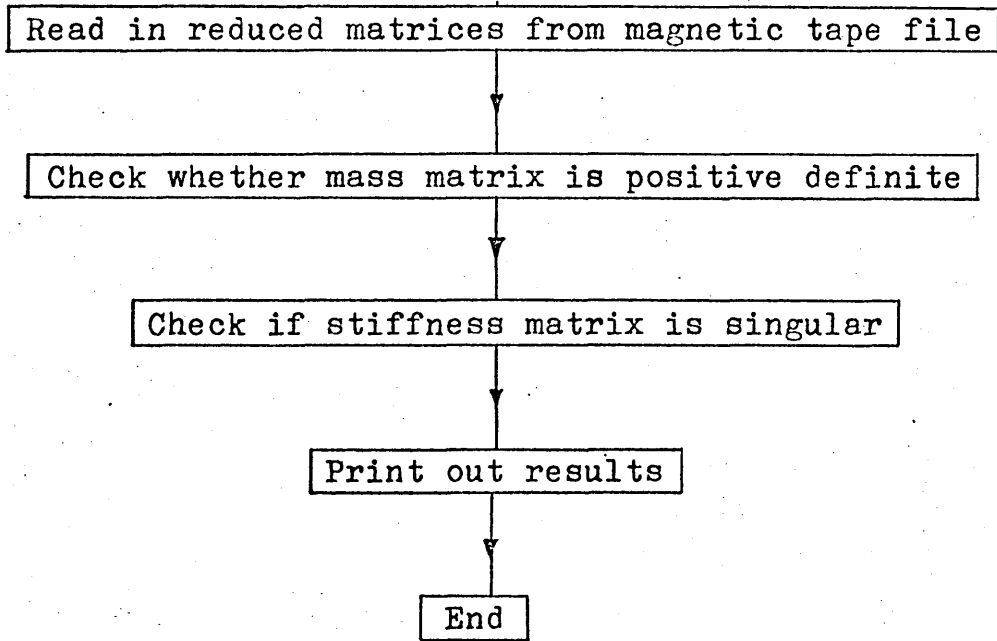


Figure 6.5 Computer program MOJFEM4 flowchart.

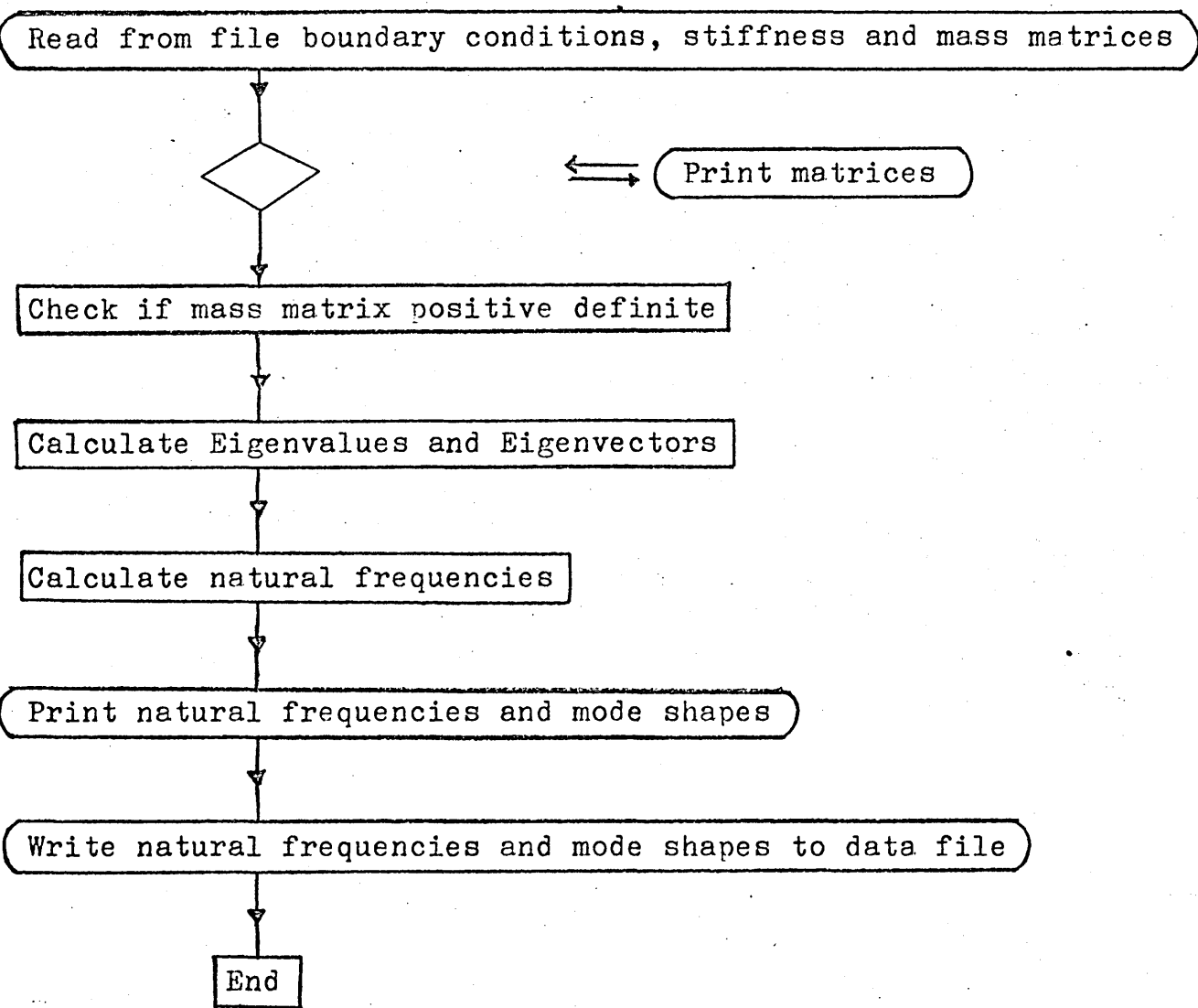
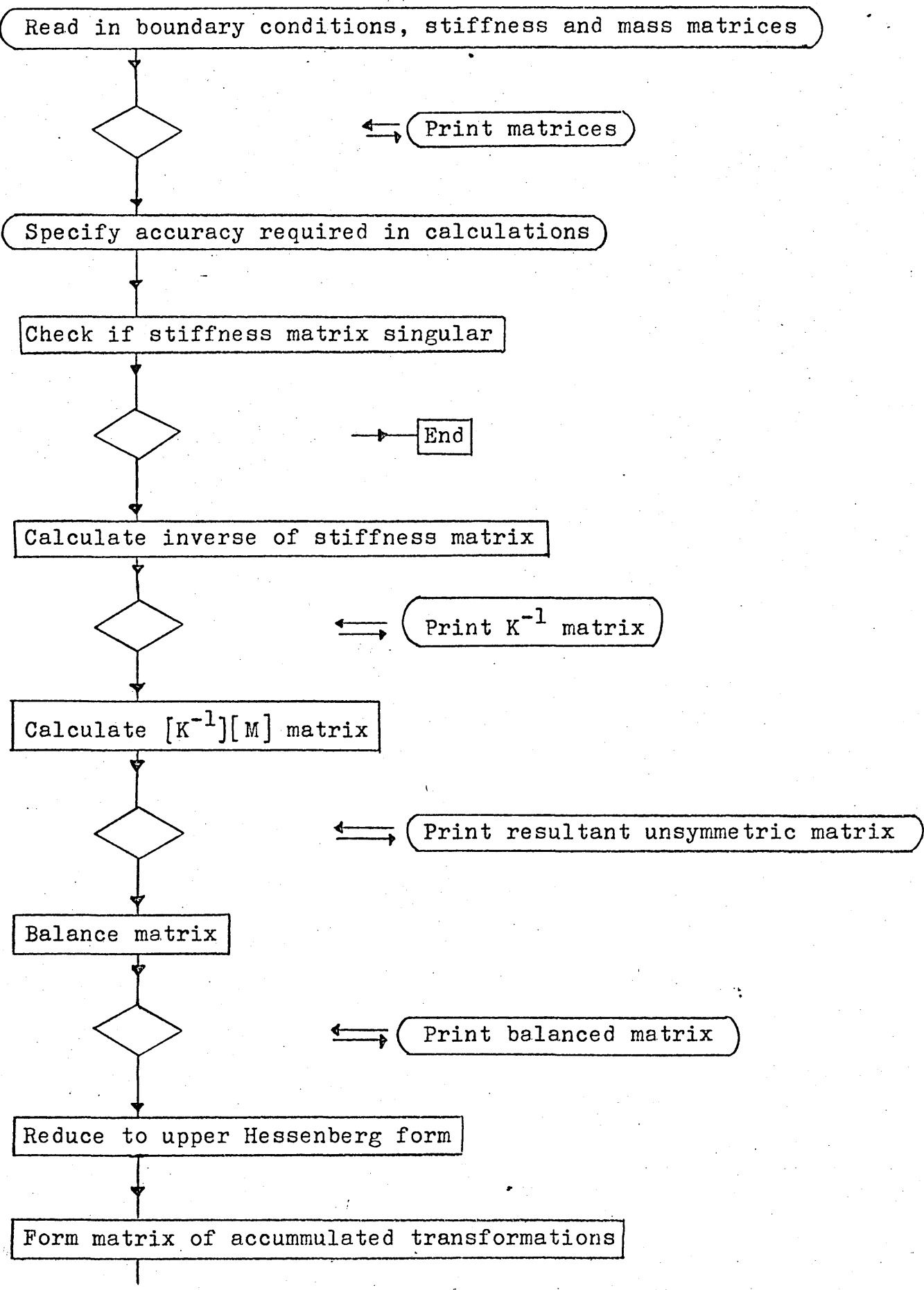


Figure 6.6 Computer program MOJFEMD (optional) flowchart.



Compute Eigenvalues and Eigenvectors of upper Hessenberg matrix

Calculate natural frequencies from Eigenvalues

Print natural frequencies

Calculate Eigenvectors of original problem

Print Eigenvectors of structure

Write to data file

End

Figure 6.7 Computer program MOJFEM5 flowchart.

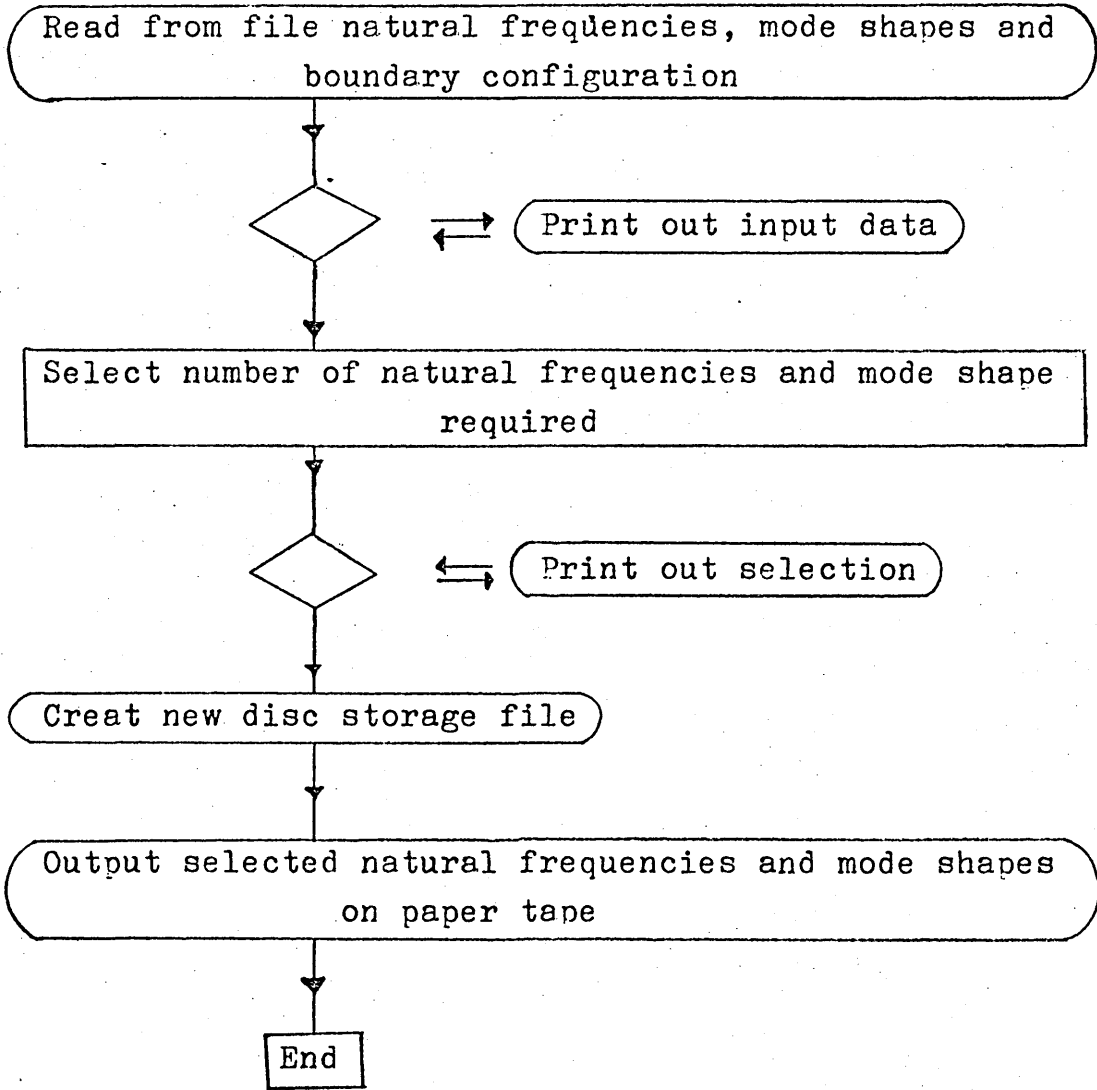


Figure 6.8 Computer program MOJFEM6 flowchart.

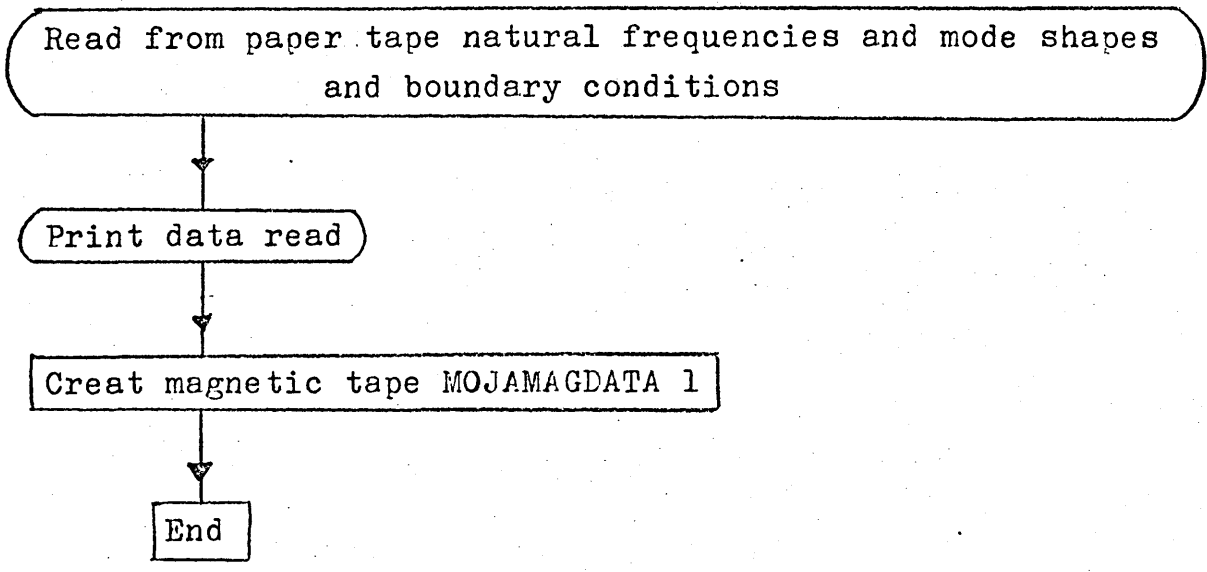
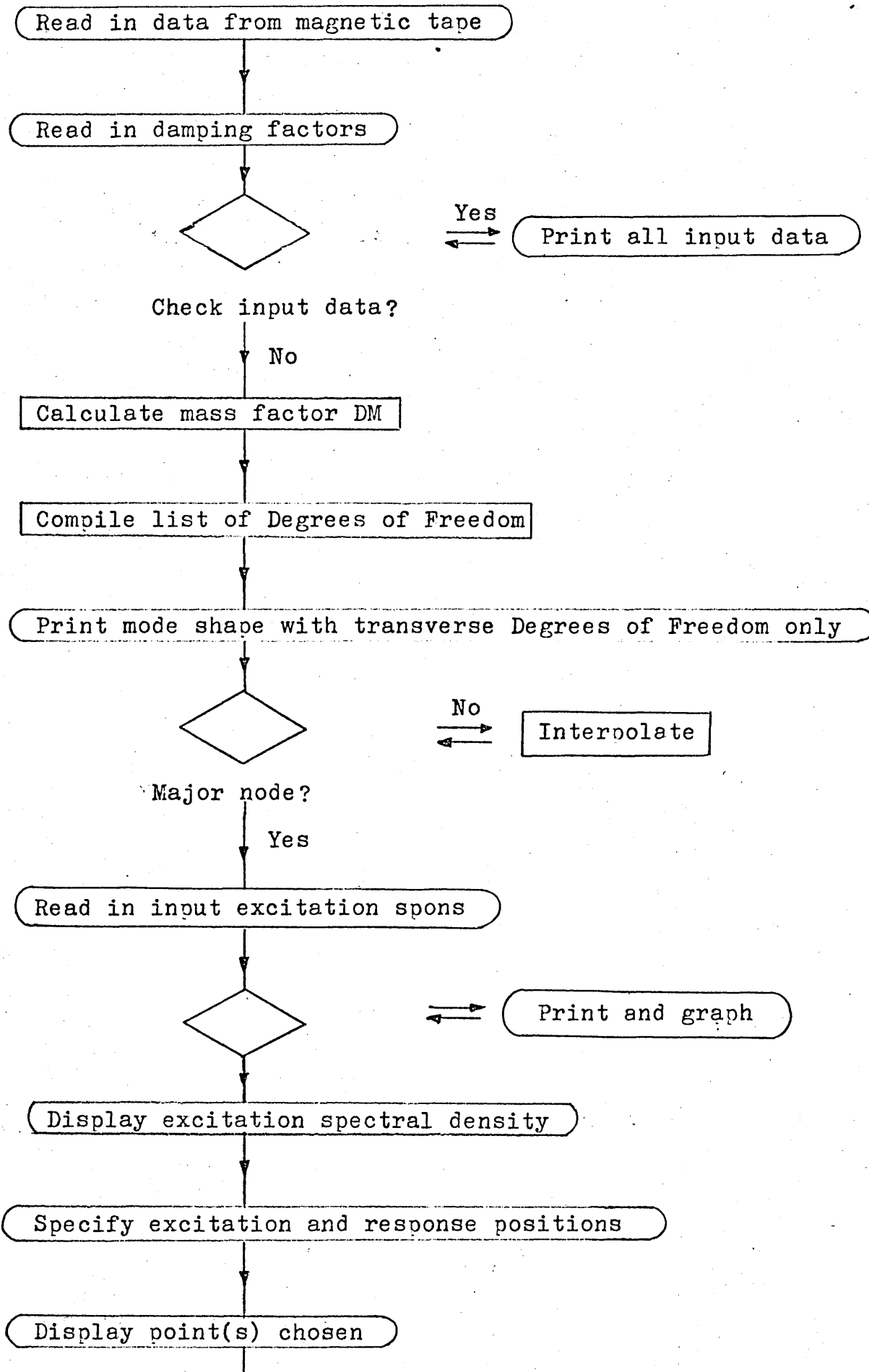
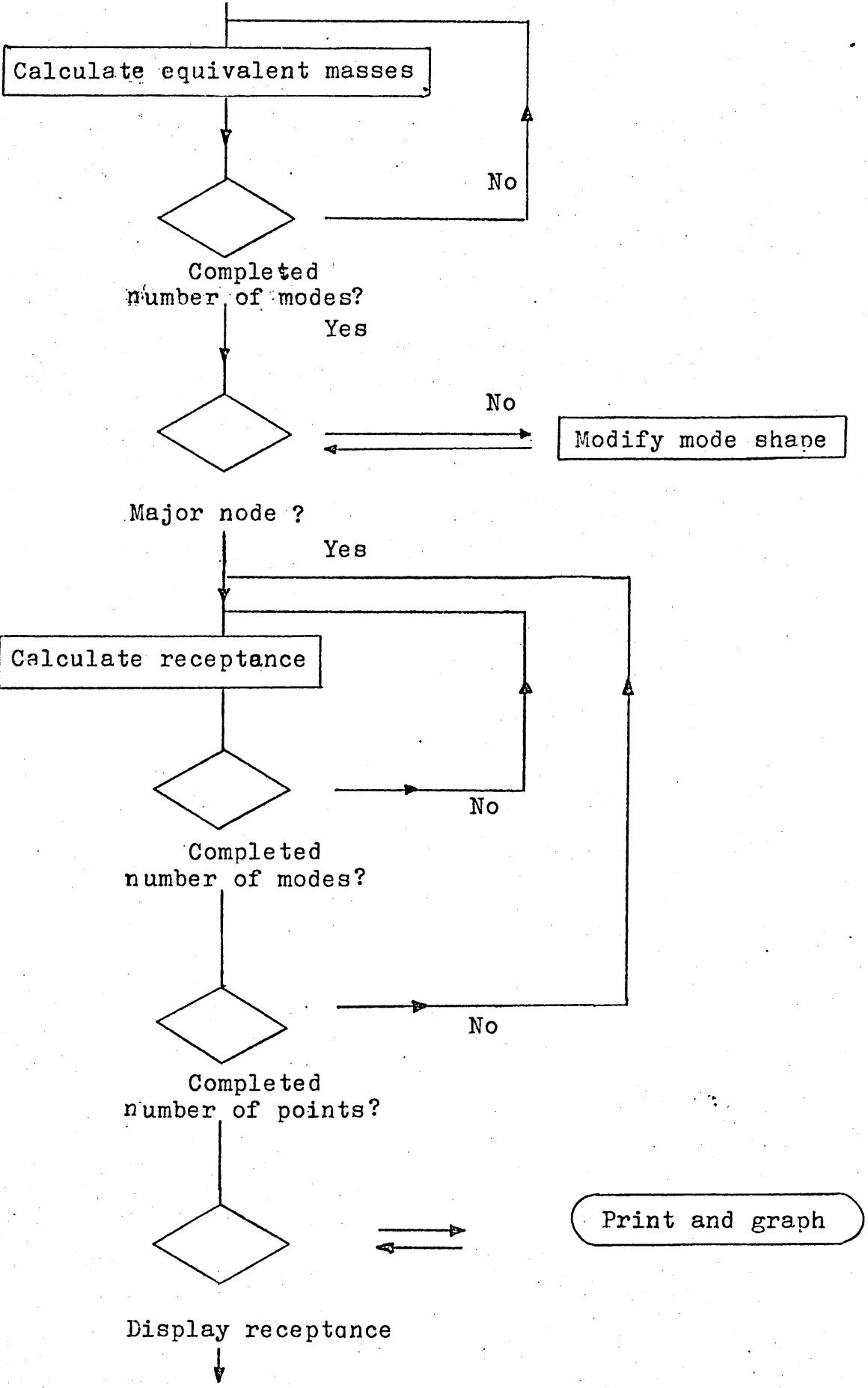


Figure 6.9 Computer program MOJFEM7 flowchart.





Calculate response spectral density

Print and graph response spectral density

Print maximum frequency

End

1907 computer. This is because having calculated the natural frequencies and mode shapes of the structure, the receptances of the box at a large number of points and calculations of the response spectral densities can be obtained. These are run as small express jobs while can be executed more economically and with faster turn round times on the local computer with graph plots produced.

MOJFEM7 fig. 6.9 computes the response power spectral density at any chosen point from natural frequencies and normal modes of the box given the damping factors and the excitation power spectral density. A peripheral graph plot of the excitation and the response power spectral density is output with an additional line printer output for more accurate checking purposes.

The following is a table of the various programs, the core requirements and the solution times for the twenty-four element-mesh idealisation shown in fig. 6.1.

<u>Program</u>	<u>Core (Kwords)</u>	<u>Time (Sec.)</u>
MOJFEM1	39	4.0
MOJFEM2	57	0.8
MOJFEM3	44	6.5
MOJFEM4	55	17.0
MOJFEMD (optional)	70	88.0
MOJFEM5	24	0.3
MOJFEM6	18	10.0
MOJFEM7	19	72.0

Summary

In this chapter results of the investigation of natural frequencies and mode shapes of beams, plates and boxes are presented. Further results of work leading up to the response of the box structure to random excitation are also presented.

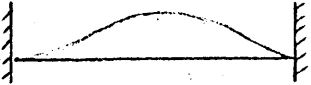
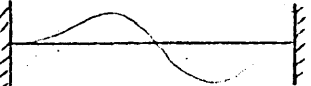
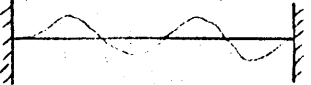
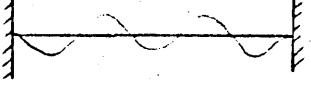
7.1 Natural frequencies and mode shapes

Section 5.3.1 describes how the natural frequencies and mode shapes of beams, plates and box structures were obtained. The natural frequencies and mode shapes of a beam simply supported at both ends and a beam fully fixed at both ends are presented in Table 7.1. The first five natural frequencies and mode shapes of a plate fully fixed all round are presented in Table 7.2.

The twenty-one natural frequencies of an open ended folded plate box type structure, fixed at the four corners of its base, existing within the frequency range 0 to 100 Hz are given in Table 7.3. Their corresponding mode shapes are illustrated in fig. 7.1 to 7.11. The first mode predicted at 5.6 Hz was not checked experimentally as equipment available only measured down to 20 Hz. However, a swaying mode was apparent at a very low frequency which seemed to correspond to this mode. The other modes have been stimulated experimentally and both the experimental and predicted results are presented here.

Table 7.1

Results of beam analysis (fully-fixed ends)

Mode shape	Natural frequency (Hz.)			Damping factor (η)
	Exact	Energy ^(FE)	Expt.	
	43.8	43.9	43.2	0.020
	121.0	123.0	117.0	0.007
	238.1	240.0	223.9	0.006
	392.0	397.0	361.0	0.004
	585.0	592.0	545.0	0.003

Results of beam analysis (simply-supported ends)

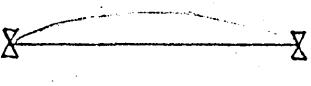
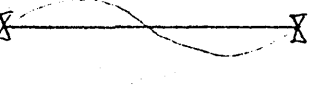
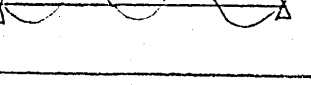
Mode shape	Natural frequency (Hz.)			Damping factor (η)
	Exact	Energy ^(FE)	Expt.	
	19.5	19.5	13.8	0.018
	78.1	78.1	62.0	0.007
	176.0	176.0	145.0	0.008
	313.0	313.0	289.0	0.006
	488.0	488.0	458.0	0.003

Table 7.2 Results of plate investigation (fixed all round)

Length = 0.78m.
 Width = 0.22m.
 Thickness = 0.00061m.

Mode shape		Natural frequency		
m	n	Expt.	F.E.	Energy
2	2	53.3 Hz	67.2	69.1
3	2	69.5	75.0	74.7
4	2	79.5	84.1	84.9
5	2	92.5	101.4	99.8
6	2	111.0	118.5	120.1

m = Number of half-wavelengths in x direction.
 n = Number of half-wavelengths in y direction.

The finite element analysis is made using 8 elements.

The results of Tables 7.1 and 7.2 were obtained principally to show that the finite element programs were working satisfactorily. The close agreement between the finite element results and other calculated results showed this to be the case. The experimentally obtained natural frequencies for the plate and for the simply supported beam are both low. This can be attributed to the fact that the required boundary conditions in these cases were not fully achieved in the experimental apparatus. No action was taken to improve these boundary conditions as these structures did not form a major part of the work.

AnalyticalExperimental

5.6 Hz	-
22.4	24.6 Hz
27.6	27.2
31.8	32.8
36.4	37.0
38.1	42.4
47.0	49.5
48.5	53.1
49.0	55.1
54.3	58.6
59.0	62.4
62.7	66.8
67.9	68.2
69.2	70.8
70.3	72.7
70.9	74.7
75.0	77.6
80.0	84.4
81.0	88.0
91.0	96.5
98.0	105.6

Table 7.3 Natural frequencies of box structure

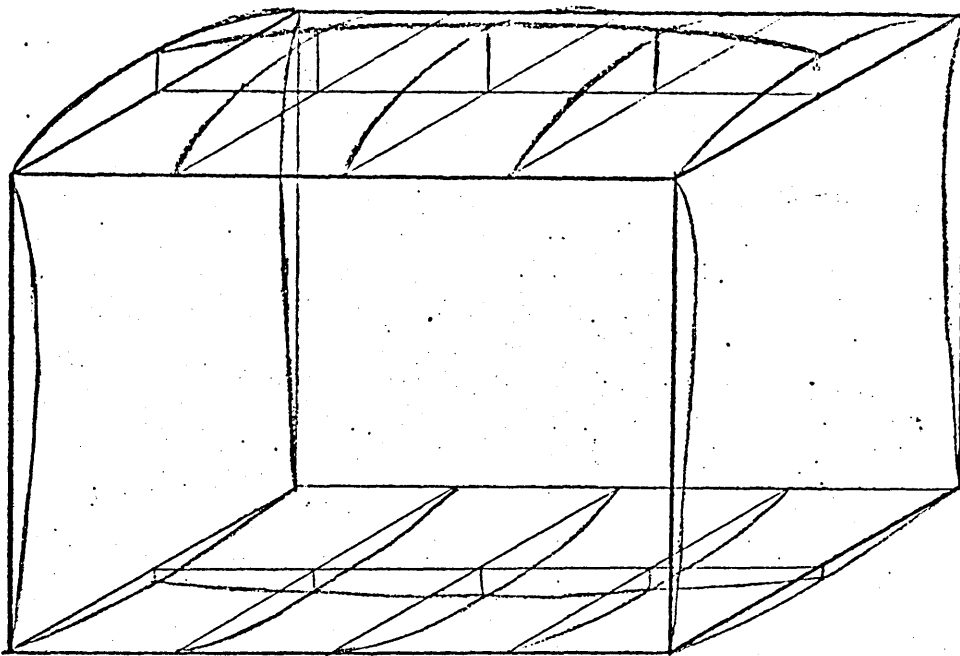
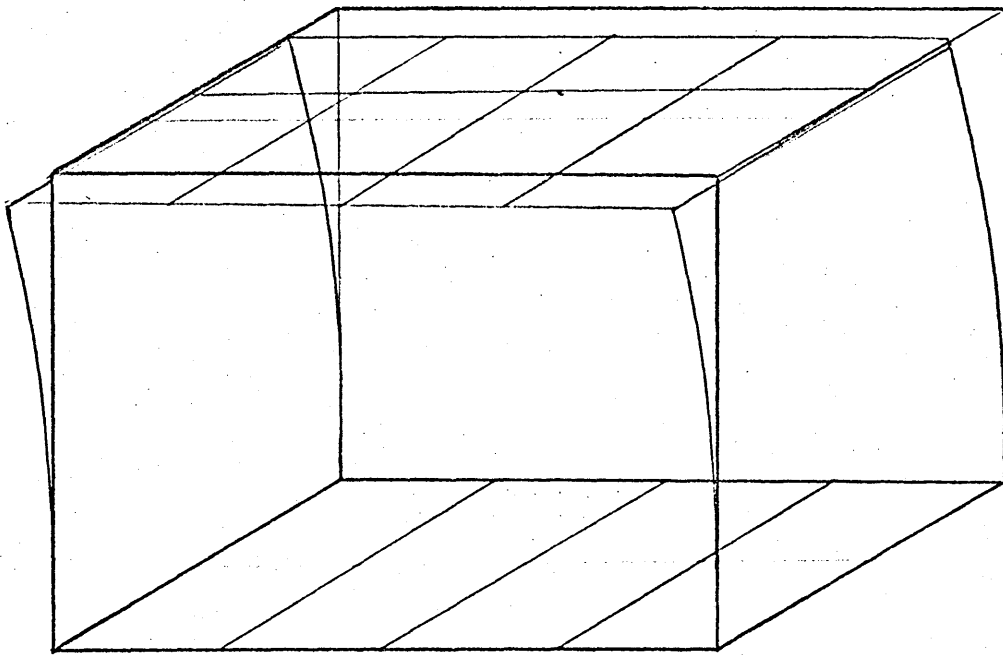


Figure 7.1 1st. and 2nd. mode shapes of the box.

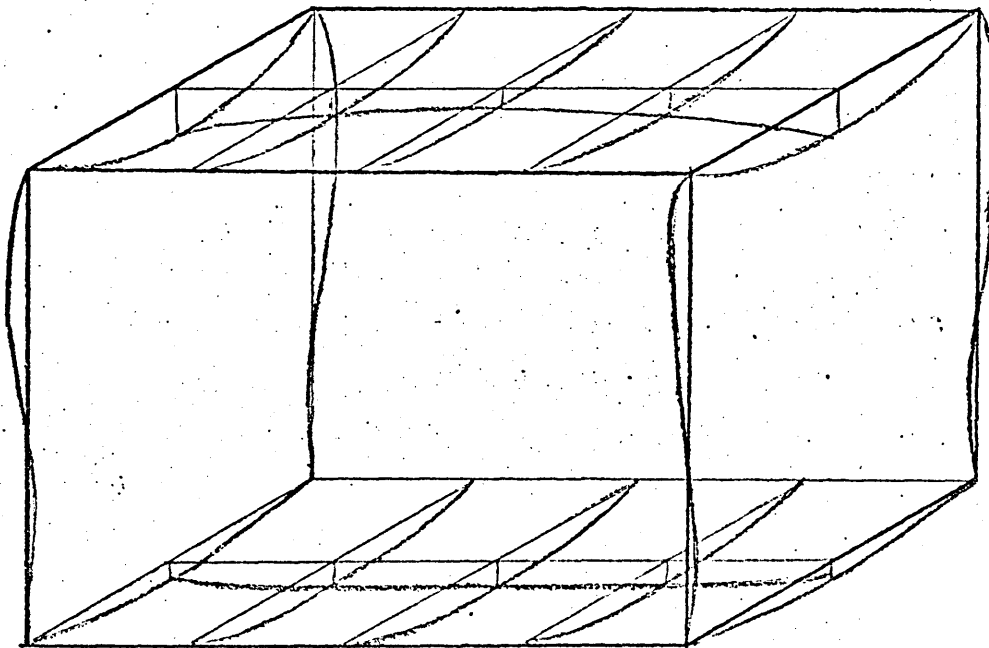
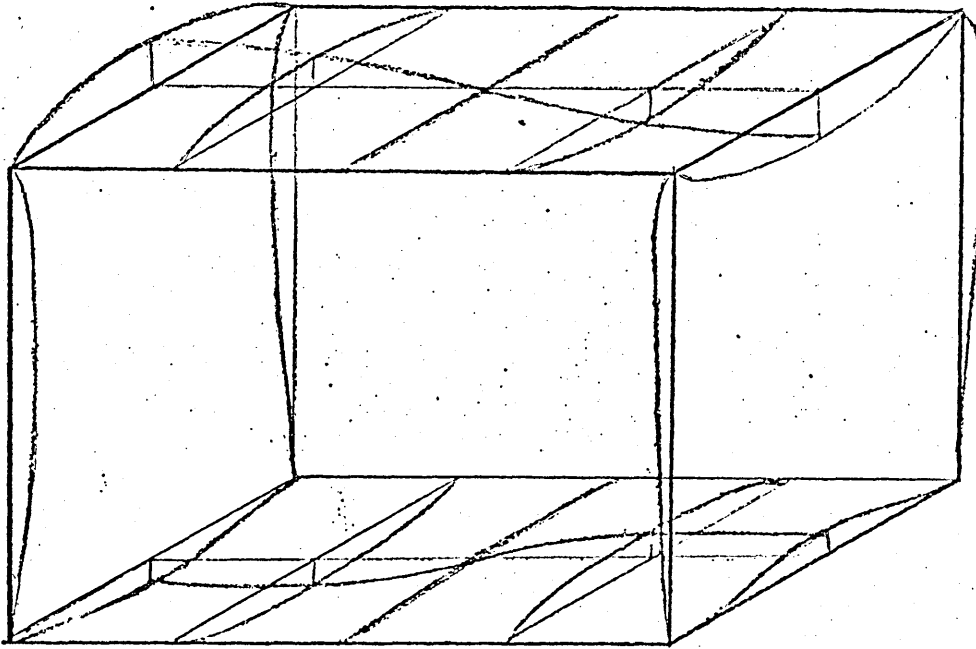


Figure 7.2 3rd. and 4th. mode shape of box.

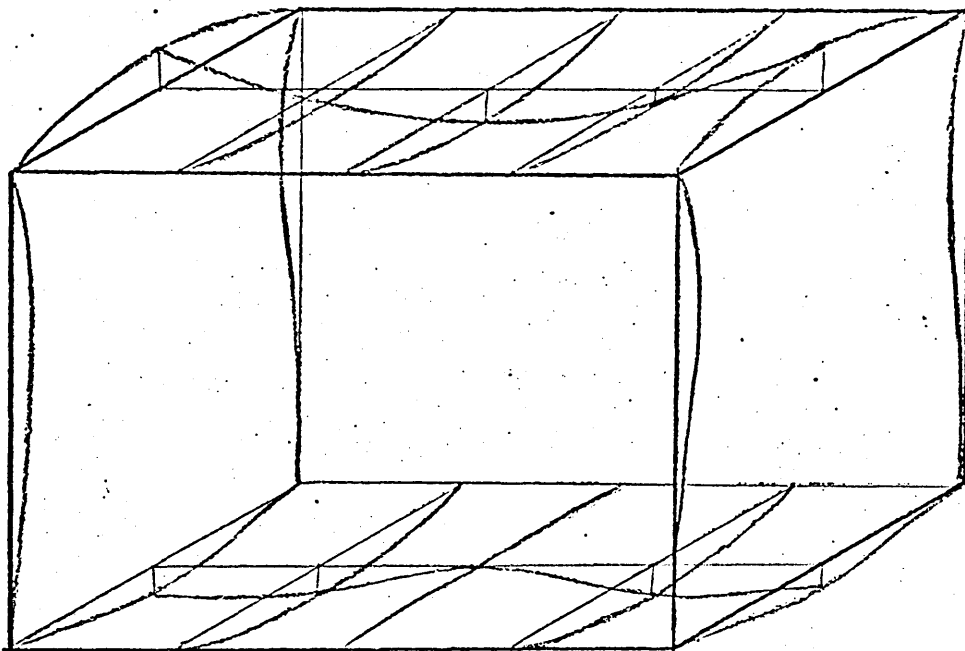
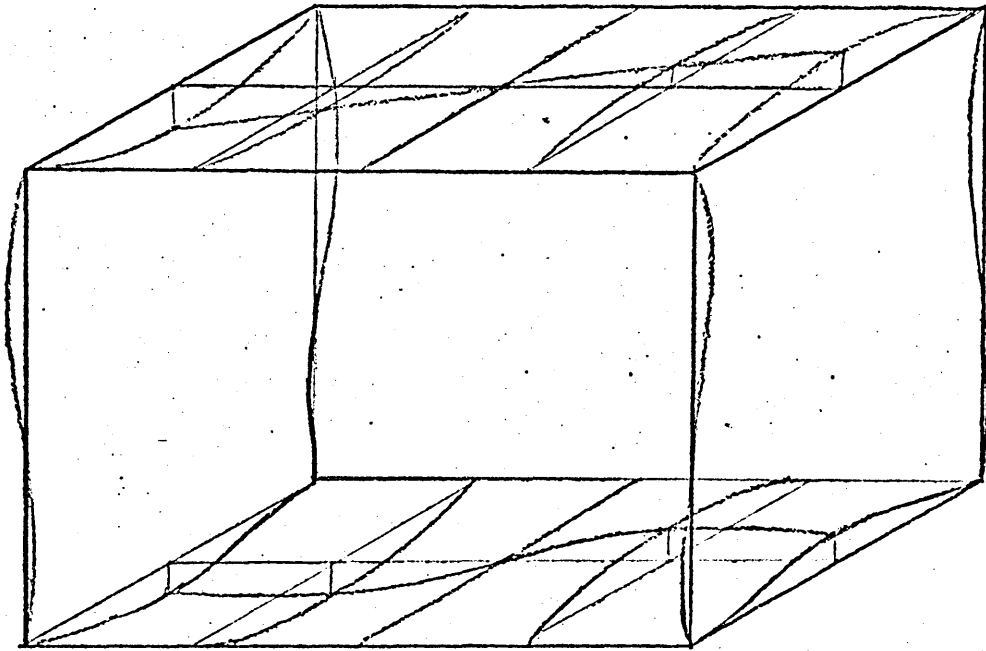


Figure 7.3 5th. and 6th. mode shapes of the box.

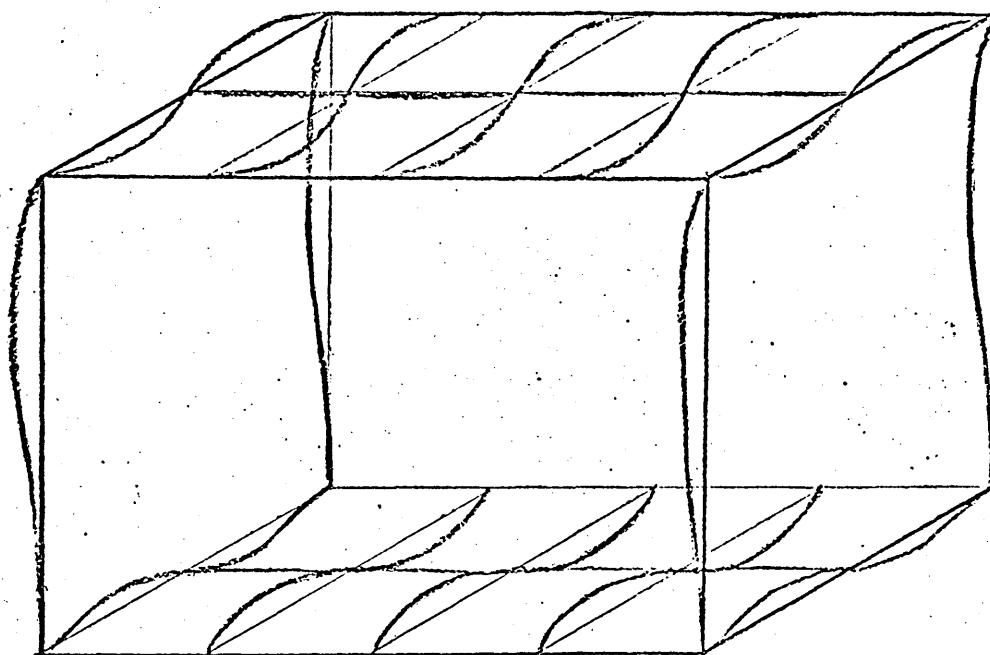
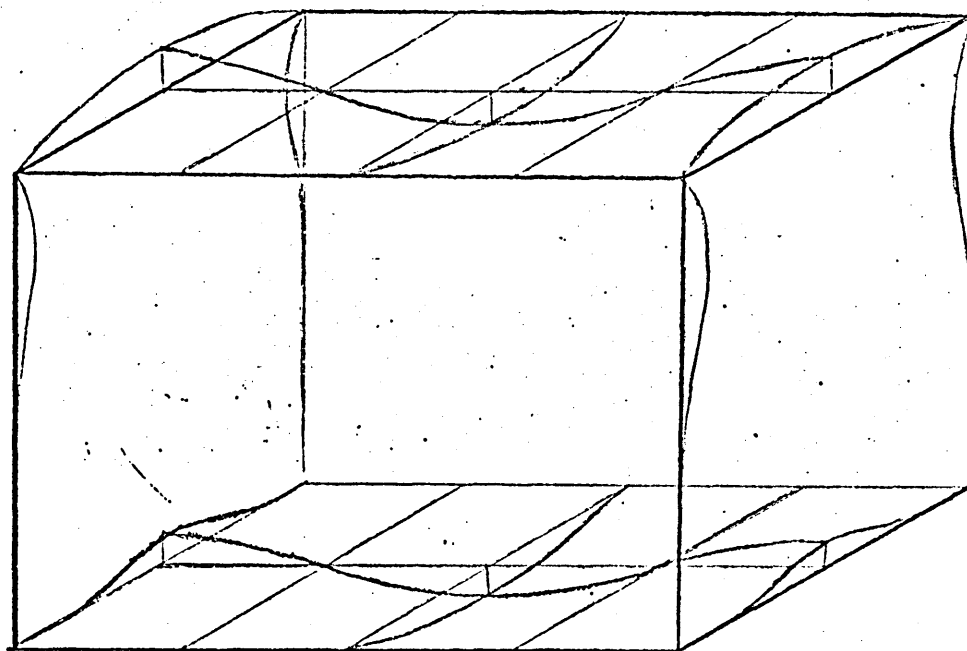


Figure 7.4 7th. and 8th. mode shapes of the box.

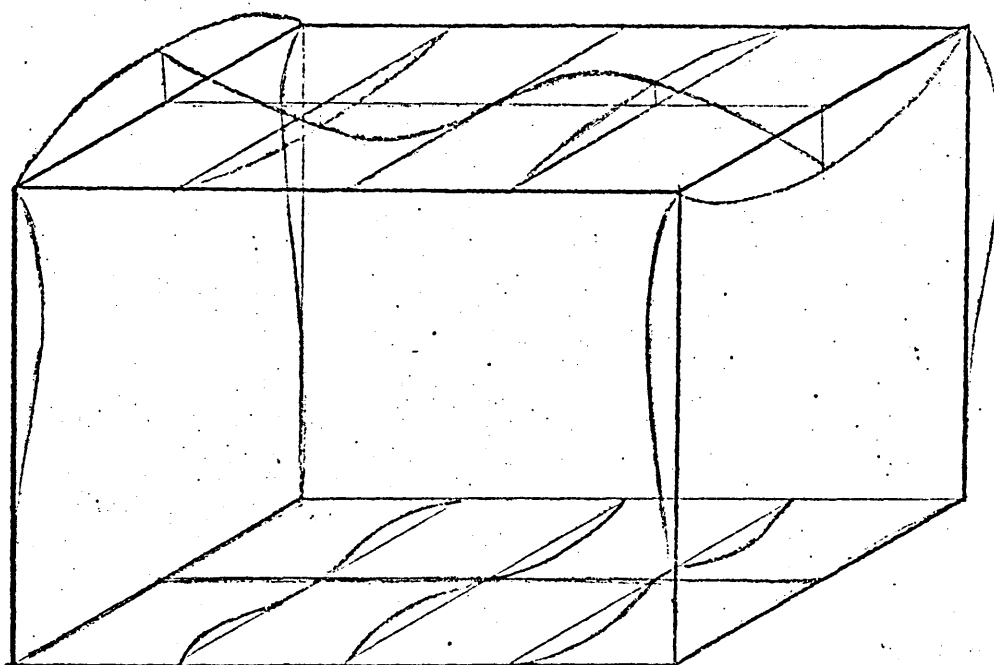
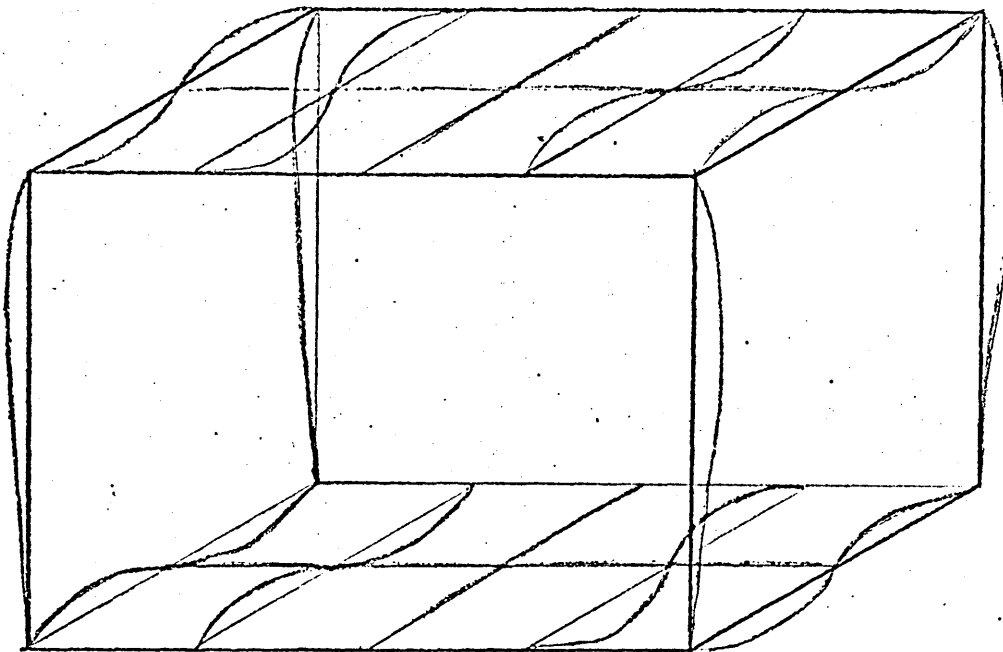


Figure 7.5 9th. and 10th. mode shapes of the box.

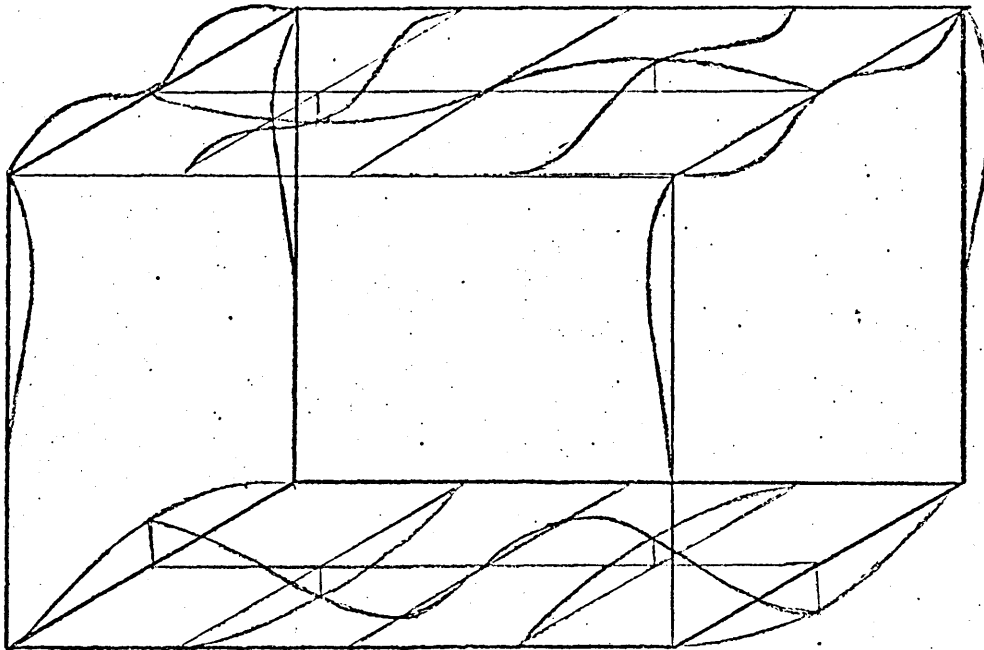
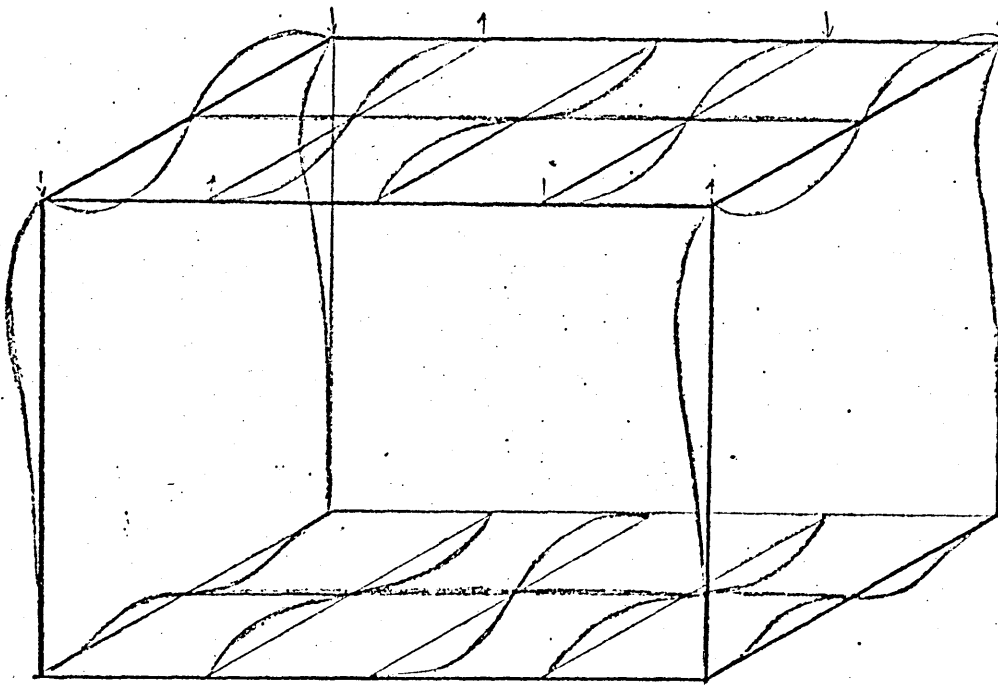


Figure 7.6 11th. and 12th. mode shapes of the box.

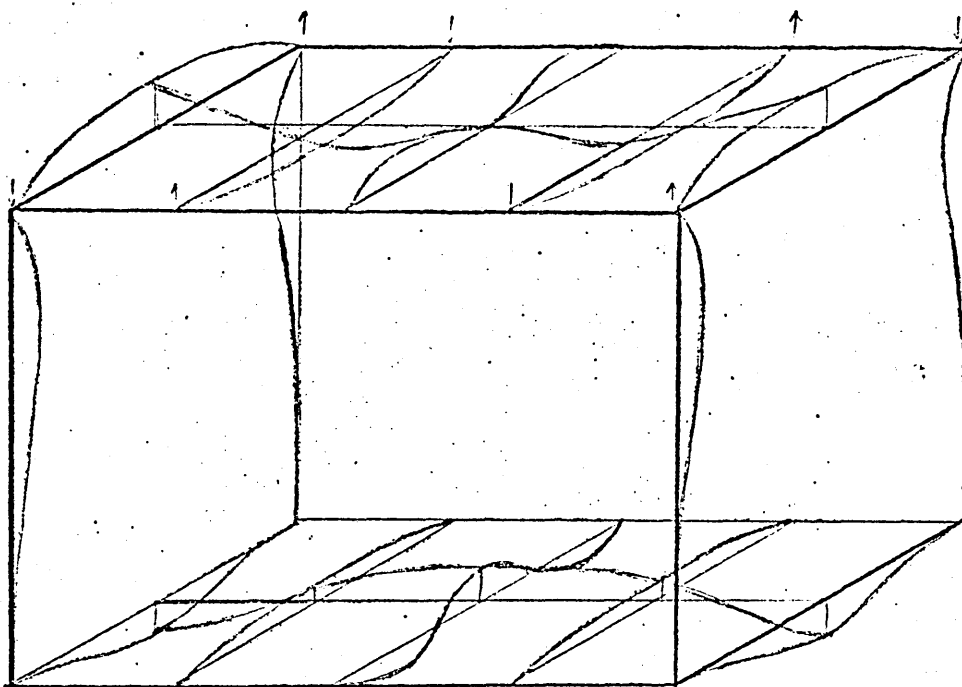
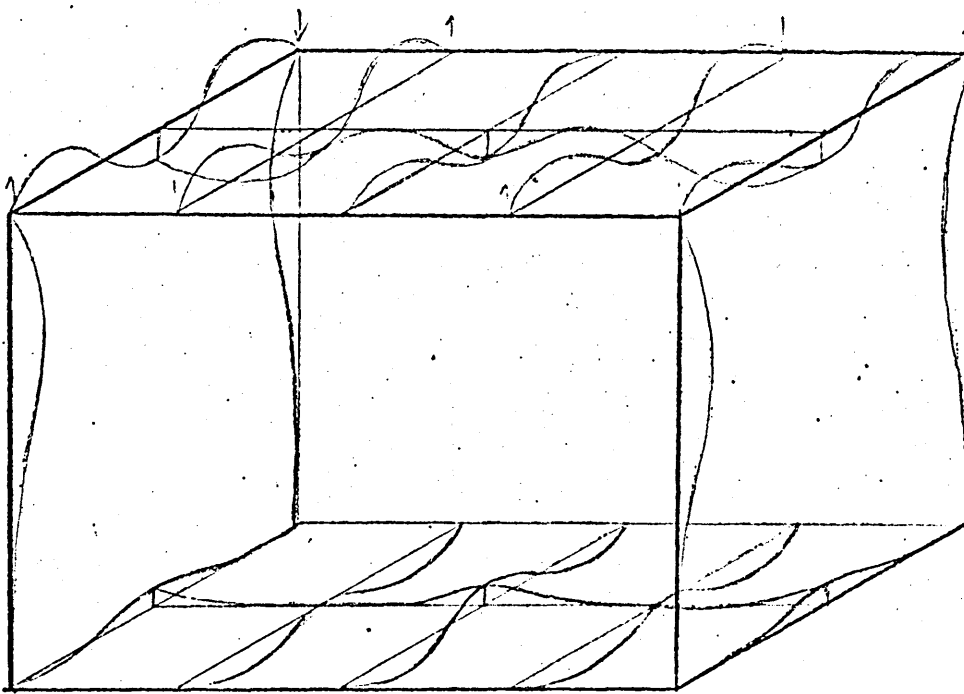


Figure 7.7 13th. and 14th. mode shapes of the box.

θ_2
also
present

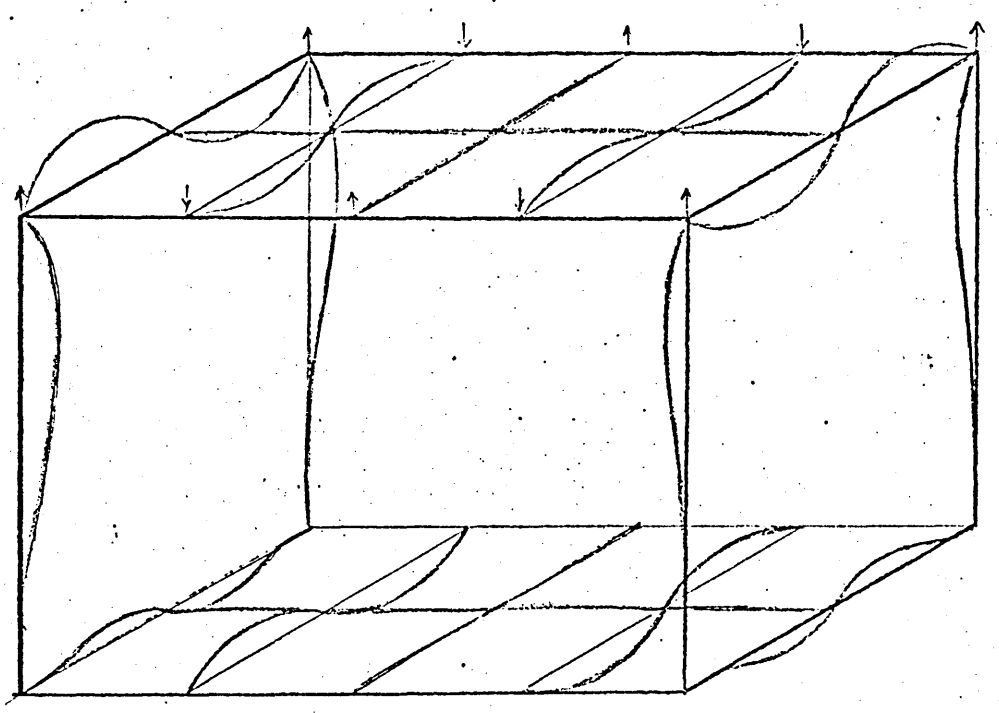
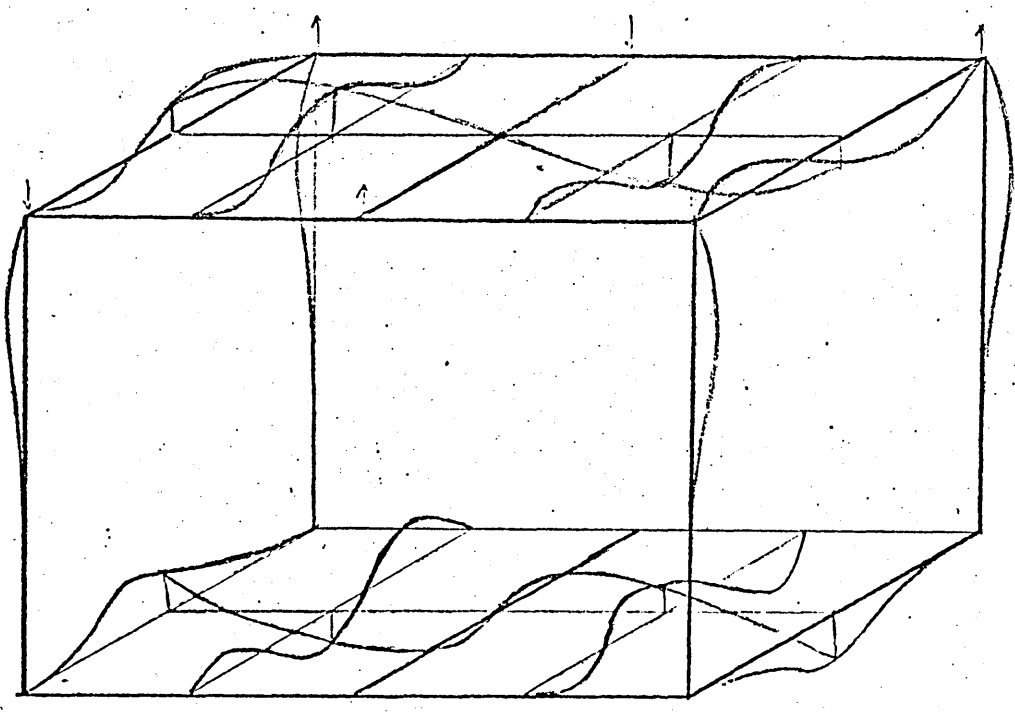


Figure 7.8 15th. and 16th. mode shapes of the box.

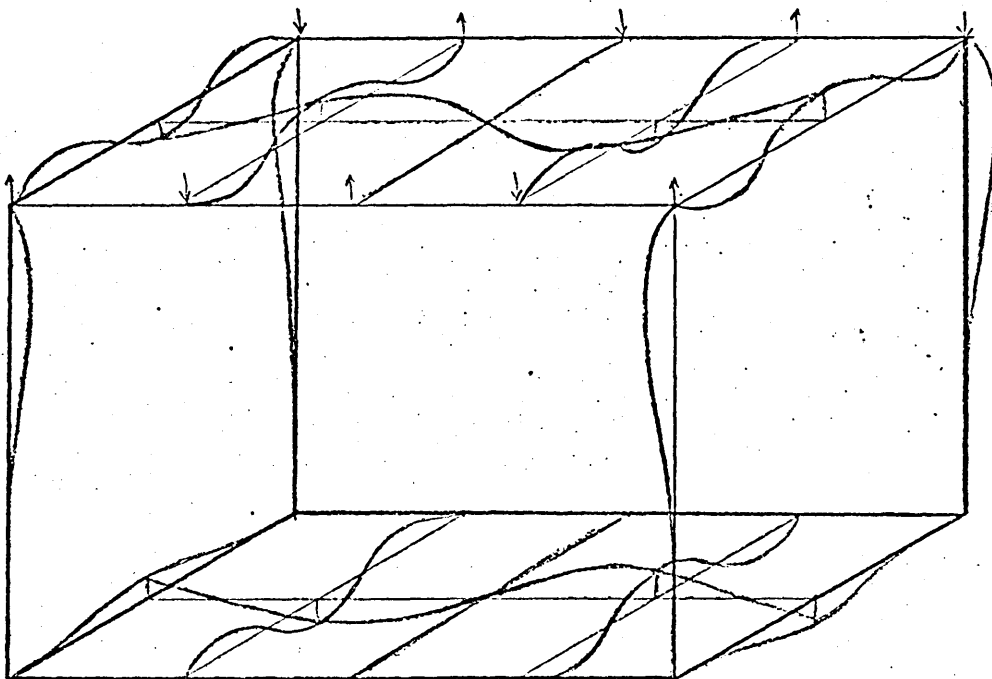
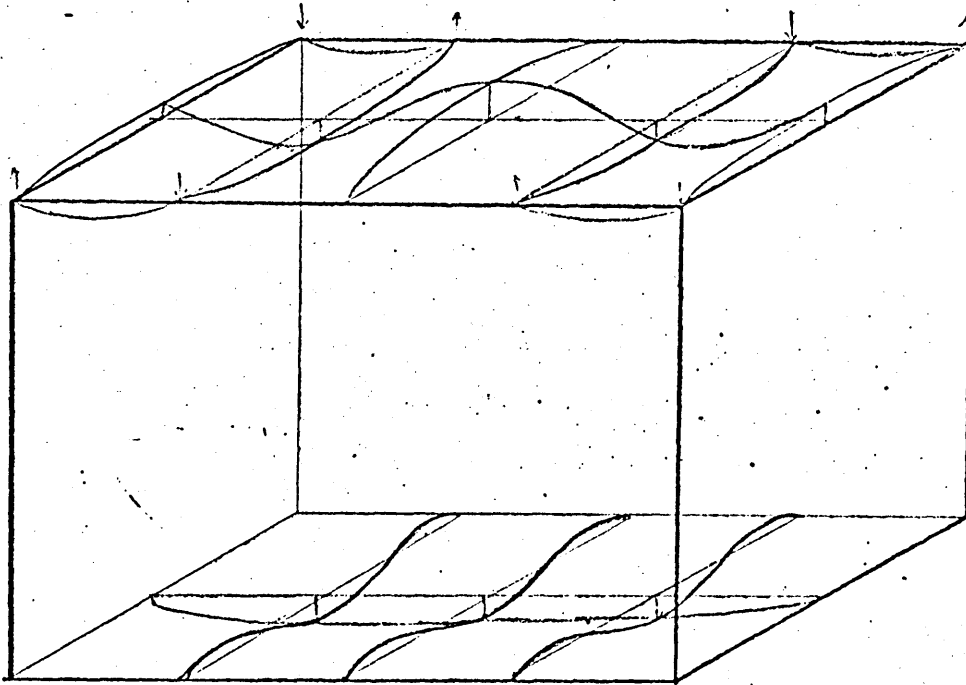


Figure 7.9 17th. and 18th. mode shapes of the box.

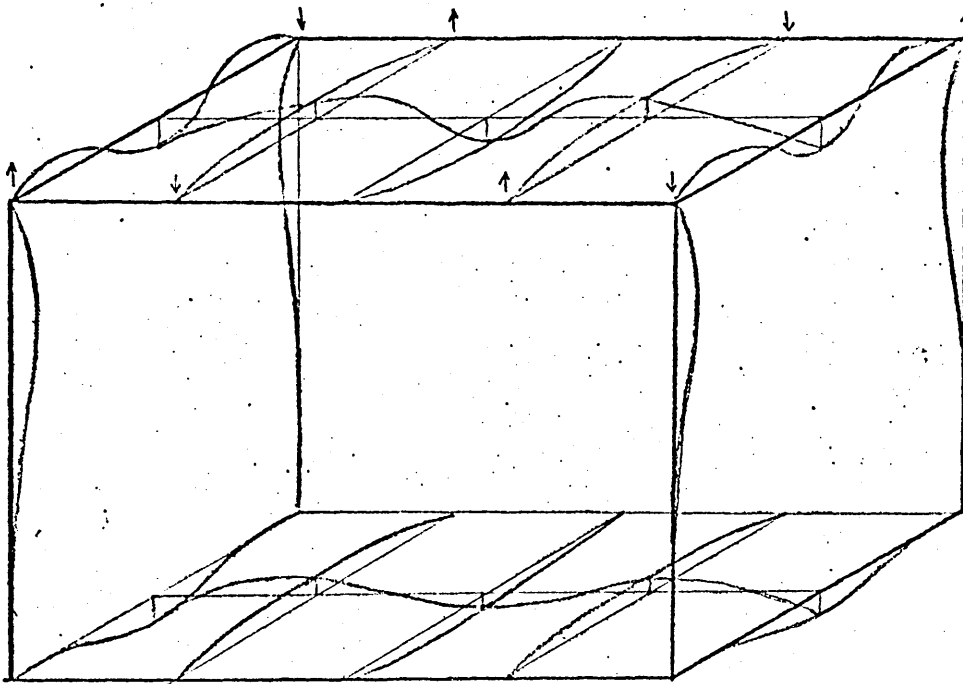
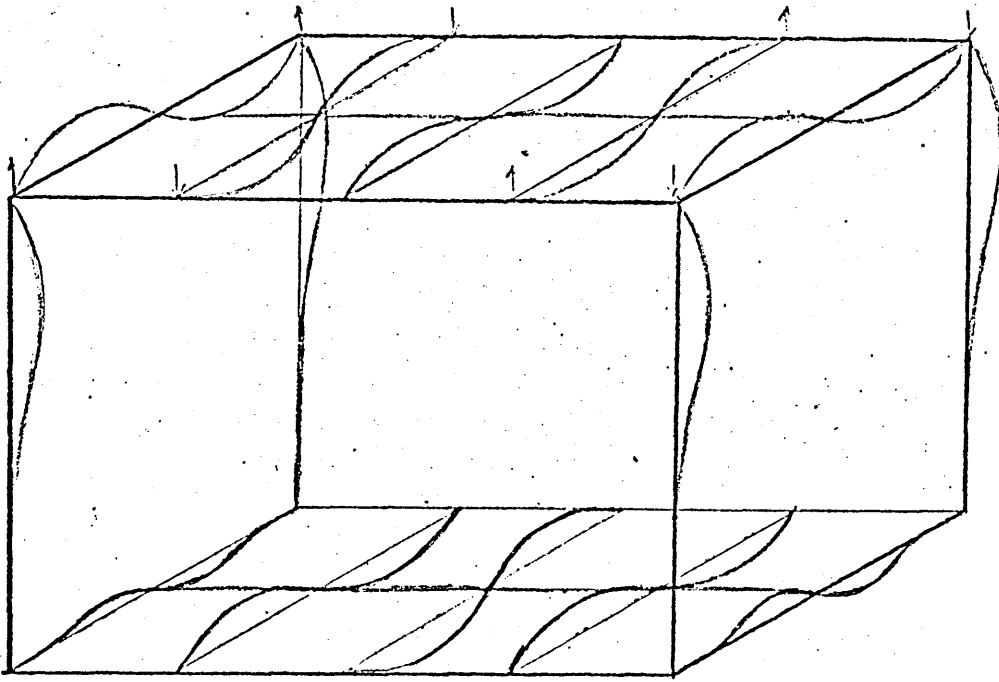


Figure 7.10 19th. and 20th. mode shapes of the box.

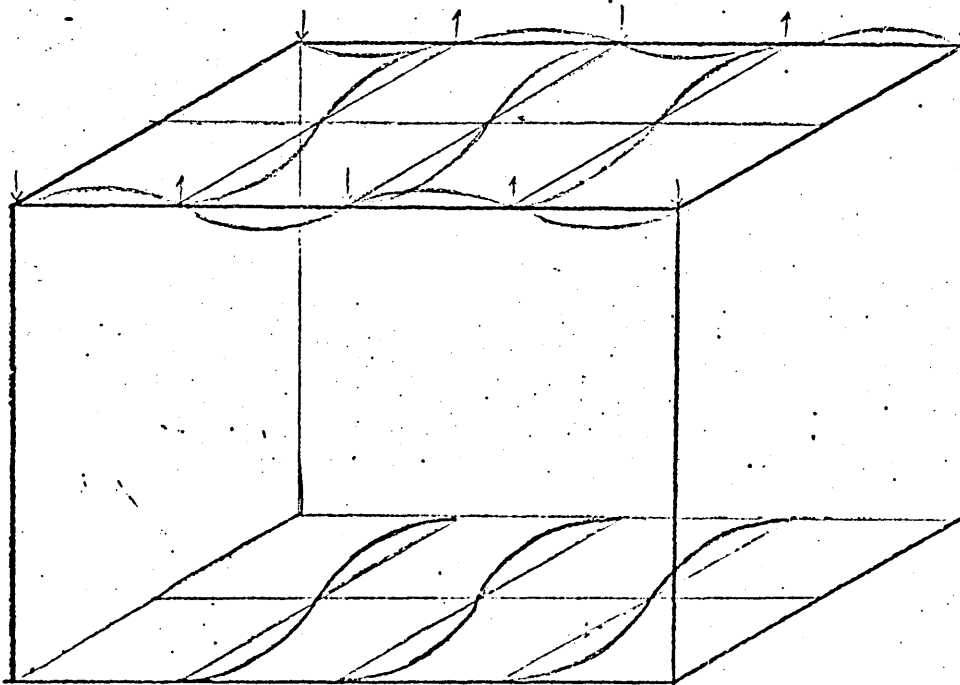


Figure 7.11 21st. mode shape of the box.

The response of the open ended box is presented here in the form of its power spectral density. The excitation used experimentally and simulated on the computer predictions (fig. 7.12) is a filtered PRBS signal applied to the non-contacting exciter probe developed. The results have been obtained using three different techniques for comparison purposes,

(a) using the box receptance as calculated from the natural frequencies and mode shapes predicted by a finite element analysis of the structure, and with the excitation power spectral density and damping factors obtained experimentally.

(b) as obtained using the cross correlation of the excitation and response signals giving the system impulse response function which is Fourier transformed to give the box receptance described in section 3.4. This is then used as in (a).

(c) by narrow band frequency analysis of the vibration response of the box structure using equipment described in chapter 5.

For spectral density calculations because of the symmetry of the problem only a quarter of the top surface of the box is illustrated in fig. 7.13. An average of the results for the other remaining part of the box has been taken because of slight differences obtained possibly due to differences in material composition or incurred during manufacture of the box. The results of the response power spectral density predicted is compared with those obtained experimentally for the seven points on the quarter box as shown in the figure. Less accurate experimental values were obtained along the edges of the box. This may be due to difficulties experienced during the manufacture of the box (a) in the cutting of the plates which make up the sides and in (b) soldering the plates to form the sides at right angles to one another.

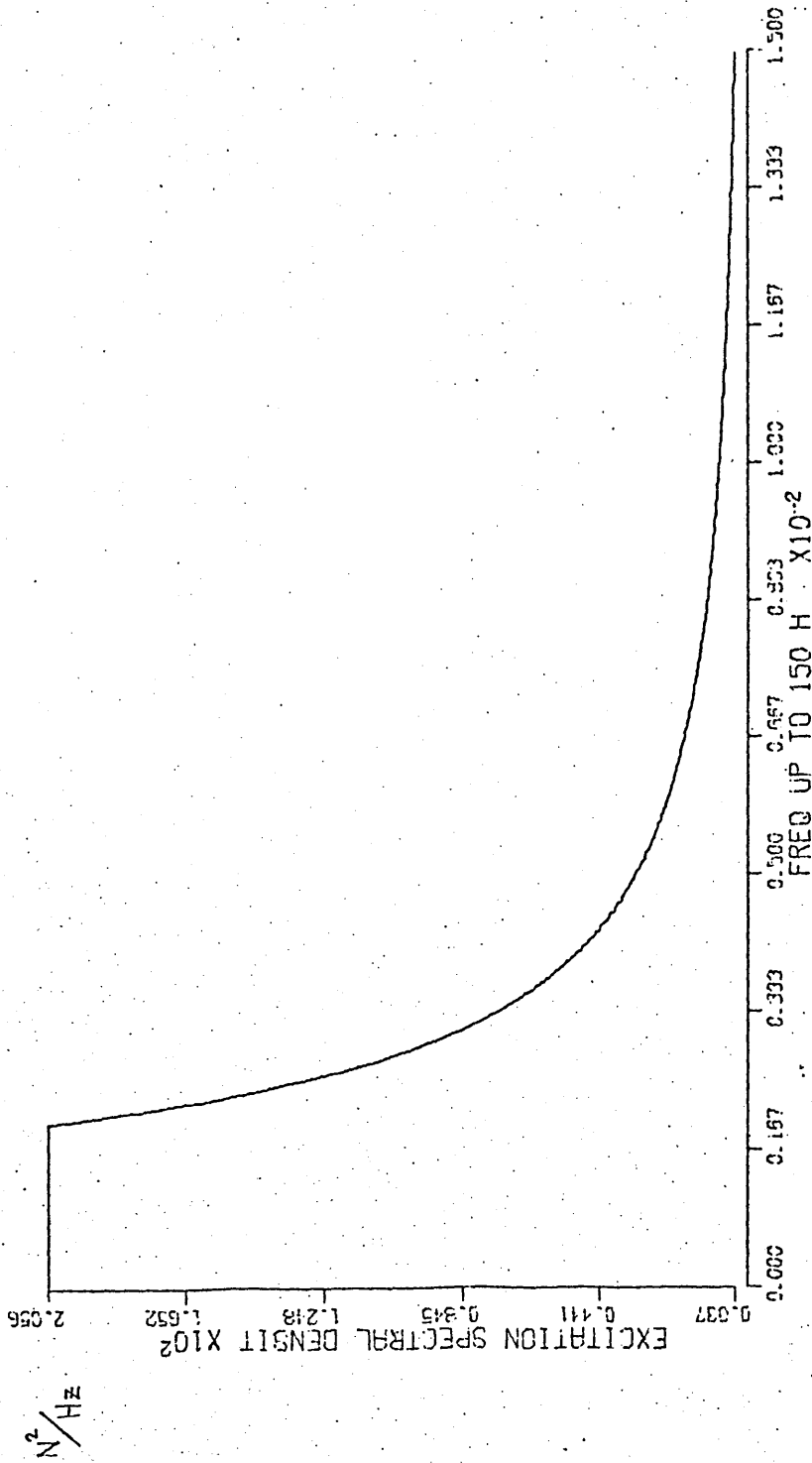


Figure 7.12 The excitation power spectral density used.

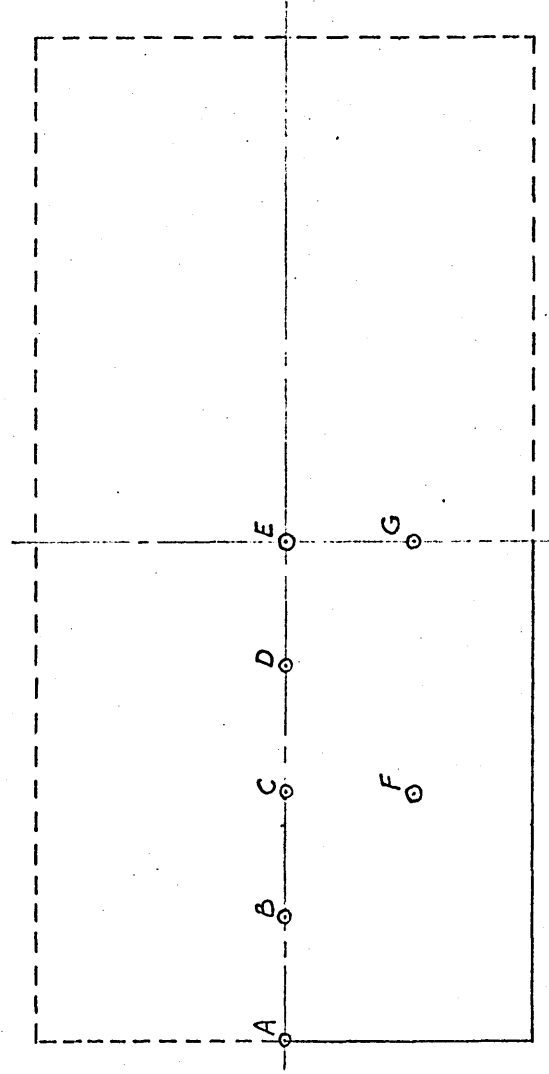
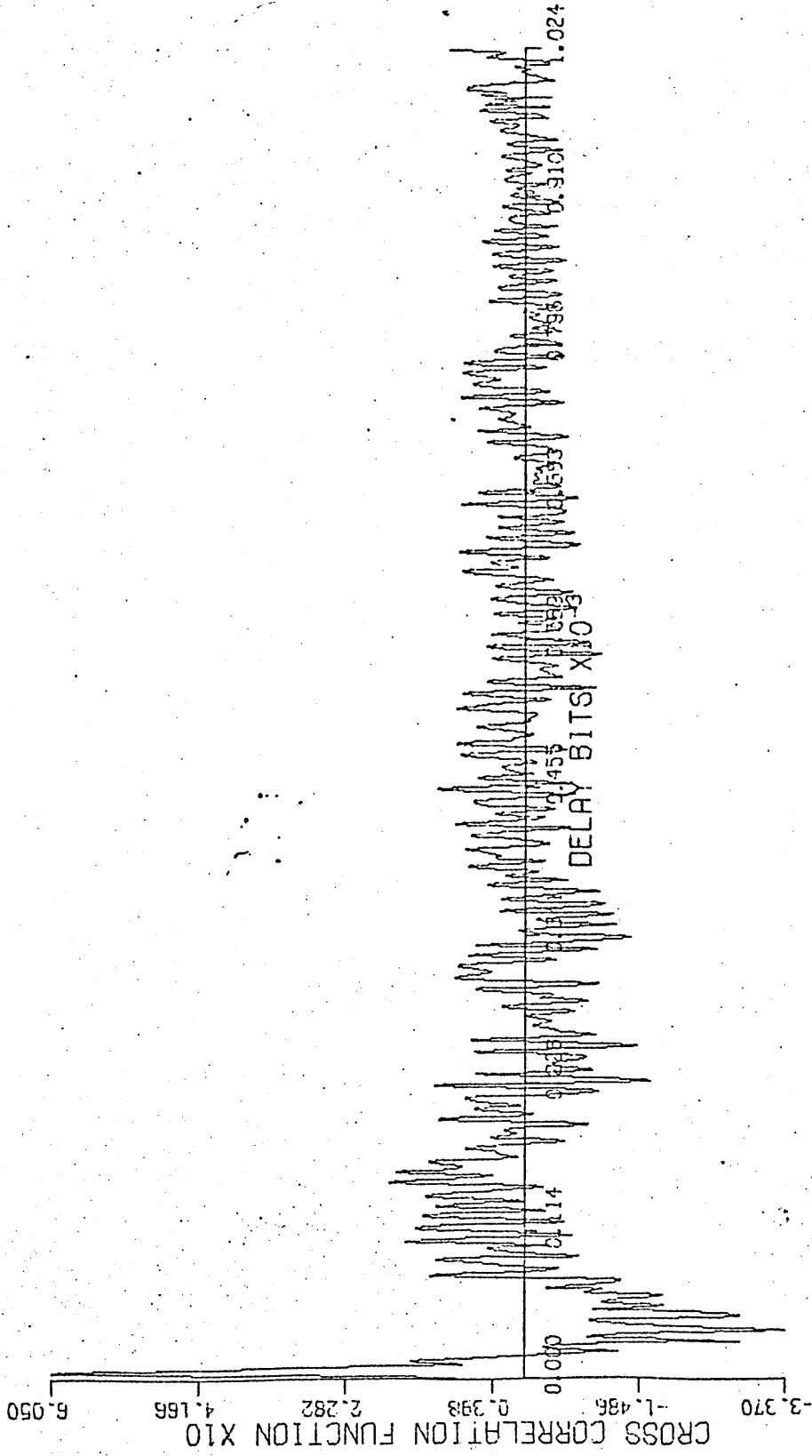


Fig. 7.13 Showing the points for which results are presented.

The excitation signal used in the tests is a PRBS signal with a true RMS level of 0.3 V. The input-output cross correlation function was obtained experimentally in the form of a paper tape to be Fourier transformed on the computer. A typical trace of the impulse response function of the box as obtained during the work is plotted by the Fourier transform program (fig. 7.14 & 7.15). From this the response of the box computed by the computer program is obtained and also displayed on a graph plot. Typical results using various degrees of smoothing for a 512 point function are shown in fig. 7.16 to 7.18 and those for a 1024 point function, fig. 7.19 to 7.21.

Figure 7.22 is a typical trace of the receptance of the box structure calculated from the natural frequencies and mode shapes obtained using a finite element analysis. The PRBS excitation signal is fed into the non-contacting exciter probe for which a typical excitation power spectral density into the box structure as shown in (fig. 7.12) is obtained. This is used in the calculation of the typical box response power spectral density (fig. 7.23) from the receptance obtained.

The response power spectral density of the box to this excitation obtained using the finite element prediction of the box receptance is shown in the chain-dotted lines in fig. 7.24 to 7.30. The full lines in the figures represent experimental results obtained from the cross correlation of the excitation and response signals. Poor results were obtained using direct narrow band frequency analysis of the response signal and are not included in the figures.



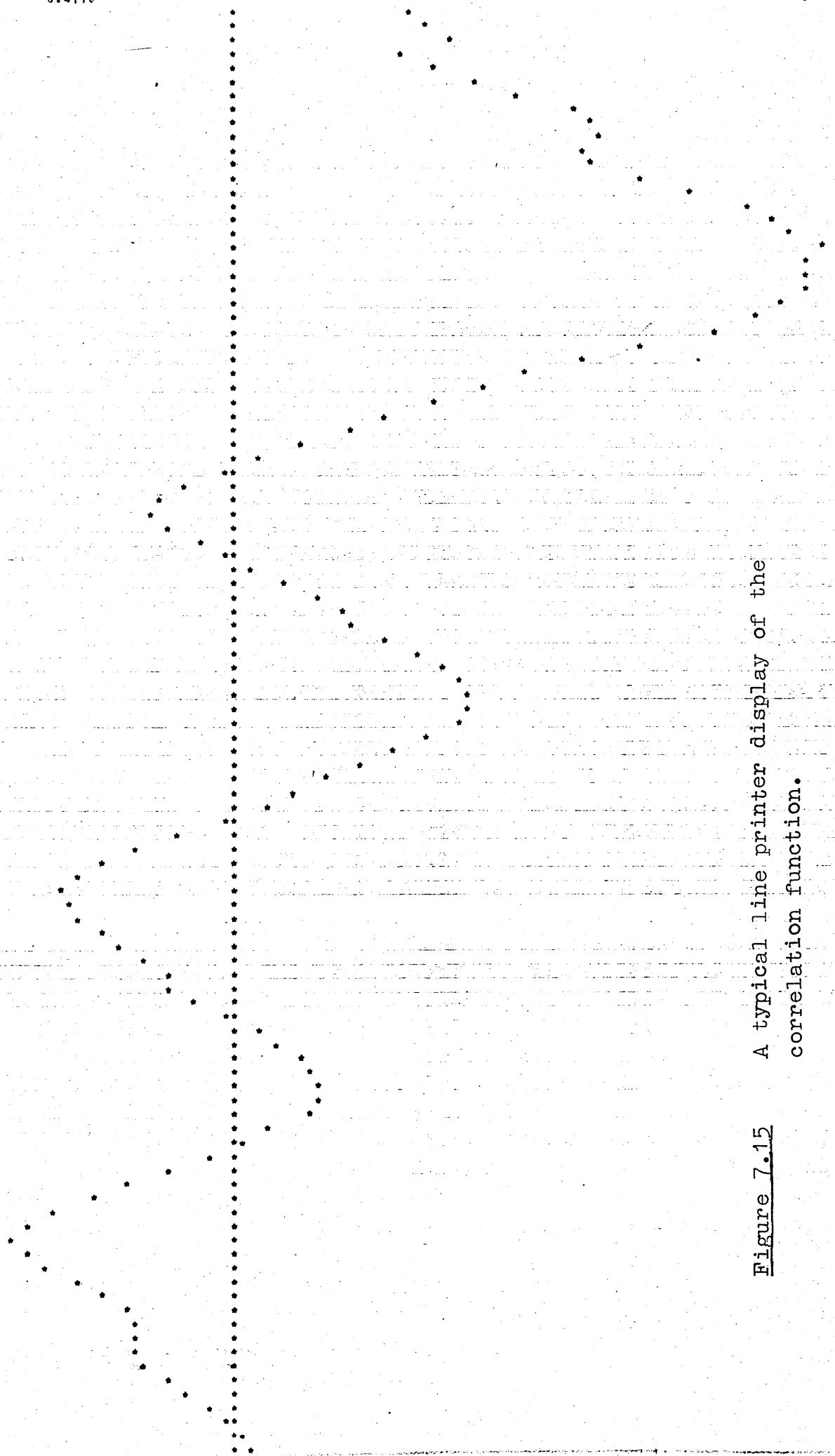


Figure 7.15 A typical line printer display of the correlation function.

0=	2.860F-01
1=	3.150F-01
2=	3.650F-01
3=	2.820F-01
4=	3.330F-01
5=	4.060F-01
6=	4.740F-01
7=	5.650F-01
8=	5.940F-01
9=	6.120F-01
10=	5.790F-01
11=	5.910F-01
12=	6.760F-01
13=	7.690F-01
14=	8.610F-01
15=	9.000F-01
16=	9.290F-01
17=	9.800F-01
18=	9.530F-01
19=	9.590F-01
20=	9.530F-01
21=	9.150F-01
22=	8.800F-01
23=	8.000F-01
24=	6.750F-01
25=	5.800F-01
26=	4.030F-01
27=	4.160F-01
28=	3.310F-01
29=	2.550F-01
30=	1.910F-01
31=	1.110F-01
32=	4.600F-02
33=	-2.000F-02
34=	-8.500F-02
35=	-1.280F-01
36=	-1.350F-01
37=	-1.090F-01
38=	-5.600F-02
39=	-2.100F-02
40=	3.200F-02
41=	8.600F-02
42=	1.440F-01
43=	1.850F-01
44=	1.990F-01
45=	2.440F-01
46=	3.040F-01
47=	3.440F-01
48=	3.680F-01
49=	3.940F-01
50=	3.940F-01
51=	3.770F-01
52=	3.250F-01
53=	2.670F-01
54=	2.060F-01
55=	1.530F-01
56=	1.010F-01
57=	5.300F-02
58=	-1.400F-02
59=	-9.200F-02
60=	-1.650F-01
61=	-2.220F-01
62=	-2.690F-01
63=	-2.880F-01
64=	-2.810F-01
65=	-2.620F-01
66=	-2.300F-01
67=	-1.890F-01
68=	-1.500F-01
69=	-1.170F-01
70=	-1.050F-01
71=	-6.700F-02
72=	-1.100F-02
73=	4.100F-02
74=	7.500F-02
75=	1.100F-01
76=	1.290F-01
77=	1.390F-01
78=	1.390F-01
79=	1.180F-01
80=	6.000F-02
81=	1.000F-02
82=	-4.800F-02
83=	-1.100F-01
84=	-1.830F-01
85=	-2.420F-01
86=	-3.110F-01
87=	-3.550F-01
88=	-3.700F-01
89=	-3.540F-01
90=	-3.150F-01
91=	-2.630F-01
92=	-2.200F-01
93=	-1.850F-01
94=	-1.700F-01
95=	-1.700F-01
96=	-1.660F-01
97=	-1.490F-01
98=	-1.160F-01
99=	-8.200F-02
100=	-4.500F-02
101=	-1.900F-02
102=	1.100F-02
103=	3.100F-02

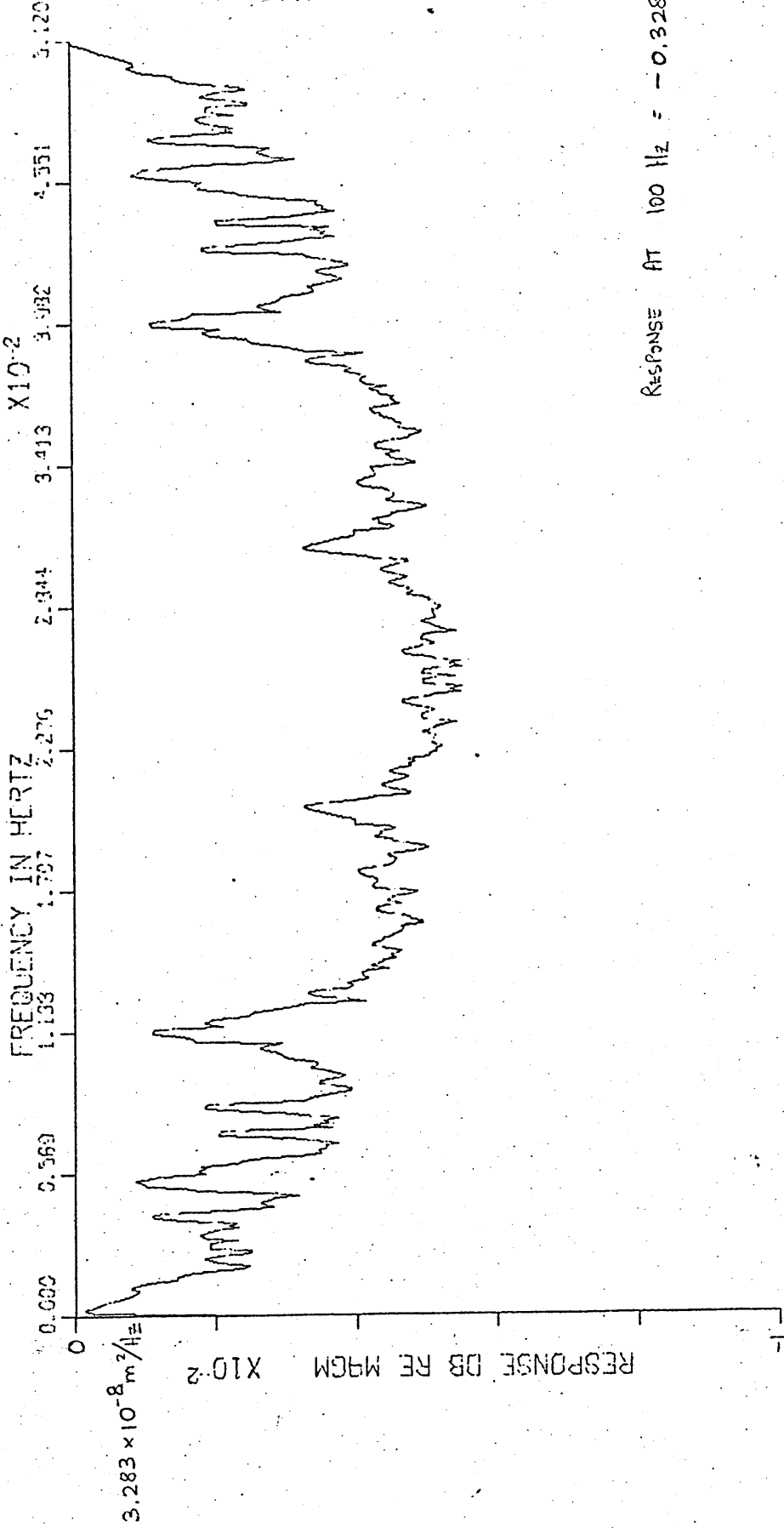
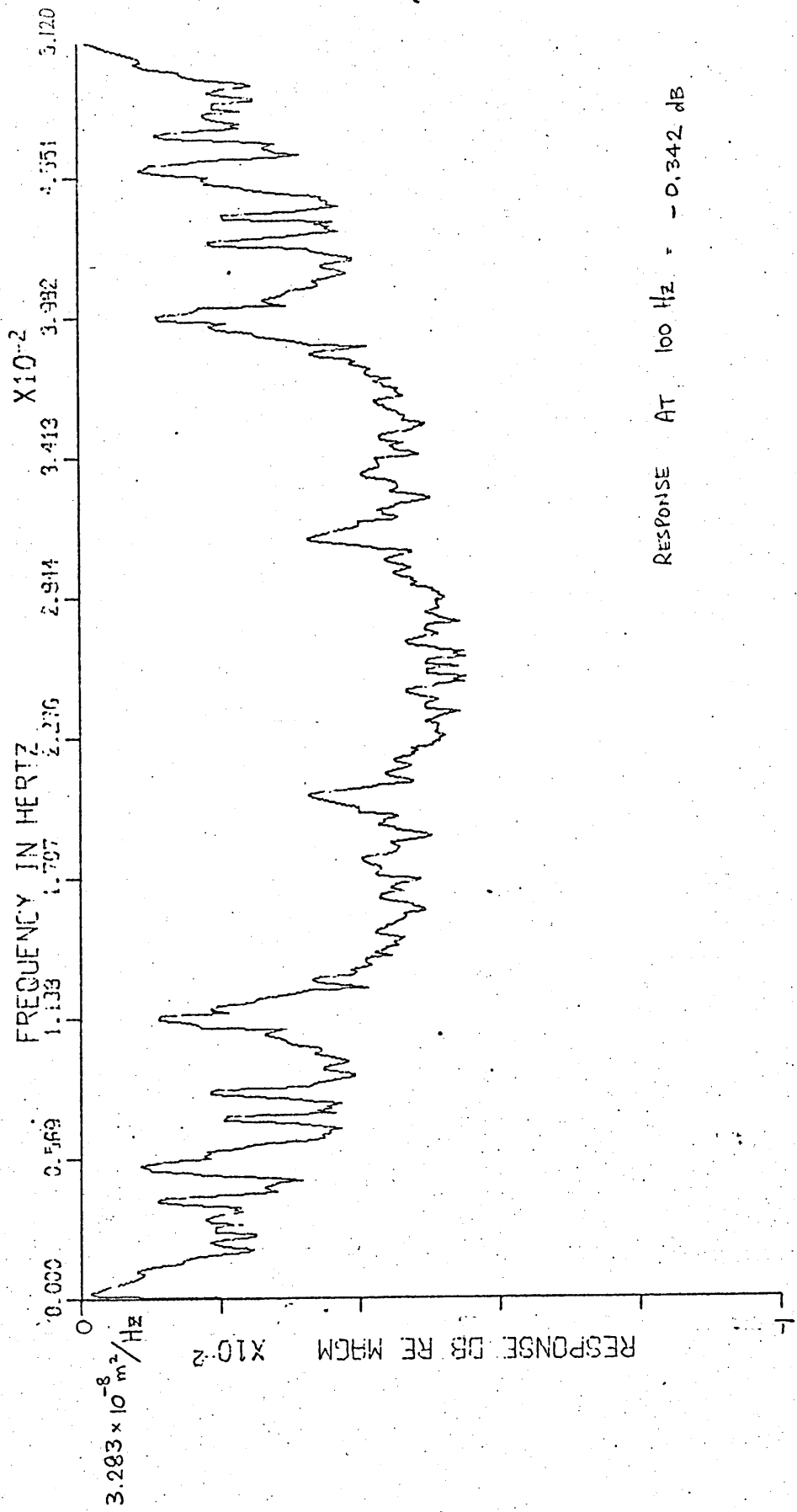


Figure 7.16 Box response to random excitation from the 512 point correlation function (non smoothed).



RESPONSE AT 100 Hz = -0.342 dB

Figure 7.17 The 512 point response PSD curve using a three point smoothing.

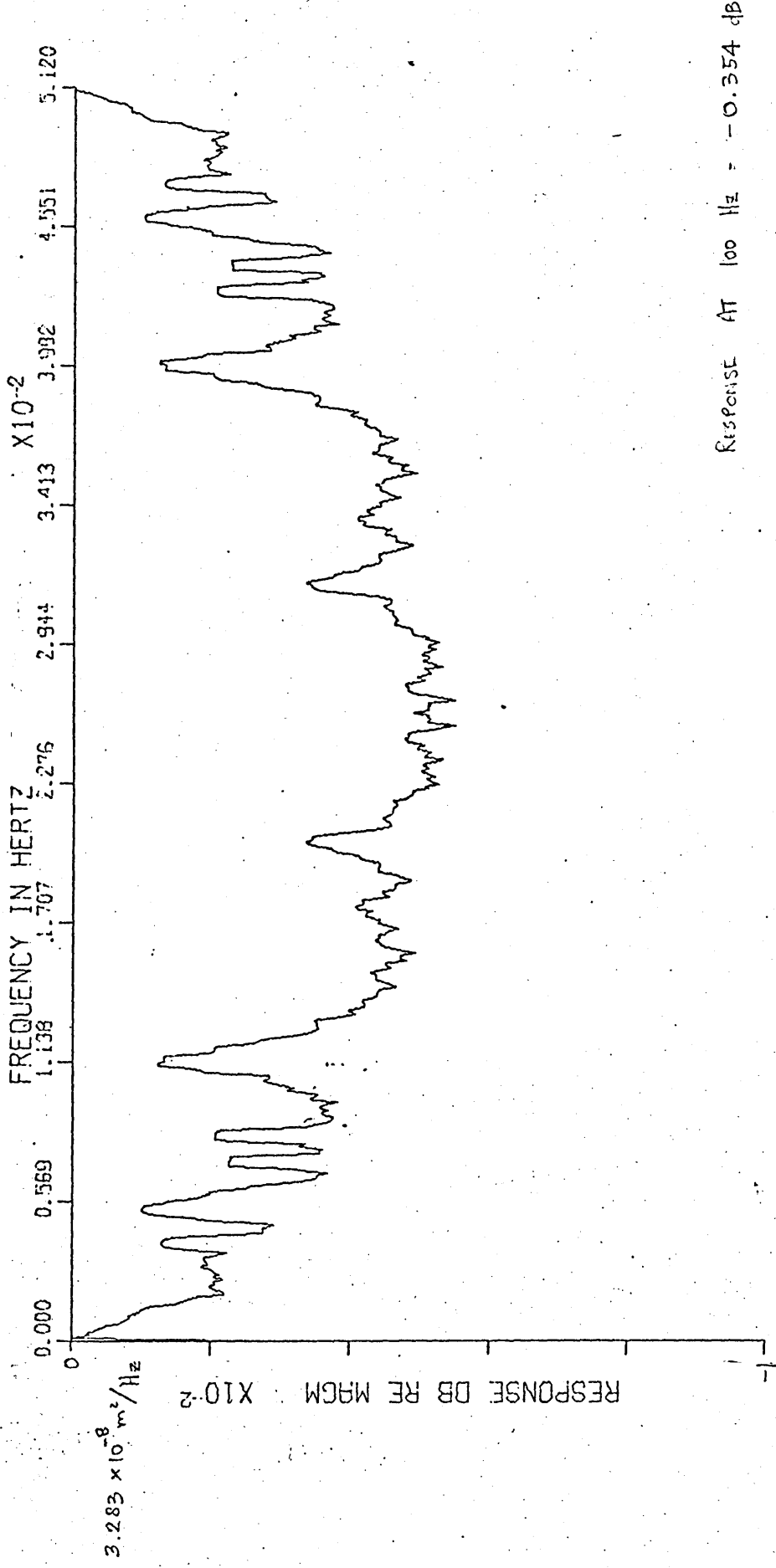
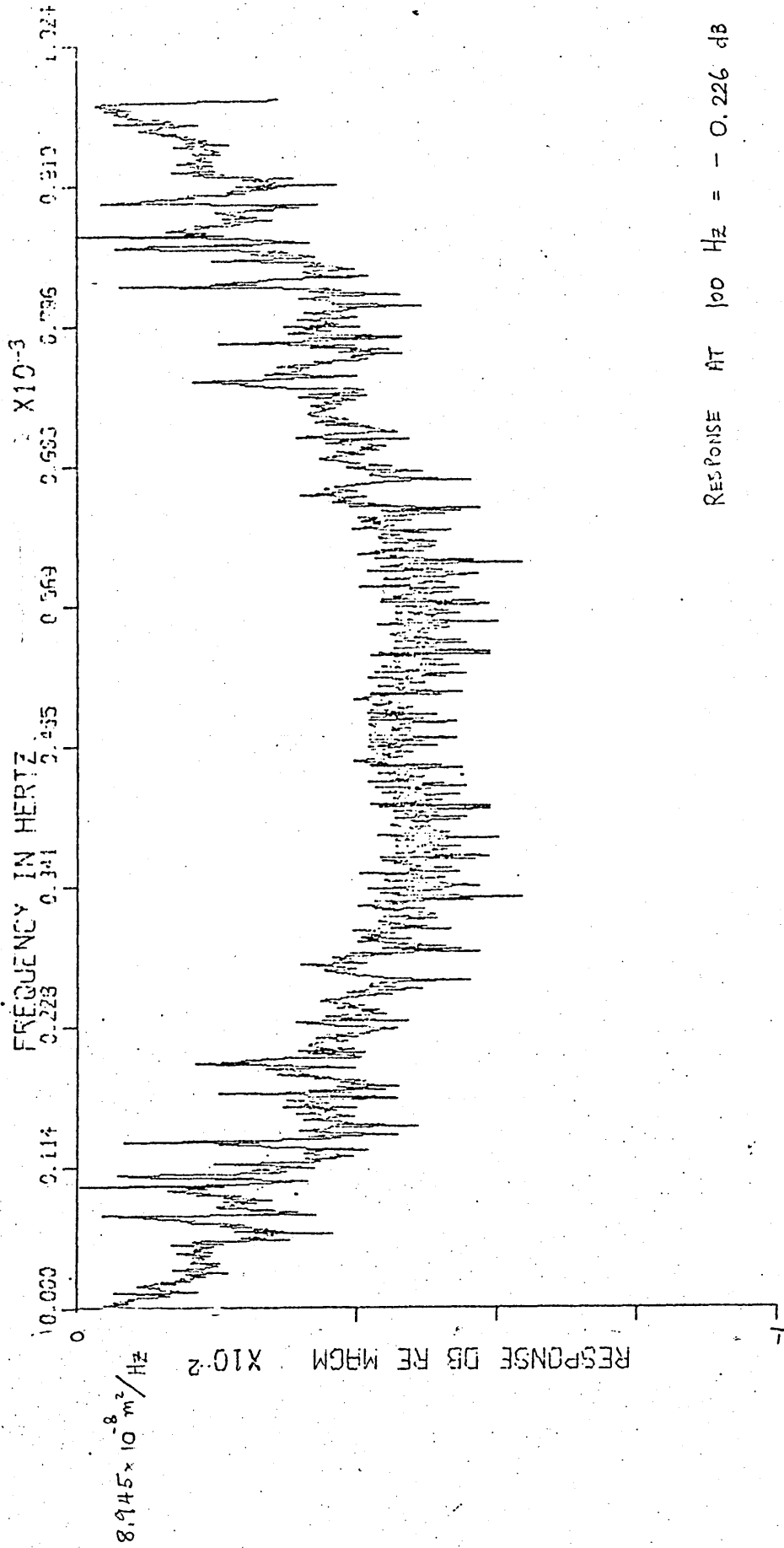


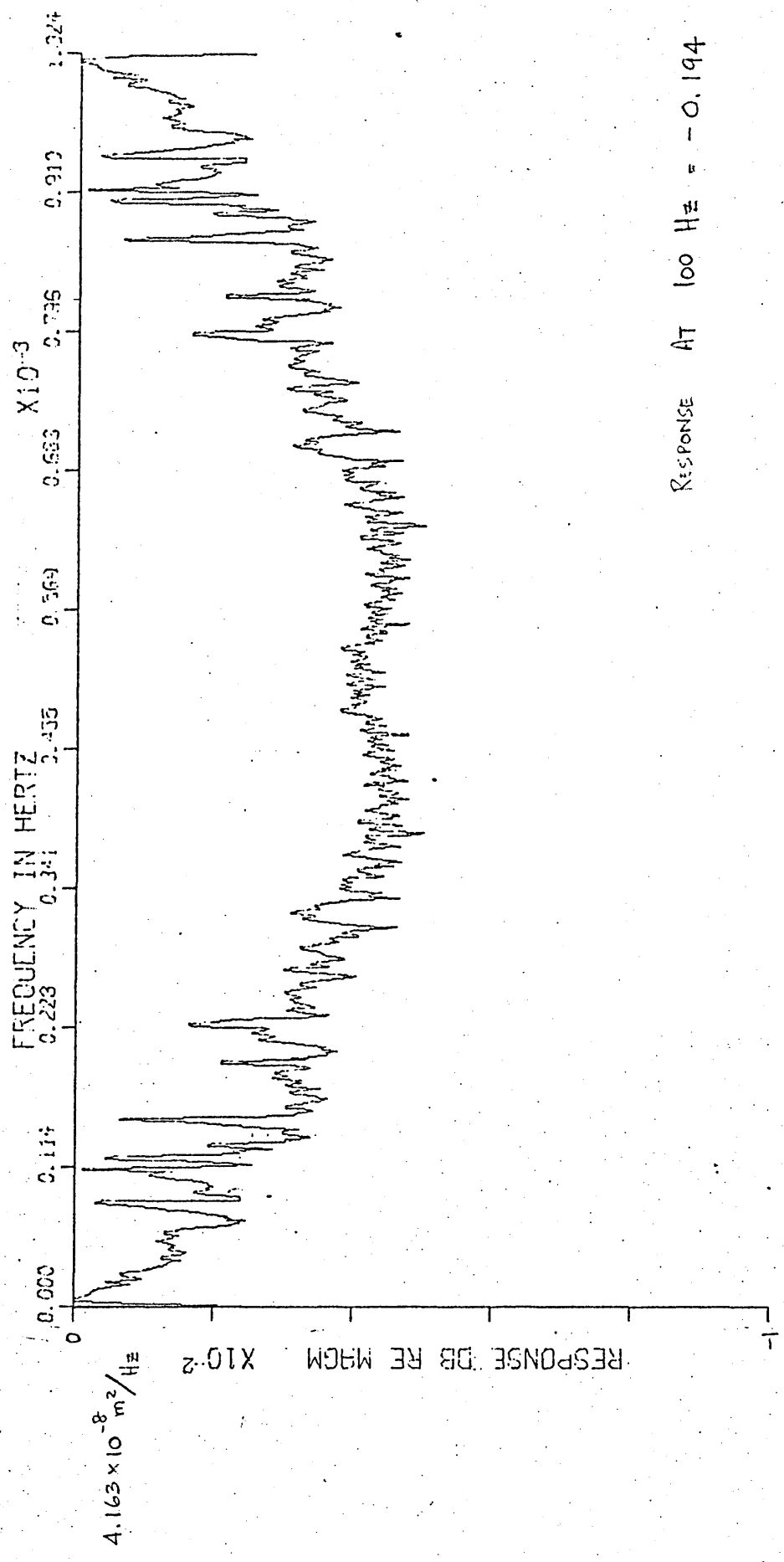
Figure 7.18 The 512 point response PSD curve using a five point smoothing.



RESPONSE AT 100 Hz = - 0.226 dB

Figure 7.19

A graph of a nonsmoothed 1024 point response power spectral density computed.



RESPONSE AT 100 Hz = -0.194

Figure 7.20 The 1024 point response PSD curve using a three point smoothing.

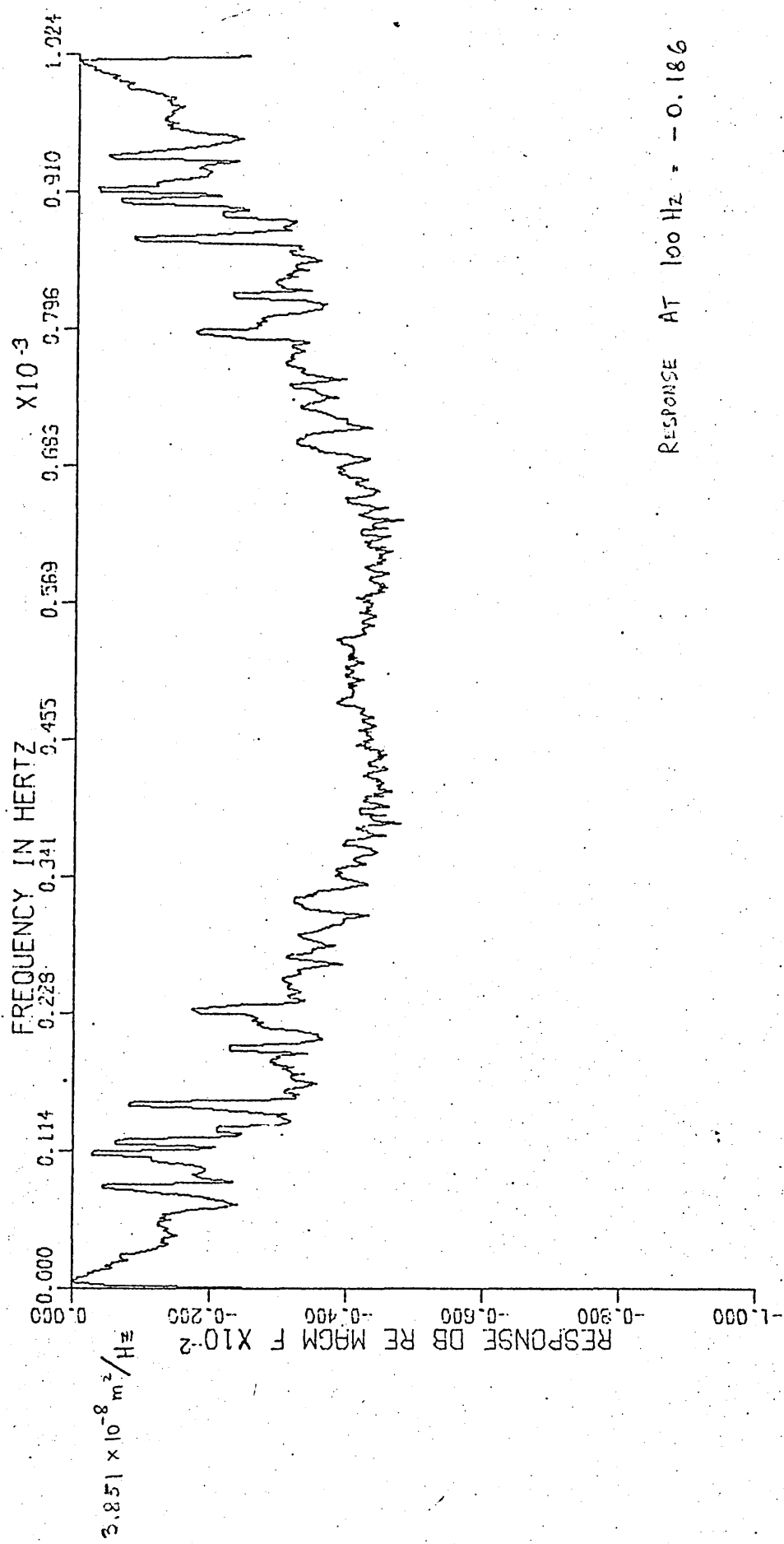


Figure 7.21 The 1024 point response PSD curve using a five point smoothing

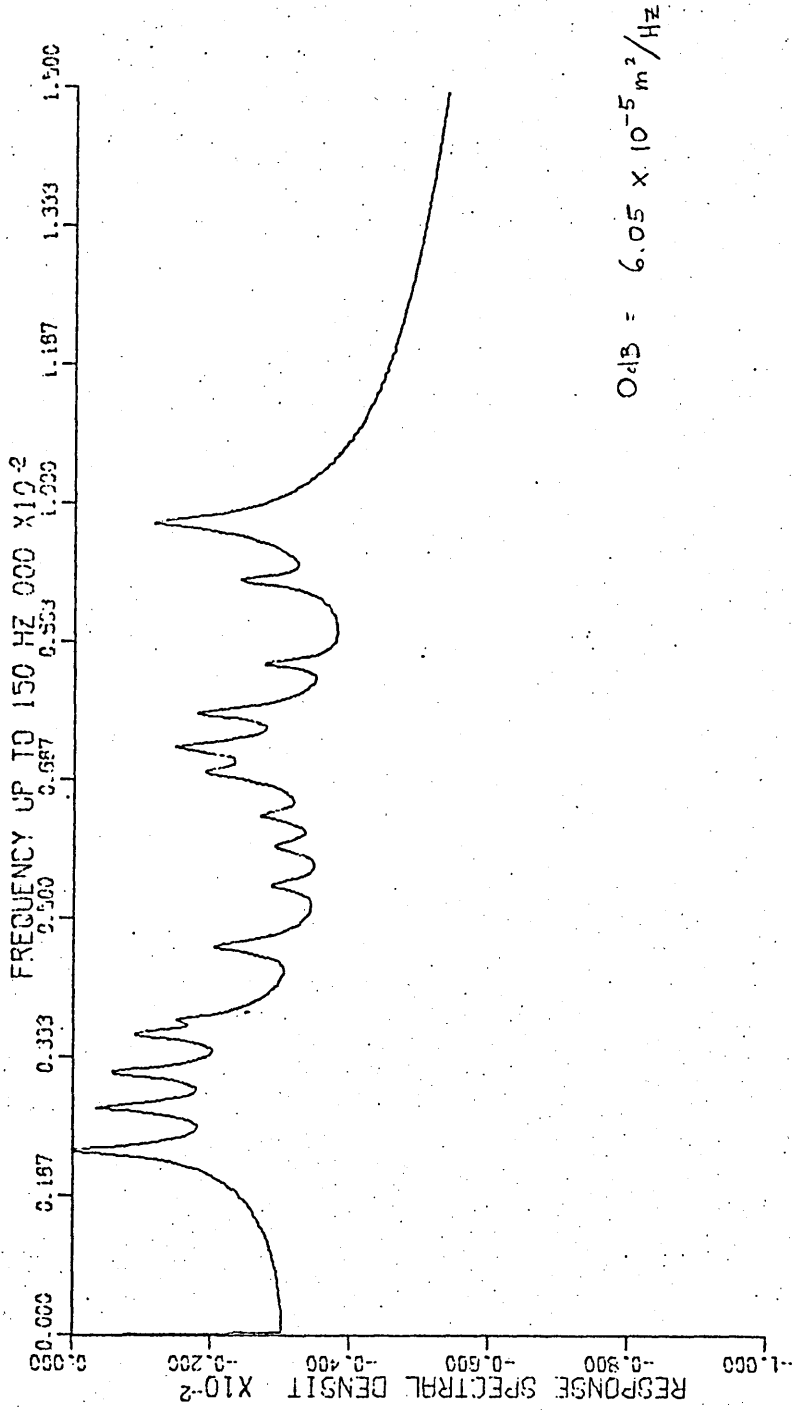


Figure 7.22 A plot of the typical box receptance² calculated using finite element results.

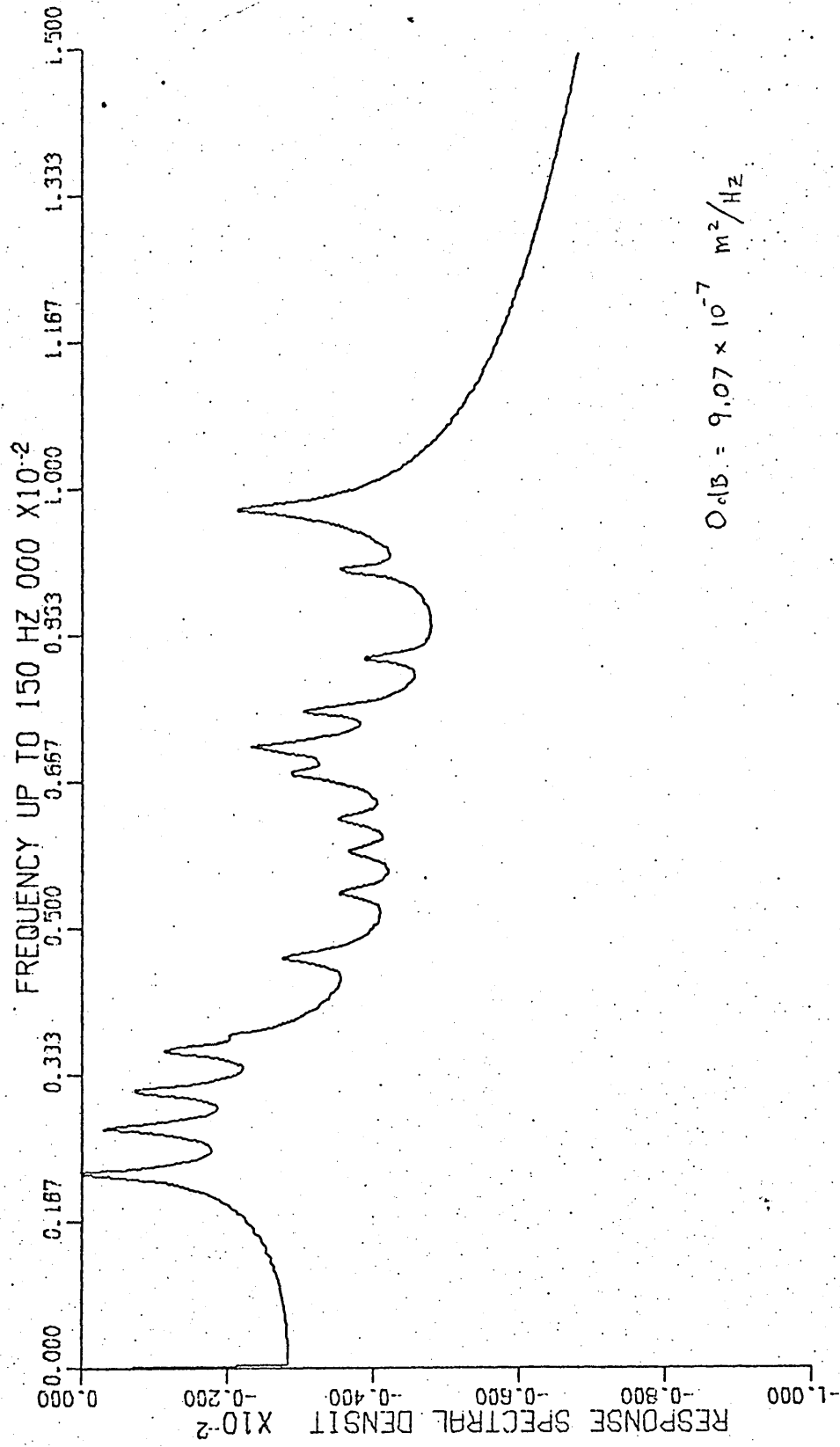


Figure 7.23 A typical response power spectral density calculated using the finite element results.

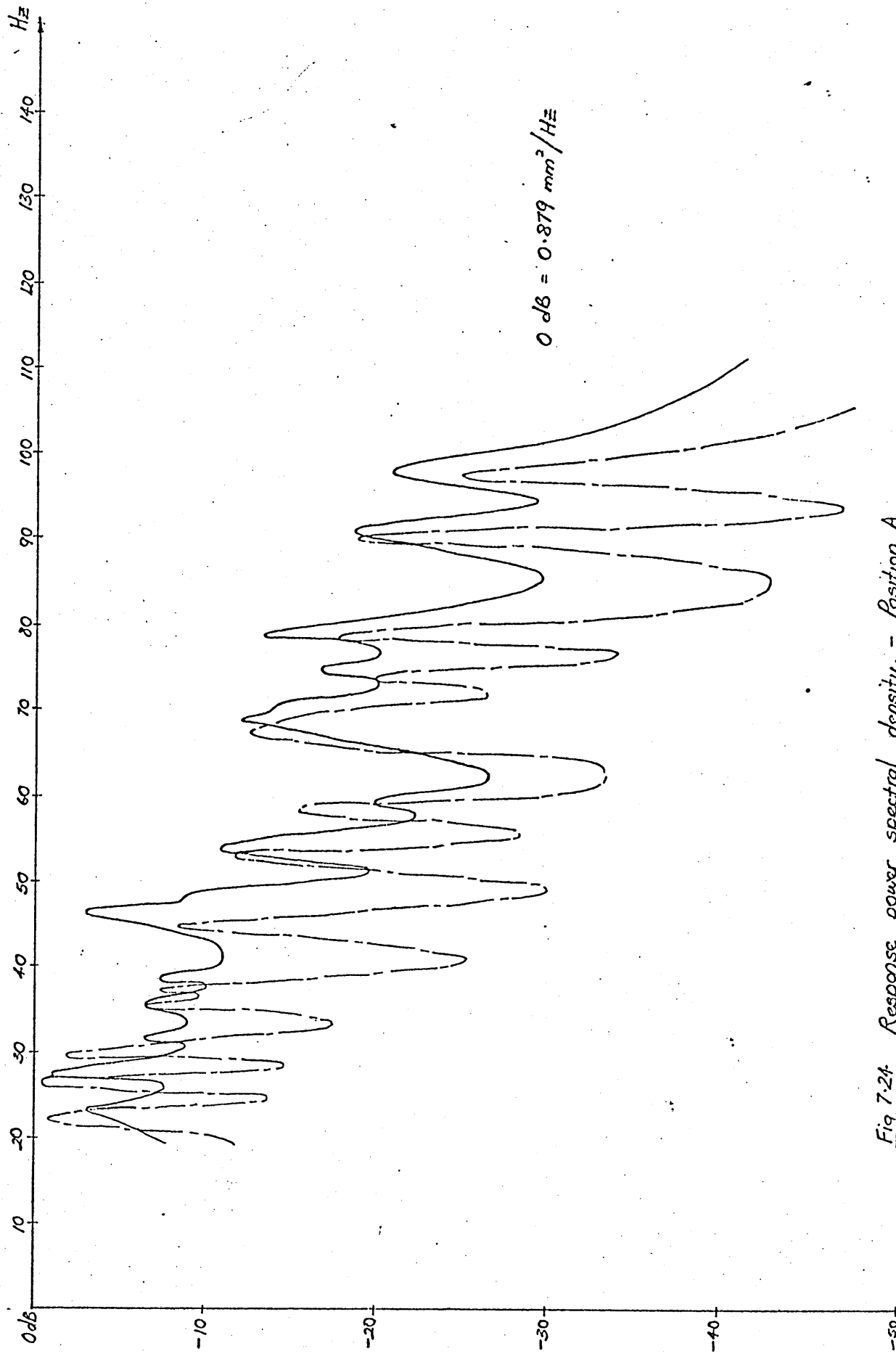


Fig 7.24 Response power spectral density. - Position A

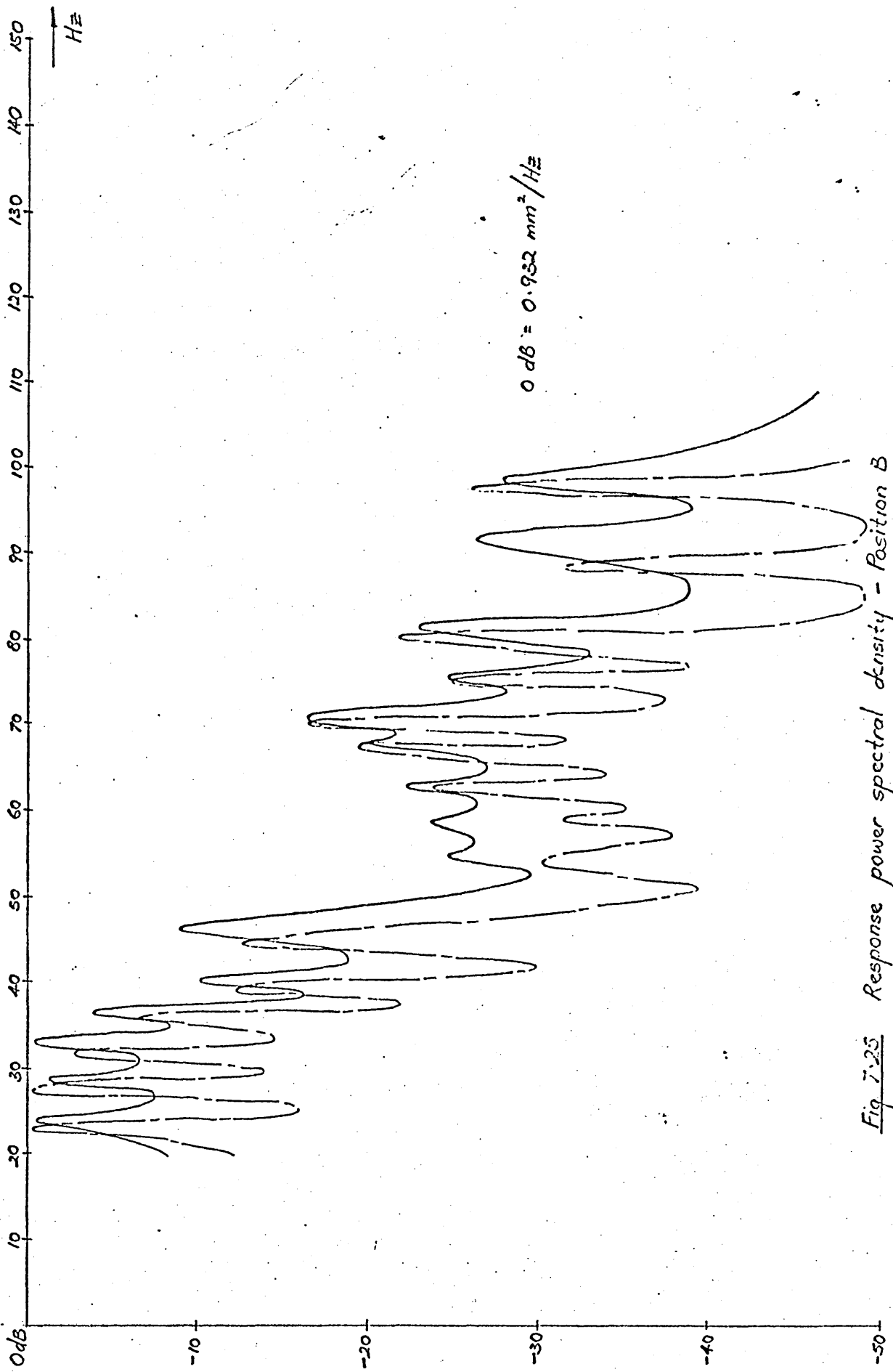


Fig 7.25 Response power spectral density - Position B

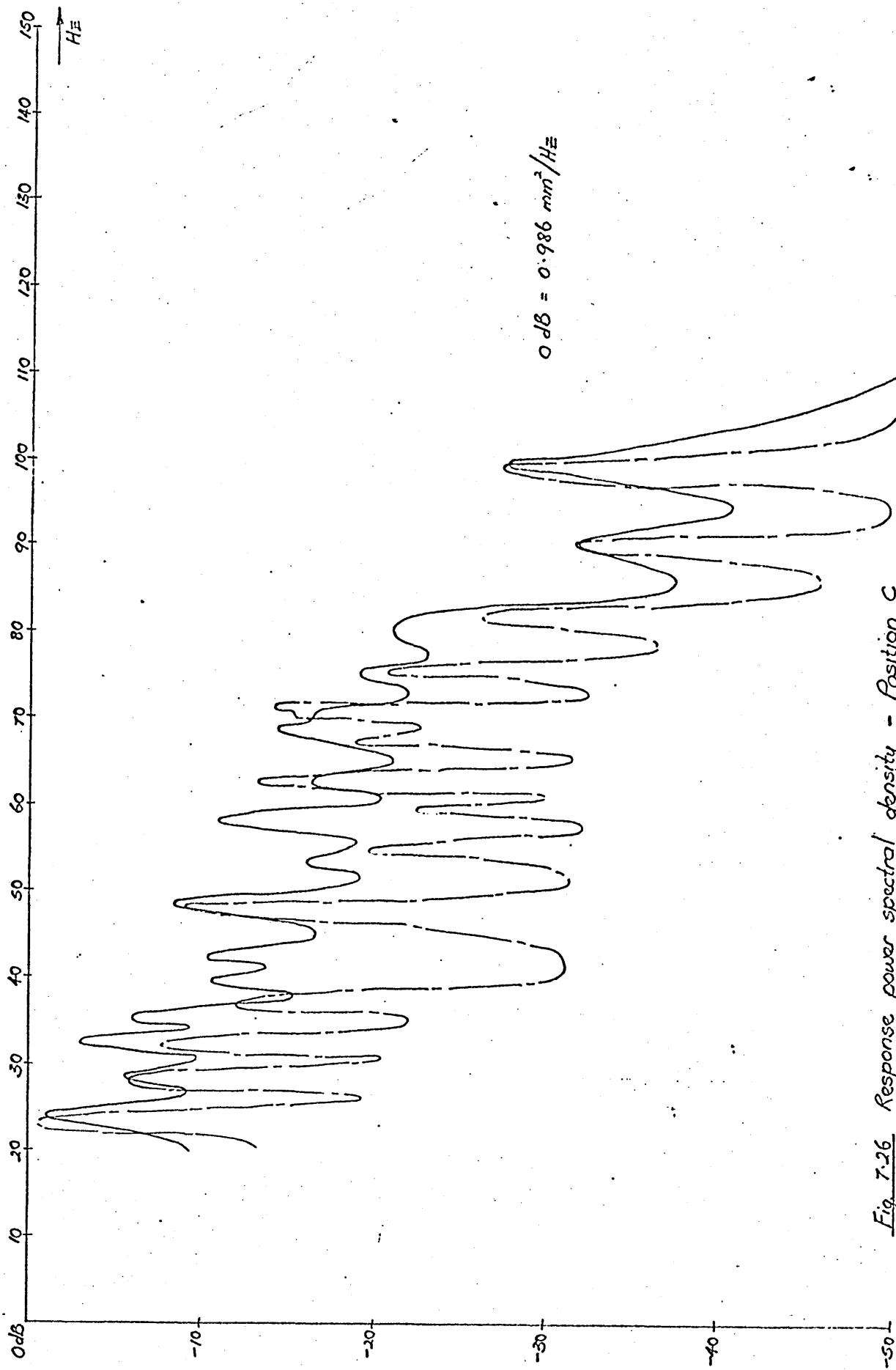


Fig. 7-26 Response power spectral density - Position C

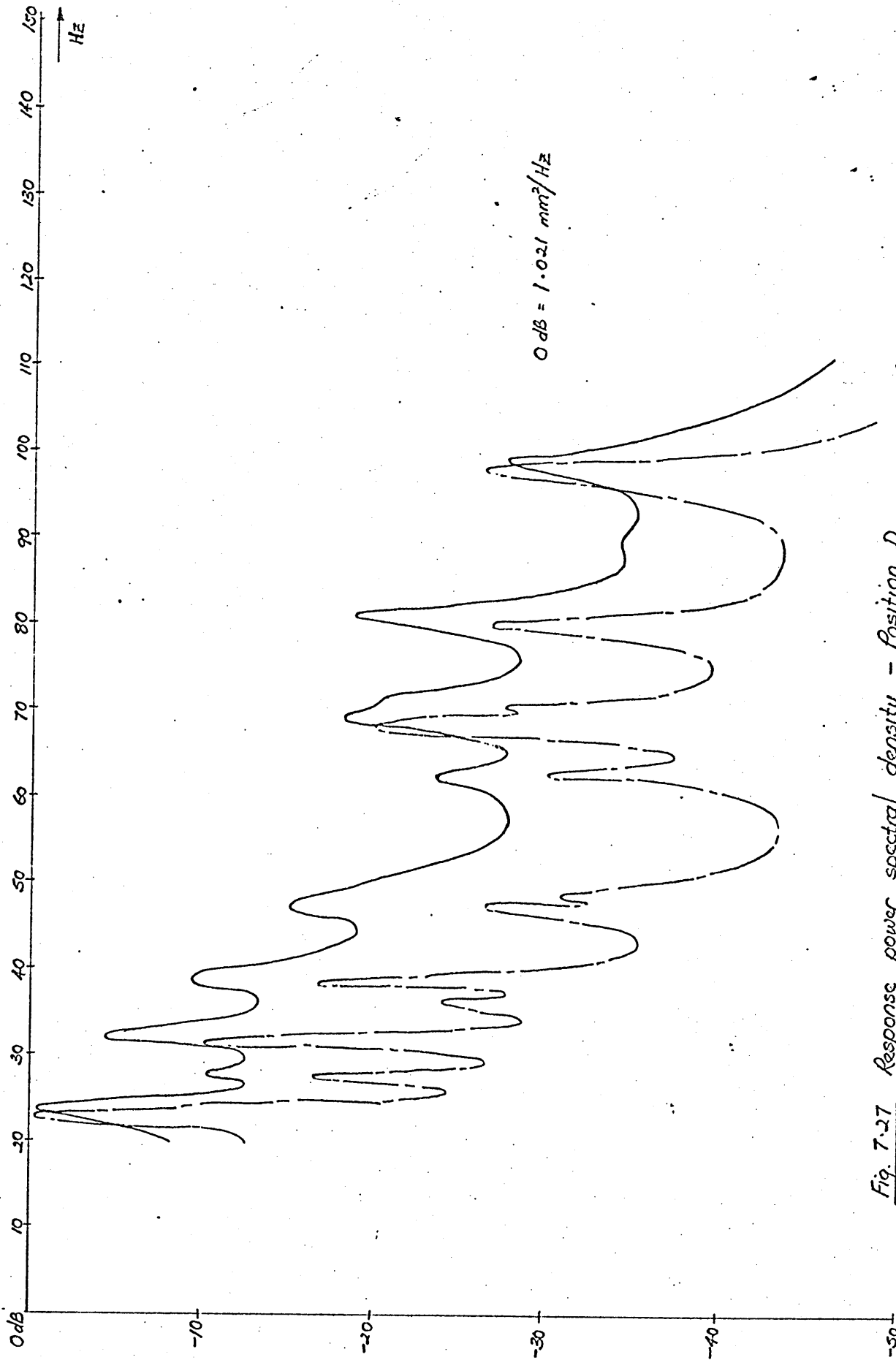


Fig. 7.27 Response power spectral density - Position D

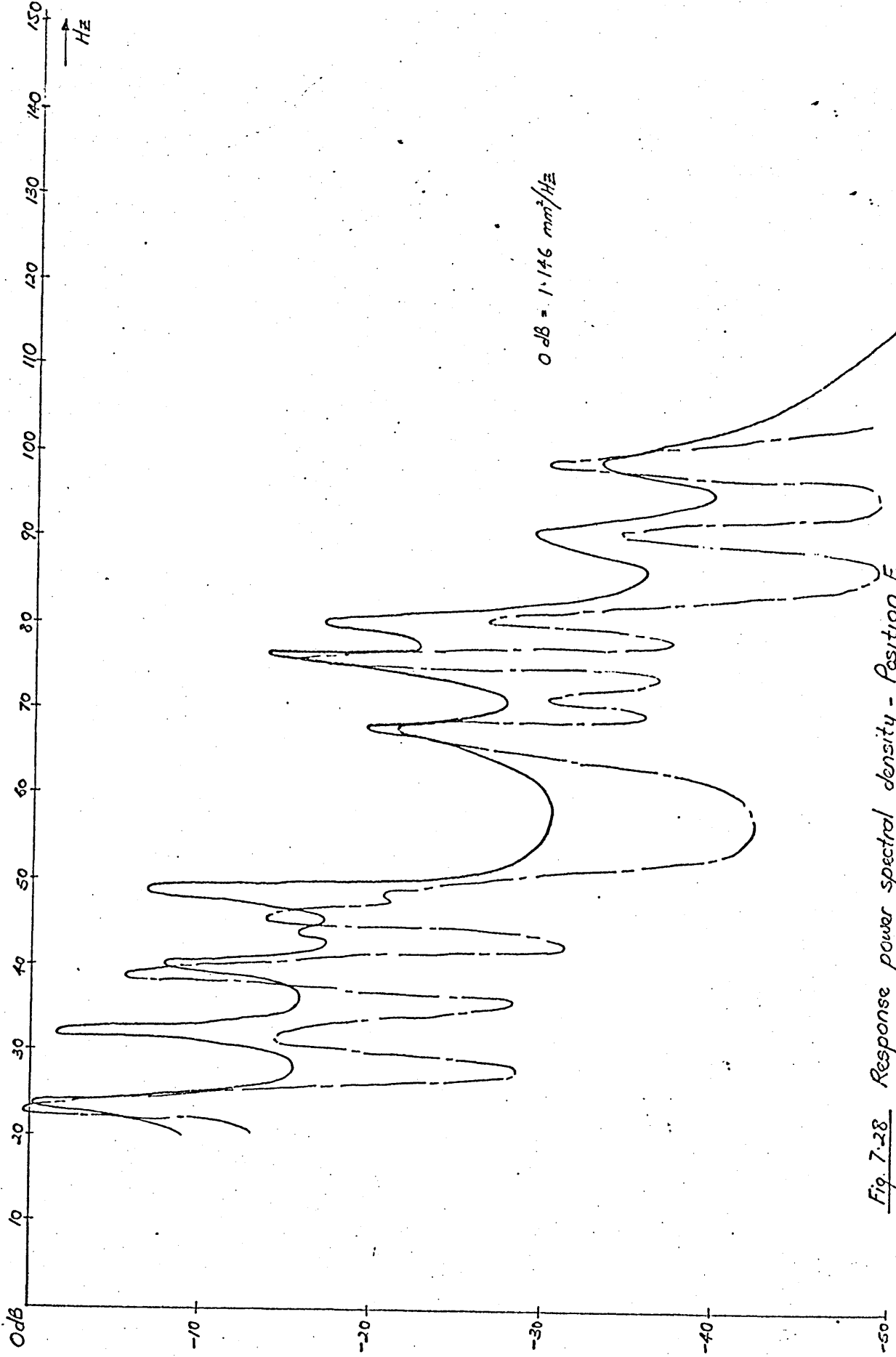


Fig. 7.28 Response power spectral density - Position E

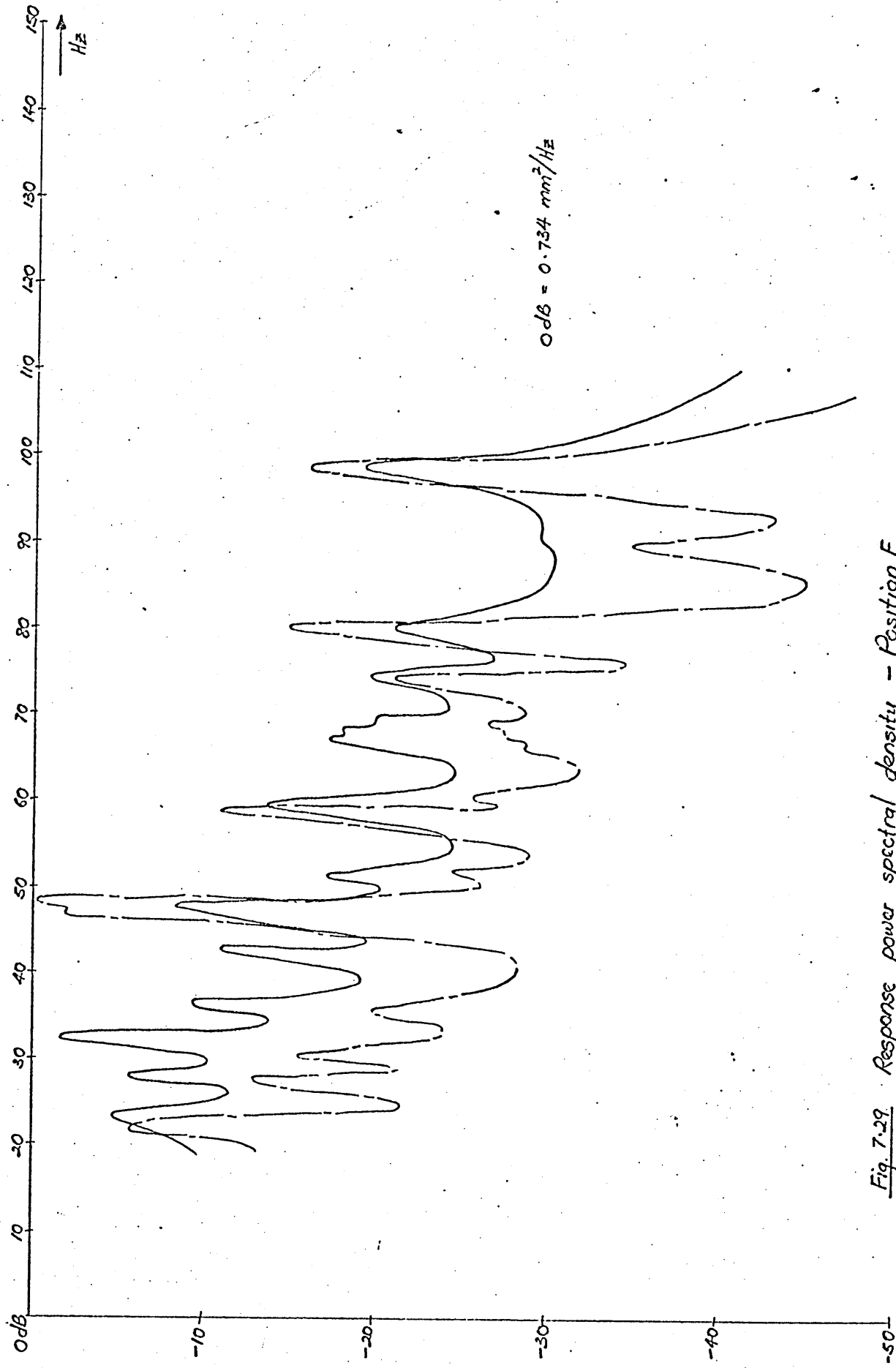


Fig. 7.29 Response power spectral density - Position F

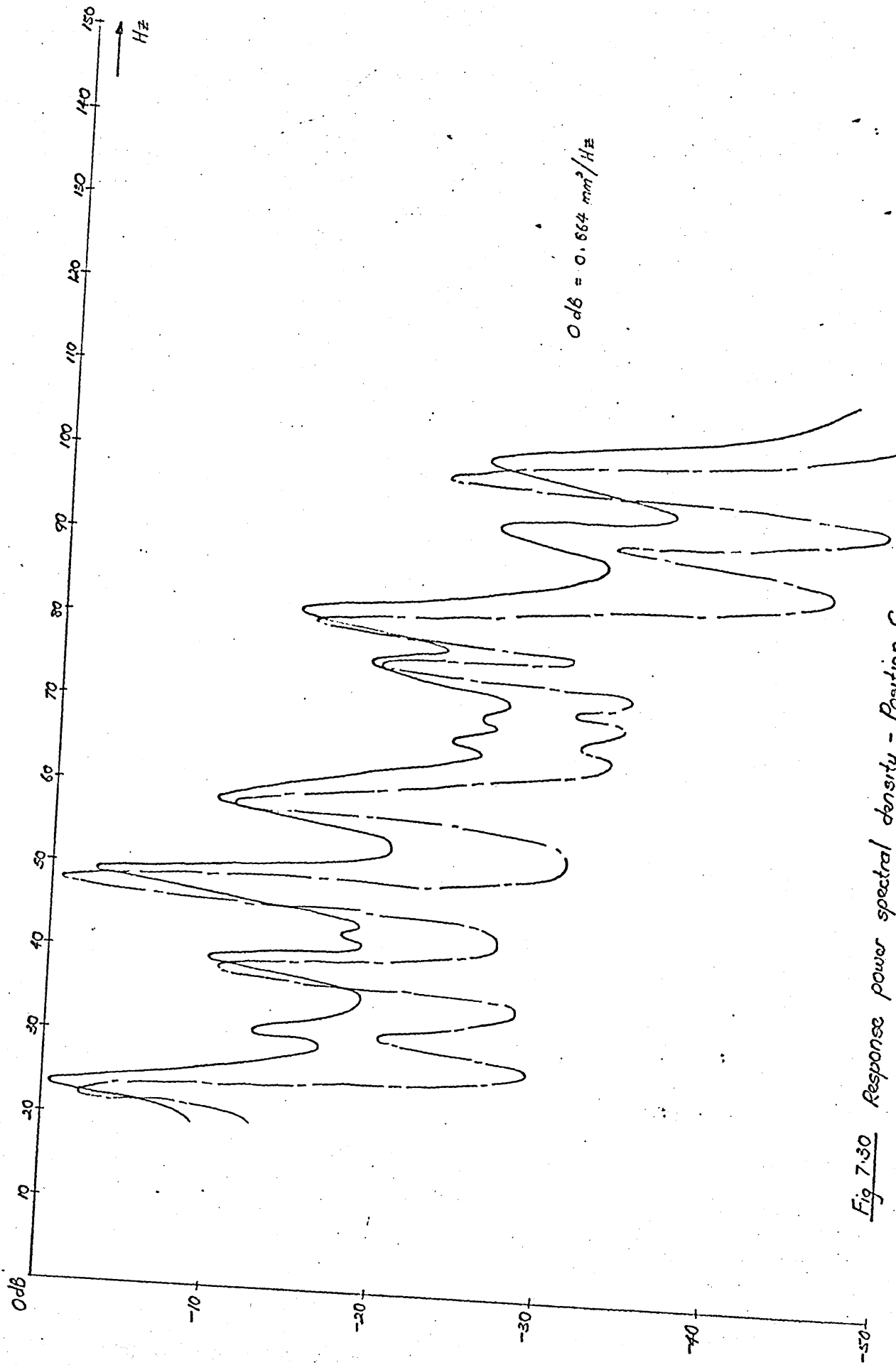


Fig 7.30 Response power spectral density - Position G

From the results given in the previous chapter it will be seen that the techniques chosen for this work in the analysis of folded plate box type structures have worked satisfactorily. The finite element method has been successfully applied to predict natural frequencies, and mode shapes and used to predict the power spectral density of the response of the box structures to random vibration. This is compared with actual experimental values obtained. The techniques used in the experimental investigation using the equipment developed during this project provides results which form a close basis of comparison with the predicted values.

Using the finite element method of analysis, the natural frequencies and the corresponding mode shapes were obtained for the simple beam, plate as well as the box structure. The finite element prediction of their natural frequencies were found to be within 5 % of the experimental values obtained. The computer program suite developed to analyse the box structure consists of seven subprograms each reading off information from the previous from a magnetic disc file, using it, and then writing the new information back to the file for the next subprogram. This strategy was found to be suitable for such a complex structure because of the reduced computer core requirements and the provision of built in checks at the end of each stage. Any errors can be detected and the computation stopped and corrected without the computation going on until the very end.

The analysis of the box structure for its natural frequencies and normal modes using the finite element method even in the relatively crude model chosen gave results which compare well with those obtained experimentally. This shows that the choice of the method for the analysis of this type of structure is well justified. Also the simple four node rectangular element used with its twelve degrees of freedom in bending and eight degrees of freedom in stretching is shown to be adequate for the range of frequencies investigated as is

the coarse mesh employed. The finite element method often gives a lower bound solution but in general this is not known unless conforming elements are used [50]. Although theoretically the accuracy obtained in such an analysis is expected to converge to the exact solution as the mesh size is refined, this is limited by the size of the computer storage available. Refinement of mesh size requires increased computer storage that rapidly become prohibitive especially in a dynamic analysis where two large matrices, the mass and the stiffness matrices have to be manipulated simultaneously. Some existing techniques for reducing the size of these matrices are reviewed in Appendix 2. The simplest way of reducing the mass matrix is to use lumped masses but this may lead to some lowering of accuracy (Zienkiewicz [20]). Techniques such as substructuring and reduction of degrees of freedom by condensation also allow the larger problems to be fitted onto the smaller computers using backing store but at the expense of increased computing time.

Methods considering only the transverse degrees of freedom (Vysloulch et al [51]) have been tried. More recently the use of reduced numbers of degrees of freedom per node eg. by using loof elements (Irons [52]) or relaxed continuity elements (Patterson & Heng [53]) have been developed.

Despite the disadvantage of the tapering shape of the force spectrum produced, the closeness of agreement between natural frequencies and mode shapes predicted and actual experimental values justifies the use of the non-contacting exciter/pickup probe developed since contacting transducers may shift the natural frequencies or distort the corresponding mode shapes obtained. The overheating and frequency doubling effects of the non-contacting exciter have been overcome although the lower force output at the higher frequencies may lead to inaccuracies in that region. It is anticipated that this frequency dependance caused by what is basically an inductance circuit may be overcome using an active resistance-capacitance circuit in parallel with the exciter probe. In the present work this was not done and in the prediction of the response

power spectral density of the box, this was taken into account in the specification of the input power spectral density. The non-contacting vibration pickup probe would probably be more accurate than conventional contacting ones especially on the light structures investigated. It was found that this capacitance probe was fully applicable over the frequency range, gap distance and amplitudes of vibration used.

In the use of discrete excitation to measure natural frequencies and mode shapes of the box structure, the closeness of the higher modes and the necessarily low level of excitation to maintain linearity allowed only the lower natural frequencies and mode shapes to be easily identifiable. Also because the tests were performed in a laboratory situated close to a busy main road, considerable extraneous noise was detected which may excite resonance modes adjacent to the one under investigation. The upper frequency limit chosen of 100 Hz was found to be sufficient, containing over twenty modes and furthermore it became difficult to distinguish between several adjacent modes which were closely bunched together just above 100 Hz. The ascertainment of mode shapes required repeated measurements taken at a sufficiently large number of points on the structure to determine the resonance mode. This became increasingly tedious especially at the higher modes.

The correlation technique has been used to give the impulse response function from which the receptance of the box system is obtained. The calculation of the cross correlation function, although more practicable than measuring the structural impulse response function, is often both time consuming and laborious. The use of the PRBS signal considerably eases the calculations and yet retains the requirement of being random white noise for the correlation calculations. Also its parameters are easily set to approximate a random signal in its frequency content, excitation amplitude and probability distribution and yet is completely repeatable. The PRBS correlation method used to obtain the receptance of the box structure gave frequencies within 5 % of the predicted values. In some cases especially at the higher frequencies it is perhaps more reliable than those obtained using sine wave

tests because extraneous noise is eliminated during the correlation phase. Because of this and despite the generally lower level of the excitation signals used, whilst agreeing with the frequencies obtained by the sine sweep test to within 1 %, the clear superiority of the correlation technique employed is illustrated in its giving consistent results throughout in the calculation of the response power spectral density. The use of the automatically recorded cross correlation function on the PRBS system built up, considerably eased a task which took up to nine hours for a 1024 point correlation. This also enabled better results to be obtained, taken overnight during the quieter late evenings, and early mornings.

The FFT computer program which calculates the receptance of the structure from its impulse response function is completely general and can be used for beam plates or box structures. Data input is chosen to be in the form of paper tape which is easily stored and also is not easily shuffled unlike the more conventional data cards. The provision of output in the form of drawings as well as values on the line printer gives an accurate and fast means of checking both input data as well as calculated values. Graph plots are also produced for ease of storage and display purposes.

The natural frequencies and mode shapes of the box calculated using the finite element method was used to derive the receptance of the box structure using experimentally obtained damping factors. Calculation of receptance from natural frequencies and mode shapes obtained using the finite element method, is carried out using

$$|\alpha(if)|^2 = \frac{\sum_r [w_r(x_A)]^2 [w_r(x_B)]^2}{M_r^2 [16\pi^4 \{ (f_r^2 - f^2)^2 + \eta_r f_r^4 \}]} \quad (8.1)$$

Although only the top surface of the box structure is considered, the method is however applicable to all sides of the box taking each side in turn. Only natural frequencies up to 100 Hz were considered and therefore the 21 natural frequencies and mode shapes in that region are used. For the

calculation of α only these natural frequencies and mode shapes play an important part; higher ones have a negligible contribution. This part of the finite element computer program is completely general; beams, plates and boxes may be analysed by the input of its natural frequencies and mode shapes at specified points and corresponding damping factors. The excitation power spectral density produced by the non-contacting exciter probe was not a flat one despite the use of a substantially white PRBS signal. This also had to be taken into account in the computation.

The response of the box type structure is obtained in the form of its power spectral density, using equation (8.2)

$$S_d(\omega) = |\alpha(i\omega)|^2 S_p(\omega) \quad (8.2)$$

This is commonly used in the calculation of response mean square value, probability distribution, etc. in random work. The response power spectral density of the box structure obtained experimentally compares satisfactorily with the predicted values especially in the lower frequency region. In this region the predicted response power spectral density agrees with the experimental values obtained to within 1 dB (about 25 % difference). At the higher frequencies however the predicted results appear to be attenuated. Average discrepancy between predicted spectral density values and actual values here are in the region of 4-5 dB. This may perhaps be caused by the following:

- (a) slight differences (up to 5 %) between computed and actual natural frequencies (since the computed natural frequencies were used in the prediction of the response power spectral densities),
- (b) the lower excitation output at the higher frequency region by the non-contacting probe and therefore greater interference effects,
- (c) inaccuracies involved in the manufacture of the box, and
- (d) a review of the damping assumptions used may also be applicable.

The apparatus, techniques employed and computer software developed during this project forms a convenient point from which extension to a two exciter investigation of random excitation of light folded plate box type structures may be carried out. Although a PRBS signal is used, a true random signal is easily substituted if a suitable correlator is available. Also from equation 8.2 the analysis is not limited to that of a flat excitation spectrum. The design of a compact exciter pickup probe resulted in measurement of excitation and response at the same point of the structure. Again the analysis is also applicable to investigations where the structure is excited at one point and measured at a different point.

Plate 1 The original vibration table.

Table 1

the original impression table.

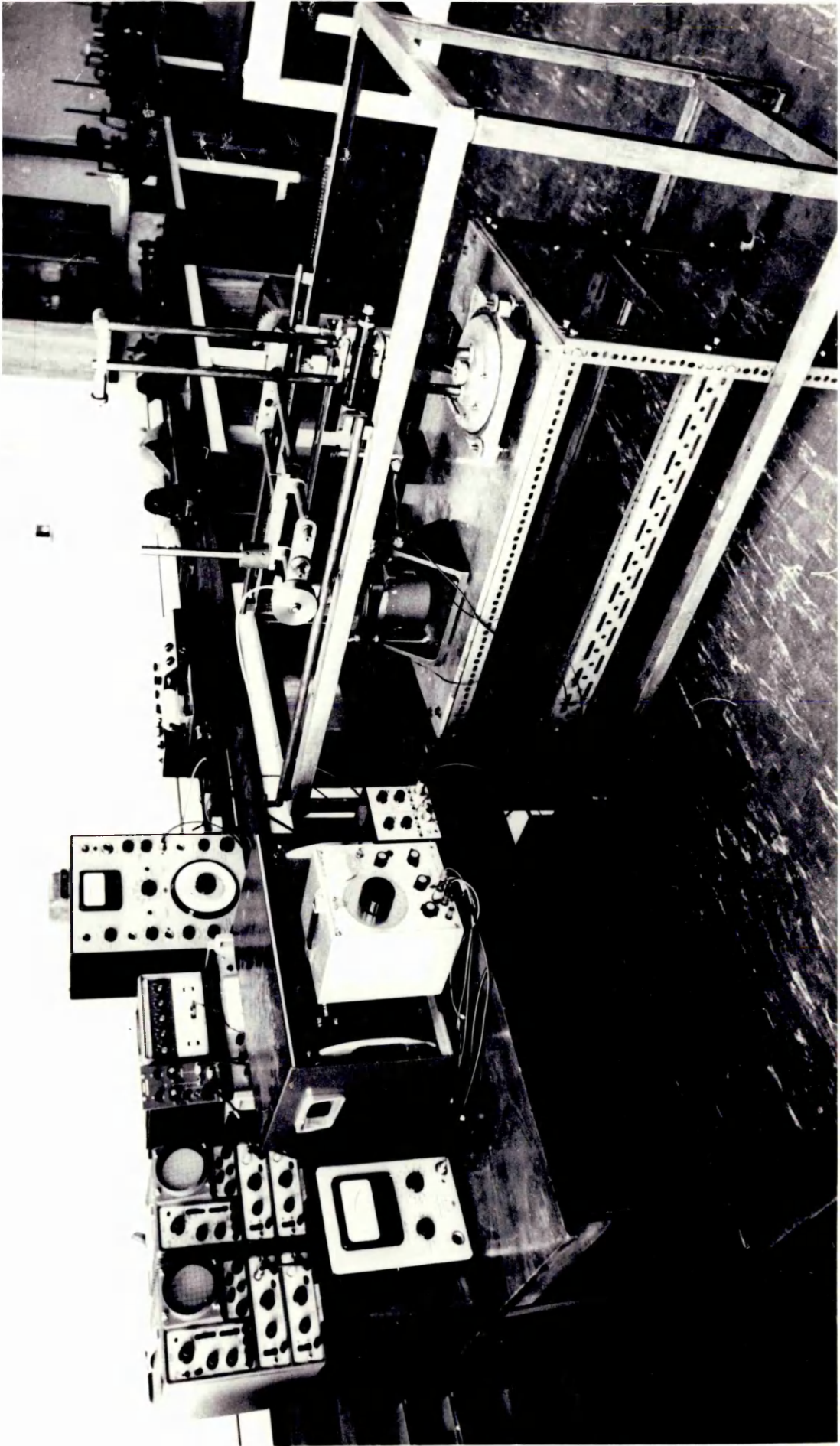
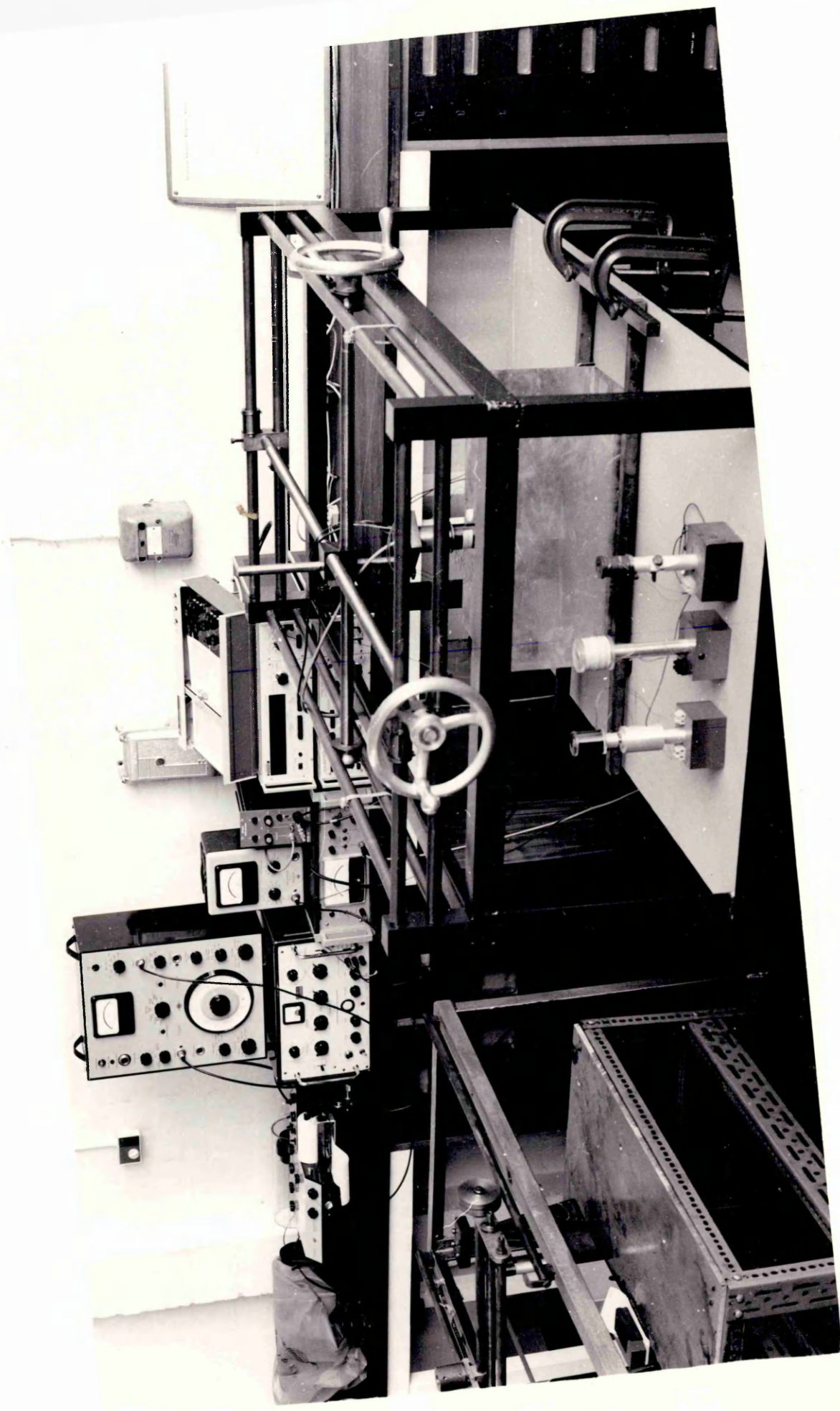


Plate 2 The redesigned vibration table.

БІЛГІС

Діагностика аеріації повітря.



The linear fine adjustment mechanism.

Plate 3

The skew fine adjustment mechanism.

Plate 11

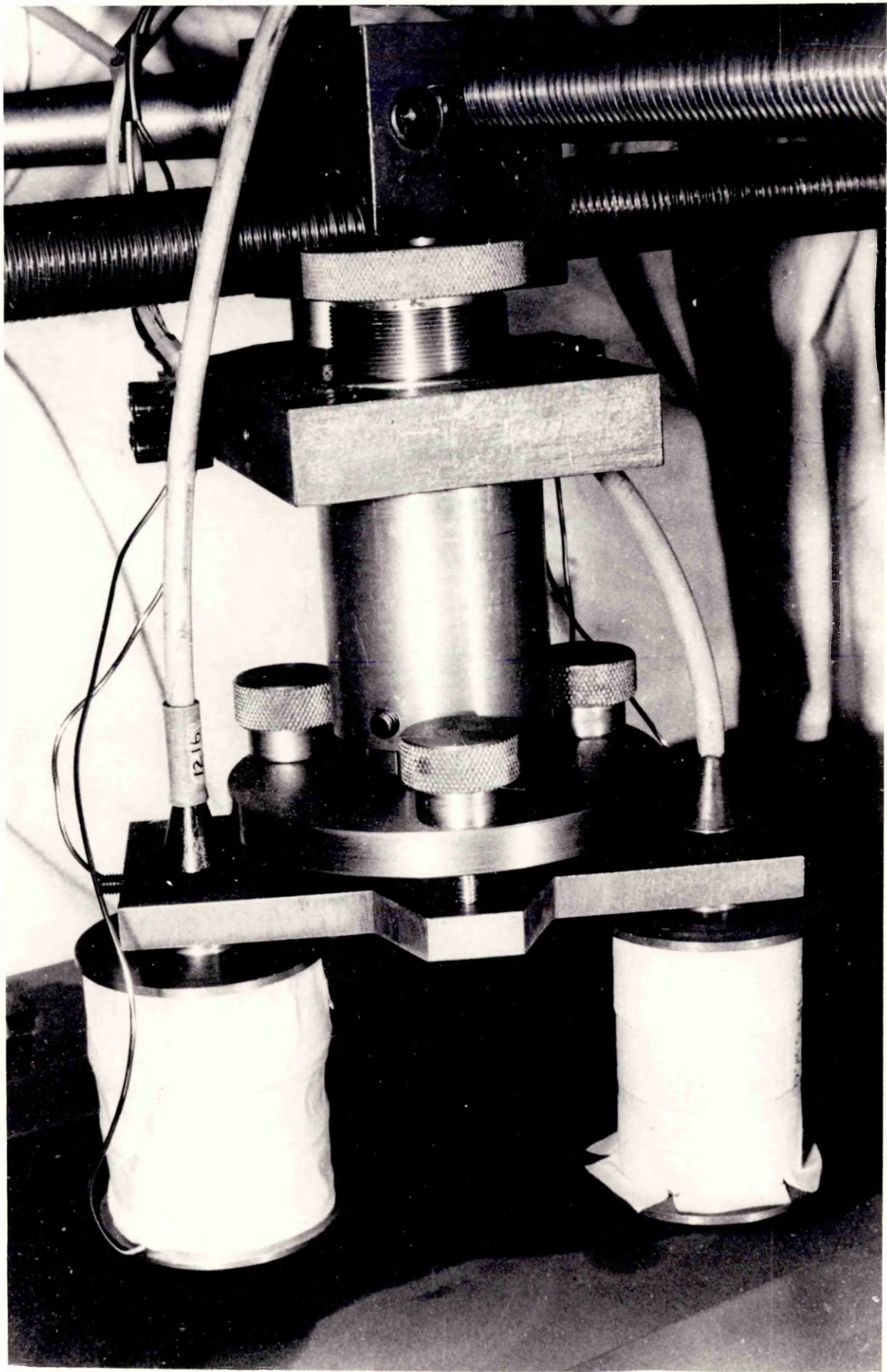


Plate 5 The plate with fully fixed edges.

Бјста 2

Две бјста мизу инја фикс едгес.

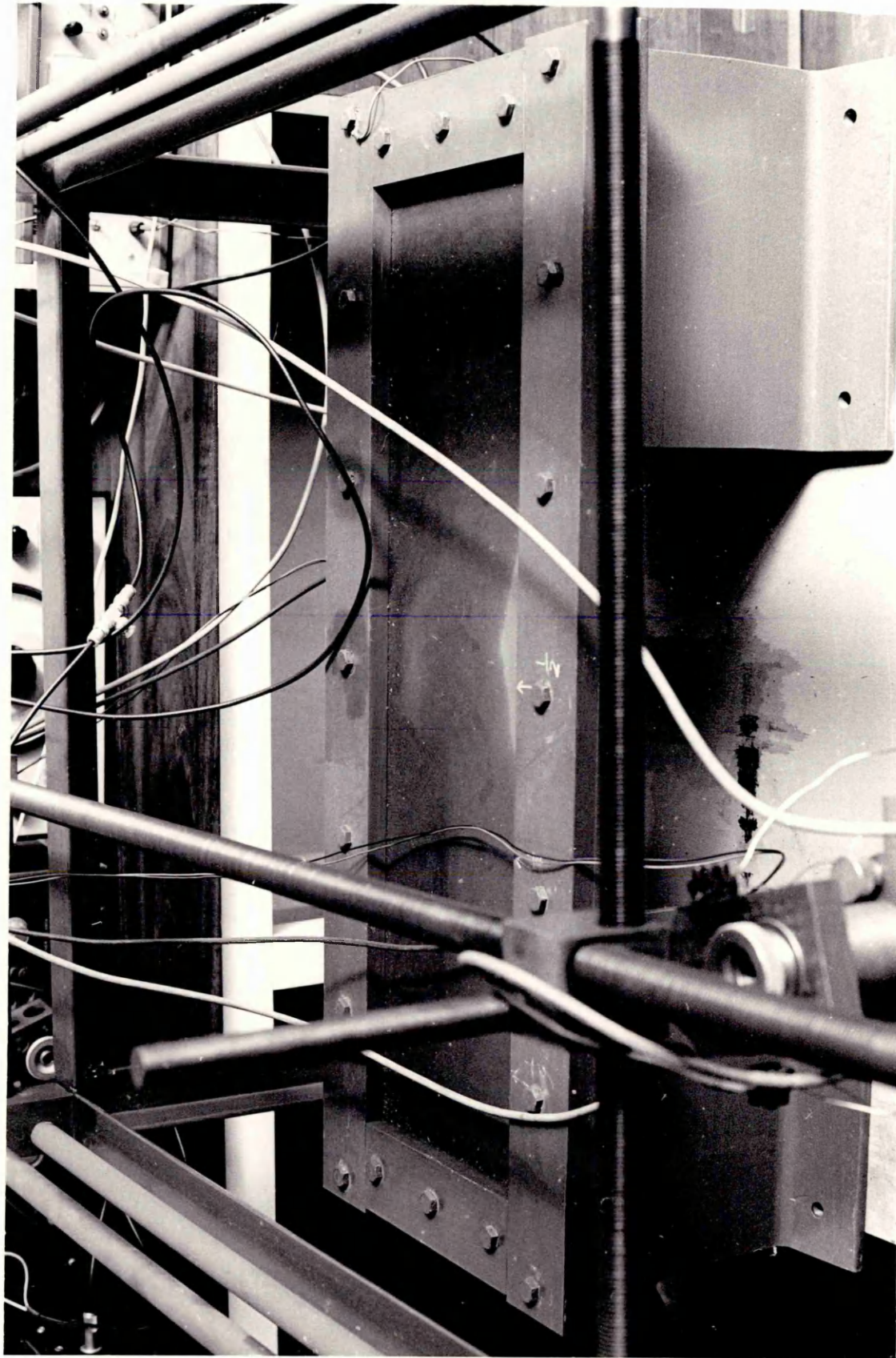


Plate 6 A fixed corner of the box structure.

Figure 9

A fixed corner of the box structure.

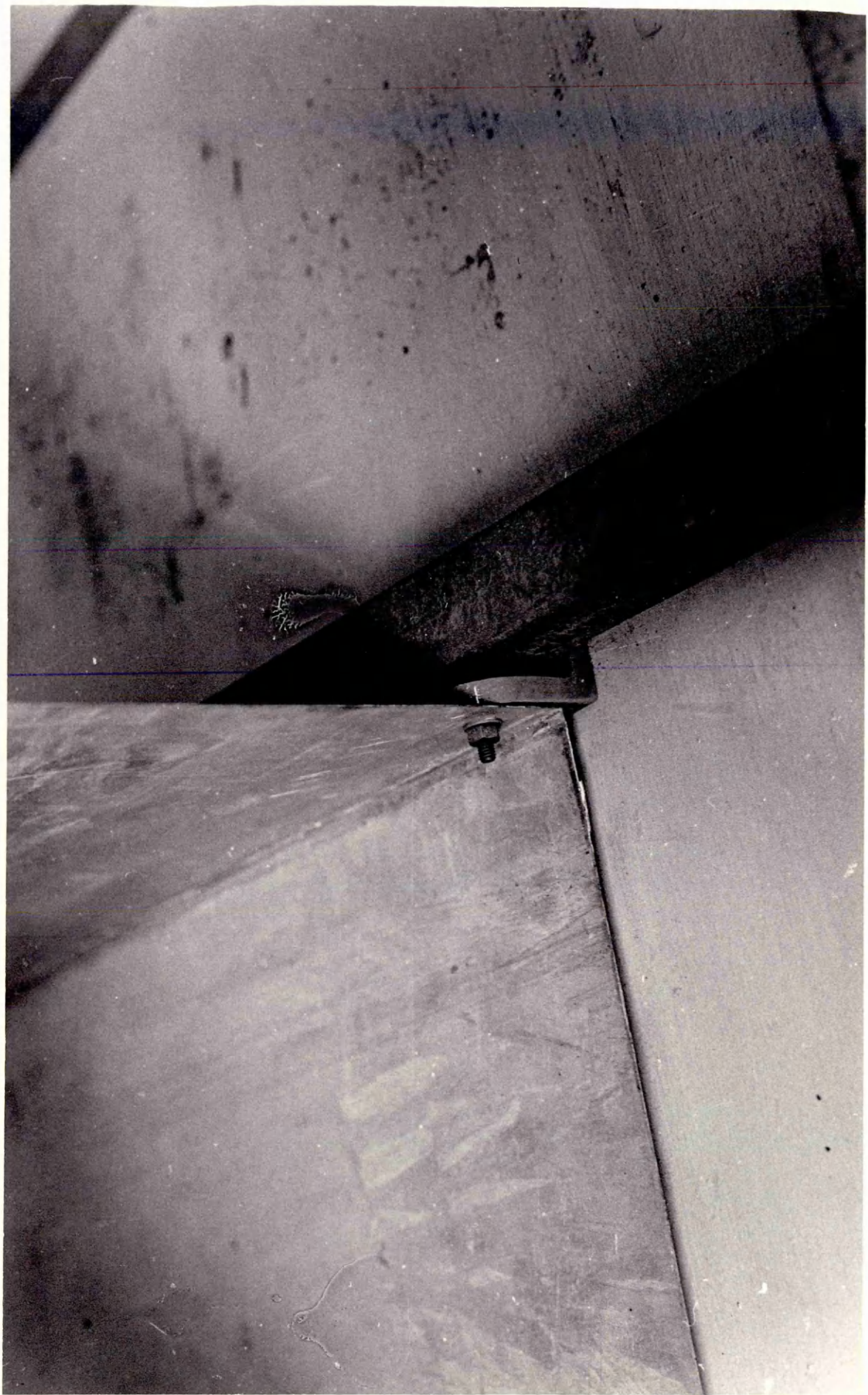


Plate 7 Close up view of the calibration of the capacitance displacement transducer.

State 1

Close nb view of the caption of, the substance of the management financial.

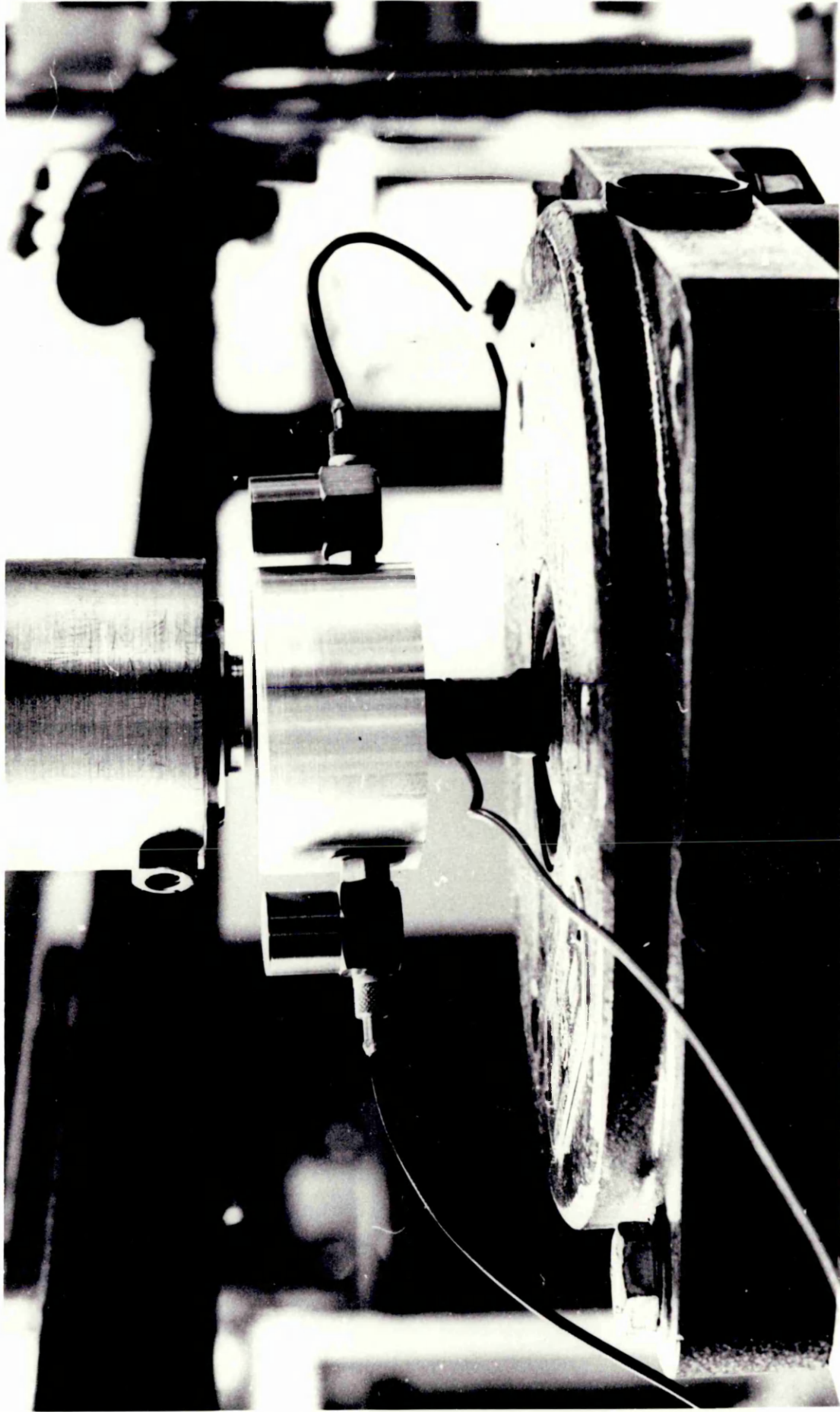


Plate 8 Instrumentation for calibration of the displacement transducer.

Figure 8 Instrumentation for calibration of the gravimetric balance.

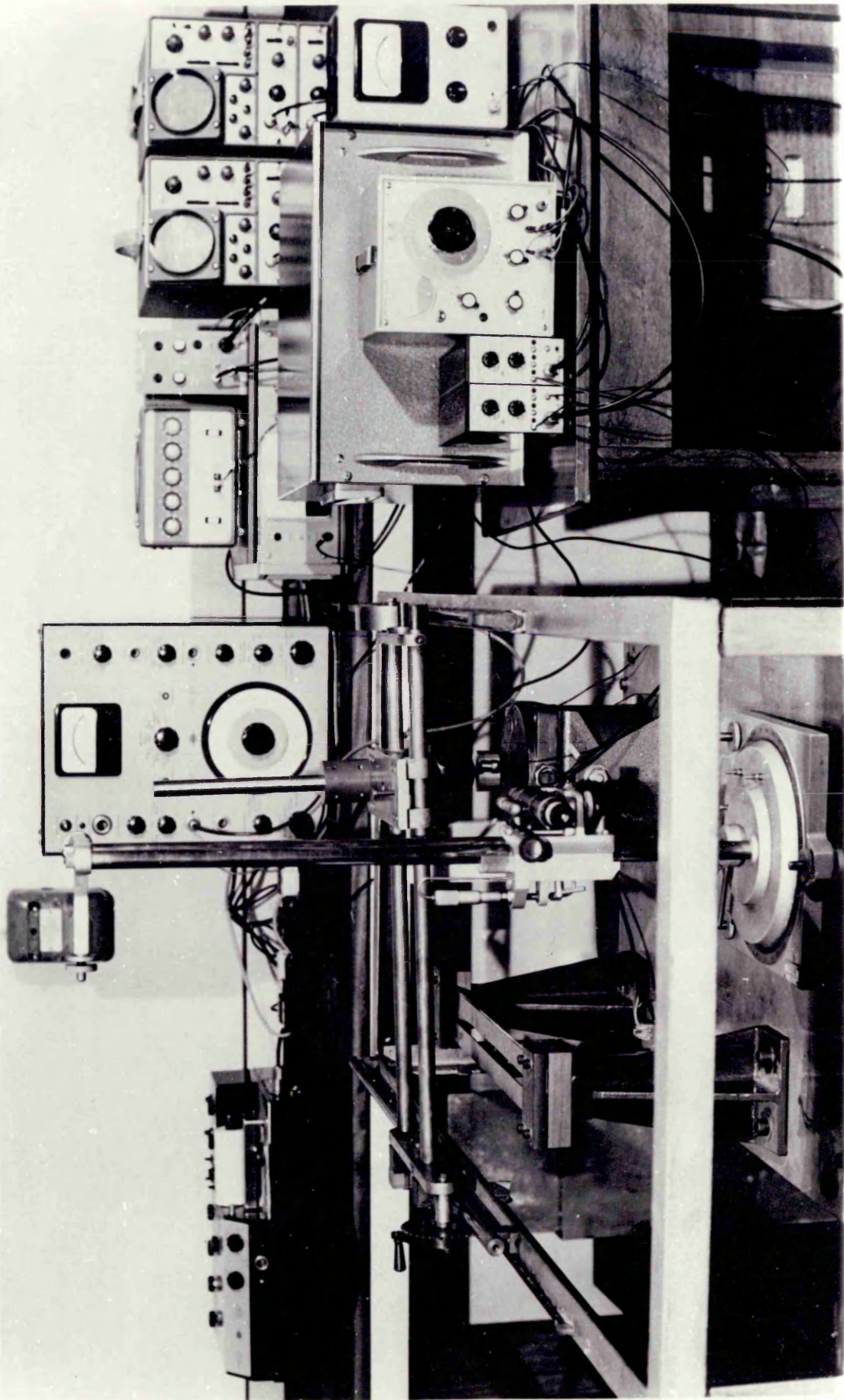


Plate 9 Calibration of noncontacting exciter using a simple beam experiment.

FIGURE 3 Description of nonconforming exciter using a simple beam experiment.

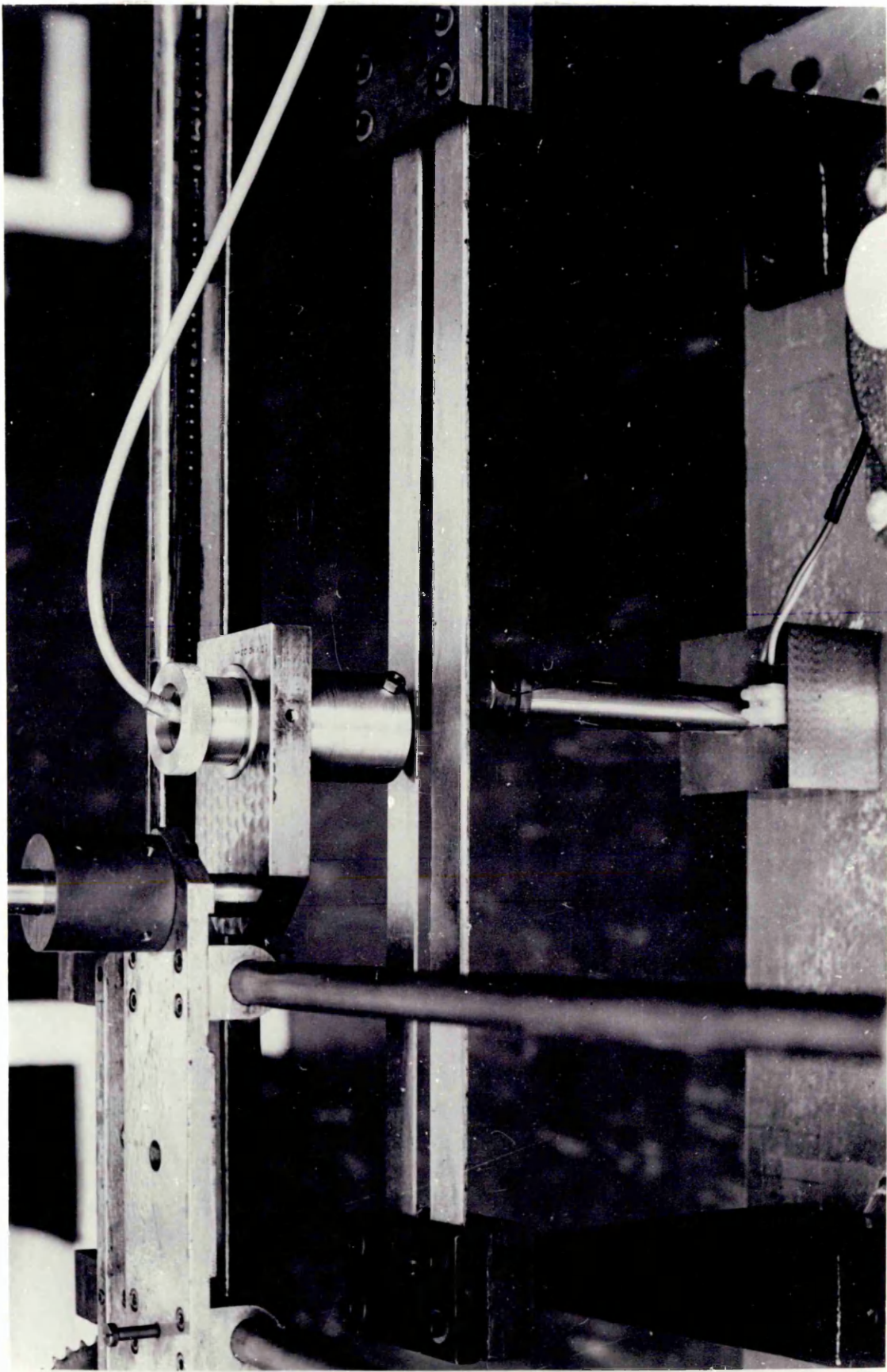


Plate 10

The housing for the piezoelectric force transducer
used for the calibration of the exciter.

Plate 10

The housing for the piezoelectric force transducer used for the calibration of the exciter.

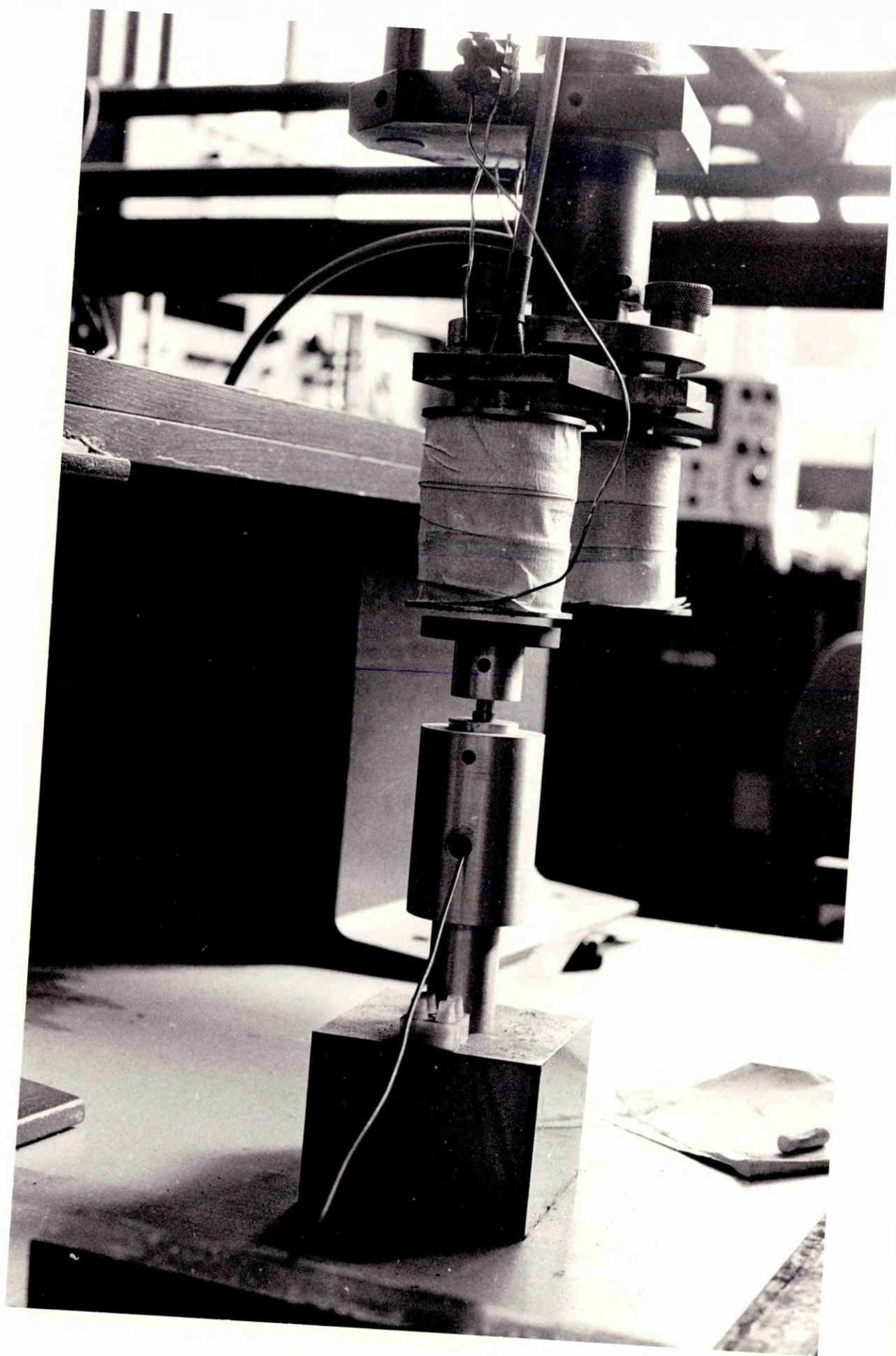


Plate 11 Some of the electromagnetic noncontacting exciters developed.

BTAT1111

some of the electromagnetic noncupaccine exofers generated.

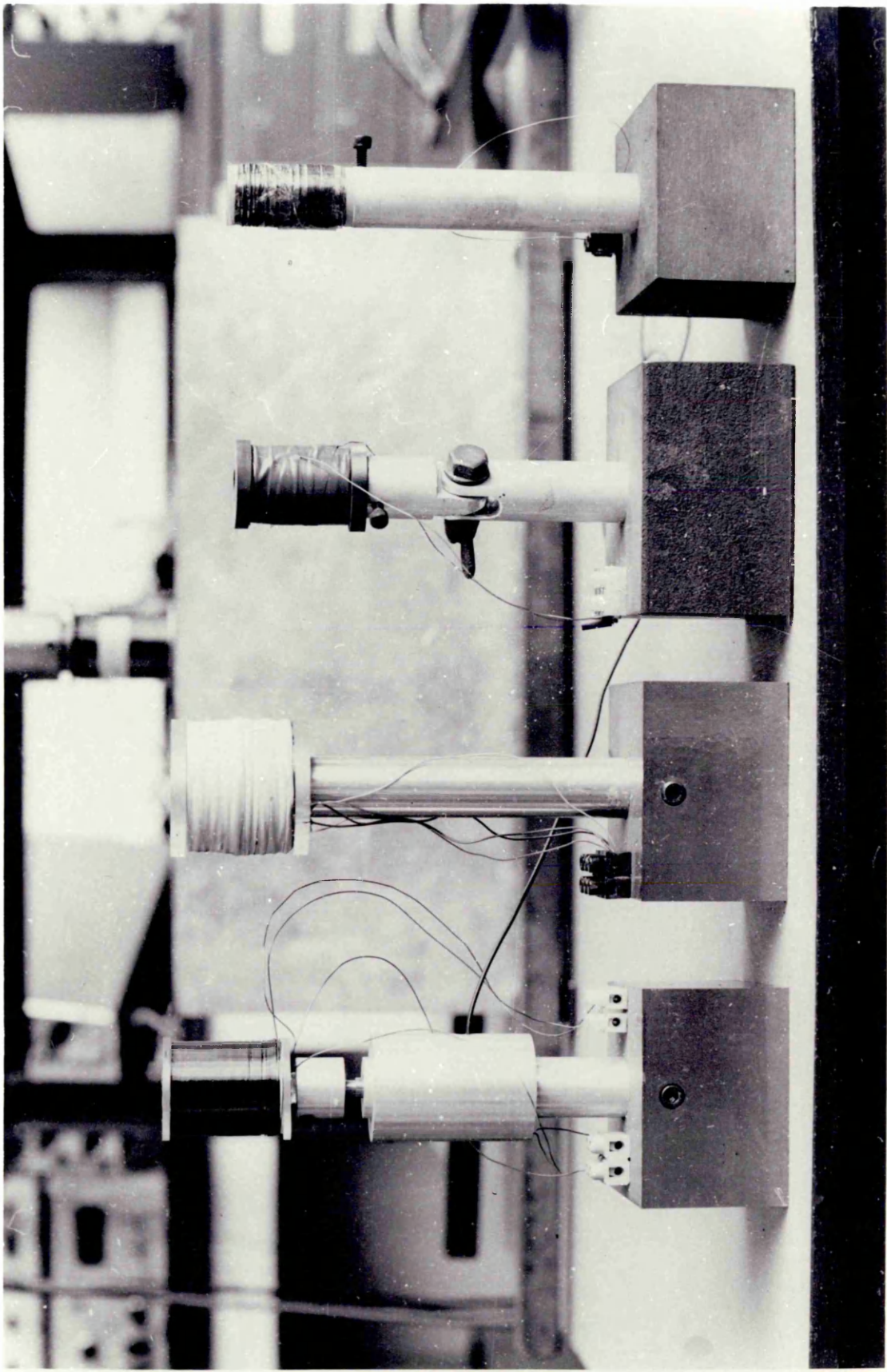


Plate 12 The combined exciter/pickup in position over the box structure.

BTBTE 15

The company excitedly picked in position over the box structure.

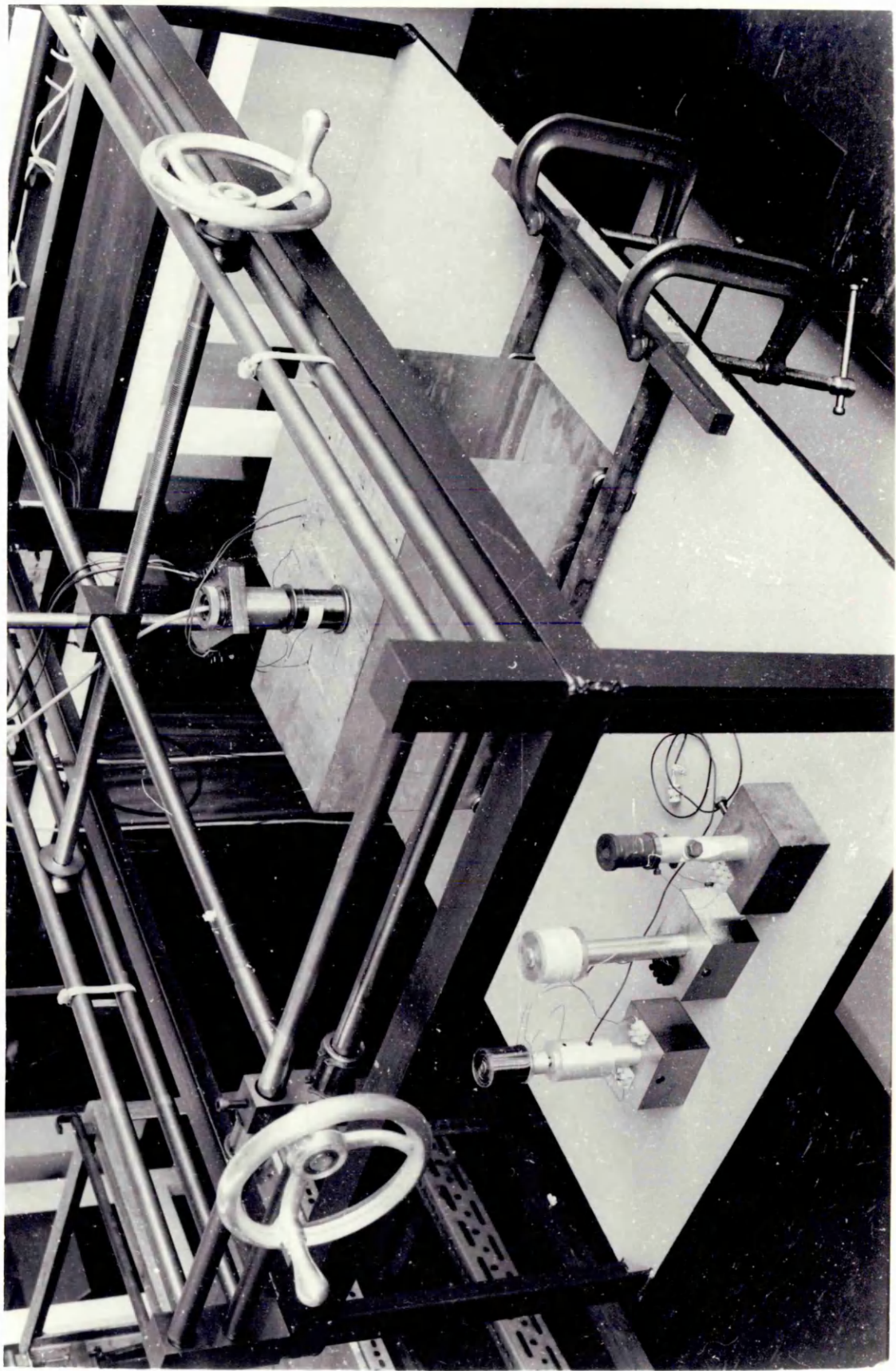


Plate 13 Frequency analysis using constant percentage frequency analyser

БІЛГІЛІК Өлөңдөнүсүз кыргыздын өнөрүнүн бергендерге үндөнүсүз кыргыздын

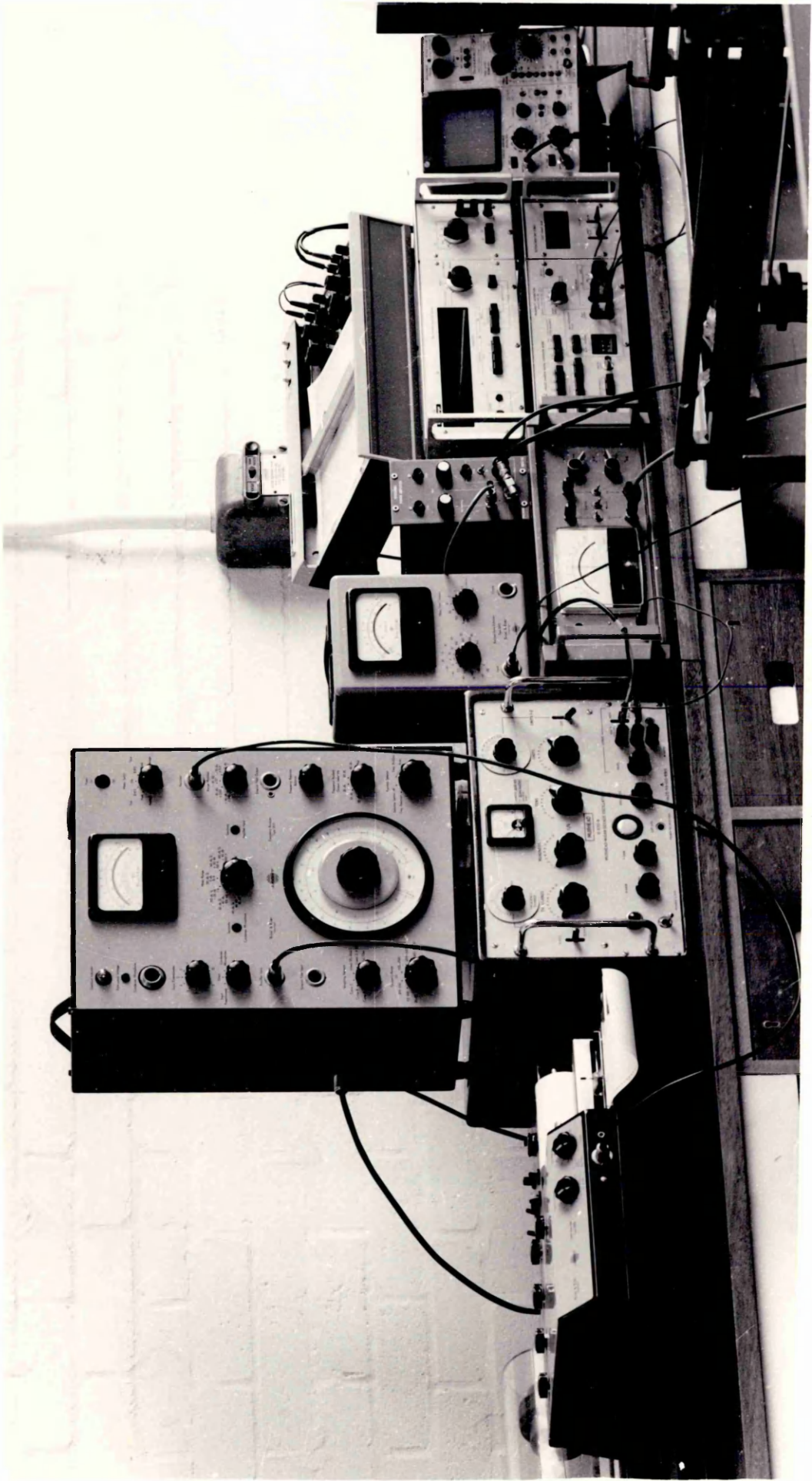


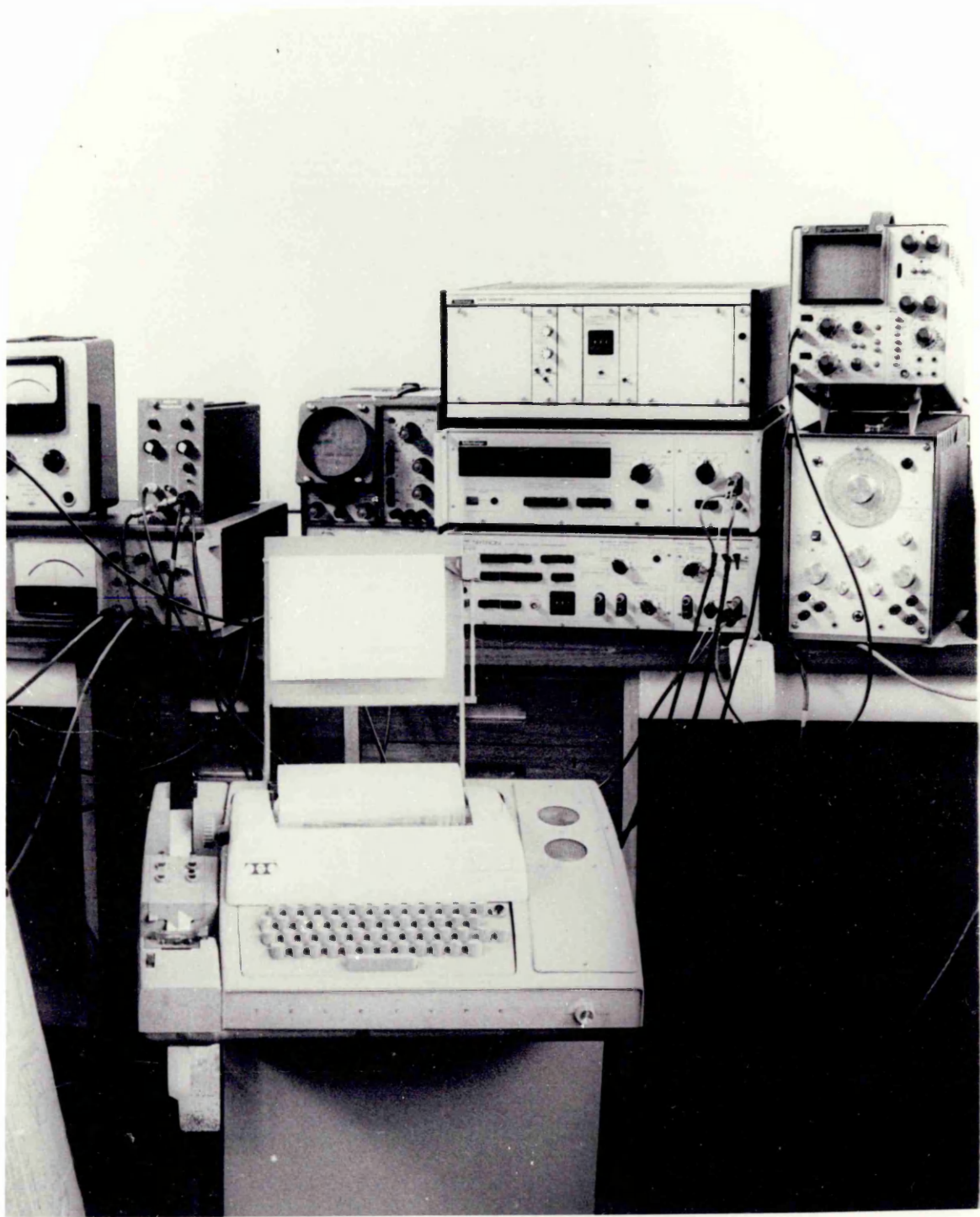
Plate 14 Constant bandwidth frequency analyser

Plate 15

The PRBS instrumentation used for the automatic generation of the cross correlation function on paper tape.

The PRBS instrumentation used for the automatic generation of the cross correlation function on paper tape.

Plate 15



REFERENCES

1. Miles, J.W.,
On structural fatigue under random loading,
Journal of Aeronautical Sciences, Vol. 21, 1954
2. Robson, J.D.,
An introduction to Random Vibrations,
Edinburgh University Press, 1963
3. Crandal, S.H.,
Random Vibrations,
M.I.T. Press, Cambridge, Mass., 1958
4. Bishop, R.E.D., and Johnson, D.C.,
The Mechanics of Vibrations,
Cambridge University Press, 1960
5. Crandal, S.H.,
The Role of Damping in Vibration Theory,
Journal of Sound and Vibration, Vol. 11, 1970
6. Abrahamson, A.L.,
Natural frequencies and normal modes of a four plate
structure,
Journal of Sound and Vibration, Vol. 28, 1973
7. Ritz, W.,
Annalen der Physik,
Vierte Folge, Vol. 28, 1909
8. Young, E.,
The vibration of rectangular plates by the Ritz Method,
Journal of Applied Mechanics, Vol. 17, 1950
9. Timoshenko, S.,
Vibration problems in Engineering,
3rd Edition D. Van Nostrand 1955

10. Warburton, G.B.,
The Vibration of Rectangular Plates,
Proceeding of the Institution of Mechanical Engineers, 1954
11. Leissa, A.W.,
The Free Vibrations of Rectangular Plates,
Journal of Sound and Vibrations, Vol. 31, 1973
12. Dickinson, S.M., and Warburton, G.B.,
Vibration of Box-type structures,
Journal of Mechanical Engineering Science, Vol. 9, 1967
13. Uhrig, R.,
The Transfer Matrix Method seen as one method of Structural
Analysis among others,
Journal of Sound and Vibration, Vol. 4, 1966
14. Dickinson, S.M., and Warburton, G.B.,
Natural Frequencies of Plate Systems using the Edge
Effect Method,
Journal of Mechanical Engineering Science, Vol. 9, 1967
15. Heng, R.B.W.,
Prediction of performance of centrally pivotted thrust
pads,
Final year project, University of Sheffield, 1971
16. Chang, A.,
An improved finite difference method for plate vibrations,
International Journal of Numerical Methods in Engineering,
Vol. 2, 1972
17. Turner, M.J., Clough, R.W., Martin, H.C., and Topp, L.J.,
Stiffness and Deflection Analysis of Complex Structures,
Journal of Aero Space Sciences, Vol. 23, 1956

18. Melosh, R.J.,
A Stiffness Matrix for the Analysis of Thin Plates
in Bending,
Journal of Aero Space Sciences, Vol. 28, 1961
19. Zienkiewicz, O.C., and Cheung, Y.K.,
The Finite Element Method for analysis of Elastic
Isotropic and Orthotropic slabs,
Proceedings of the Institution of Civil Engineers,
Vol. 28, 1964
20. Dawe, D.J.,
A finite Element Approach to Plate Vibration Problems,
Journal of Mechanical Engineering Science, Vol. 7, 1965
21. Proc. Conf. Matrix Methods in Structural Mechanics 1966
(AFFDL-TR-66-80),
Wright - Patterson Air Base
22. Prezemieniecki, J.S.,
Theory of Matrix Structural Analysis,
McGrw-Hill, 1968
23. Zienkiewicz, O.C.,
The Finite Element Method in Engineering Science,
2nd Edition, McGraw-Hill, 1971
24. Rockey, K.C., and Evans, H.R.,
A finite Element Solution for Folded Plates,
International Conference on Space Structures,
Battersea, 1966
25. Handa, K.N.,
Analysis of In-plane Vibrations of Box-type structures
by a Finite Element Method,
Journal of Sound and Vibration, Vol. 21, 1972

26. Ali, R., Hedges, J.L., and Mills, B.,
Computer Aided Design applied to a model of a chassis
type structure using Finite Element Techniques,
Proceedings of the Automobile Division of the Institution
of Mechanical Engineers, Vol. 184, 1969/70
27. Davis, W.D.T.,
Random Signal Testing for evaluating System Dynamics,
Wireless World, August 1966
28. Jones, F.,
Impulse Testing of Dynamic Systems,
Electronic Engineering, May 1967
29. Cooley, J.W., and Turkey, J.W.,
An Algorithm for the Machine Calculations of Complex
Fourier Series,
Mathematics of Computation, Vol. 19, 1965
30. Bingham, C., Godfrey, M.D., and Turkey, J.W.,
Modern Techniques of Power Spectrum Estimation,
I.E.E. trans, Audio and Elec.acc., Vol. AU-15, June 1967
31. Cochran, W.T., Cooley, J.W., et. al.,
What is the Fast Fourier Transform,
I.E.E. trans. Audio and Electroacoustics, Vol. AU-15,
June 1967
32. Clough, R.W., and Johnson, C.P.,
A Finite Element Approximation for the Analysis of
Thin Shells,
International Journal of Solid Structures, Vol. 4, 1968
33. Gere, J.M., and Weaver, W.,
Analysis of framed structures,
Van Nostrand, 1965
34. Nottingham Algorithm Group Computer Scientific Subroutine
Manual

35. Wilkinsin, J.H.,
The Algebraic Eigenvalue problem,
Clarendon Press, 1965
36. Franklin, J.N.,
Matrix Theory
Prentice-Hall Applied Mathematics series, 1968
37. Wiener, N.,
Random Theory,
M.I.T. Press, 1958
38. Jenkins, G.M., and Watts, D.G.,
Spectral Analysis and its Applications,
Holden-Day Inc., 1968
39. Newland, D.E.,
An Introduction to Random Vibrations and Spectral
Analysis, to be published
40. Pseudo-Random Binary Sequence Generator Handbook
JM 1861
Solartron Schlumberger
41. Plukett, R.,
Experimental Measurement Of Mechanical Impedance
or Mobility,
J. App. Mechanics, ASME Transaction, Vol. 21/3, 1954
42. Dunn, J.W.,
Measurement Techniques for the Analysis of Forced
structural Vibration.
Proceedings of the Institution of Mechanical
Engineers, Vol 182/37, 1968
43. Pandered, J.W., and Bishop, R.E.D.,
A critical introduction to some industrial resonance
testing techniques (and three other articles)
Journal of Mechanical Engineering Science, Vol 5
No. 4, 1963

44. Shapiro, U.,
An Experimental Investigation into response
distribution in coupled Plate Systems,
Ph.D. Thesis, University of Warwick, 1971
45. McNulty, G.J.,
U.S.A.F. Technical Report, AFSDL / TR / 67 / 97,
Wright-Patterson Air Force Base,
Ohio, 1967.
46. Blackman, R.B., and Tukey, J.W.,
The measurement of Power Spectra,
Dover Publications Inc., New York, 1959
47. Myklestad, N.O.,
The concept of Complex Damping,
Journal of Applied Mechanics, Vol 19, 1952
48. Kennedy, C.C., and Pancu, C.D.P.,
Use of vectors in vibration measurement and
analysis
J. Aeronautical Science, Vol 14, 1947
49. Bert, C.W.,
Material damping - An Introductory Review of
Mathematical Models, Measures and Experimental
Techniques,
Journal of Sound and Vibration, Vol 29, 1973
50. Rao, Murty and Rao,
Bounds for eigenvalues in some vibration problems,
International Journal of Numerical Methods in
Engineering, Vol 5, 1974
51. Vysloulch, V.A., Kandidov, V.P., and Chesnokov, S.S.,
Reduction of the degrees of Freedom in solving
Dynamic Problems by the Finite Element Method,
Int. Journal of Numerical Methods in Engineering,
Vol. 7, 1973

52. Irons, B.,
The Semi-loof Shell Element,
Proceedings of Conference on Finite Elements for
Thin Shells and Curved Members, Cardiff, May 1974

53. Patterson, C., and Heng, R.,
Finite Elements with Relaxed Continuity for Folded
Plate Structures,
Conference on Computing Developments in Experimental
and Numerical Stress Analysis, Nottingham, Sept 1975

54. Irons, B.M.,
A Frontal Solution Program for Finite Element
Analysis,
Int. Jnl. for Numerical Methods in Engineering,
Vol 2, 1970

Appendices

1. The element mass and stiffness matrices
2. The solution algorithms
3. The Finite Element computer program suite
4. The Fast Fourier Transform computer program
5. The experimental apparatus
6. Calibration of vibration pickup transducer
7. Calibration of exciter

Appendix 1

The stiffness and mass matrices

(a) The 24 x 24 stiffness matrix K

The lower triangle of the symmetrical matrix is given below

where A = length

B = width

$$P = \frac{A}{B}$$

v = poisson's ratio

t = thickness

$$C = \frac{Et^3}{12(1 - \nu^2)AB}$$

$$D = \frac{Et}{12(1 - \nu^2)}$$

$$\begin{aligned} K(1,1) &= D((4.0/P)+(2.0x(1.0-\nu)xP)) \\ K(2,1) &= D(3.0x(1.0+\nu)/2.0) \\ K(2,2) &= D((4.0xP)+(2.0x(1.0-\nu)/P)) \\ K(3,1) &= 0 \\ K(3,2) &= 0 \\ K(3,3) &= C((4.0xP^2)+(4.0/P^2)+2.8-(0.8x\nu)) \\ K(4,1) &= 0 \\ K(4,2) &= 0 \\ K(4,3) &= C(((2.0xP^2)+(0.2)+(0.8x\nu))xB) \\ K(4,4) &= C(((4.0xP^2/3.0)+(4.0x(1.0-\nu)/15.0))x(B^2)) \\ K(5,1) &= 0 \\ K(5,2) &= 0 \\ K(5,3) &= C(((2.0/P^2)+(0.2)+0.8x\nu))x(-A)) \\ K(5,4) &= C(-\nu xAxB) \\ K(5,5) &= C(((4.0/(3.0xP^2))+((4.0x(1-\nu))/15.0x(AxA))) \\ K(6,1) &\text{ to } K(6,6) = 0 \\ K(7,1) &= D((2.0/P)-(2.0x(1.0-\nu)xP)) \\ K(7,2) &= D(-3.0x(1.0-3.0x\nu)/2.0) \\ K(7,3) &\text{ to } K(7,6) = 0 \\ K(7,7) &= D((4.0/P)+(2.0x(1.0-\nu)xP)) \\ K(8,1) &= D(3.0x(1.0-(3.0x\nu))/2.0) \\ K(8,2) &= D((-4.0xP)+((1.0-\nu)/P)) \\ K(8,3) &\text{ to } K(8,6) = 0 \\ K(8,7) &= D(-3.0x(1.0+\nu)/2.0) \\ K(8,8) &= D((4.0xP)+(2.0x(1.0-\nu)/P) \\ K(9,1) &= 0 \\ K(9,2) &= 0 \\ K(9,3) &= C((2.0/P^2)-(4.0xP^2)-2.8+(4.0x\nu/5.0)) \\ K(9,4) &= C(((2.0xP^2)+((1.0-\nu)/5.0))x(-B)) \\ K(9,5) &= C(((1.0/P^2)+((1.0+(4.0x\nu))/5.0))xA) \\ K(9,6) &\text{ to } K(9,8) = 0 \\ K(9,9) &= C((4.0xP^2)+(2.8)-(0.8x\nu)+(4.0/P^2)) \\ K(10,1) &= 0 \\ K(10,2) &= 0 \\ K(10,3) &= C(((2.0xP^2)+(1.0-\nu)/5.0xB) \\ K(10,4) &= C(((2.0xP^2/3.0)+((1-\nu)/15.0))x(BxB)) \\ K(10,5) &= 0 \\ K(10,6) &\text{ to } K(10,8) = 0 \\ K(10,9) &= C(((2.0xP^2)+(0.2)+(0.8x\nu))x(-B)) \\ K(10,10) &= C(((4.0xP^2/3.0)+(4.0x(1.0-\nu))/15.0)x(BxB)) \end{aligned}$$

$K(11,1) = 0$
 $K(11,2) = 0$
 $K(11,3) = C(((1.0+(4.0xv))/5.0))xA$
 $K(11,4) = 0$
 $K(11,5) = C(((2.0/(3.0xP^2))=(4.0x(1.0-v)/15.0))x(AxA))$
 $K(11,6) \text{ to } K(11,8) = 0$
 $K(11,9) = C((-2.0/P^2)-(0.8xv))xA$
 $K(11,10) = C(vxAxB)$
 $K(11,11) = C(((4.0/3.0xP^2))+(4.0x(1.0-v)/15.0))x(AxA)$
 $K(12,1) \text{ to } K(12,12) = 0$
 $K(13,1) = D((-2.0/P)-((1.0-v)xP))$
 $K(13,2) = D((-3.0x(1.0+v)/2.0))$
 $K(13,3) \text{ to } K(13,6) = 0$
 $K(13,7) = D((-4.0/P)+((1.0-v)xP))$
 $K(13,8) = D((-3.0x(1-(3.0xv))/2.0))$
 $K(13,9) \text{ to } K(13,12) = 0$
 $K(13,13) = D((4.0/P)+(2.0x(1.0-v)xP))$
 $K(14,1) = D(-3.0x(1.0+v)/2.0)$
 $K(14,2) = D((-2.0xP)-((1.0-v)/P))$
 $K(14,3) \text{ to } K(14,6) = 0$
 $K(14,7) = D((3.0x(1.0-(3.0xv))/2.0))$
 $K(14,8) = D((2.0xP)-(2.0x(1.0-v)/P))$
 $K(14,9) \text{ to } K(14,12) = 0$
 $K(14,13) = D((3.0x(1.0+v)/2.0))$
 $K(14,14) = D((4.0x(1.0-v)/P))$
 $K(15,1) = 0$
 $K(15,2) = 0$
 $K(15,3) = C((-2.0xP^2)-(2.0/P^2)+(2.8)-(0.8xv))$
 $K(15,4) = C((-P^2+((1-v)/15.0))xB)$
 $K(15,5) = C((-1.0/P^2)+((1-v)/5.0))x(-A)$
 $K(15,6) \text{ to } K(15,8) = 0$
 $K(15,9) = C((-2.0x((2.0/P^2)-(14.0-(4.0xv))/5.0))$
 $K(15,10) = C((-P^2+(1.0+(4.0xv))/5.0))x(B)$
 $K(15,11) = C(((2.0/P^2)+((1.0-v)/5.0))xA)$
 $K(15,12) \text{ to } K(15,14) = 0$
 $K(15,15) = C((4.0xP^2)+(4.0/P^2)+(2.8)-(0.8xv))$
 $K(16,1) = 0$
 $K(16,2) = 0$
 $K(16,3) = C((P^2-((1-v)/5.0))x(B))$
 $K(16,4) = C(((P^2/3.0)+((1-v)/15.0))x(BxB))$
 $K(16,5) \text{ to } K(16,8) = 0$
 $K(16,9) = C((-P^2+(1.0+(4.0xv))/5.0)xB)$
 $K(16,10) = C(((2.0xP^2)/3.0)-((4.0x(1.0-v))/15.0))x(BxB)$
 $K(16,11) \text{ to } K(16,14) = 0$
 $K(16,15) = C((-2.0xP^2)-(0.2)-(0.8xv))xB$
 $K(16,16) = C(((4.0xP^2/3.0)+(4.0x(1-v)/15.0))x(BxB))$
 $K(17,1) = 0$
 $K(17,2) = 0$
 $K(17,3) = C((1.0/P^2)-((1-v)/5.0))x(-A)$
 $K(17,4) = 0$
 $K(17,5) = C(((1.0/(3.0xP^2))+((1-v)/15.0))x(AxA))$
 $K(17,6) \text{ to } K(17,8) = 0$
 $K(17,9) = C(((2.0/P^2)+((1.0-v)/5.0))x(-A))$
 $K(17,10) = 0$
 $K(17,11) = C(((2.0/(3.0xP^2))-((1.0-v)/15.0))+(AxA))$
 $K(17,12) \text{ to } K(17,14) = 0$
 $K(17,15) = C(((2.0/P^2)+(0.2)+(0.8xv))x(A))$
 $K(17,16) = C(-vxAxB)$
 $K(17,17) = C(((4.0/(3.0xP^2))+4.0x(1-v)/15.0))x(AxA)$
 $K(18,1) \text{ to } K(18,18) = 0$

$K(19,1) = D((-4.0/P) + ((1.0-v) \times P))$
 $K(19,2) = D((3.0 \times (1.0 - (3.0 \times v)) / 2.0))$
 $K(19,3) \text{ to } K(19,6) = 0$
 $K(19,7) = D((-2.0/P) - ((1.0-v) \times P))$
 $K(19,8) = D((3.0 \times (1.0 + v) / 2.0))$
 $K(19,9) \text{ to } K(19,12) = 0$
 $K(19,13) = D((2.0/P) - (2.0 \times (1.0 - v) \times P))$
 $K(19,14) = D((-3.0 \times (1.0 - (3.0 \times v)) / 2.0))$
 $K(19,15) \text{ to } K(19,18) = 0$
 $K(19,19) = D((4.0/P) + (2.0 \times (1.0 - v) \times P))$
 $K(20,1) = D((-3.0 \times (1.0 - (3.0 \times v)) / 2.0))$
 $K(20,2) = D((2.0 \times P) - (2.0 \times (1.0 - v) / P))$
 $K(20,3) \text{ to } K(20,6) = 0$
 $K(20,7) = D((3.0 \times (1.0 + v) / 2.0))$
 $K(20,8) = D((-2.0 \times P) - ((1.0 - v) / P))$
 $K(20,9) \text{ to } K(20,12) = 0$
 $K(20,13) = D((3.0 \times (1.0 - (3.0 \times v)) / 2.0))$
 $K(20,14) = D((-4.0 \times P) + ((1.0 - v) / P))$
 $K(20,15) \text{ to } K(20,18) = 0$
 $K(20,19) = D((-3.0 \times (1.0 + v) / 2.0))$
 $K(20,20) = D((4.0 \times P) + (2.0 \times (1.0 - v) / P))$
 $K(21,1) = 0$
 $K(21,2) = 0$
 $K(21,3) = C(-2.0 \times ((2.0/P^2) - P^2) - ((14.0 - (4.0 \times v)) / 5.0))$
 $K(21,4) = C((-P^2 + ((1.0 + (4.0 \times v)) / 5.0)) \times B)$
 $K(21,5) = C(((2.0/P^2) + ((1.0 - v) / 5.0)) \times A)$
 $K(21,6) \text{ to } K(21,8) = 0$
 $K(21,9) = C(-2.0 \times P^2 - (2.0/P^2) + (2.8) - (0.8 \times v))$
 $K(21,10) = C((P^2 - ((1 - v) / 5.0)) \times B)$
 $K(21,11) = C(((1.0/P^2) - ((1 - v) / 5.0)) \times (A))$
 $K(21,12) \text{ to } K(21,14) = 0$
 $K(21,15) = C((2.0 \times ((1.0/P^2) - (2.0 \times P^2))) - ((14.0 - (4.0 \times v)) / 5.0))$
 $K(21,16) = C(((2.0 \times P^2) + ((1.0 - v) / 5.0)) \times B)$
 $K(21,17) = C(((1.0/P^2) - ((1.0 + (4.0 \times v)) / 5.0)) \times A)$
 $K(21,18) \text{ to } K(21,20) = 0$
 $K(21,21) = C((4.0 \times P^2) + (4.0/P^2) + (2.8) - (0.8 \times v))$
 $K(22,1) = 0$
 $K(22,2) = 0$
 $K(22,3) = C(((P^2) - ((1.0 + (4.0 \times v)) / 5.0)) \times B)$
 $K(22,4) = C(((2.0 \times P^2 / 3.0) - (4.0 \times (1.0 - v) / 15.0)) \times (B \times B))$
 $K(22,5) \text{ to } K(22,8) = 0$
 $K(22,9) = C((P^2 - ((1 - v) / 5.0)) \times (-B))$
 $K(22,10) = C((P^2 / 3.0) + ((1 - v) / 15.0)) \times (B \times B)$
 $K(22,11) \text{ to } K(22,14) = 0$
 $K(22,15) = C((2.0 \times P^2) + ((1.0 - v) / 5.0)) \times (-B)$
 $K(22,16) = C((2.0 \times P^2 / 3.0) - ((1.0 - v) / 15.0)) \times (B \times B)$
 $K(22,17) \text{ to } K(22,20) = 0$
 $K(22,21) = C(((2.0 \times P^2) + (0.2) + (0.8 \times v)) \times (B))$
 $K(22,22) = C(((4.0 \times P^2 / 3.0) + (4.0 \times (1 - A) / 15.0)) \times (B \times B))$

K(23,1) = 0
 K(23,2) = 0
 K(23,3) = C(((2.0/P²)+((1.0-v)/5.0))x(-A))
 K(23,4) = 0
 K(23,5) = C((2.0/3.0xP²))-((1.0-v)/15.0))x(AxA))
 K(23,6) to K(23,8) = 0
 K(23,9) = C((-1.0/P²)+((1-v)/5.0))xA
 K(23,10) = 0
 K(23,11) = C(((1.0/(3.0xP²))+((1-v)/15.0))x(AxA))
 K(23,12) to K(23,14) = 0
 K(23,15) = C(((1.0/P²)-((1.0+(4.0xv))/5.0))xA)
 K(23,16) = 0
 K(23,17) = C(((2.0/(3.0xP²))- (4.0x(1.0-v)/15.0))x(AxA))
 K(23,18) to K(23,20) = 0
 K(23,21) = C(((2.0/P²)+(0.2)+(0.8xv))xA)
 K(23,22) = C(vxAxB)
 K(23,23) = C(((4.0/(3.0xP²))+ (4.0x(1-v)/15.0))x(AxA))
 K(24,1) to K(24,24) = 0

(b) The 24 x 24 mass matrix M

The lower triangle of the symmetrical matrix
is given below where

A = length

B = width

ρ = density / unit area

multiply throughout by $\frac{\rho AB}{176400}$

M(1,1) = 19600
M(2,1) = 0
M(2,2) = 19600
M(3,1) = 0
M(3,2) = 0
M(3,3) = 24178.0
M(4,1) = 0
M(4,2) = 0
M(4,3) = 3227 x B
M(4,4) = 560 x B x B
M(5,1) = 0
M(5,2) = 0
M(5,3) = -3227 x A
M(5,4) = -441.0 x A x B
M(5,5) = 560.0 x A x A
M(6,1) to M(6,6) = 0
M(7,1) = 9800
M(7,2) to M(7,6) = 0
M(7,7) = 19600
M(8,1) = 0
M(8,2) = 9800
M(8,3) to M(8,7) = 0
M(8,8) = 19600
M(9,1) = 0
M(9,2) = 0
M(9,3) = 8582.0
M(9,4) = 1918.0 x B
M(9,5) = -1393.0 x A
M(9,6) to M(9,8) = 0
M(9,9) = 24178.0
M(10,1) = 0
M(10,2) = 0
M(10,3) = -1918.0 x B
M(10,4) = -420.0 x B x B
M(10,5) = 294.0 x A x B
M(10,6) to M(10,8) = 0
M(10,9) = -3227.0 x B
M(10,10) = 560.0 x B x B
M(11,1) = 0
M(11,2) = 0
M(11,3) = -1393 x A
M(11,4) = -294.0 x A x B
M(11,5) = 280.0 x A x A
M(11,6) to M(11,8) = 0
M(11,9) = -3227.0 x A
M(11,10) = 441.0 x A x B
M(11,11) = 560.0 x A x A

M(12,1) to M(12,12) = 0
M(13,1) = 4900
M(13,2) to M(13,6) = 0
M(13,7) = 9800
M(13,8) to M(13,12) = 0
M(13,13) = 19600
M(14,1) = 0
M(14,2) = 4900
M(14,3) to M(14,7) = 0
M(14,8) = 9800
M(14,9) to M(14,13) = 0
M(14,14) = 19600
M(15,1) = 0
M(15,2) = 0
M(15,3) = 2758.0
M(15,4) = 812.0 x B
M(15,5) = -812.0 x A
M(15,6) to M(15,8) = 0
M(15,9) = 8582.0
M(15,10) = -1393.0 x B
M(15,11) = -1918.0 x A
M(15,12) to M(15,14) = 0
M(15,15) = 24178.0
M(16,1) = 0
M(16,2) = 0
M(16,3) = -812.0 x B
M(16,4) = -210.0 x B x B
M(16,5) = 196.0 x A x B
M(16,6) to M(16,8) = 0
M(16,9) = -1393 x B
M(16,10) = 280.0 x B x B
M(16,11) = 294.0 x A x B
M(16,12) to M(16,14) = 0
M(16,15) = -3227.0 x B
M(16,16) = 560.0 x B x B
M(17,1) = 0
M(17,2) = 0
M(17,3) = 812.0 x A
M(17,4) = 196.0 x A x B
M(17,5) = -210.0 x A x A
M(17,6) to M(17,8) = 0
M(17,9) = 1918.0 x A
M(17,10) = -294.0 x A x B
M(17,11) = -420.0 x A x A
M(17,12) to M(17,14) = 0
M(17,15) = 3227.0 x A
M(17,16) = -441.0 x A x B
M(17,17) = 560.0 x A x A
M(18,1) to M(18,18) = 0

M(19,1) = 9800
M(19,2) = 0
M(19,3) to M(19,6) = 0
M(19,7) = 4900
M(19,8) to M(19,12) = 0
M(19,13) = 9800
M(19,14) to M(19,18) = 0
M(19,19) = 19600
M(20,1) = 0
M(20,2) = 9800
M(20,3) to M(20,7) = 0
M(20,8) = 4900
M(20,9) = M(20,13) = 0
M(20,14) = 9800
M(20,15) to M(20,19) = 0
M(20,20) = 19600
M(21,1) = 0
M(21,2) = 0
M(21,3) = 8582.0
M(21,4) = 1393 x B
M(21,5) = - 1918.0 x A
M(21,6) to M(21,8) = 0
M(21,9) = 2758.0
M(21,10) = - 812.0 x B
M(21,11) = - 812.0 x A
M(21,12) to M(21,14) = 0
M(21,15) = 8582.0
M(21,16) = - 1918.0 x B
M(21,17) = 1393.0 x A
M(21,18) to M(21,20) = 0
M(21,21) = 24178.0
M(22,1) = 0
M(22,2) = 0
M(22,3) = 1393.0 x B
M(22,4) = 280.0 x B x B
M(22,5) = - 294.0 x A x B
M(22,6) to M(22,8) = 0
M(22,9) = 812.0 x B
M(22,10) = - 210.0 x B x B
M(22,11) = - 196.0 x A x B
M(22,12) to M(22,14) = 0
M(22,15) = 1918.0 x B
M(22,16) = - 420.0 x B x B
M(22,17) = 294.0 x A x B
M(22,18) to M(22,20) = 0
M(22,21) = 3227.0 x B
M(22,22) = 560.0 x B x B
M(23,1) = 0
M(23,2) = 0
M(23,3) = 1918.0 x A
M(23,4) = 294.0 x A x B
M(23,5) = - 420.0 x A x A
M(23,6) to M(23,8) = 0
M(23,9) = 812.0 x A

M(23,10) = - 196.0 x A x B
M(23,11) = - 210.0 x A x A
M(23,12) to M(23,14) = 0
M(23,15) = 1393.0 x A
M(23,16) = - 294.0 x A x B
M(23,17) = 280.0 x A x A
M(23,20) = 0
M(23,21) = 3227.0 x A
M(23,22) = 441.0 x A x B
M(23,23) = 560.0 x A x A
M(24,1) to M(24,24) = 0

The computer solution algorithms

- 2.1 Brief notes on current techniques available for economising on the computer core space required using the finite element method of analysis.

- 2.2 Listing of the standard library computer subroutines used. Acknowledgements are due to the Nottingham Algorithm Group from whom descriptions of their scientific subroutines which were used in the computer analysis performed are here reproduced.

The finite element analysis of the three dimensional folded plate structure required a very large core storage in order to solve for the natural frequencies and mode shapes of the structure. The simple and rather coarse mesh used, shown in figure 2.12, gave a 146 x 146 matrix for the stiffness as well as the mass matrices. This required a 70K computer core storage which is often not available on smaller computers or even if available, together with a long computer solution time, is consequently very costly. The results are also likely to be excessive and is accurate only at the lower frequencies. In fact only a quarter of the eigenvalues computed is likely to be accurate enough for engineering purposes.

Although not used in the program developed, for prospective students of the finite element technique, savings in core space may be achieved although often at the expense of increased computing time by methods,

- a) using the full stiffness matrix - most accurate but very demanding on core storages.
- b) banded K - the stiffness matrix is stored banded, resulting in a storage saving but at the cost of an increased solution time.
- c) frontal solution - reduction or condensation of selected degrees of freedom and solving only the 'front' where unnecessary degrees of freedom at stage are eliminated and put on to a disc backing store to relieve core storage.
- d) substructuring - use of compound elements made up of collections of normal elements.

The first two requires little explanation and core savings are achieved utilising the matrices' symmetry and sparseness outside the diagonal band.

Frontal solution

Here only the current active degrees of freedom are kept in the core during the solution [45]. All other degrees of freedom are reduced out of the core after all information relating to them is complete. These are stored in a peripheral storage device such as disc or magnetic tape and the method is especially advantageous for matrices where the bandwidth varies considerably.

The elimination takes place as follows. Basically what we have is a very large linear set of simultaneous equations. When all the information relating to a particular variable is complete then that variable may be eliminated since it can be expressed in terms of the other variables.

$$[K]\{d\} = \{F\} \quad (A.2.1)$$

$$\text{or } \sum_{j=1}^n K_{ij}d_j = F_i \text{ for } i = 1 \rightarrow n$$

for $i = k$ (i.e. the k th equation)

$$\sum_{j=1}^n K_{kj}d_j = F_k$$

$$\therefore d_k = \frac{1}{K_{kk}} \left[- \left(\sum_{y=1}^n K_{ky}d_y \right) + F_k \right] \text{ for } y \neq k \quad (A.2.2)$$

This is then used in all the remaining $(n - 1)$ equations to give a reduced form of (A.2.1)

$$\text{so that } \left(\sum_{j=1}^n K_{ij}d_j \right) - K_{ik}d_k = F_i - \frac{K_{ik}}{K_{kk}} \left[- \left(\sum_{y=1}^n K_{ky}d_y \right) + F_k \right]$$

for $y \neq k$

on rearranging, for $y \neq k$

$$\begin{aligned} \sum_{j=1}^n (K_{ij}d_j) - \sum_{y=1}^n \left(\frac{K_{ky}d_y K_{ik}}{K_{kk}} \right) - K_{ik}d_k \\ = F_i - F_k \frac{K_{ik}}{K_{kk}} \end{aligned}$$

hence

$$\sum_{j=1}^n (K_{ij} - \frac{K_{ik}K_{kj}}{K_{kk}}) d_j = F_i - F_k \frac{K_{ik}}{K_{kk}} \quad (A.2.3)$$

Thus using this method the N equations can be reduced to N - 1 and so on.

Using equation (A.2.2) which is stored on peripheral a back substitution can be performed to determine d_k . Equation (A.2.3) can be derived from (A.2.1)^k by replacing

$$K_{ij} \quad \text{by} \quad (K_{ij} - \frac{K_{ik}K_{kj}}{K_{kk}}) \quad \text{and}$$

$$F_i \quad \text{by} \quad (F_i - \frac{F_k K_{ik}}{K_{kk}})$$

where d_k is the degree of freedom to be eliminated.

The mass terms are modified to

$$M_{ij} = M_{ij} - (M_{ik} \frac{K_{kj}}{K_{kk}}) - M_{kj} \frac{K_{ik}}{K_{kk}} + \frac{K_{ik}K_{kj}M_{kk}}{(K_{kk})^2}$$

Thus the net result is that the kth row and column of the stiffness and mass matrices are eliminated in the modified matrices in which terms need only be altered if d_i and d_j are both coupled to d_k (figure A.2.1).

Substructuring

The dynamic analysis of the three dimensional structure requires a very large core storage and sometimes even use of the front solution is not sufficient. Because the problem is so large even the active degrees of freedom themselves require more core storage than is available, substructuring is therefore necessary.

Substructuring is the name given to the reduction of the structure into giant compound elements. Thus only the nodes at which these 'substructures' join are used. In a dynamic analysis the mass matrix is reduced to those at

banded matrix

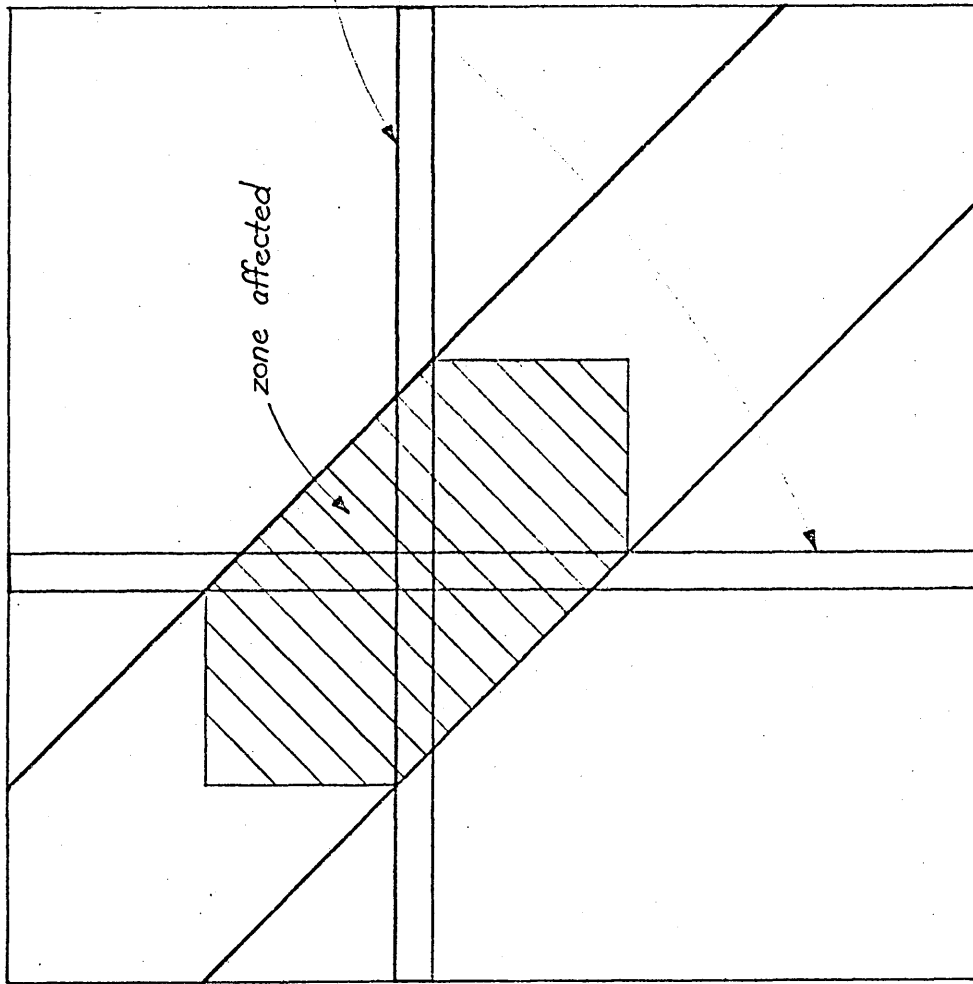


Fig A 2-1

these nodes plus the 'master freedoms' specified.

A backing store is used to store the reduced out matrices and the substructure matrices are then used to produce the complete system matrix. The eigenvalue problem of the master degrees of freedom is then solved and a back substitution is carried out to determine the displacement of the 'slave' freedoms 's' on a static basis. The choice of s is based on the observation that for the lower modes of vibration of a structure it is possible to neglect the effect of local inertia forces. The assumption is made that s in relation to nearby unknowns d' is given by static considerations. The inertia associated with s is not neglected but it is not allowed to affect the relationship between s and d' .

The method introduces errors almost negligible if the following conditions are satisfied:

- 1) if rotational rather than translational freedoms are eliminated.
- 2) degrees of freedom close to clamped or hinged boundaries and other freedoms having little inertia effects in the mode of interest are eliminated.
- 3) only the first n/3 eigenvalues of the n degrees of freedom chosen is required.
- 4) retention of at least one master freedom to represent each of the rigid body modes of the structure.

Here the method is briefly to first partition the stiffness matrix [K] and the displacements {U} into

$$K = \begin{bmatrix} K_{11} & K_{12} \\ K_{21} & K_{22} \end{bmatrix}$$

$$U = \begin{Bmatrix} U_1 \\ U_2 \end{Bmatrix}$$

where U_1 contains the retained displacements and U_2 the

remaining. U_2 is then obtained from the static equilibrium eqn. $\{F\} = [K] \{U\}$ by assuming that the external forces F_2 corresponding to the displacements U_2 are all equal to zero. Therefore $\{U_2\} = -[K_{22}^{-1}][K_{21}]\{U_1\}$. The resulting condensed mass matrix is then

$$[M_c] = [A_c]^T [M] [A_c]$$

where $A_c = \begin{bmatrix} 1 \\ -K_{22}^{-1} K_{21} \end{bmatrix}$

$$\begin{aligned} \text{Therefore } M_c &= \begin{bmatrix} 1 & -\frac{K_{21}}{K_{22}} \end{bmatrix} [M] \begin{bmatrix} 1 \\ -\frac{K_{21}}{K_{22}} \end{bmatrix} \\ &= \begin{bmatrix} 1 & -\frac{K_{21}}{K_{22}} \end{bmatrix} \begin{bmatrix} M_{11} - M_{12} \frac{K_{21}}{K_{22}} \\ M_{21} - M_{22} \frac{K_{21}}{K_{22}} \end{bmatrix} \\ &= M_{11} - M_{12} \frac{K_{21}}{K_{22}} - M_{21} \frac{K_{21}}{K_{22}} + M_{22} \left\{ \frac{K_{21}}{K_{22}} \right\}^2 \end{aligned}$$

where $\frac{K_{21}}{K_{22}} = [K_{22}]^{-1} [K_{21}]$

The result is considerably reduced stiffness and mass matrices, the dimensions of which correspond to the number of terms retained in U_1 .

1. SUBROUTINE FO2AEF(A,IA,B,IB,N,R,V,IV,DL,E,IFAIL)
2. Eigenvalues and eigenvectors of $(A-\lambda B)x=0$, where A is real symmetric and B is real symmetric positive definite, by Householder's method and the QL algorithm.
3. Language FORTRAN IV.
4. Description

The problem is reduced to the standard symmetric eigenproblem using Cholesky's method to decompose B into triangles $B=LL^T$, where L is lower triangular. Then $Ax=\lambda Bx$ implies $(L^{-1}AL^{-T})(L^Tx)=\lambda(L^Tx)$, hence the eigenvalues of $Ax=\lambda Bx$ are those of $Py=\lambda y$, where P is the symmetric matrix $L^{-1}AL^{-T}$. Householder's method is used to tridiagonalise the matrix P and the eigenvalues are found using the QL algorithm. An eigenvector Z of the derived problem is related to an eigenvector x of the original problem by $Z=L^Tx$. The eigenvectors Z are determined using the QL algorithm and are normalised so that $Z^TZ=1$, the eigenvectors of the original problem are then determined by solving $Z=L^Tx$ and are normalised so that $x^TBx=1$.

5. References

- MARTIN, R.S., WILKINSON, J.H. Reduction of the symmetric eigenproblem $Ax=\lambda Bx$ and related problems to standard form. Num. Math., Band 11, 1968, pp 99-110.
- MARTIN, R.S., REINSCH, C., WILKINSON, J.H. Householder's tridiagonalisation of a symmetric matrix. Num. Math., Band 11, 1968, pp 181-195.
- BOWDLER, H., MARTIN, R.S., REINSCH, C., WILKINSON, J.H. The QL and QR algorithms for symmetric matrices. Num. Math., Band 11, 1968, pp 293-306.

6. Parameters

A - the name of a two dimensional REAL ARRAY of at least (N,N)

elements. On entry it should contain the real symmetric matrix A in $(A-\lambda B)x=0$, the upper triangle only is needed. On exit the strict upper triangle will be unchanged. The lower triangle is used as work space. (See section 12).

- IA - an INTEGER quantity, the first dimension of A , $IA \geq N$.
- B - the name of a two dimensional REAL ARRAY of at least (N,N) elements. On entry it should contain the elements of the symmetric positive definite matrix B in $(A-\lambda B)x=0$, the upper triangle only is needed. On exit the upper triangle will be unchanged, the strict lower triangle is used as workspace.
- IB - an INTEGER quantity, the first dimension of B , $IB \geq N$.
- N - an INTEGER quantity, the order of matrix A .
- R - the name of a one dimensional REAL ARRAY of at least (N) elements, on exit it will contain the eigenvalues of $(A-\lambda B)x=0$ in order of increasing magnitude.
- V - the name of a two dimensional REAL ARRAY of at least (N,N) elements. On exit it will contain the eigenvectors of $(A-\lambda B)x=0$ in column order corresponding to the eigenvalues, i.e. $V(I,J)$, where $I=1,N$ corresponds to eigenvalue $R(J)$. (See section 12).
- IV - an INTEGER quantity, the first dimension of V , $IV \geq N$.
- DL - the name of a one dimensional REAL ARRAY of at least (N) elements used as work space.
- E - the name of a one dimensional REAL ARRAY of at least (N) elements used as work space.

IFAIL - an INTEGER variable. On entry the value of IFAIL determines the mode of failure in the routine. On exit IFAIL indicates successful use of the routine or acts as an error indicator.

If, on entry, $IFAIL=0$ (hard failure) the program will terminate with a failure message if any error is detected.

If, on entry, $IFAIL=1$ (soft failure) control returns to the calling sequence within the program if any error is detected by the routine. No failure message will be printed.

On exit $IFAIL=0$ for a successful call of the routine. For other exit values of IFAIL, and their meanings, see section 7.

It is essential, if the soft failure option is used, that the value of IFAIL is tested on exit.

7. Error Indicators

IFAIL=1 Failure in F01AEF, matrix B is not positive definite possibly due to rounding errors.

IFAIL=2 Failure in F02AMF, more than 30 iterations are needed to isolate any one eigenvalue.

If the hard failure option is employed and the routine fails because of the error labelled by I, the message printed is LIBRARY FAILS IN F02AEF WITH ERROR I.

8. Auxiliary Routines

This subroutine calls subroutines F01AEF, F01AJF, F02AMF, F01AEF and P01AAF.

9. Timing

For a matrix of order 10 the procedure takes 0.1 seconds.

For a matrix of order 20 the procedure takes 0.9 seconds.

For a matrix of order 30 the procedure takes 2.9 seconds.

10. Storage

The compiled subroutine and auxiliary subroutines require 1667 words. There are no internally declared arrays.

11. Accuracy

In general the accuracy of this subroutine is very high. However, if B is ill-conditioned with respect to inversion the eigenvalues and eigenvectors could be inaccurately determined. The answers to the test cases were always accurate to 9 significant figures.

12. Further Comments

If the subroutine is called with the same name for the arrays A and V then the eigenvectors will overwrite the real symmetric matrix A.

13. Example

To find the eigenvalues and eigenvectors of the problem $Ax = \lambda Bx$ where A is the symmetric matrix

10.0	2.0	3.0	1.0	1.0
	12.0	1.0	2.0	1.0
		11.0	1.0	-1.0
			9.0	1.0
				15.0

and B is the positive definite matrix

```

12.0  1.0  -1.0  2.0  1.0
      14.0  1.0  -1.0  1.0
      16.0  -1.0  1.0
      12.0  -1.0
      11.0

```

a short program could be

```

MASTER TESTEIGRV
DIMENSION A(5,5),B(10,10),EVEC(5,5),EVAL(10),WKS1(5),WKS2(100)
N=5
DO 1 I=1,N
  READ(1,100)(A(I,J),J=I,N)
1  CONTINUE
DO 2 I=1,N
  READ(1,100)(B(I,J),J=I,N)
2  CONTINUE
100 FORMAT(5F0.0)
    I=1
    CALL FOZAEF(A,N,B,10,N,EVAL,EVEC,5,WKS1,WKS2,I)
    IF(I.EQ.0) GOTO 10
    WRITE(2,200)I
200  FORMAT(1H0, 'FAILURE, IFAIL=', I5)
    STOP
10  DO 3 I=1,N
    WRITE(2,201)I,EVAL(I),(EVEC(J,I),J=1,N)
3  CONTINUE
201  FORMAT(1H0, 'LAMDA',I2,'=',1PE16.9//'EIGENVECTOR'//10
1(1X,1PE16.9//))
    STOP
    END
    FINISH

```

Results

LAMDA 1 = 4.327872110E-01

EIGENVECTOR

```

1.345905740E-01
-6.129472247E-02
-1.579025622E-01
1.094657877E-01
-4.147301179E-02

```

LAMDA 2 = 6.636627484E-01

EIGENVECTOR

```

8.291980649E-02
1.531483957E-01
-1.186036679E-01
-1.828130418E-01
3.561720369E-03

```

LAMDA 3 = 9.438590047E-01

EIGENVECTOR

-1.917100316E-01

1.589912115E-01

-7.483907094E-02

1.374689295E-01

-8.897789234E-02

LAMDA 4 = 1.109284540E 00

EIGENVECTOR

1.420119599E-01

1.424199505E-01

1.209976230E-01

1.255310152E-01

7.692207282E-03

LAMDA 5 = 1.492353233E 00

EIGENVECTOR

-7.638671787E-02

1.709800187E-02

-6.666453367E-02

8.604800930E-02

2.894334142E-01

14. Keywords

Householder

Eigenvalues

Eigenvectors

Standard Eigenproblem

Appendix 3

The finite element suite of computer programs developed

A listing of the set of computer programs developed to analyse folded plate box structure.

```
LDSET(PRESET=NGINF,MAP=B/ZZZZMP)
LGO(PL=6000)
CATALOG(TAPE3,MOJDAT1 ,FO=ASIS,ST=S6A)
#####
```

```
PROGRAM STRUCT(INPUT,TAPE1=INPUT,OUTPUT,TAPE2=OUTPUT,TAPE3)
LEVEL 2,K
```

```
C THIS PROGRAM COMPUTES THE STIFFNESS MATRIX OF A BOX OF NXNYNZ ELEMENT
C.....FROM 3 STANDARD PLATE ELEMENTS WHOSE STIFFNESS MATRICES ARE COMPUTED
C.....THESE ELEMENTS ARE ROTATED AND MERGED INTO A BOX. THE
C INERTIA MATRIX IS SIMILARLY OBTAINED AND THESE COMPLETED BOX MATRICES
C ARE STORED IN DATAFILE MO//DATA
```

```
DIMENSION K(24,24),Q(24,24)
INTEGER ORDER
INTEGER E
REAL KK(24,24),P,Y,LENGTH,WIDTH,KJ
REAL K(180,180),K1(24,24)
COMMON/UPPER/K
```

```
NX=4
NY=2
NZ=1
```

```
C ... LENGTH IS LENGTH OF BOX
C.....WIDTH IS WIDTH OF BOX
```

```
LENGTH=0.515
WIDTH=0.255
HEIGHT=0.255
A=LENGTH/FLOAT(NX)
B=WIDTH/FLOAT(NY)
C=HEIGHT/FLOAT(NZ)
```

```
C.....V=POISSON'S RATIO
V=0.3
```

```
C.....H=THICKNESS OF PLATE
```

```
H=0.00054
Y=(2.06E11)
V=0.3
```

```
C.....RHO=DENSITY OF PLATE
```

```
RHO=7800.0*H
N=24
ORDER=(NX+1)*(NY+1)*(NZ+1)*6
DO 4 I = 1,ORDER
DO 4 J = 1,ORDER
4 K(I,J) = 0.0
```

```
CALL BEND1(KK,N,A,B,V,Y,H,RHO)
CALL CLEAR(K1)
CALL PLAIN1 (K1,N,A,B,V,Y,H,RHO,KK)
CALL REORDER(N,KK,KJ)
CALL ROTATE1 (K1,KK,Q,R)
CALL COMPLET (K,NZ,ORDER,R,N,NX,NY,1 )
CALL COMPLET (K,NZ,ORDER,R,N,NX,NY,2 )
```

```
C.....CALL ROTATE2 (K1,KK,Q,R)
```

```
C.....CALL COMPLET (K,NX,ORDER,R,N,NY,NZ,3)
```

```
C.....CALL COMPLET (K,NX,ORDER,R,N,NY,NZ,4)
```

```
CALL BEND1(KK,N,A,C,V,Y,H,RHO)
CALL CLEAR(K1)
```

```
CALL PLAIN1 (K1,N,A,C,V,Y,H,RHO,KK)
```

```
CALL REORDER(N,KK,KJ)
```

```
CALL ROTATE3 (K1,KK,Q,R)
```

```
CALL COMPLET (K,NY,ORDER,R,N,NX,NZ,5)
```

```
CALL COMPLET (K,NY,ORDER,R,N,NX,NZ,6)
```

```
REWIND 3
```

```
WRITE (3) K
```

```
C.....USE K ANDKK MATRIX FOR INERTIA MATRIX
```

```
DO14 I = 1,ORDER
```

```
DO14 J = 1,ORDER
```

```
14 K(I,J) = 0.0
```

```
CALL BEND2(KK,N,A,B,V,Y,H,RHO)
```

```
CALL CLEAR(K1)
```

```
CALL PLAIN2 (K1,N,A,B,V,Y,H,RHO,KK)
```

```
CALL REORDER(N,KK,KJ)
```

```
CALL ROTATE1 (K1,KK,Q,R)
```

```
CALL COMPLET (K,NZ,ORDER,R,N,NX,NY,1 )
```

```
CALL COMPLET (K,NZ,ORDER,R,N,NX,NY,2 )
```

```
C.....CALL ROTATE2 (K1,KK,Q,R)
```

```
C.....CALL COMPLET (K,NX,ORDER,R,N,NY,NZ,3)
```

```
C.....CALL COMPLET (K,NX,ORDER,R,N,NY,NZ,4)
```

```
CALL BEND2(KK,N,A,C,V,Y,H,RHO)
```

```
CALL CLEAR(K1)
```

```
CALL PLAIN2 (K1,N,A,C,V,Y,H,RHO,KK)
```

```
CALL REORDER(N,KK,KJ)
```

```
CALL ROTATE3 (K1,KK,Q,R)
```

```
CALL COMPLET (K,NY,ORDER,R,N,NX,NZ,5)
```

```
CALL COMPLET (K,NY,ORDER,R,N,NX,NZ,6)
```

```
C.....STORE MATRIX UNFORMATTED IN MAG TAPE
```

```
WRITE (5) K
```

```
ENDFILE 3
```

```
REWIND 3
```

```
STOP
```

```
END
```

```

SUBROUTINE BEND 1 (KK,N,A,B,V,E,T,RHO)
REAL          KK(N,N)          ,P,A,B,V
C,.....CLEAR KK MATRIX
DO 1 I=1,N
DO 1 J=1,N
1 KK(I,J)=0.0
C,.....COMPUTE LOWER TRIANGULAR KK MATRIX
C,.....N=12 SIGNIFIES BENDING N=24 FOR BENDING + STRETCHING
IF(N.EQ,12) GO TO 10
IF(N.EQ,24) GO TO 20
10 I=1
C,.....THIS GIVES A 12 X 12 MATRIX
J=3
WRITE(2,11)
11 FORMAT(//'THIS IS FOR PLATE BENDING ONLY')
GO TO 50
20 I=3
WRITE(2,21)
21 FORMAT(//'THIS IS FOR PLATE BENDING AND STRETCHING')
J=6
C,.....THIS GIVES A 24 X 24 MATRIX
GO TO 50
50 P=(A/B)**2
J2=J*2
J3=J*3
KK(I,1)=(4.0*P)+(4.0/P)+2.8-(0.8*V)
KK(I+1,1)=((2.0*P)+(0.2)+(0.8*V))*B
KK(I+1,1+1)=((4.0*P/3.0)+(4.0*(1.0-V)/15.0))*(B**2)
KK(I+2,1)=((2.0/P)+(0.2)+(0.8*V))*(-A)
KK(I+2,1+1)=-V*A*B
KK(I+2,1+2)=((4.0/(3.0*P))+((4.0*(1-V))/15.0))*(A*A)
KK(I+J,1)=(2.0/P)-(4.0*P)-2.8+(4.0*V/5.0)
KK(I+J,1+1)=((2.0*P)+(1.0-V)/5.0))*(-B)
KK(I+J,1+2)=((-1.0/P)+((1.0+(4.0*V))/5.0))*A
KK(I+J,1+J)=(4.0*P)+(4.0/P)+(2.8)-(0.8*V)
KK(I+J+1,1)=((2.0*P)+(1.0-V)/5.0))*B
KK(I+J+1,1+1)=((2.0*P/3.0)-((1-V)/15.0))*(B*B)
KK(I+J+1,1+2)=0.0
KK(I+J+1,1+J)=((2.0*P)+(0.2)+(0.8*V))*(-B)
KK(I+J+1,1+J+1)=((4.0*P/3.0)+(4.0*(1.0-V)/15.0))*(B*B)
KK(I+J+2,1)=((-1.0/P)+((1.0+(4.0*V))/5.0))*A
KK(I+J+2,1+1)=0.0
KK(I+J+2,1+2)=((2.0/(3.0*P))-((4.0*(1.0-V))/15.0))*(A*A)
KK(I+J+2,1+J)=((-2.0/P)-(0.2)-(0.8*V))*A
KK(I+J+2,1+J+1)=V*A*B
KK(I+J+2,1+J+2)=((4.0/(3.0*P))+((4.0*(1.0-V))/15.0))*(A*A)
KK(I+J2,1)=(-2.0*P)-((2.0/P)+(2.8)-(0.8*V)
KK(I+J2,1+1)=(-P+((1-V)/15.0))*B
KK(I+J2,1+2)=((-1.0/P)+((1-V)/5.0))*(-A)
KK(I+J2,1+J)=(-2.0*((2.0/P)-P)-((14.0-(4.0*V))/5.0)
KK(I+J2,1+J+1)=((-P+(1.0+(4.0*V))/5.0))*B)
KK(I+J2,1+J+2)=((2.0/P)+((1.0-V)/5.0))*A
KK(I+J2,1+J2)=((4.0*P)+(4.0/P)+(2.8)-(0.8*V)
KK(I+J2+1,1)=(P-((1-V)/5.0))*B)
KK(I+J2+1,1+1)=((P/3.0)+((1-V)/15.0))*(B*B)
KK(I+J2+1,1+2)=0.0
KK(I+J2+1,1+J)=(-P+(1.0+(4.0*V))/5.0))*B
KK(I+J2+1,1+J+1)=(((2.0*P)/3.0)-((4.0*(1.0-V))/15.0))*(B*B)
KK(I+J2+1,1+J+2)=0.0
KK(I+J2+1,1+J2)=((-2.0*P)-(0.2)-(0.8*V))*B
KK(I+J2+1,1+J2+1)=((4.0*P/3.0)+(4.0*(1-V)/15.0))*(B*B)
KK(I+J2+2,1)=((1.0/P)-((1-V)/5.0))*(-A)
KK(I+J2+2,1+1)=0.0
KK(I+J2+2,1+2)=((1.0/(3.0*P))+((1-V)/15.0))*(A*A)
KK(I+J2+2,1+J)=((2.0/P)+((1.0-V)/5.0))*(-A)
KK(I+J2+2,1+J+1)=0.0
KK(I+J2+2,1+J+2)=((2.0/(3.0*P))-((1.0-V)/15.0))*(A*A)
KK(I+J2+2,1+J2)=((2.0/P)+(0.2)+(0.8*V))*A)
KK(I+J2+2,1+J2+1)=-V*A*B
KK(I+J2+2,1+J2+2)=((4.0/(3.0*P))+((4.0*(1-V))/15.0))*(A*A)
KK(I+J3,1)=-2.0*((2.0/P)-P)-((14.0-(4.0*V))/5.0)
KK(I+J3,1+1)=(-P+((1.0+(4.0*V))/5.0))*B
KK(I+J3,1+2)=((2.0/P)+((1.0-V)/5.0))*A
KK(I+J3,1+J)=-((2.0*P)-((2.0/P)+(2.8)-(0.8*V)
KK(I+J3,1+J+1)=(P-((1-V)/5.0))*B)
KK(I+J3,1+J+2)=((1.0/P)-((1-V)/5.0))*A)
KK(I+J3,1+J2)=((2.0*((1.0/P)-((2.0*P)-((14.0-(4.0*V))/5.0)
KK(I+J3,1+J2+1)=((2.0*P)+(1.0-V)/5.0))*B)
KK(I+J3,1+J2+2)=((1.0/P)-((1.0+(4.0*V))/5.0))*A)
KK(I+J3,1+J3)=((4.0*P)+(4.0/P)+(2.8)-(0.8*V)
KK(I+J3+1,1)=(P-((1.0+(4.0*V))/5.0))*B)
KK(I+J3+1,1+1)=((2.0*P/3.0)-((4.0*(1.0-V))/15.0))*(B*B)
KK(I+J3+1,1+2)=0.0
KK(I+J3+1,1+J)=(P-((1-V)/5.0))*(-B)
KK(I+J3+1,1+J+1)=((P/3.0)+((1-V)/15.0))*(B*B)
KK(I+J3+1,1+J+2)=0.0
KK(I+J3+1,1+J2)=((2.0*P)+(1.0-V)/5.0))*(-B)
KK(I+J3+1,1+J2+1)=((2.0*P/3.0)-((1.0-V)/15.0))*(B*B)

```

```

KK(I+J3+1,I+J3+1)=((4.0*P/3.0)+(4.0*(1-V)/15.0))*(B+B)
KK(I+J3+2,1)=((2.0/P)+((1.0-V)/5.0))*(-A)
KK(I+J3+2,1+1)=0.0
KK(I+J3+2,1+2)=((2.0/(3.0*P))-((1.0-V)/15.0))*(A+A)
KK(I+J3+2,1+J)=((-1.0/P)+((1-V)/5.0))*A
KK(I+J3+2,1+J+1)=0.0
KK(I+J3+2,1+J+2)=((1.0/(3.0*P))+((1-V)/15.0))*(A+A)
KK(I+J3+2,1+J2)=((1.0/P)-((1.0+(4.0*V))/5.0))*A
KK(I+J3+2,1+J2+1)=0.0
KK(I+J3+2,1+J2+2)=((2.0/(3.0*P))-((4.0*(1.0-V)/15.0))*(A+A)
KK(I+J3+2,1+J3)=((2.0/P)+(0.2)+(0.8*V))*A
KK(I+J3+2,1+J3+1)=V*A*B
KK(I+J3+2,1+J3+2)=((4.0/(3.0*P))+((4.0*(1-V)/15.0))*(A+A)
C.....MULTIPLY BY FACTOR
DO 54 I=1,N
DO 54 J=1,I
54 KK(I,J)=(KK(I,J))*(E*(T+3))/(12.0*(1.0-(V+2)))*A*B)
C.....COMPLETE UPPER MATRIX TRIANGLE
NH1=N-1
DO 55 I=1,NH1
IA1=I+1
DO 55 J=IA1,N
55 KK(I,J)=KK(J,I)
C.....WRITE COMPLETE ELEMENT STIFFNESS MATRIX
WRITE(2,00) ((KK(I,J),J=1,N),I=1,N)
60 FORMAT (1H1,'*KK MATRIX'//(' ',12E10.4))
RETURN
END

SUBROUTINE PLAIN1 (KK,N,A,B,V,E,T,RHO,K1)
REAL K1(N,N)
REAL KK(N,N)
C.....N = 8 SIGNIFIES PLAIN STRAIN, N = 24 FOR BENDING AND STRETCHING
IF(N.EQ.8) GO TO 10
IF(N.EQ.24) GO TO 20
STOP
10 WRITE(2,11)
11 FORMAT(//'THIS IS FOR PLAIN STRAIN ONLY')
J=2
GO TO 30
20 J=6
C.....THIS GIVES A 8 X 8 MATRIX
30 J2=J+2
C.....NOTE THAT P = (A/B) NOT (A/B+2)
P=A/B
KK(1,1)=(4.0/P)+(2.0*(1.0-V)*P)
KK(2,1)=3.0*(1.0+V)/2.0
KK(2,2)=(4.0*P)+(2.0*(1.0-V)/P)
KK(1+J,1)=(2.0/P)-((2.0*(1.0-V)*P)
KK(1+J,2)=-3.0*(1.0-3.0*V)/2.0
KK(1+J,1+J)=(4.0/P)+(2.0*(1.0-V)*P)
KK(1+J+1,1)=3.0*(1.0-(3.0*V))/2.0
KK(1+J+1,2)=(-4.0*P)+((1.0-V)/P)
KK(1+J+1,1+J)=-3.0*(1.0+V)/2.0
KK(1+J+1,1+J+1)=(4.0*P)+(2.0*(1.0-V)/P)
KK(1+J2,1)=(-2.0/P)-((1.0-V)*P)
KK(1+J2,2)=(-3.0*(1.0+V)/2.0)
KK(1+J2,1+J)=(-4.0/P)+((1.0-V)*P)
KK(1+J2,1+J+1)=(-3.0*(1-(3.0*V))/2.0)
KK(1+J2,1+J2)=(4.0/P)+(2.0*(1.0-V)*P)
KK(1+J2+1,1)=-3.0*(1.0+V)/2.0
KK(1+J2+1,2)=(-2.0*P)-((1.0-V)/P)
KK(1+J2+1,1+J)=(3.0*(1.0-(3.0*V))/2.0)
KK(1+J2+1,1+J+1)=(2.0*P)-((2.0*(1.0-V)/P)
KK(1+J2+1,1+J2)=(3.0*(1.0+V)/2.0)
KK(1+J2+1,1+J2+1)=(4.0*P)+(2.0*(1.0-V)/P)
J3=J+3
KK(1+J3,1)=(-4.0/P)+((1.0-V)*P)
KK(1+J3,2)=(3.0*(1.0-(3.0*V))/2.0)
KK(1+J3,1+J)=(-2.0/P)-((1.0-V)*P)
KK(1+J3,1+J+1)=(3.0*(1.0+V)/2.0)
KK(1+J3,1+J2)=(2.0/P)-((2.0*(1.0-V)*P)
KK(1+J3,1+J2+1)=(-3.0*(1.0-(3.0*V))/2.0)
KK(1+J3,1+J3)=(4.0/P)+(2.0*(1.0-V)*P)
KK(1+J3+1,1)=(-3.0*(1.0-(3.0*V))/2.0)
KK(1+J3+1,2)=(2.0*P)-((2.0*(1.0-V)/P)
KK(1+J3+1,1+J)=(3.0*(1.0+V)/2.0)
KK(1+J3+1,1+J+1)=(-2.0*P)-((1.0-V)/P)
KK(1+J3+1,1+J2)=(3.0*(1.0-(3.0*V))/2.0)
KK(1+J3+1,1+J2+1)=(-4.0*P)+((1.0-V)/P)
KK(1+J3+1,1+J3)=(-3.0*(1.0+V)/2.0)
KK(1+J3+1,1+J3+1)=(4.0*P)+(2.0*(1.0-V)/P)
C.....MULTIPLY BY COMMON FACTOR
DO 34 I=1,N
DO 34 J=1,I
34 KK(I,J)=(KK(I,J))*(E*T)/(12.0*(1.0-(V+2)))
C.....COMPLETE UPPER MATRIX TRIANGLE
NH1=N-1
DO 35 I=1,NH1
IA1=I+1
DO 35 J=IA1,N
35 KK(I,J)=KK(J,I)
DO 38 I=1,N
DO 38 J=1,N
38 K1(I,J)=K1(I,J)+KK(I,J)
WRITE(2,40) ((K1(I,J),J=1,N),I=1,N)

```

```

      I=1
      NO=N
1013 I=I+1
      IF(I.EQ, NO) GO TO 1112
      J=1
1011 IF(K1(I,J),NE,K1(J,I)) GO TO 1111
      J=J+1
      IF(J.LT,I) GO TO 1011
      GO TO 1013
1111 WRITE (2,1012) (I,J,K1(I,J) ,K1(J,I))
1012 FORMAT(///' UNSYMMETRICAL MATRIX'///' ERRUK POSITION IS  ',2I3,////' ')
      I=I+1,2F12.4)
      IF(I.LT,NO ) GO TO 1013
1112 CONTINUE

```

```

      RETURN
      END

```

```

      SUBROUTINE BEHD 2 (MM,N,A,B,V,E,T,RHO)
      REAL MM(N,N),P,A,B,V
C..... CLEAR MM MATRIX
      DO 1 I=1,N
      DO 1 J=1,N
      1 MM(I,J)=0.0

C..... N=12 SIGNIFIES BENDING N=24 FOR BENDING + STRETCHING
      IF(N.EQ,12) GO TO 10
      IF(N.EQ,24) GO TO 20
      10 I=1
      WRITE(2,11)
      11 FORMAT(//'THIS IS FOR PLATE BENDING ONLY')
      J=3
C..... THIS GIVES A 12 X 12 MATRIX
      GO TO 50
      20 I=3
      WRITE(2,21)
      21 FORMAT(//'THIS IS FOR PLATE BENDING AND STRETCHING')
      J=6
C..... THIS GIVES A 24 X 24 MATRIX
      GO TO 50
      50 P=(A/B)**2
      J2=J*2
      J3=J*3
      MM(I,1)=24178.0
      MM(I+1,1)=5227*B
      MM(I+1,1+1)=560*B*B
      MM(I+2,1)=-3227*A
      MM(I+2,1+1)=-441.0*A*B
      MM(I+2,1+2)=560.0*A*A
      MM(I+J,1)=8582.0
      MM(I+J,1+1)=1918.0*B
      MM(I+J,1+2)=-1593.0*A
      MM(I+J,1+J)=24178.0
      MM(I+J+1,1)=-1918.0*B
      MM(I+J+1,1+1)=-420.0*B*B
      MM(I+J+1,1+2)=294.0*A*B
      MM(I+J+1,1+J)=-3227.0*B
      MM(I+J+1,1+J+1)=560.0*B*B
      MM(I+J+2,1)=-1593*A
      MM(I+J+2,1+1)=-294.0*A*B
      MM(I+J+2,1+2)=280.0*A*A
      MM(I+J+2,1+J)=-3227.0*A
      MM(I+J+2,1+J+1)=441.0*A*B
      MM(I+J+2,1+J+2)=560.0*A*A
      MM(I+J2,1)=2758.0
      MM(I+J2,1+1)=812.0*B
      MM(I+J2,1+2)=-812.0*A
      MM(I+J2,1+J)=8582.0
      MM(I+J2,1+J+1)=-1593.0*B
      MM(I+J2,1+J+2)=-1918.0*A
      MM(I+J2,1+J2)=24178.0
      MM(I+J2+1,1)=-812.0*B
      MM(I+J2+1,1+1)=-210.0*B*B
      MM(I+J2+1,1+2)=196.0*A*B
      MM(I+J2+1,1+J)=-1393*B
      MM(I+J2+1,1+J+1)=280.0*B*B
      MM(I+J2+1,1+J+2)=294.0*A*B
      MM(I+J2+1,1+J2)=-3227.0*B
      MM(I+J2+1,1+J2+1)=560.0*B*B
      MM(I+J2+2,1)=812.0*A
      MM(I+J2+2,1+1)=196.0*A*B
      MM(I+J2+2,1+2)=-210.0*A*A
      MM(I+J2+2,1+J)=1918.0*A
      MM(I+J2+2,1+J+1)=-294.0*A*B
      MM(I+J2+2,1+J+2)=-420.0*A*A
      MM(I+J2+2,1+J2)=3227.0*A
      MM(I+J2+2,1+J2+1)=-441.0*A*B
      MM(I+J2+2,1+J2+2)=560.0*A*A
      MM(I+J3,1)=8582.0
      MM(I+J3,1+1)=1593*B
      MM(I+J3,1+2)=-1918.0*A
      MM(I+J3,1+J)=2758.0
      MM(I+J3,1+J+1)=-812.0*B
      MM(I+J3,1+J+2)=-812.0*A

```

```

MM(I+J3,1+J2+1)=-1918,0*B
MM(I+J3,1+J2+2)=1395,0*A
MM(I+J3,1+J3)=24178,0
MM(I+J3+1,1)=1395,0*B
MM(I+J3+1,1+1)=260,0*A*B
MM(I+J3+1,1+2)=-294,0*A*B
MM(I+J3+1,1+J)=812,0*B
MM(I+J3+1,1+J+1)=-210,0*B*B
MM(I+J3+1,1+J+2)=-196,0*A*B
MM(I+J3+1,1+J2)=1918,0*B
MM(I+J3+1,1+J2+1)=-420,0*B*B
MM(I+J3+1,1+J2+2)=294,0*A*B
MM(I+J3+1,1+J3)=5227,0*B
MM(I+J3+1,1+J3+1)=560,0*B*B
MM(I+J3+2,1)=1918,0*A
MM(I+J3+2,1+1)=294,0*A*A
MM(I+J3+2,1+2)=-420,0*A*A
MM(I+J3+2,1+J)=812,0*A
MM(I+J3+2,1+J+1)=-196,0*A*B
MM(I+J3+2,1+J+2)=-210,0*A*A
MM(I+J3+2,1+J2)=1395,0*A
MM(I+J3+2,1+J2+1)=-294,0*A*B
MM(I+J3+2,1+J2+2)=280,0*A*A
MM(I+J3+2,1+J3)=5227,0*A
MM(I+J3+2,1+J3+1)=441,0*A*B
MM(I+J3+2,1+J3+2)=560,0*A*A

```

```

C.....MULTIPLY BY COMMON FACTOR
DO 74 I=1,N
DO 74 J=1,I
74 MM(I,J)=(MM(I,J))*RHU*A*B/176400
C.....COMPLETE UPPER INERTIA MATRIX TRIANGLE.
NM1=N-1
DO 75 I=1,NM1
IA1=I+1
DO 75 J=IA1,N
75 MM(I,J)=MM(J,I)
C.....WRITE COMPLETED ELEMENT INERTIA MATRIX
WRITE(2,80) ((MM(I,J),J=1,N),I=1,N)
80 FORMAT (1H1,'MM MATRIX'////(' ',12E10,4))
RETURN
END

```

```

####S
****

```

```

SUBROUTINE PLAIN2 (MM,N,A,B,V,E,T,RHD,K1)
REAL K1(N,N)
REAL MM(N,N)
C..... N = 8 SIGNIFIES PLAIN STRAIN, N = 24 FOR BENDING AND STRETCHING
IF(N.EQ,8) GO TO 10
IF(N.EQ,24) GO TO 20
STOP
10 WRITE(2,11)
11 FORMAT(//'THIS IS FOR PLAIN STRAIN ONLY')
J=2
GO TO 30
20 J=6
30 J2=J+2
P=A/B
C..... THIS GIVES A 8 X 8 MATRIX
C..... COMPUTE INERTIA MATRIX
MM(1,1)=4,0
MM(2,1)=0,0
MM(2,2)=4,0
MM(1+J,1)=2,0
MM(1+J,2)=0,0
MM(1+J,1+J)=4,0
MM(1+J+1,1)=0,0
MM(1+J+1,2)=2,0
MM(1+J+1,1+J)=0,0
MM(1+J+1,1+J+1)=4,0
MM(1+J2,1)=1,0
MM(1+J2,2)=0,0
MM(1+J2,1+J)=2,0
MM(1+J2,1+J+1)=0,0
MM(1+J2,1+J2)=4,0
MM(1+J2+1,1)=0,0
MM(1+J2+1,2)=1,0
MM(1+J2+1,1+J)=0,0
MM(1+J2+1,1+J+1)=2,0
MM(1+J2+1,1+J2)=0,0
MM(1+J2+1,1+J2+1)=4,0
J3=J+3
MM(1+J3,1)=2,0
MM(1+J3,2)=0,0
MM(1+J3,1+J)=1,0
MM(1+J3,1+J+1)=0,0
MM(1+J3,1+J2)=2,0
MM(1+J3,1+J2+1)=0,0
MM(1+J3,1+J3)=4,0
MM(1+J3+1,1)=0,0
MM(1+J3+1,2)=2,0
MM(1+J3+1,1+J)=0,0
MM(1+J3+1,1+J+1)=1,0

```

```

      MM(1+J3+1,1+J2)=0,0
      MM(1+J3+1,1+J2+1)=2,0
      MM(1+J5+1,1+J5)=0,0
      MM(1+J3+1,1+J5+1)=4,0
C.....MULTIPLY BY COMMON FACTOR
      DO 50 I=1,N
      DO 50 J=1,i
      50 MM(I,J)=(MM(I,J)*RHO*A*B/36,0)
C.....COMPLETE UPPER TRIANGULAR MATRIX
      NM1=N-1
      DO 60 I=1,NM1
      IA1=I+1
      DO 60 J=IA1,N
      60 MM(I,J)=MM(J,I)
      DO 38 I=1,N
      DO 38 J=1,N
      38 K1(I,J)=K1(I,J)+MM(I,J)
      WRITE (2,70)
      70 FORMAT (' TRANSLATIONAL INERTIA MATRIX COMPLETED')
      WRITE(2,40) ((K1(I,J),J=1,N),I=1,N)
      40 FORMAT (1H1,'MM MATRIX'////(' ',12E10,4))
      RETURN
      END

```

```

      SUBROUTINE REORDER (N, K,KJ)
      REAL K( N,N ),KJ
      C      RENUMBER NODAL SYSTEM
C.....INTERCHANGE NODE 2 AND 4 ROWS
      DO 60 I=7,12,1
      DO 60 J=1,24,1
      KJ=K(I+12,J)
      K(I+12,J)= K(I,J)
      60 K(I,J)=KJ
C.....INTERCHANGE NODE 2 AND 4 COLUMNS
      DO 70 J=7,12,1
      DO 70 I=1,24,1
      KJ=K(I,J+12)
      K(I,J+12)=K(I,J)
      70 K(I,J)=KJ
C.....REORDER NODAL SYSTEM
C.....INTERCHANGE NODE 3 AND 4 ROWS
      DO 80 I=13,18,1
      DO 80 J=1,24,1
      KJ=K(I+6,J)
      K(I+6,J)=K(I,J)
      80 K(I,J)=KJ
C.....INTERCHANGE NODE 3 AND 4 COLUMNS
      DO 90 J=13,18
      DO 90 I=1,24
      KJ=K(I,J+6)
      K(I,J+6)=K(I,J)
      90 K(I,J)=KJ
      100 WRITE(2,100)((K(I,J),J=1,24 ),I=1,24 )
      100 FORMAT('REORDERED ELEMENT MATRIX'////(' ',10F12,4))

      RETURN
      END

```

```

      SUBROUTINE ROTATE1 (R,K,K1,S)
      DIMENSION R(24,24), S(24,24)
      REAL K(24,24),K1(24,24)
      DO 5 I=1,24
      DO 5 J=1,24
      S(I,J)=0,0
      K1(I,J)=0,0
      5 R(I,J)=0,0
      DO 10 I=1,24
      10 K(I,I)=1,0
      WRITE(2,40) ((R(I,J),J=1,24),I=1,24)
C.....POST-MULTIPLY BY R
      DO 50 I=1,24
      DO 50 J=1,24
      DO 50 L=1,24
      50 K1(I,J)=K1(I,J)+(K(I,L)*R(L,J))
      DO 52 I=1,24
      DO 52 J=1,24
      DUMMY=R(I,J)
      R(I,J)=R(J,I)
      R(J,I)=DUMMY
      52 CONTINUE
      WRITE(2,40) ((R(I,J),J=1,24),I=1,24)
C.....PRE-MULTIPLY BY R TRANSPOSED
      DO 55 I=1,24
      DO 55 J=1,24
      DO 55 L=1,24
      55 S (I,J)=S (I,J)+(R(I,L)*K1(L,J))
      40 FORMAT(24F5,2)
      WRITE (2,60) ((S (I,J),J=1, 24),I=1,24)
      60 FORMAT ('1ROTATED ELEMENTAL MATRIX'////(' ',12E10,4))
      RETURN
      END

```

```

SUBROUTINE ROTATEZ (K,K1,S)
REAL K(24,24),K1(24,24)
DIMENSION R(24,24), S(24,24)
DO 5 I=1,24
DO 5 J=1,24
S(I,J)=0.0
K1(I,J)=0.0
5 R(I,J)=0.0
DO 10 I=1,24,3
J=I+1
10 R(I,J)= 1.0
DO 20 I=2,24,3
J=I+1
20 R(I,J)=1.0
DO 30 I=3,24,3
J=I-2
30 R(I,J)=1.0
WRITE(2,40) ((R(I,J),J=1,24),I=1,24)
40 FORMAT(24F5,2)
C.....POST-MULTIPLY BY R
DO 50 I=1,24
DO 50 J=1,24
DO 50 L=1,24
50 K1(I,J)=K1(I,J)+(K(I,L)*R(L,J))
DO 52 I=1,24
DO 52 J=1,24
DUMMY=R(I,J)
R(I,J)=R(J,I)
R(J,I)=DUMMY
52 CONTINUE
WRITE(2,40) ((R(I,J),J=1,24),I=1,24)
C.....PRE-MULTIPLY BY R TRANSPOSED
DO 55 I=1,24
DO 55 J=1,24
DO 55 L=1,24
55 S (I,J)=S (I,J)+(R(I,L)*K1(L,J))
WRITE (2,60) ((S (I,J),J=1, 24),I=1,24)
60 FORMAT ('ROTATED ELEMENTAL MATRIX'///(' ',12E10.4))
RETURN
END

```

```

SUBROUTINE ROTATE3 (R,K,K1,S)
REAL K(24,24),K1(24,24)
DIMENSION R(24,24), S(24,24)
DO 5 I=1,24
DO 5 J=1,24
S(I,J)=0.0
K1(I,J)=0.0
5 R(I,J)=0.0
DO 10 I=1,24,3
J=I
10 R(I,J)= 1.0
C.....POST-MULTIPLY BY R
DO 20 I=2,24,3
J=I+1
20 R(I,J)=1.0
DO 30 I=3,24,3
J=I-1
30 R(I,J)=-1.0
WRITE(2,40) ((R(I,J),J=1,24),I=1,24)
40 FORMAT(24F5,2)
C.....PRE-MULTIPLY BY R TRANSPOSED
DO 50 I=1,24
DO 50 J=1,24
DO 50 L=1,24
50 K1(I,J)=K1(I,J)+(K(I,L)*R(L,J))
DO 52 I=1,24
DO 52 J=1,24
DUMMY=R(I,J)
R(I,J)=R(J,I)
R(J,I)=DUMMY
52 CONTINUE
WRITE(2,40) ((R(I,J),J=1,24),I=1,24)
DO 55 I=1,24
DO 55 J=1,24
DO 55 L=1,24
55 S (I,J)=S (I,J)+(R(I,L)*K1(L,J))
WRITE (2,60) ((S (I,J),J=1, 24),I=1,24)
60 FORMAT ('ROTATED ELEMENTAL MATRIX'///(' ',12E10.4))
RETURN
END

```

```

SUBROUTINE COMPLET (K,NZ,NO,KK,NS,NX,NY,NA)
LEVEL 2,K
REAL KK(NS,NS),K(NO,NO)
INTEGER E
C.....WRITE (2,1003) ((KK(J, JJ),JJ=1,NS),J=1,NS)
I1=(NX+1)*(NY+1)+6
NK=(NX+1)*6
N1=(NX+1)*(NZ+1)+6
IF((NA.EQ.1).OR.(NA.EQ.2))N1=(NX+1)*NZ+6
NJ=6
IF((NA.EQ.3).OR.(NA.EQ.4)) NJ=(NZ+1)*6
C.....COMPLETE MATRIX FOR WHOLE PLATE FROM ELEMENT MATRICES
I=-5

```

```

C.....IT DENOTES STARTING POINT AND INCREMENTAL X,
IT=1-(NJ)
NH=HK
IF (NA, EQ, 2) IT=IT+(NX+1)*(NY+1)*HZ*6
IF (NA, EQ, 4) IT=IT+(NZ*6)
IF (NA, EQ, 6) IT=IT+((NX+1)*HZ*6)
10 I=1+6
IT=IT+(NJ)
IF (I, EQ, 1) GO TO 100
IF (NH, GT, (NK)) GO TO 30
C.....DOUBLE POINT FIRST ROW FOLLOWS
IF (I, LT, (NN-5)) GO TO 200
IF (I, EQ, (NN-5)) GO TO 300
IF (I, GT, (I1-NK)) GO TO 40
25 IF (I, EQ, (NN+1)) GO TO 400
C.....QUADRUPEL POINTS ROWS FOLLOWS
IF (I, EQ, (NN+1)) NN=NN+NK
30 IF (I, LT, (NN-5)) GO TO 800
IF (I, EQ, (NN-5)) GO TO 500
IF (I, LT, (I1-NK)) GO TO 25
40 CONTINUE
IF (I, EQ, (NN+1)) GO TO 600
C
DOUBLE POINTS ROWS FOLLOWS
IF (I, LT, (I1-5)) GO TO 700

```

```

C.....THIS LEAVES ONLY ROWS OF LAST NODE

```

```

E = 19
M = IT - NJ - N1
101 N=1
L=IT
102 DO 105 J=1,6
MM = M+J-1
K(L,MM) = KK(E,J)+K(L,MM)
K(L,MM+NJ)=KK(E,J+6)+K(L,MM+NJ)
K(L,MM+N1) = KK(E,J+12)+K(L,MM+N1)
K(L,MM+N1+NJ) = KK(E,J+18)+K(L,MM+N1+NJ)
105 CONTINUE
L=L+1
E=E+1
N=N+1
IF (N, LT, 7) GO TO 102
GO TO 1000

```

```

100 E=1
M=IT
C.....ROWS 1 TO 6
GO TO 101

```

```

300 E=7
M=IT-NJ
C.....ROWS OF CORNER NODES
GO TO 101

```

```

600 E=13
M=IT-N1
C.....CORNER NODES OF LAST NODE
GO TO 101

```

```

200 E = 7
M=IT-NJ
250 L=IT
N=1
251 CONTINUE

```

```

C.....COMPUTE DOUBLE POINTS ROW
DO 255 J=1,6
MM=M+J-1
K(L,MM)=KK(E,J)+K(L,MM)
NJ2=NJ+2
K(L,MM+NJ)= KK(E,J+6)+KK(E-6,J)+K(L,MM+NJ)
K(L,MM+NJ2)= KK(E-6,J+6)+K(L,MM+NJ2)
K(L,MM+N1) = KK(E,J+12)+K(L,MM+N1)
K(L,MM+N1+NJ)= KK(E,J+18)+KK(E-6,J+12)+K(L,MM+N1+NJ)
K(L,MM+N1+NJ2)= KK(E-6,J+18)+K(L,MM+N1+NJ2)
255 CONTINUE
E=E+1
L=L+1
N=N+1
IF (N, LT, 7) GO TO 251
GO TO 1000

```

```

400 L=IT
M=IT-N1
E=13
N=1
C.....ROWS OF LEFT HAND EDGE NODES

```

```

401 DO 420 J=1,6
MM=M+J-1
K(L,MM)=KK(E,J)+K(L,MM)
K(L,MM+NJ) = KK(E,J+6) + K(L,MM+NJ)
K(L,MM+N1) = KK(E,J+12)+KK(E-12,J)+K(L,MM+N1)
K(L,MM+N1+NJ) = KK(E,J+18) + KK(E-12,J+6) + K(L,MM+N1+NJ)
K(L,MM+N1+N1+NJ) = KK(E-12,J+18) + K(L,MM+N1+N1+NJ)
420 K(L,MM+N1+N1) = KK(E-12,J+12)+K(L,MM+N1+N1)
N=N+1
E=E+1
L=L+1
IF (N, LT, 7) GO TO 401

```

```

GO TO 1000
500 L=IT
E=19
M=IT-N1-NJ
N=1
C.....ROWS OF R.H. EDGE NODES
501 DO 510 J=1,6
MM=M+J-1
K(L,MM)=KK(E,J)+K(L,MM)
K(L,MM+NJ)=KK(E,J+6)+K(L,MM+NJ)
K(L,MM+N1)=KK(E,J+12)+KK(E-12,J)+K(L,MM+N1)
K(L,MM+N1+NJ)=KK(E,J+18)+KK(E-12,J+6)+K(L,MM+N1+NJ)
K(L,MM+N1+N1)=KK(E-12,J+12)+K(L,MM+N1+N1)
K(L,MM+N1+N1+NJ)=KK(E-12,J+18)+K(L,MM+N1+N1+NJ)
510 CONTINUE
N=N+1
E=E+1
L=L+1
IF(N,LT,7) GO TO 501
GO TO 1000

700 L=IT
E=19
N=1
C.....COMPUTE DOUBLE POINTS ROWS 88
M=IT-N1-NJ
GO TO 250

800 IF(NN,EQ,(NK*2)) GO TO 801
GO TO 855
C.....COMPUTE K MATRIX ROWS FIRST OF QUADRUPLE POINTS ROWS
801 IF(L,GT,(NN-N1+7)) GO TO 861
M=IT-N1-NJ
L=IT
N=1
E=19
810 DO 820 J=1,6
MM=M+J-1
K(L,MM)=KK(E,J)+K(L,MM)
K(L,MM+NJ)=KK(E,J+6)+KK(E-6,J)+K(L,MM+NJ)
N2=NJ*2
803 K(L,MM+N2)=KK(E-6,J+6)+K(L,MM+N2)
MM=M+J-1+N1
K(L,MM)=KK(E,J+12)+KK(E-12,J)+K(L,MM)
K(L,MM+NJ)=KK(E,J+18)+KK(E-12,J+6)+KK(E-6,J+12)+KK(E-18,J)
+K(L,MM+NJ)
805 K(L,MM+N2)=KK(E-6,J+18)+KK(E-18,J+6)+K(L,MM+N2)
MM=M+J-1+N1+N1
K(L,MM)=KK(E-12,J+12)+K(L,MM)
K(L,MM+NJ)=KK(E-12,J+18)+KK(E-18,J+12)+K(L,MM+NJ)
820 K(L,MM+N2)=KK(E-18,J+18)+K(L,MM+N2)
L=L+1
N=N+1
E=E+1
IF(N,LT,7) GO TO 810

840 CONTINUE
GO TO 1000

C IF NY IS MORE THAN 3
C.....COMPUTE QUAD POINTS ROWS FROM FIRST ROW OF QUAD POINTS
C.....POSSIBLE ERROR BUILD-UP FROM USING THESE ROWS
855 CONTINUE
L=IT
N=1
IAN1A6=IT+N1+NJ+5
ITM1M6=IT-N1-NJ
850 DO 851 J=ITM1M6,IAN1A6
852 K(L,J)=K(L-N1,J-N1)
851 CONTINUE
L=L+1
N=N+1
IF(N,LT,7) GO TO 850
GO TO 1000

C.....COMPUTE QUAD POINTS ROW ONE, SECOND POINT ONWARDS
861 CONTINUE
L=IT
N=1
IAN1A6=IT+N1+NJ+5
ITM1M6=IT-N1-NJ
860 DO 862 J=ITM1M6,IAN1A6
862 K(L,J)=K(L-NJ,J-NJ)
L=L+1
N=N+1
IF(N,LT,7) GO TO 860
GO TO 1000

1000 IF(L,LT,(NK-NJ))GO TO 10
IF(NA,LE,4) GO TO 1050
IF(L,EQ,((NK-NJ+1)*2)) IT=((NK+1)*NZ+6)+IT
IF(L,EQ,((NK-NJ+1)) ) IT=((NK+1)*NZ+6)+IT
1050 IF(L,LT,(11-5)) GO TO 10

C.....PRINT COMPLETED K MATRIX

```

```

      NAUX=NX
      NX=11
      IF ((NA,NE,1),AND,(NA,NE,2)) GO TO 1054
      WRITE (2,1052)
1052  FORMAT (///' PLATE IN XY PLANE ONLY'/)
      GO TO 1065
1054  IF ((NA,NE,3),AND,(NA,NE,4)) GO TO 1058
      WRITE (2,1056)
1056  FORMAT (///' PLATES IN XY AND YZ PLANES'/)
      GO TO 1065
1058  WRITE (2,1060)
1060  FORMAT (///' PLATES IN XY AND YZ AND ZX PLANES'/)
1065  CONTINUE
      WRITE(2,1001)
1001  FORMAT(' COMPLETED MATRIX'///)
C.....THIS IS TO REMOVE PRINTOUT INSTRUCTIONS
C.....DO 1005 I=1,NO
      WRITE(2,1002)
1002  FORMAT(' ')
      WRITE(2,1003)(K(I,J),J=1,NO)
1003  FORMAT(10E12,4)
1005  CONTINUE
      I=1
1013  I=I+1
      IF(I,EQ, NO) GO TO 1112
      J=1
1011  IF(K(I,J),NE,K(J,I)) GO TO 1111
      J=J+1
      IF(J,LT,I) GO TO 1011
      GO TO 1013
1111  WRITE (2,1012) (I,J,K(I,J),K(J,I))
1012  FORMAT (///' UNSYMMETRICAL MATRIX'///' ERROR POSITION IS ',2I3,///' ',
1' ',2F12,4)
      IF(I,LT,NO) GO TO 1013
1112  CONTINUE

      NX=NAUX
      RETURN
      END

```

```

/*
JOB MUJFEM2,;ESJJS,CP76(T40,P2000)
ATTACH (TAPE3,MUJDAT1 ,FU=ASIS,ST=S6A)
ATTACH (AFILE,LIBMAGFTNLCH,LD=LIBAPPL)
LIBRARY(AFILE)
FTN.
LDSET(PRESET=NGINF,MAP=B/ZZZMP)
LGU(PL=6000)
REWIND(TAPE3)
COPY(TAPE3,TAPE9)
CATALOG(TAPE9,MUJDAT1 ,FU=ASIS,ST=S6A)
****
PROGRAM STRUCT(INPUT,TAPE1=INPUT,OUTPUT,TAPE2=OUTPUT,TAPE3,TAPE4)
LEVEL 2,K,S

```

```

C.....THIS PROGRAM TAKES THE STIFFNESS AND MASS MATRICES AS GIVEN BY MASTER PLAT
C READ IN FROM MAG TAPE. THE INERTIA MATRIX IS SIMILARLY MODIFIED 18
C AND RECORDED IN DISCFILE BOTH TAKING INTO ACCOUNT BOUNDARY CONDITIONS
      REAL K(180,180),KK(6,6),LENGTH, PEINT(156)
      REAL S(146,146)
      INTEGER ORDER
      INTEGER W(180)
      COMMON/UPPER/K,S
      NX=5
      NY=3
      NZ=2
      READ (3) K
      ORDER=NX*NY*NZ*6
      N=ORDER
      DO 10 I=1,N
10  W(I)=1
      DO 15 I=1,N,6
      IF(I,EQ,1) GO TO 11
      IF(I,EQ,25) GO TO 11
      IF(I,EQ,61) GO TO 11
      IF(I,EQ,85) GO TO 11
      GO TO 15
11  CONTINUE
      J=0
12  W(I+J)=0
      J=J+1
      IF(J,LT,6) GO TO 12
15  CONTINUE
C.....THIS ELIMINATES THETA FOR EMPTY FIELDS
      NYM2=NY-2
      DO 50 JJ=1,NYM2
      DO 50 J=1,NX
      JK=(NX*6)+(6*J+JJ)
      JKK=(NX*NY*6)+JK
      W(JK)=0
      W(JKK)=0
50  CONTINUE
      M=0
      DO 16 I=1,N
      IF(W(I),EQ,0) GO TO 16
      M=M+1
16  CONTINUE

```

```

WRITE(2,1)M
17 FORMAT(' M = ',110)
WRITE(2,1)
1 FORMAT(' ')
NXM6=NX*6
WRITE (2,60)
60 FORMAT(' DEGREES OF FREEDOM REDUCED OUT'//)
DO 19 I=1,N, NXM6
II=(NXM6)+I-1
WRITE(2,18)(W(J),J=I,II)
18 FORMAT(50I4)
19 CONTINUE
WRITE (2,46)
46 FORMAT('1STIFFNESS MATRIX OF REDUCED PLATE')
C.....IW=1 FOR PRINT
IW=2
CALL BNDRY (K,N,W,S,M,1,IW)
CALL SYMET(S,M)
CALL WRTP(S,1,M)
C USE K AND KK MATRIX FOR INERTIA MATRIX
READ (3) K
WRITE (2,64)
64 FORMAT('1INERTIA MATRIX OF STIFFENED PLATE')
CALL BNDRY (K,N,W,S,M,2,IW)
CALL SYMET(S,M)
REWIND 3
WRITE (5) W
CALL WRTP(S,2,M)
ENDFILE 3
REWIND 3
STOP
END

```

```

SUBROUTINE BNDRY (K,N,W,S,A,B,C)
LEVEL 2,K,S
REAL S(A,A),K(N,N)
INTEGER A,B
INTEGER C
INTEGER W(N)
C THIS SUBROUTINE ALLOWS FOR SATISFACTION OF THE BOUNDARY CONDITIONS AND AT
C THE SAME TIME REDUCES REDUNDANT ROWS AND COLUMNS OF THE MATRIX
L=1
C.....DEALS WITH ROWS
DO 100 I=1,N
C W(I) = 0 IF DEGREE OF FREEDOM ELIMINATED
IF (W(I).EQ.0) GO TO 100
C THIS ELIMINATES ROW
M=L
C.....DEALS WITH COLUMNS
DO 90 J=1,N
IF (W(J).EQ.0) GO TO 90
S(L,M)=K(I,J)
M=M+1
90 CONTINUE
L=L+1
100 CONTINUE
M=M-1
IF (A.EQ.M) GO TO 110
STOP
110 CONTINUE
C COMPLETE LOWER TRIANGULAR MATRIX
C.....ROUND TO BE SYMMETRICAL
MM1=M-1
DO 120 J=1, MM1
JA1=J+1
DO 120 I= JA1 ,M
120 S(I,J)=S(J,I)
WRITE (2,140) M
140 FORMAT (' ', ' MATRIX SIZE IS ',I3)
IF(C.NE.1) GO TO 143
DO 142 I = 1,M
WRITE (2,141) ((S(I,J),J=1,M))
141 FORMAT ('0',(12E10,4))
142 CONTINUE
143 CONTINUE
RETURN
END

```

```

SUBROUTINE WRTP(S,B,A)
LEVEL 2,S
REAL S(A,A)
INTEGER A,B
C.....THIS SUBROUTINE WRITES REDUCED MATRICES TO DISCFILE
WRITE (4) S
IF (B.EQ.1) GO TO 200
REWIND 4
READ (4) S
WRITE(3) S
READ (4) S
WRITE(3) S
WRITE(2,89)
89 FORMAT('// DATAFILE 'MOJDAT ' HAS NOW BFEN REDUCED BY BOUNDARY')
200 RETURN
END

```

```

SUBROUTINE SYMET(S,M)
LEVEL 2,S
DIMENSION S(N,N)
C..... THIS SUBROUTINE CHECKS MATRICES ARE SYMMETRICAL AFTER REDUCTION
DO 5 I=2,M
IM1=I-1
DO 5 J=1,IM1
IF(S(I,J).EQ.S(J,I)) GO TO 100
WRITE (2,10) I,J,S(I,J),S(J,I)
100 FORMAT(' UNSYMMETRICAL MATRIX AT ',2I5,/' ' ,2E10,4)
5 CONTINUE
CONTINUE
RETURN
END

```

```

SUBROUTINE DEDET(K,M,I,DET,REINT,IT,S)
REAL K(1,I),S(M,M),REINT(M)
LEVEL 2,K,S
DO 30 I1=1,M
DO 30 J =1,M
K(I1,J)=S(I1,J)
30 CONTINUE
CALL F05AAF(S,M,M ,DET,REINT,IT)
WRITE(2,71)DET
71 FORMAT(' DET = ',E20,10)
IF(IT,EQ,0) GO TO 85
IF(IT,EQ,1) GO TO 65
IF(IT,EQ,2) GO TO 75
65 CONTINUE
WRITE(2,70)I
70 FORMAT(' SINGULAR MATRIX AT ',I4)
WRITE(2,72)(K(I,J2),J2=1,I)
WRITE(2,72)(S(I,J2),J2=1,I)
WRITE(2,72)(K(J2,I),J2=1,I)
WRITE(2,72)(S(J2,I),J2=1,I)
72 FORMAT(6E15,7)
STOP
75 CONTINUE
WRITE(2,80)I
80 FORMAT(I4,' VERY LARGE DETERMINANT VALUE DETECTED')
WRITE(2,72)(K(I,J2),J2=1,I)
WRITE(2,72)(S(I,J2),J2=1,I)
WRITE(2,72)(K(J2,I),J2=1,I)
WRITE(2,72)(S(J2,I),J2=1,I)
STOP
85 CONTINUE
WRITE(2,90)I
90 FORMAT(I4,' MATRIX IS CONFIRMED NON SINGULAR')
100 CONTINUE
DO 200 I1=1,M
DO 200 J =1,M
200 S(I1,J)=K(I1,J)
RETURN
END

```

```

/*
JOB MUJFEM3, :ESJJS,CP76(T40,P2000)
ATTACH(TAPE3,MUJDAT1 ,FU=ASIS,ST=S6A)
ATTACH(AFIL,LIBNAGFINLCH, ID=LIBAPPL)
LIBRARY(AFIL)
FTN,
LDSET(PRESET=NGINF,MAP=B/ZZZMP)
LGO(PL=2000)
#####

```

```

PROGRAM POSDEF(INPUT,TAPE1=INPUT,OUTPUT,TAPE2=OUTPUT,TAPE3)
LEVEL 2,K,M,C
INTEGER IW(180)
REAL K(146,146),M(146,146),C(146)
COMMON/UPPER/K,M,C
READ(3)IW
READ(3)K
READ(3)M
IF=1
CALL F01AEF(146,K,146,M,146,C,IF)
IF(IF,EQ,1) WRITE(2,10)
10 FORMAT(' M NOT POSITIVE DEFINITE')
IF(IF,EQ,0) WRITE(2,20)
20 FORMAT(' M IS POSITIVE DEFINITE')
STOP
END

```

```

/*
JOB MUJFEMD, :ESJJS,CP76(T5//,P0000)
ATTACH(TAPE3,MUJDAT1 ,FU=ASIS,ST=S6A)
ATTACH( AFIL,LIBNAGFINLCH, ID=LIBAPPL)
FTN(UPT=2)
LIBRARY(AFIL)
LDSET(PRESET=NGINF,MAP=B/ZZZMP)
LGO(PL=3000)
REWIND(TAPE3)
COPY(TAPE3,TAPE4)
CATALOG(TAPE4,MUJDAT1 ,FU=ASIS,ST=S6A)

```

```

#####
PROGRAM SOLVE(INPUT,TAPE1=INPUT,OUTPUT,TAPE2=OUTPUT,TAPE3)
LEVEL 2,K,M,A
LEVEL 2,BB,BL,W,Z
COMMON/UPPER/K,M,A
COMMON/LOWER/BB,BL,W,Z
C,.... THIS PROGRAM SOLVES EIGENVALUES AND EIGENVECTORS FROM K AND M MATRICES
DIMENSION BB(146),BL(146),W(146),IW(146)
REAL K(146,146),M(146,146),A(146,146)
INTEGER Z(146)
N=146
NE=146
C,.... NW EQUAL ZERO FOR NO MATRIX PRINTOUT
NW=0
READ (3) IW
READ (3) K
READ (3) M
REWIND 3
WRITE (2,4)
4 FORMAT(' K MATRIX'//)
IF (NW,EQ,0) GO TO 15
5 FORMAT ('// ( 9F12.4)')
DO 6 I=1,N
WRITE(2,5)(K(I,J),J=1,N)
6 CONTINUE
WRITE(2,8)
8 FORMAT(' ')
WRITE(2,10)
10 FORMAT ('M MATRIX'//)
DO 14 I=1,N
WRITE(2,11)
11 FORMAT (' ')
WRITE(2, 5)(M(I,J),J=1,N)
14 CONTINUE
15 CONTINUE
IF=1
C EPS GIVES ACCURACY REQUIRED
EPS=1,0E-11
DO 13 I=1,N
DO 13 J=1,N
13 A(I,J) = 0,0
C,.... INVERT K MATRIX
CALL F01AAF (K,N,N,A,N,BL,IF)
IF(IF,EQ,0) GO TO 20
IF (IF,NE,1) GO TO 18
WRITE (2,17)
17 FORMAT (' MATRIX SINGULAR ')
18 WRITE(2,21)
21 FORMAT('NO IMPROVEMENT IN ITERATION')
GO TO 30
20 WRITE (2,23)
23 FORMAT ('UNSUCCESSFUL INVERSION ')
30 CONTINUE
IF (NW,EQ,0) GO TO 32
WRITE (2,31)
31 FORMAT ('INVERTED K MATRIX FOLLOWS')
WRITE(2,5) ((A(I,J),J=1,N),I=1,N)
32 CONTINUE
IF (NW,EQ,0) GO TO 40
WRITE(2,8)
WRITE(2, 5)((K(I,J),J=1,N),I=1,N)
WRITE(2,8)
WRITE(2, 5)(BL(I),I=1,N)
WRITE(2,8)
40 CONTINUE
WRITE(2,19)IF
19 FORMAT(15)
C,.... COMPLETE UPPER TRIANGLE
C,.... MULTIPLY 1/K AND M MATRICES
IF = 1
CALL F01CKF (K,A,M,N,N,N,BL,N,1,IF)
IF (IF,EQ,0) GO TO 46
WRITE (2,45) IF
45 FORMAT (140, ' ERROR DETECTED ',15)
STOP
46 CONTINUE
WRITE(2,48)
48 FORMAT(' KM MATRIX OBTAINED')
IF(NW,EQ,0) GO TO 49
WRITE (2,47) ((K(I,J),J=1,N),I=1,N)
47 FORMAT (' KM MATRIX'// (10F12.4))
49 CONTINUE
C,.... BALANCE UNSYMMETRICAL MATRIX
CALL F01ATF(N,2,K,N,IX,IY,BB)
WRITE(2,6)
WRITE(2,51)
51 FORMAT(' BALANCED MATRIX')
IF (NW,EQ,0) GO TO 57
WRITE(2, 5)((K(I,J),J=1,N),I=1,N)
WRITE (2,5) (BB(I),I=1,N)
WRITE(2,55)IX,IY
55 FORMAT(2110)
57 CONTINUE
C,.... REDUCE TO UPPER HESSENBERG FORM
CALL F01AKF(N,IX,IY,K,N,Z)
CALL F01APE (N,IX,IY,Z,K,N,A,N)
C,.... COMPUTE EIGENVALUES AND EIGENVECTORS OF UPPER HESSENBERG MATRIX
IF = 1
CALL F02APF (N,IX,IY,EPS,K,N,A,N,W,BL,Z,IF)

```

```

IF(IF,NE,1) STOP
WRITE(2,75)
75 FORMAT('OMORE THAN 50 ITERATIONS NECESSARY IN ONE SOLUTION')
71 CONTINUE
WRITE (2,75) (Z(1),I=1,N)
73 FORMAT (' NO OF ITERATIONS =',I5)
WRITE(2,8)
WRITE (2,50) NE
50 FORMAT(1H1,'NO OF EIGENVALUES COMPUTED =',I4//)
WRITE (2,60) (W(1),I=1,NE)
60 FORMAT(1H , 'EIGENVALUFS'//(1X,10E12.6) )
IF (NW,EQ,0) GO TO 61
WRITE (2,60)(BL(1),I=1,NE)
61 CONTINUE
DO 63 I=1,NE
IF(W(1),LT,0.0) GO TO 62
GO TO 63
62 WRITE(2,64)I
64 FORMAT(' NEGATIVE EIGENVALUE AT ',I5)
W(1)=-W(1)
63 W(1)=(SQRT(1./W(1)))/(2.0*3.142)
WRITE(2,65) (W(1),I=1,NE)
65 FORMAT (1H ,/, ' NATURAL FREQUENCIFS (HERTZ)'//(1X,5F12.4))
C.....RANSFORM EIGENVECTORS OF BALANCED MATRIX TO ORIGINAL MATRIX
CALL F01AUF(N,IX,IY,N,6B,A,N)
WRITE(2,80)
80 FORMAT('EIGENVECTORS')
74 FORMAT(9F13,6)
DO 90 J=1,N
WRITE(2,11)
WRITE (2,74)(A(I,J),I=1,N)
90 CONTINUE
100 CONTINUE
REWIND 3
WRITE (3) IW
WRITE (3) A
WRITE (3) W
STOP
END

```

#####

/*/*

```

JOB MUJFEM4, :ESJJS,CP76(T40,P2000)
ATTACH(TAPE3,MUJDAT1 ,FO=ASIS,ST=S6A)
ATTACH( AFILE,LIBNAGFTNLCH,ID=LIBAPPL)
FTN(OPT=2)
LIBRARY(AFILE)
LDSET(PRESET=NGINF,MAP=B/ZZZHP) .
LGO(PL=4000)
REWIND(TAPE3)
COPY(TAPE3,TAPE9)
CATALOG(TAPE9,MUJDAT1 ,FO=ASIS,ST=S6A)

```

#####

```

PROGRAM SOLVE(INPUT,TAPE1=INPUT,OUTPUT,TAPE2=OUTPUT,TAPE3)
LEVEL 2,K,M,A
LEVEL 2,BB,BL,W,Z
COMMON/UPPER/K,M,A
COMMON/LOWER/BB,BL,W,Z
C.....THIS PROGRAM SOLVES EIGENVALUES AND EIGENVECTORS FROM K AND M MATRICES
DIMENSION BB(146),BL(146),W(146),IW(146)
REAL K(146,146),M(146,146),A(146,146)
INTEGER Z(146)
N=146
NE=146
C.....NW EQUAL ZERO FOR NO MATRIX PRINTOUT
NW=0
READ (3) IW
READ (3) K
READ (3) M
REWIND 3
WRITE (2,4)
4 FORMAT(' K MATRIX'////)
IF (NW,EQ,0) GO TO 15
5 FORMAT (//( 9F12.4))
DO 6 I=1,N
WRITE(2,5)(K(I,J),J=1,N)
6 CONTINUE
WRITE(2,8)
8 FORMAT(' ')
WRITE(2,10)
10 FORMAT ('M MATRIX'////)
DO 14 I=1,N
WRITE(2,11)
11 FORMAT (' ')
WRITE(2, 5)(M(I,J),J=1,N)
14 CONTINUE
15 CONTINUE
IF=1
CALL F02AEF(K,N,M,N,N,W,A,N,BL,BB,IF)
IF(IF,EQ,0) GO TO 20
IF (IF,NE,1) GO TO 18
WRITE (2,17)
17 FORMAT (' MATRIX NOT POSITIVE DEFINITE')
18 WRITE(2,21)
21 FORMAT('NO IMPROVEMENT IN ITERATION')
GO TO 30
20 WRITE (2,23)
23 FORMAT ('USUCCESSFUL COMPUTATION')

```

```

30 CONTINUE
WRITE(2,80)
80 FORMAT('EIGENVECTORS')
74 FORMAT('F13,6)
70 FORMAT ('//', '15,' MODE SHAPE CORRESPONDING TO NATFREQ'//AFTD,3)
DO 90 J=1,N
W(J) = (SQRT(W(J)))/(6,284)
WRITE(2,70) J,W(J)
WRITE(2,11)
WRITE(2,74)(A(1,J),I=1,N)
90 CONTINUE
100 CONTINUE
WRITE(2,60) (IW(I),I=1,180)
60 FORMAT(60I2)
REWIND 3
WRITE(3) IW
WRITE(3) A
WRITE(3) W
STOP
END

####
****
/*
JOB MUJFEM5, :ESJJS,CP76(T24,P2000)
ATTACH(TAPE3,MUJDAT1 ,FO=ASIS;ST=S6A)
FTN.
LGO(PL=3000)
REWIND(TAPE3)
COPY(TAPE5,SCRATCH)
CATALOG(SCRATCH,MUJDAT2 ,FO=CONF,ST=S6A)
####
PROGRAM SPDNS(INPUT,TAPE1=INPUT,OUTPUT,TAPE2=OUTPUT,TAPE5)
LEVEL 2,A,W,IW
COMMON/UPPER/A,W,IW
C..... THIS PROGRAM READS NATURAL FREQUENCIES AND MODE SHAPES OF BOX
C..... AND OUTPUTS SELECTED ONES ON DISC TO PAPER TAPE
DIMENSION A(146,146),W(146),IW(180)
READ(3)IW
READ(3)A
READ(3)W
N=146
NT=180
1 FORMAT(' ')
5 FORMAT(' DEGREES OF FREEDOM REDUCED OUT '///)
9 FORMAT(//(9E13,4))
10 FORMAT(//(9F13,6))
11 FORMAT(50I4)
70 FORMAT ('//', '15,' MODE SHAPE CORRESPONDING TO NATFREQ'//AFTD,3//)
WRITE(2,1)
WRITE(2,1)
WRITE(2,5)
WRITE(2,11)(IW(I),I=1,NT)
WRITE(2,1)
WRITE(2,10)( W(I),I=1,N)
DO 20 J=2,21
WRITE(2,70) J,W(J)
WRITE(2,9) (A(1,J),I=1,N)
20 CONTINUE
REWIND 3
C..... SELECT TWENTY NATURAL FREQUENCIES AND MODES SHAPES OF BOX WITHIN
C..... FREQUENCY RANGE 20 TO 100 HZ AND WRITE TO PAPER TAPE FILE
C..... ONLY CONSIDERING UPPER SURFACE OF BOX
K=62
DO 50 J=2,21
WRITE(3,9) (A(1,J),I=K,N)
50 CONTINUE
WRITE(3,10) (W(I),I=2,21)
WRITE(3,11) (IW(I),I=91,NT)
STOP
END

```

####

```

JOB MUJFEM6,1905M30B,HENG
DISPLAY '4514 MUJAMAGDATA1 33000512 OUT'
FORTRAN 1,CRO(MUJ6PRUG),LTRU (DAT1),100,1000
****

```

```

DOCUMENT MUJ6PROG
PROGRAM(MUJ61905M0JB)
INPUT 1 = CRU
OUTPUT 2 = LPO
INPUT 4 = TR0
USE 3= MTU(MUJAMAGDATA1)
TRACE 2
END
MASTER TAPE
DIMENSION A(85,20),W(20),IW(90)
9 FORMAT((9E13,4),//)
10 FORMAT (9F13,6)
11 FORMAT(50I4)
REWIND 5
C.....WRITE FIRST TWENTY NAT FREQ AND MODE SHAPE TO PAPER TAPE
C.....ONLY CONSIDERING UPPER SURFACE OF BOX
N=85
K=1
DO 20 J=1,20

```

```

      READ (4,9) (A(I,J),I=K,N)
      WRITE(2,9) (A(I,J),I=K,N)
20  CONTINUE
      WRITE (5) A
      READ (4,10) (W(I),I=1,20)
      WRITE (5) W
      WRITE (2,10) (W(I),I=1,20)
      READ (4,11) (IW(I),I=1,90)
      WRITE (5) IW
      WRITE (2,11) (IW(I),I=1,90)
      ENDFILES
      STOP
      END
      FINISH
****

#SWITCH

JOB HOJFEM7,1905M30B,HENG
DISPLAY '4514 HOJAMAGDATA1 33000512 IM'
FORTRAN 1,CRU(HOJ7PROG),CRU(HOJTDATA), 75,1000
****
      DOCUMENT HOJ7PROG
      LIBRARY (FD,SUBGROUPSRGP)
      LIBRARY(ED,SUBGROUPSRF7)
      PROGRAM(HOJ71905HOJC)
      COMPACT DATA
      INPUT 1=CRU
      OUTPUT 2=LPO
      INPUT 3=HTU(HOJAMAGDATA1)
      NO TRACE
      END
      MASTER RESPONSE
      REAL M(20)
      DIMENSION A(512),SX(512),SY(512)
      DIMENSION IW(90),EN(20),F(20),W(90,20),R(102),X(85,20)
      DIMENSION DL(9),V(9),BCA(14)
      DIMENSION WDF(20),WDFCV(20)
      DATA BCA(1)/27HEXCITATION SPECTRAL DENSITY/
      DATA BCA(5)/18HFREQ UP TO 150 HZ /
      DATA BCA(7)/25HRESPONSE SPECTRAL DENSITY/
      DATA BCA(10)/23H FREQUENCY UP TO 150 HZ/
      KEWIND 5
C,....,15 TRANSVERSE DEGREES OF FREEDOM ON TOP PLATE
      NTRANS=15
      NMODE=20
      N=90
      READ(3)X
      READ(3)F
      READ(3)IW
      NF=512
C,....,CALL PRINP(X,F,IW)
      FMAX=150
      FMIN=FMAX/512,0
      READ (1,10) (EN(I),I=1,NMODE)
10  FORMAT(10F8,4)
      WRITE(2,10) (F(I),I=1,20)
      WRITE(2,10) (FN(I),I=1,NMODE)
      DM = ((0.78*0.22*0.00061)*7800,0)/FLOAT(NTRANS)
      FQ=0,0
      DO 15 I=1,NF
      A(I)=0,0
15  CONTINUE
      DO 9 J=1,20
      K=1
      DO 9 I=1,90
      W(I,J)=X(K,J)
      IF(IW(I).EQ.1) GO TO 8
      K=K+1
      W(I,J)=0,0
8  CONTINUE
      K=K+1
9  CONTINUE
      WRITE (2,4)
4  FORMAT(/' DEFLECTIONS IN MODES '/')
      WRITE (2,5) ((W(I,J),I=3,4,6),J=1,20)
5  FORMAT (/ (9E13,5))
C,....,HNODE=0,5 INDICATESHALFWAY NODE POINTS TO BE INTERPOLATED
C,....,FOR ADDITIONAL SPDNS POINTS
      HNODE=1,0
      HNODE=0,5
      IF(HNODE.GT.0,5) GO TO 18

      CALL INTH(W,WDF,WDFCV)
18  CONTINUE
C,....,INPUT SPECTRAL DENSITY
      CALL INSPDNS(SX,NF,FMIN)
      CALL GRAPH (SX,NF,0,0,SY,BCA,1,R,FMAX)
C,....,NB VALUE IS CHANGED AFTER PLOTTING
      CALL INSPDNS(SX,NF,FMIN)
C,....,RESPONSE AT DEGREE OF FREEDOM K

      K=39
      K=33
      K=27
      K=21
      K=15
      K=9
      K=3

```

K=87
K=81
K=75
K=69
K=63
K=57
K=51
K=45

```
C.....PLATE EXCITED AT DEGRFE OF FREEDOM L
L=K
20 CONTINUE
WRITE (2,200) K,L
200 FORMAT (' RESPONSE AT NODE*,15,* TO EXCITATION AT NODE*,15)
C.....I CONTROLS NO OF NAT FREQ AND MODF SHAPES USED
C.....J CONTROLS NO OF TRANSVERSE DEGREES OF FREEDOM
DO 1000 IJ=1,512
FQ=FMIN*(FLOAT(IJ))
DO 60 I=1,NMODE
M(I)=0.0
DO 50 J=3,N+6
50 M(I)=M(I)+((W(J,1)**2)*DM)
C.....TO TAKE INTO ACCOUNT THE OTHER 3 SIDES
C.... M(I)=M(I)*3.0
M(I)=M(I)*4.0
60 CONTINUE
C.....THIS CALCULATES MODULUS OF RECEPTANCE
C.....COMPUTE SQUARE OF MOD OF RECEPTANCE
IF( MNODE.GT.0.5) GO TO 80
C.....FOR ADDITIONAL NODES
DO 70 I=1,20
W(L,I)=WDFCV(I)
70 CONTINUE
80 CONTINUE

C.....A(IJ) IS RECEPTANCE SQUARED
DO 100 I=1,NMODE
100 A(IJ)=A(IJ) +(((W(L,I)*W(K,1))**2)/(((M(I)**2)+(
1(((F(I)**2)-(FQ**2))**2)+((EN(I)**2)*(F(I)**4))))))
A(IJ)=A(IJ)/(16.0*(5.142**4))
1000 CONTINUE
C.....CALL GRAPH2(N,DL,NO,V,W,BCD,DCX,IM,R)
CALL SPDNS (A,SX,SY,NF)
CALL GRAPH (SY,NF,50,U,SX,BCA,2,R,FMAX)
WRITE(2,1001) FMAX
1001 FORMAT (/' FMAX = ',F10.3)
STOP
END
SUBROUTINE INTM(W,WDF,WDFCV)
DIMENSION W(90,20)
DIMENSION WDF(20),WDFCV(20)
ELENG=0.13
IST=39
IST=45
IST=51
IST=9
IST=15
IST=21
IST=33
ISTEP=30
ISTEP=6
JST=IST+ISTEP
IF(ISTEP.EQ.30) GO TO 20
ICR=IST+2
JCR=JST+2
GO TO 30
20 CONTINUE
ICR=IST+1
JCR=JST+1
30 CONTINUE
DO 40 I=1,20
WDF(I)=(W(IST,I)+W(JST,I))/2.0
WDFCV(I)=WDF(I)+(ELENG*(W(ICR,I)-W(JCR,I))/8.0)
40 CONTINUE
WRITE(2,10) (WDF(I),I=1,20)
WRITE(2,10) (WDFCV(I),I=1,20)
10 FORMAT(' ',/(12E10.4))
RETURN
END

SUBROUTINE INSPDNS(SX,NF,FMIN)
DIMENSION SX(NF)
DO 5 I=1,68
SX(I)=8.40/(((FLOAT(69))*FMIN)**2)
5 CONTINUE
DO 10 I=69,NF
SX(I)=8.40/(((FLOAT(I))*FMIN)**2)
10 CONTINUE
RETURN
END

SHORTLIST
SUBROUTINE PRINP(X,F,IW)
DIMENSION X(85,20),F(20),IW(90)
WRITE(2,500) ((X(I,J),I=1,85), J=1,20)
WRITE (2,600) (F (I),I=1,20)
WRITE(2,700)(IW(I),I=1,90)
500 FORMAT (/'(9E13.4))
600 FORMAT (/'(9F13.4))
```

```

700 FORMAT (5014)
RETURN
END

SUBROUTINE SPDNS (A,SX,SY,N)
DIMENSION A(N),SX(N),SY(N)
C..... THIS COMPUTES THE SPECTRAL DENSITY OF RESPONSE TO INPUT SPD
WRITE (2,40) (A(I),I=1,N)
DO 20 I=1,N
SY(I) = A(I)*SX(I)
20 CONTINUE
WRITE(2,50)
30 FORMAT (' SPECTRAL DENSITY OF RESPONSE')
WRITE (2,40) (SY(I),I=1,N)
40 FORMAT (12E10,3)
RETURN
END

SUBROUTINE GRAPH (B,N,LOG,NSKIP,X,BCD,IJ,LN,FMAX)
C..... B IS A POSITIVE REAL ARRAY
C..... LOG IS SET TO 0 FOR LINAR GRAPH AND 50 FOR LOG GRAPH
C..... NSKIP IS NO OF ENTERIES TO BE SKIPPED
INTEGER G
REAL MAGNEG
REAL MAGH,MAGN,B(N),LN(102)
DIMENSION X(N)
DIMENSION BCD(14)
DATA BL,ST/1H,1H*/
IF (LOG,NE,50,AND,LOG,NE,0) GO TO 100
GO TO 200
100 WRITE (2,110)
110 FOKMAT (' NO DB SCALE SPECIFIED')
STOP

200 WRITE (2,210) N
210 FORMAT (' N IS HARMONIC NUMBER =',I6/)
IF (LOG,EQ,0) GO TO 220
DO 205 I = 1,N
205 IF(B(I)) 211,213,213
211 WRITE (2,212)
212 FORMAT (' ERROR DETECTED LOG OF NEGATIVE NUMBER')
STOP

213 CONTINUE
WRITE (2,215) B(1)
215 FORMAT (' A(C) OMITTED FROM GRAPH, A(0) =',1P2E12,3)
AUX = B(1)
B(1) = 0.0
C..... PUT THE LARGEST POSITIVE OR LEAST NEGATIVE VALUE EQ MAGH
220 MAGH = B(1)
230 DO 290 I=2,N
MAGN = B(I)
240 IF (MAGH - MAGN) 250,290,290
250 MAGH = MAGN
290 CONTINUE
IF (LOG,EQ,0) GO TO 500
WRITE (2,300) MAGH
300 FORMAT (T90,'ZERO DB =',1PE12,3/)
E=2.0
IF(E,EQ,1.0) WRITE(2,310)
IF(E,EQ,2.0) WRITE(2,311)
310 FORMAT(2X,'-100',7X,'-90',7X,'-80',7X,'-70',7X,'-60',7X,'-50',7X,
1'-40',7X,'-30',7X,'-20',7X,'-10',9X,'0')
311 FORMAT (3X,'-50',7X,'-45',7X,'-40',7X,'-35',7X,'-30',7X,'-25',7X,
1'-20',7X,'-15',7X,'-10',8X,'-5',9X,'0')
DO 320 I = 1,102
320 LN(I) = EL

ALMAGH=1.0E-40
DO 330 I = 27N,(NSKIP+1)
F = 10.0*ALOG10(MAGH/(B(I)+ALMAGH))
B(I)=F
G = 101.5 - (F+E)
IF (G,LT,1) GO TO 380
LN(G) = ST
380 K = I-1
WRITE (2,340) K,LN,F
340 FORMAT (I5,10ZAT,' = ',F10,3)
IF (G,GE,1) LN(G) = BL
330 CONTINUE
H(1) = AUX
DO 350 K = 1,N
350 X(K) = ((FLOAT(K-1)) + 9.0)/(FLOAT(N))
DO 400 I=1,N
400 B(I)=-((B(I)+5.0)/100.0)
CALL HGPLUT (0.0,0.0,1,1)
CALL HGPLUT (-2.0,2.0,1,4)
CALL HGPAXIS (0.0,-5.0,BCD(7), 25.5,0.0,90.0,-100.0,20.0)
AXIL=FMAX/9.0
CALL HGPAXIS (0.0,0.0,BCD(10),27, 9.0,0.0,0.0,AXIL)
CALL HGPLUT (0.0,0.0,3,0)
N=N-1
CALL HGPLINE(X,0,N,-1)
CALL HGPLUT (1,0,1,0,1,2)
RETURN
500 CONTINUE
C..... PUT LARGEST NEGATIVE VALUE AS MAGNEG.
MAGNEG = B(1)

```

```

DO 296 I = 2,N
MAGN = B(I)
IF (MAGNEG - MAGN) 296,296,295
295 MAGNEG = MAGN
296 CONTINUE
C.....FIND X AXIS
M = (INT(((ABS(MAGNEG)/(MAGN-MAGNEG))+100.0)+1.0))
IF (MAGNEG.GT.0.0) M = 1.0
IF (MAGN.LT.0.0) M = 101.0
WRITE (2,505) MAGNEG,MAGN
505 FORMAT (' THIS MUST BE NEGATIVE',40X,' THIS MUST BE POSITIVE',/
1' ',F10.4,80X,F10.4)
LN(M) = ST
IF(M.EQ.1.0) GO TO 512
DO 510 J=1,M-1
510 LN(J) = BL
512 CONTINUE
IF(M.EQ.101.0) GO TO 514
DO 511 J=M+1,102
511 LN(J) = BL
514 CONTINUE
IF(IJ.EQ.1) GO TO 521
C.....PLOT ON LINE PRINTER
DO 525 I=1,N,(NSKIP+1)
F = B(I)
IF (M.NE.1.0) GO TO 515
C.....G IS SCALE FACTOR
G = ((F/MAGN)+100.0)+1.0
513 IF(M.NE.101.0) GO TO 515
G = M-((F/MAGNEG)+100.0)
515 G = (100.0*((F-MAGNEG)/(MAGN-MAGNEG)))+1.0
LN(G) = ST
K = I-1
WRITE (2,520) LN,K,F
520 FORMAT (10Z1,14,'*',1PE14.3)
IF (G.NE.M) LN(G) = BL
525 CONTINUE
521 CONTINUE
C INITIALISE PLOTTER
CALL HGFPLOT(0.0,0.0,0.1,1)
C ASSIGN ORIGIN
AM = ((MAGN/(MAGN-MAGNEG))+5.00)+2.0
CALL HGFPLOT (-2.0,AM,1,4)
AM=AM-2.0
C PUT IN X AXIS
C POSITION PEN AT X AXIS
CALL HGFPLOT (0.0,0.0,3,0)
AXIL=FMAX/9.0
C DRAW IN X AXIS
CALL HGPAXIS (0.0,0.0,BCD(5),-18, 9.0,0.0,0.0,AXIL)
AAM=(MAGN-MAGNEG)/5.0
AMH=-5.0+AM
IF(IJ.EQ.1) GO TO 545
IF(IJ.EQ.2) GO TO 546
545 CALL HGPAXIS (0.0,AMH,BCD(1),26.5,0.90,0,MAGNEG,AAM)
GO TO 547
546 CALL HGPAXIS (0.0,AMH,BCD(7),26.5,0.90,0,MAGNEG,AAM)
547 CONTINUE
C SCALE GRAPH
DO 550 K = 1,N
550 X(K) = ((FLOAT(K-1))+ 9.0)/(FLOAT(N))
C SCALE Y COORDINATES
IF(MAGN.LT.ABS(MAGNEG)) GO TO 555
AA=MAGN
GO TO 560
555 AA=ABS(MAGNEG)
560 CONTINUE
DO 600 I = 1,N
600 B(I)=(B(I)*AM)/MAGN
C COMMENCE PLOT
CALL HGPLINE (X,B,N,1)
C END PLOT
CALL HGFPLOT (1.0,1.0,1,2)
CONTINUE
RETURN
END

FINISH

```

```

****
DOCUMENT HOJTDATA
.0180 .0150 .0125 .0105 .0100 .0095 .0091 .0085 .0080 .0076
.0070 .0067 .0064 .0060 .0057 .0054 .0050 .0040 .0030 .0020

```

The Fourier Transform computer programs

The computer programs MOJFTM1 and MOJFTM2, developed to analyse sets of 512 and 1024 data respectively, Fourier transforming from the time to the frequency domain using the discrete Fourier transform or the fast Fourier transform algorithms.

DOCUMENT MUJFPROG

LIBRARY(ED,SUBGRUJPSRF)
 LIBRARY (ED,SUBGRUJPSRGP)
 PROGRAM(MUJF1905MUJC)
 COMPACT
 INPUT 1=TRU
 OUTPUT 2=LPO
 NO TRACE
 END

MASTER FORTFM

C.....THIS PROGRAM COMPUTES THE FOURIER TRANSFORM OF REAL DATA OF IMPULSE
 C.....WHICH IS DIVIDED BY THE FACTOR K
 C.....FOR THE RECEPTANCE OF THE COMPLETE SYSTEM WHICH IS THEN SQUARED
 C.....THIS IS THEN MULTIPLIED BY THE EXCIT PSD OF THE PRBS SIGNAL
 C.....USED AND FROM IT PSD OF THE SYSTEM RESPONSE IS OBTAINED
 C.....THIS IS IN TURN MULTIPLIED BY THE PICK UP FACTOR SQUARED TO GIVE
 C.....RESPONSE OF THE BOX STRUCTURE, N IS NO OF DATA
 C.....COMPLEX W(512)
 REAL MAGM,MAGN ,LN(102)
 DIMENSION BCD(14)
 DIMENSION C(512),D(512)
 INTEGER G
 REAL MAGNEG
 COMPLEX X(512),A(512)
 NEX=9
 N=(2**NEX)
 DO 1 I=1,N
 1 READ (1,101,END=2) C(I)
 GO TO 3
 2 DO 4 J=1,N-I+1
 4 C(J+I-1) = 0.0
 3 CONTINUE
 WRITE (2,150) I
 150 FORMAT (/' NO OF DATA INPUT = ',I5)
 101 FORMAT (F5,3/)
 DO 200 J=1,N
 200 X(J)=CHPLX(C(J),0.0)
 WRITE (2,210)N
 210 FORMAT (/' PLOT OF DATA INPUT FOLLOWS, N= ',I6)
 CALL GRAPH (C,N,U,D)
 CALL FFT(X,NEX,N,A)
 C... CALL ROOT (W,N)
 C... CALL DFT (X,W,A,N)
 C.....IMPULSE RESPONSE OF BOX PLOTTED
 C.....TABULATE FOURIER COEFFICIENTS A
 WRITE (2,220) A(1)
 220 FORMAT (/'10FT COEFFICIENTS ARE'/'/' D,C,TERM =',1PE11,3)
 WRITE (2,230) (A(J),J=2,N)
 230 FORMAT (/4(1PE14,3,1PE11,3))
 C.....RMS VALUE OF PRBS SIGNAL
 PRBS=0.8
 PRBS=0.3
 C.....EXPSD IS EXCITATION POWER SPECTRAL DENSITY USING 0.45 CLOCK FREQ
 EXPSD = (PRBS**2)/(0.45*500.0)
 C.....PLOT SPECTRAL DENSITY OF OUTPUT FROM BOX
 C.....EXPSD = 2 PI FACTORK
 FACTURK=EXPSD/6.284
 DO 250 I=1,N
 250 C(I) = CABS(A(I))/FACTURK
 WRITE (2,251) (C(I),I=1,N)
 251 FORMAT (/' SYSTEM RECEPTANCE',/' ' ',(10E12,4))
 C.....PICK UP FACTOR IN MM PER VOLT INCLUDING OUTPUT AMPLIFICATION
 PF=2.25/100.0
 DO 252 I=1,N
 252 C(I) = ((PF*C(I))**2)*EXPSD
 WRITE (2,255)N
 255 FORMAT (/' BOX RESPONSE FOLLOWS, N = ',I6)
 WRITE (2,275) (C(I),I=1,N)
 275 FORMAT (/' RESPONSE',/' ' ',(10E12,4))
 CALL GRAPH (C,N,50,U,D)
 STOP
 END
 SUBROUTINE GRAPH (B,N,LOG,NSKIP,X)
 C.....B IS A POSITIVE REAL ARRAY
 C.....LOG IS SET TO 0 FOR LINEAR GRAPH AND 50 FOR LOG GRAPH
 C.....NSKIP IS NO OF ENTERIES TO BE SKIPPED .
 INTEGER G
 REAL MAGNEG
 REAL MAGM,MAGN,B(N),LN(102)
 DIMENSION X(N)
 DIMENSION BCD(14)
 DATA BCD(1)/26HCKROSS CORRELATION FUNCTION/
 DATA BCD(5)/10HDELAY BITS/
 DATA BCD(7)/23H RESPONSE DB RE MAGM/
 DATA BCD(10)/37HFREQUENCY IN HERTZ(DC COMPONENT=)/
 DATA BL,ST/1H ,1H*/
 IF (LOG,NE,50,AND,LOG,NE,0) GO TO 100
 GO TO 200
 100 WRITE (2,110)
 110 FORMAT (' NO DB SCALE SPECIFIED')
 STOP
 200 WRITE (2,210) N

```

210 FORMAT (' N IS HARMONIC NUMBER =',I6)
    IF (LOG,EQ,0) GO TO 220
    DD 205 I = 1,N

205 IF(B(1)) 211,213,215
211 WRITE (2,21)
212 FORMAT (' ERROR DETECTED LOG OF NEGATIVE NUMBER')
    STOP

213 CONTINUE
    WRITE (2,215) B(1)
215 FORMAT (' A(0) OMITTED FROM GRAPH, A(0) =',1P2E12,5)
    AUX = B(1)
    B(1) = 0,0
C,....PUT THE LARGEST POSITIVE OR LEAST NEGATIVE VALUE EQ MAGM
220 MAGM = B(1)
230 DO 290 I=2,N
    MAGN = B(I)
240 IF (MAGM - MAGN) 250,290,290
250 MAGM = MAGN
290 CONTINUE
    IF (LOG,EQ,0) GO TO 500
    WRITE (2,300) MAGM
300 FORMAT (T90,'ZERO DB =',1PE12,5/)
    E = 2,0
    IF(E,EQ,1,0) WRITE(2,310)
    IF(E,EQ,2,0) WRITE(2,311)
310 FORMAT(2X,'-100',7X,'-90',7X,'-80',7X,'-70',7X,'-60',7X,'-50',7X,
1'-40',7X,'-30',7X,'-20',7X,'-10',9X,'0')
311 FORMAT (3X,'-50',7X,'-45',7X,'-40',7X,'-35',7X,'-30',7X,'-25',7X,
1'-20',7X,'-15',7X,'-10',8X,'-5',9X,'0')
    DD 320 I = 1,102
320 LN(I) = BL
    ALMAGM=1,UE-40
    DO 350 I = 2,N,(NSKIP+1)
    F = 10,0*ALOG10(MAGM/(B(I)+ALMAGM))
    G = 101,5 - (F*E)
    IF (G,LT,1) GO TO 380
    LN(G) = ST
380 K = I-1
    WRITE (2,340) K, LN,K,F
340 FORMAT (15,102A1,14,'=-',F7,2)
    IF (G,GE,1) LN(G) = BL
330 CONTINUE
    B(1) = AUX
    DO 350 K = 1,N
350 X(K) = ((FLOAT(K-1))* 9,0)/(FLOAT(N))
    DD 400 I = 1,N
400 B(I) =-5,0*(10,0*ALOG10(MAGM/(B(I)+1,UE-20)))/100,0)
    CALL HGPlot (0,0,0,0,1,1)
    CALL HGPlot (-2,0,2,0,1,4)
    CALL HGPAXIS (0,0,-5,0,BCD(7), 25,5,0,90,0,-100,0,10,0)
    AXISL = N/ 9,0
    CALL HGPAXIS (0,0,0,0,BCD(10),37, 9,0,0,0,0,0,AXISL)
    CALL HGPlot (0,0,0,0,3,0)
    CALL HGPLINE (X,B,N,-1)
    CALL HGPlot (1,0,1,0,1,2)
    RETURN
500 CONTINUE
C,....PUT LARGEST NEGATIVE VALUE AS MAGNEG.
MAGNEG = B(1)
DO 296 I = 2,N
MAGN = B(I)
IF (MAGNEG - MAGN) 296,296,295
295 MAGNEG = MAGN
296 CONTINUE
C,....FIND X AXIS
M = (INT(((ABS(MAGNEG)/(MAGM-MAGNEG))*100,0)+1,0))
IF (MAGNEG,GT,0,0) M = 1,0
IF (MAGM,LT,0,0) M = 101,0
WRITE (2,505) MAGNEG,MAGM
505 FORMAT (' THIS MUST BE NEGATIVE',40X,' THIS MUST BE POSITIVE',/
1' ',F10,4,80X,F10,4)
LN(M) = ST
IF (M,EQ,1,0) GO TO 512
DO 510 J=1,M-1
510 LN(J) = BL
512 CONTINUE
IF(M,EQ,101,0) GO TO 514
DO 511 J=M+1,102
511 LN(J) = BL
514 CONTINUE
DO 525 I=1,N,(NSKIP+1)
F = B(I)
IF ( M,NE,1,0) GO TO 513
G = ((F/MAGM)+100,0)+1,0
513 IF(M,NE,101,0) GO TO 515
G = M-((F/MAGNEG)+100,0)
515 G = (100,0*((F-MAGNEG)/(MAGM-MAGNEG)))+1,0
LN(G) = ST
K = I-1
WRITE (2,520) LN,K,F
520 FORMAT (102A1,14,'=',1PE14,3)
IF (G,NE,M) LN(G) = BL
525 CONTINUE
C INITIALISE PLOTTER
CALL HGPlot(0,0,0,0,1,1)
C ASSIGN ORIGIN
AM = ((MAGM/(MAGM-MAGNEG))*5,00)+2,0

```

```

CALL HG PLOT (-2.0,AM,1,4)
AM=AM-2.0
C PUT IN X AXIS
AXISL = N/ 9.0
C POSITION PEN AT X AXIS
CALL HG PLOT (0.0,0.0,5.0)
DRAW IN X AXIS
C CALL HGPAXIS (0.0,0.0,BCD(5),-10, 9.0,0.0,0.0,AXISL)
AAH=(MAGH-MAGNEG)/5.0
AMH=-5.0+AM
C CALL HGPAXIS (0.0,AMH,BCD(T),26.5,0.90,0.0,MAGNEG,AAH)
SCALE GRAPH
DO 550 K = 1,N
550 X(K) = ((FLOAT(K-1))= 9.0)/(FLOAT(N))
C SCALE Y COORDINATES
IF(MAGH.LT.ABS(MAGNEG)) GO TO 555
AA=MAGH
GO TO 560
555 AA=ABS(MAGNEG)
560 CONTINUE
DO 600 I = 1,N
600 B(I)=(B(I)+AM)/MAGH
C COMMENCE PLOT
CALL HG PLINE (X,B,N,T)
C END PLOT
CALL HG PLOT (1.0,1.0,1,2)
CONTINUE
RETURN
END
SUBROUTINE FFT(A,N,NB,B)
COMPLEX A(NB),U,W,T,B(NB)
NBD2=NB/2
NBH1=NB-1
J=1
DO 4 L=1,NBH1
IF(L.GE,J) GO TO 2
T=A(J)
A(J)=A(L)
A(L)=T
2 K=NBD2
3 IF(K.GE,J) GO TO 4
J=J-K
K=K/2
GO TO 3
4 J=J+K
PI=3.14159265359
DO 6 M=1,K
U=(1.0,0.0)
ME=2+M
K=ME/2
W=CMPLX(COS(PI/K),SIN(PI/K))
DO 5 J=1,K
DO 5 L=J,NB,ME
LPK=L+K
T=A(LPK)+U
A(LPK)=A(L)-T
5 A(L)=A(L)+T
6 U=U+W
DO 10 I=1,NB
B(I)=A(I)/(FLOAT(NB))
10 CONTINUE
RETURN
END
FINISH
****

```

#SWITCH

JOB MUJFTM2,1905H0JC,HENG
FORTRAN 1,CRU(MUJFPRUG),TRU(MUJGDATA),200,4500

DOCUMENT MUJFPRUG
LIBRARY(ED,SURGROUPSRF7)
LIBRARY (LD,SUBGROUPSRGP)
PROGRAM(MUJF1905H0JC)

COMPACT
INPUT 1=TRU
OUTPUT 2=LPO
NO TRACE
END

MASTER FORTM

C.....THIS PROGRAM COMPUTES THE FOURIER TRANSFORM OF REAL DATA OF IMPULSE
C.....WHICH IS DIVIDED BY THE FACTOR K
C.....FOR THE RECEPTANCE OF THE COMPLETE SYSTEM WHICH IS THEN SQUARED
C.....THIS IS THEN MULTIPLIED BY THE EXCIT PSD OF THE PRBS SIGNAL
C.....USED AND FROM IT PSD OF THE SYSTEM RESPONSE IS OBTAINED
C.....THIS IS IN TURN MULTIPLIED BY THE PICK UP FACTOR SQUARED TO GIVE
C.....RESPONSE OF THE BOX STRUCTURE. N IS NO OF DATA

C.....COMPLEX W(1024)
DIMENSION BCD(14)
DIMENSION C(1024),D(1024)
COMPLEX X(1024),A(1024)
INTEGER G
REAL MAGNEG
REAL MAGM,MAGN, LN(102)

NEX=10
N=(2**NEX)
DO 1 I=1,N
1 READ (1,101,END=2) C(I)
GO TO 3
2 DO 4 J=1,N-1+1
4 C(J+1-1) = 0.0
3 CONTINUE

WRITE (2,150) I
150 FORMAT (/' NO OF DATA INPUT = ',I5)
101 FORMAT (F5,3/)
DO 200 J=1,N
200 X(J)=CMPLX(C(J),0.0)
WRITE (2,210)N
210 FORMAT (/' PLOT OF DATA INPUT FOLLOWS. N = ',I6)
CALL GRAPH (C,N,U,D)
CALL FFT(X,NEX,N,A)

C... CALL ROOT (W,N)
C... CALL DFT (X,W,A,N)
C.....IMPULSE RESPONSE OF BOX PLOTTED
C.....TABULATE FOURIER COEFFICIENTS A

WRITE (2,220) A(1)
220 FORMAT (/' DFT COEFFICIENTS ARE'/'/' D.C.TERM =',1P2E11.3)
WRITE (2,250) (A(J),J=2,N)
250 FORMAT (/'(1PF14.3,1PE11.5))

C.....RMS VALUE OF PRBS SIGNAL
PRBS=0.3
C.....EXPSD IS EXCIT POWER SPECTRAL DENSITY USING 0.45 CLOCK FREQUENCY
EXPSD =(PRBS**2)/(0.45*300.0)

C.....EXPSD = 2 PI FACTOR
FACTORK=EXPSD/6.284
DO 250 I=1,N

250 C(I) = CABS(A(I))/FACTORK
WRITE (2,251) (C(I),I=1,N)
251 FORMAT (/' SYSTEM RECEPTANCE',/' ',(10E12,4))

C.....PICK UP FACTOR IN MH PER VOLT, INCLUDING OUTPUT AMPLIFICATION
PF=2.25/31.6
DO 252 I=1,N

252 C(I) = ((PFAC(I)**2)*EXPSD
C.....PLOT SPECTRAL DENSITY OF OUTPUT FROM BOX
WRITE (2,255)N

255 FORMAT (/' BOX RESPONSE FOLLOWS. N = ',I6)
WRITE (2,275) (C(I),I=1,N)
275 FORMAT (/' RESPONSE',/' ',(10E12,4))

CALL GRAPH (C,N,50,U,D)
STOP
END

SUBROUTINE DFT (X,W,A,N)
COMPLEX X(N),W(N),A(N)
A(1)=(0.0,0.0)
DO 10 J=1,N
10 A(1)=A(1)+X(J)
DO 20 L=1,(N-1)
A(L+1)=(0.0,0.0)
DO 20 M=1,N
IAK = (((M-1)*L)+1)
INDEX = IAK-(N*INT((FLOAT(IAK)-0.01)/(FLOAT(N))))
20 A(L+1)=A(L+1)+X(M)*W(INDEX)
DO 30 J=1,N
30 A(J)=A(J)/N
RETURN
END

SUBROUTINE ROOT (W,N)
COMPLEX W(N)
C.....CALCULATE THE COMMON ROOT W(J) WHERE W(J)= CEXP((-2I)*PI*J/N)

```

W(1)=(1,0,0,0)
C=N
W(2)=CEXP(CMPLX(0,0,-6.2852/C))
DO 50 J=3,N
W(J) =W(J-1)*W(2)
50 CONTINUE
RETURN
END

SUBROUTINE GRAPH (B,N,LOG,NSKIP,X)
C..... B IS A POSITIVE REAL ARRAY
C..... LOG IS SET TO 0 FOR LINEAR GRAPH AND 50 FOR LOG GRAPH
C..... NSKIP IS NO OF ENTERIES TO BE SKIPPED
INTEGER G
REAL MAGNEG
REAL MAGH,MAGN,B(N),LN(102)
DIMENSION X(N)
DIMENSION BCD(14)
DATA BCD(1)/26HCROSS CORRELATION FUNCTION/
DATA BCD(5)/10HDELAY BITS/
DATA BCD(7)/23H RESPONSE DB RE MAGH/
DATA BCD(10)/3/HFREQUENCY IN HERTZ(DC COMPONENT= )/
DATA BL,ST/1H,1H*/
IF (LOG,NE,50,AND,LOG,NE,0) GO TO 100
GO TO 200

100 WRITE (2,110)
110 FORMAT (' NO DB SCALE SPECIFIED')
STOP

200 WRITE (2,210) N
210 FORMAT (' N IS HARMONIC NUMBER =',I6/)
IF (LOG,EQ,0) GO TO 220
DO 205 I = 1,N

205 IF(B(I)) 211,213,213
211 WRITE (2,212)
212 FORMAT (' ERROR DETECTED LOG OF NEGATIVE NUMBER')
STOP

213 CONTINUE
WRITE (2,215) B(1)
215 FORMAT (' A(0) OMITTED FROM GRAPH. A(0) =',1P2E12,3)
AUX = B(1)
B(1) = 0,0
C..... PUT THE LARGEST POSITIVE OR LEAST NEGATIVE VALUE EQ MAGH
220 MAGH = B(1)
230 DO 290 I=2,N
MAGN = B(I)
240 IF (MAGH - MAGN) 250,290,290
250 MAGH = MAGN
290 CONTINUE
IF (LOG,EQ,0) GO TO 500
WRITE (2,300) MAGH
300 FORMAT (T90,'ZERO DB =',1PE12,3/)
E = 2.0
IF(E,EQ,1.0) WRITE(2,310)
IF(E,EQ,2.0) WRITE(2,311)
310 FORMAT(2X,'-100',7X,'-90',7X,'-80',7X,'-70',7X,'-60',7X,'-50',7X,
1'-40',7X,'-30',7X,'-20',7X,'-10',9X,'0')
311 FORMAT (3X,'-50',7X,'-45',7X,'-40',7X,'-35',7X,'-30',7X,'-25',7X,
1'-20',7X,'-15',7X,'-10',8X,'-5',9X,'0')
DO 320 I =1,102
320 LN(I) = BL
ALMAGH=1.0E-40
DO 350 I =2,N,(NSKIP+1)
F = 10,0*ALOG10(MAGH/(B(I)+ALMAGH))
G = 101,5 - (F*E)
IF (G,LT,1) GO TO 380
LN(G) = ST
380 K = I-1
WRITE (2,340) K,LN,K,F
340 FORMAT (I5,102A1,14,'=-',F7,2)
IF (G,GE,1) LN(G) = BL
350 CONTINUE
B(1) = AUX
DO 350 K = 1,N
350 X(K) = ((FLOAT(K-1))* 9.0)/(FLOAT(N))
DO 400 I = 1,N
400 B(I) =-5,0*(10,0*ALOG10(MAGH/(B(I)+1.0E-20))/100,0)
CALL HG PLOT (0,0,0,0,1,1)
CALL HG PLOT (-2,0,2,0,1,4)
CALL HGPAXIS (0,0,-5,0,BCD(7), 25,5,0,90,0,-100,0,20,0)
AXISL = N/ 9,0
CALL HGPAXIS (0,0,0,0,BCD(10),57, 9,0,0,0,0,0,AXISL)
CALL HG PLOT (0,0,0,0,3,0)
CALL HG PLINE (X,B,N,-1)
CALL HG PLOT (1,0,1,0,1,2)
RETURN
500 CONTINUE
C..... PUT LARGEST NEGATIVE VALUE AS MAGNEG.
MAGNEG = B(1)
DO 296 I = 2,N
MAGN = B(I)
IF (MAGNEG - MAGN) 296,296,295
295 MAGNEG = MAGN
296 CONTINUE
C..... FIND X AXIS
M = (INT((ABS( MAGNEG)/(MAGH-MAGNEG))*100,0)+1,0)

```

```

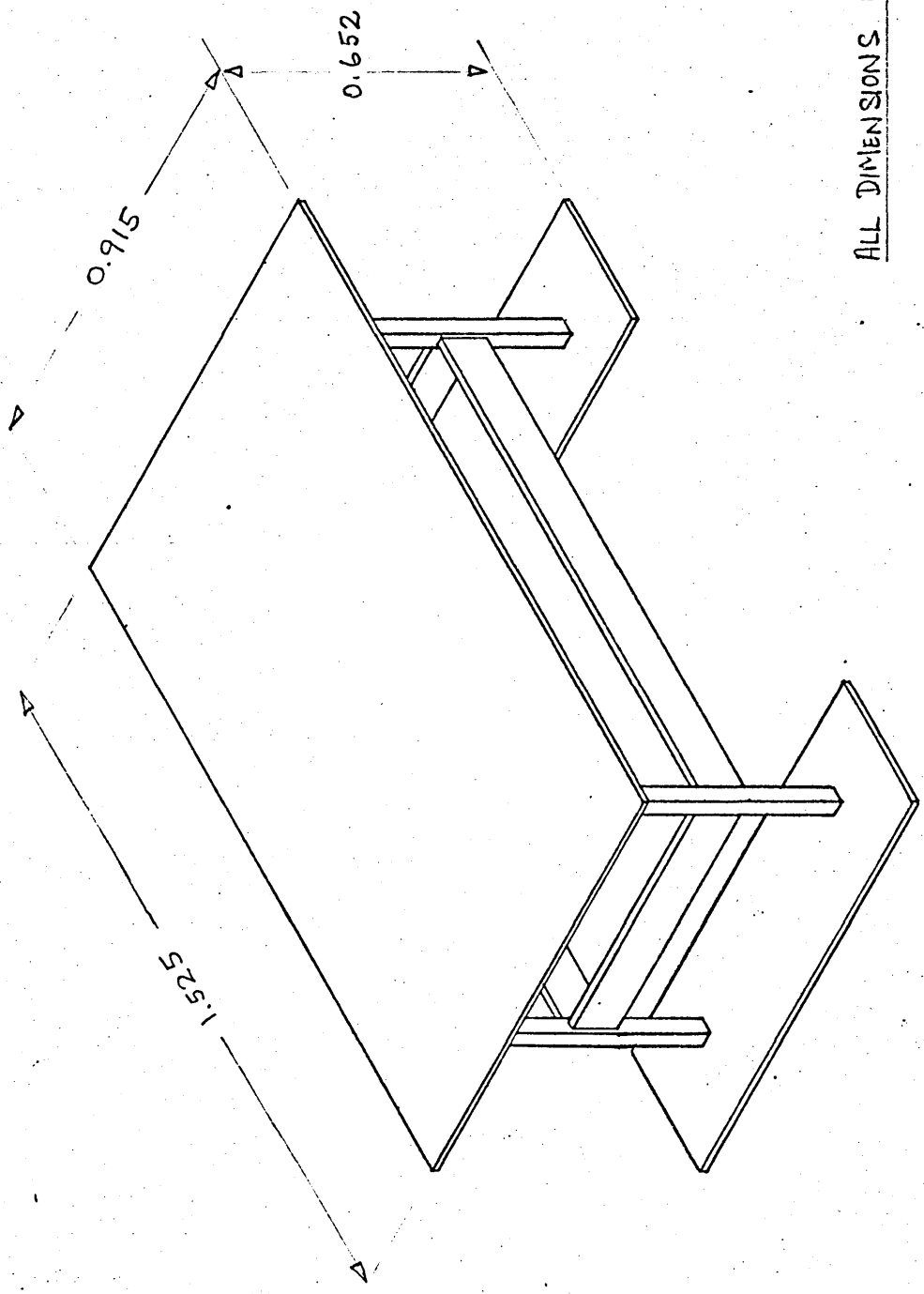
      IF (MAGNEG.GT.0.0) M = 1.0
      IF (MAGM.LT.0.0) M = 101.0
      WRITE (2,505) MAGNEG,MAGM
505  FORMAT (' THIS MUST BE NEGATIVE',40X,' THIS MUST BE POSITIVE',/
      1' ',F10.4,80X,F10.4)
      LN(M) = ST
      IF (M.EQ.1.0) GO TO 512
      DO 510 J=1,M-1
510  LN(J) = BL
512  CONTINUE
      IF (M.EQ.101.0) GO TO 514
      DO 511 J=M+1,102
511  LN(J) = BL
514  CONTINUE
      DO 525 I=1,N,(NSKIP+1)
      F = B(I)
      IF (M.NE.1.0) GO TO 513
      G = ((F/MAGM)*100.0)+1.0
513  IF (M.NE.101.0) GO TO 515
      G = M-((F/MAGNEG)*100.0)
515  G = (100.0+((F-MAGNEG)/(MAGM-MAGNEG)))+1.0
      LN(G) = ST
      K = I-1
      WRITE (2,520) LN,K,F
520  FORMAT (10Z A1,14,'=',1PE14.3)
      IF (G.NE.M) LN(G) = BL
525  CONTINUE
C     INITIALISE PLOTTER
      CALL HGPLUT(0.0,0.0,0.1,1)
C     ASSIGN ORIGIN
      AM = ((MAGM/(MAGM-MAGNEG))*5.00)+2.0
      CALL HGPLUT (-2.0,AM,1,4)
      AM=AM-2.0
C     PUT IN X AXIS
      AXISL = N/ 9.0
C     POSITION PEN AT X AXIS
      CALL HGPLUT (0.0,0.0,3,0)
C     DRAW IN X AXIS
      CALL HGPAXIS (0.0,0.0,BCD(5),-10, 9,0,0,0,0,0,AXISL)
      AAM=(MAGM-MAGNEG)/5.0
      AMH=-5.0+AM
      CALL HGPAXIS (0.0,AMH,BCD(1),26,5,0,90,0,MAGNEG,AAM)
C     SCALE GRAPH
      DO 550 K = 1,N
550  X(K) = ((FLOAT(K-1))* 9.0)/(FLUAT(N))
C     SCALE Y COORDINATES
      IF (MAGM,LT,ABS(MAGNEG)) GO TO 555
      AA=MAGM
      GO TO 560
555  AA=ABS(MAGNEG)
560  CONTINUE
      DO 600 I = 1,N
      B(I)=(B(I)*AM)/MAGM
C     COMMENCE PLOT
      CALL HGPLINE (X,B,N,1)
C     END PLOT
      CALL HGPLUT (1.0,1.0,1,2)
      CONTINUE
      RETURN
      END

SUBROUTINE FFT(A,N,NB,B)
COMPLEX A(NB),U,W,T,B(NB)
NBD2=NB/2
NBH1=NB-1
J=1
DO 4 L=1,NBH1
IF(L.GE,J) GO TO 2
T=A(J)
A(J)=A(L)
A(L)=T
2  K=NBD2
3  IF(K.GE,J) GO TO 4
J=J-K
K=K/2
GO TO 3
4  J=J+K
PI=3.14159265359
DO 6 M=1,N
U=(1.0,0.0,0)
ME=2**M
K=ME/2
W=CMPLX(COS(PI/K),SIN(PI/K))
DO 5 J=1,K
DO 5 L=J,NB,ME
LPK=L+K
T=A(LPK)*U
A(LPK)=A(L)-T
5  A(L)=A(L)+T
6  U=U*W
DO 10 I=1,NB
B(I)=A(I)/(FLOAT(NB))
10 CONTINUE
RETURN
END
FINISH
****
#SWITCH

```

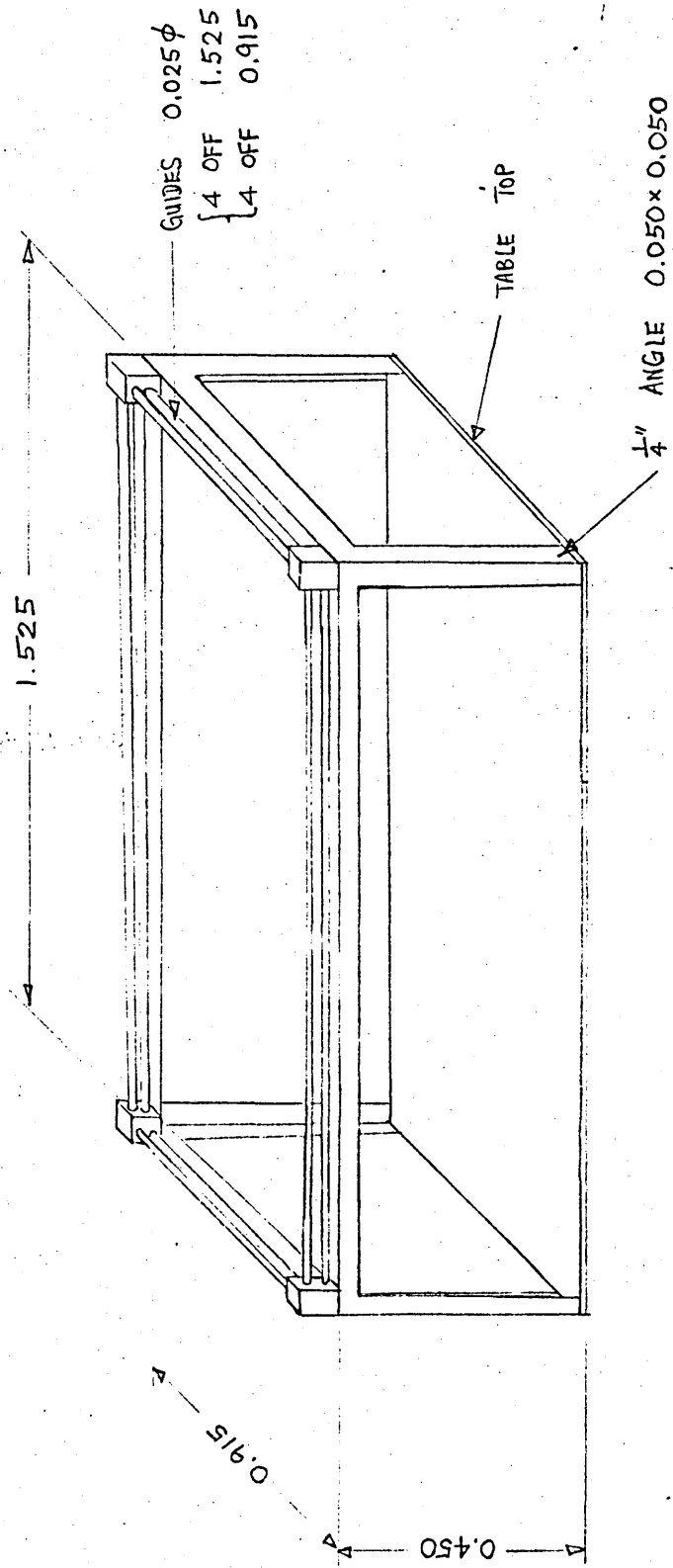
Appendix 5

Diagrams and illustrations of the experimental apparatus
developed



ALL DIMENSIONS IN METRES

FIG A.5.1. THE VIBRATION TABLE



ALL DIMENSIONS IN METRES

FIG A.5.2. FRAMEWORK FOR TRANSVERSE GEAR

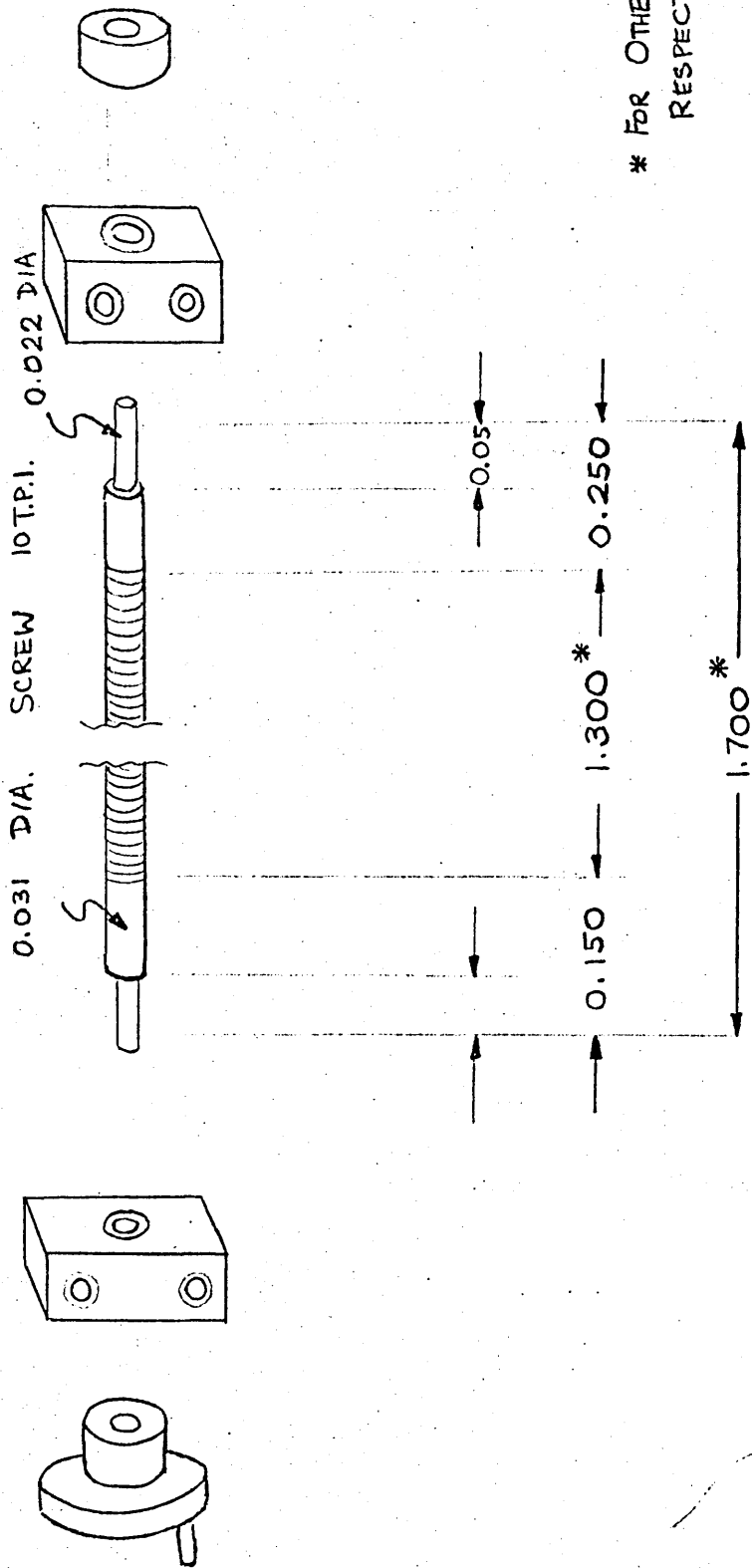


Fig. A.5.3 LEADSCREW + ASSEMBLY (2 OFF)

ALL DIMENSIONS IN METRES

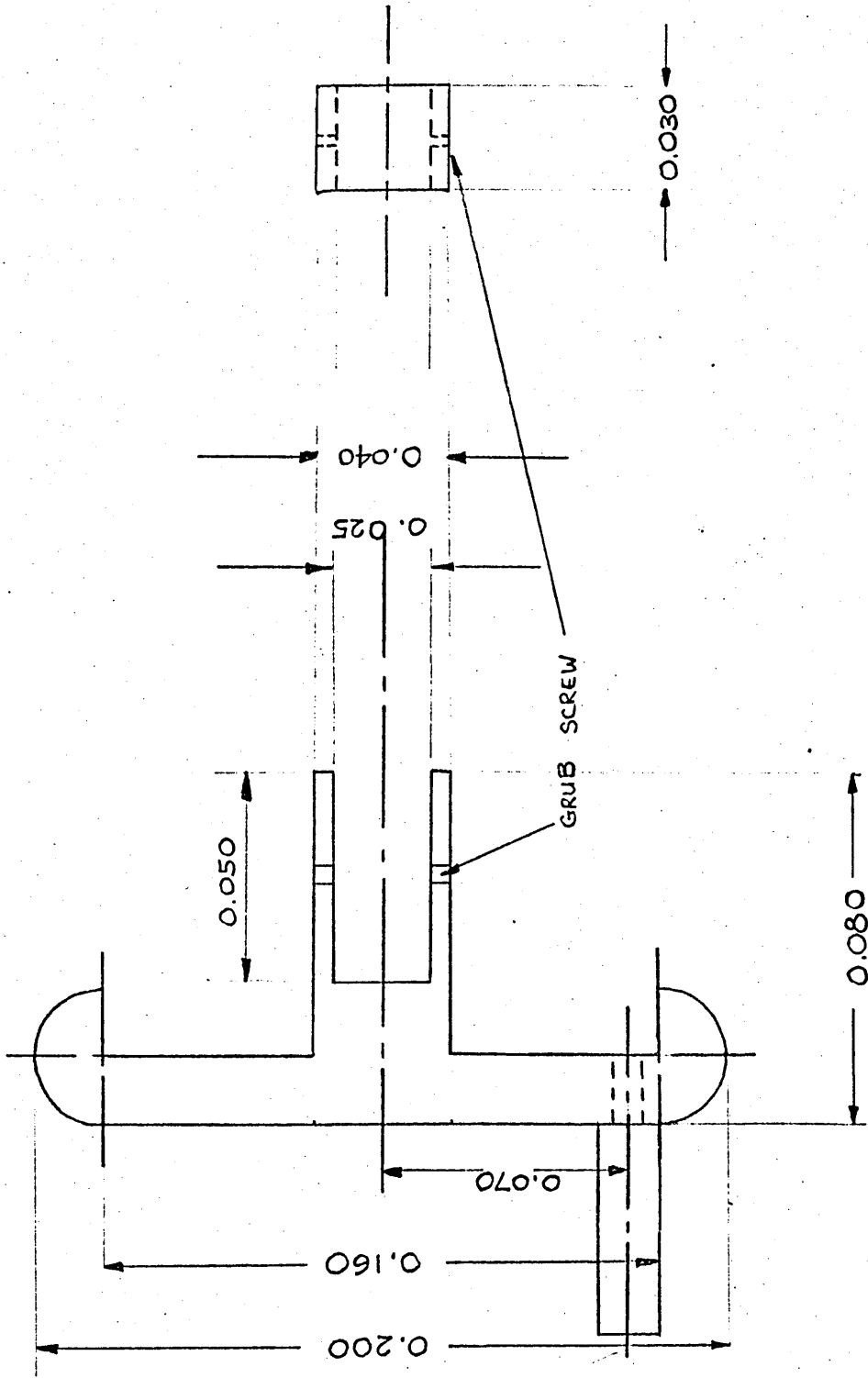
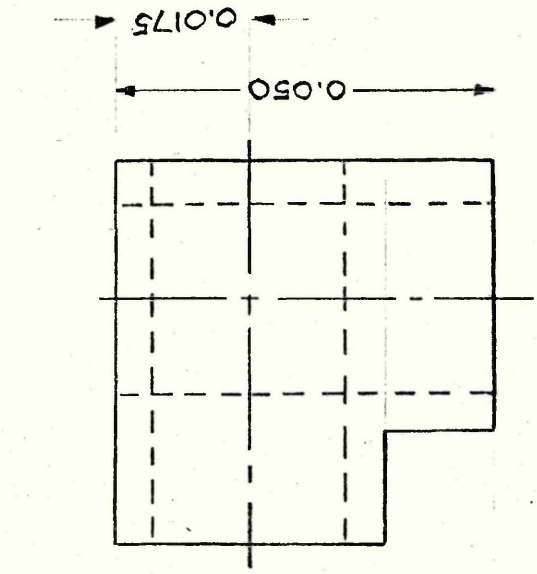


FIG. A.5.4. HANDWHEEL AND ENDSTOP (2 OFF EACH)

SCALE 1:2



FULL SCALE

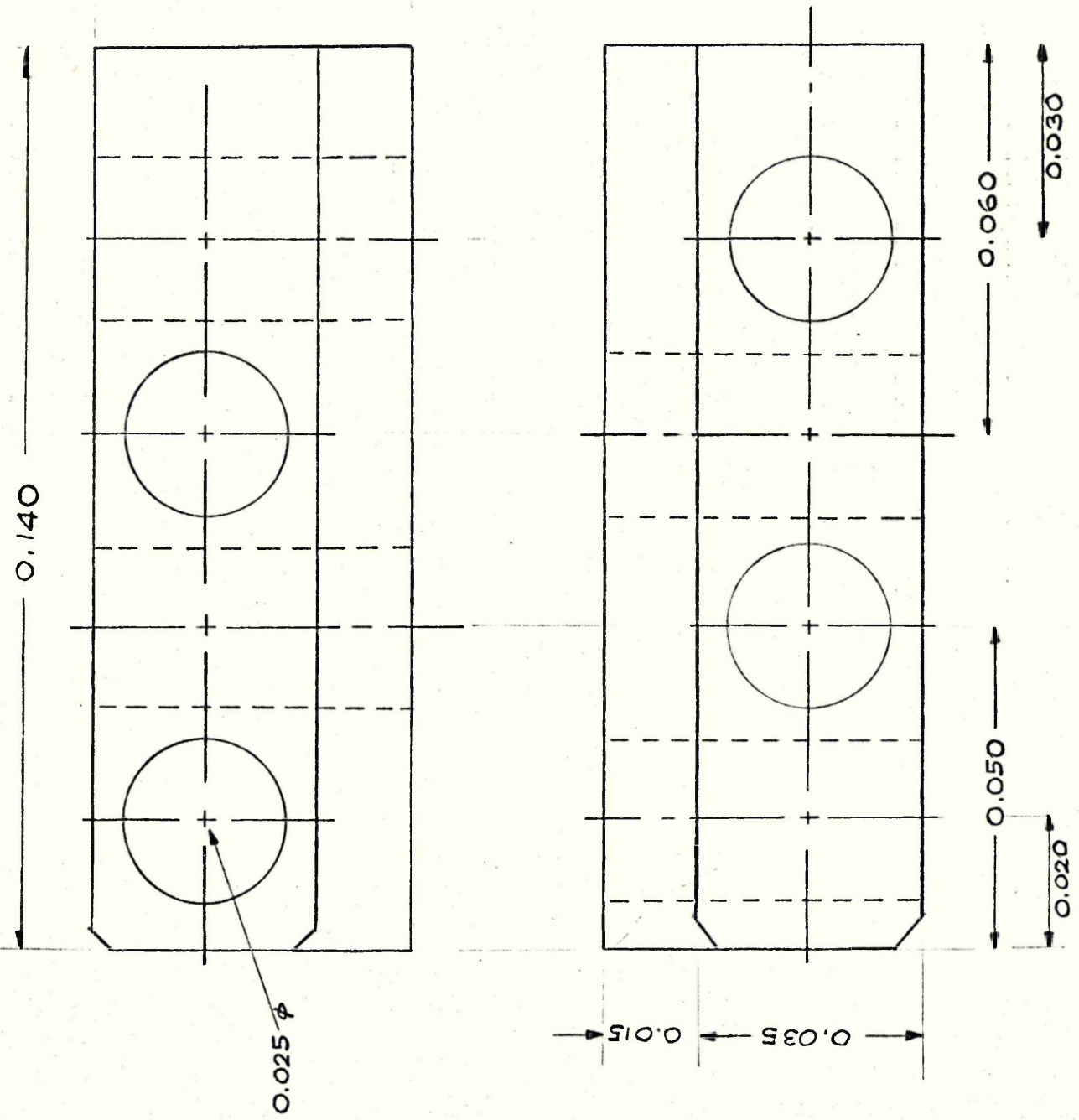
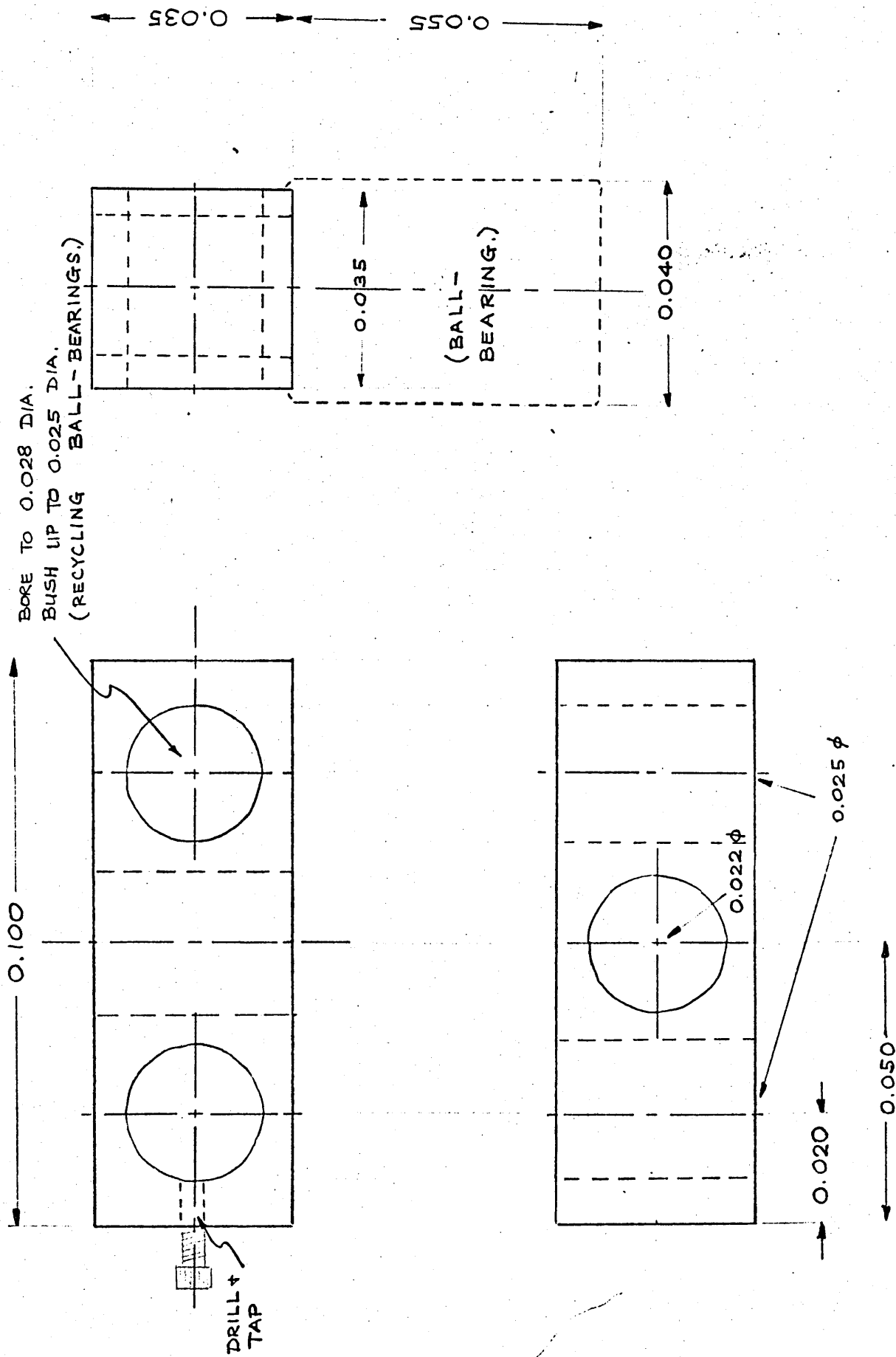


FIG. A.5.5. CORNER SUPPORTS (4 OFF)



FULL SCALE

FIG A.5.6. THE BEARINGS (2 OFF)

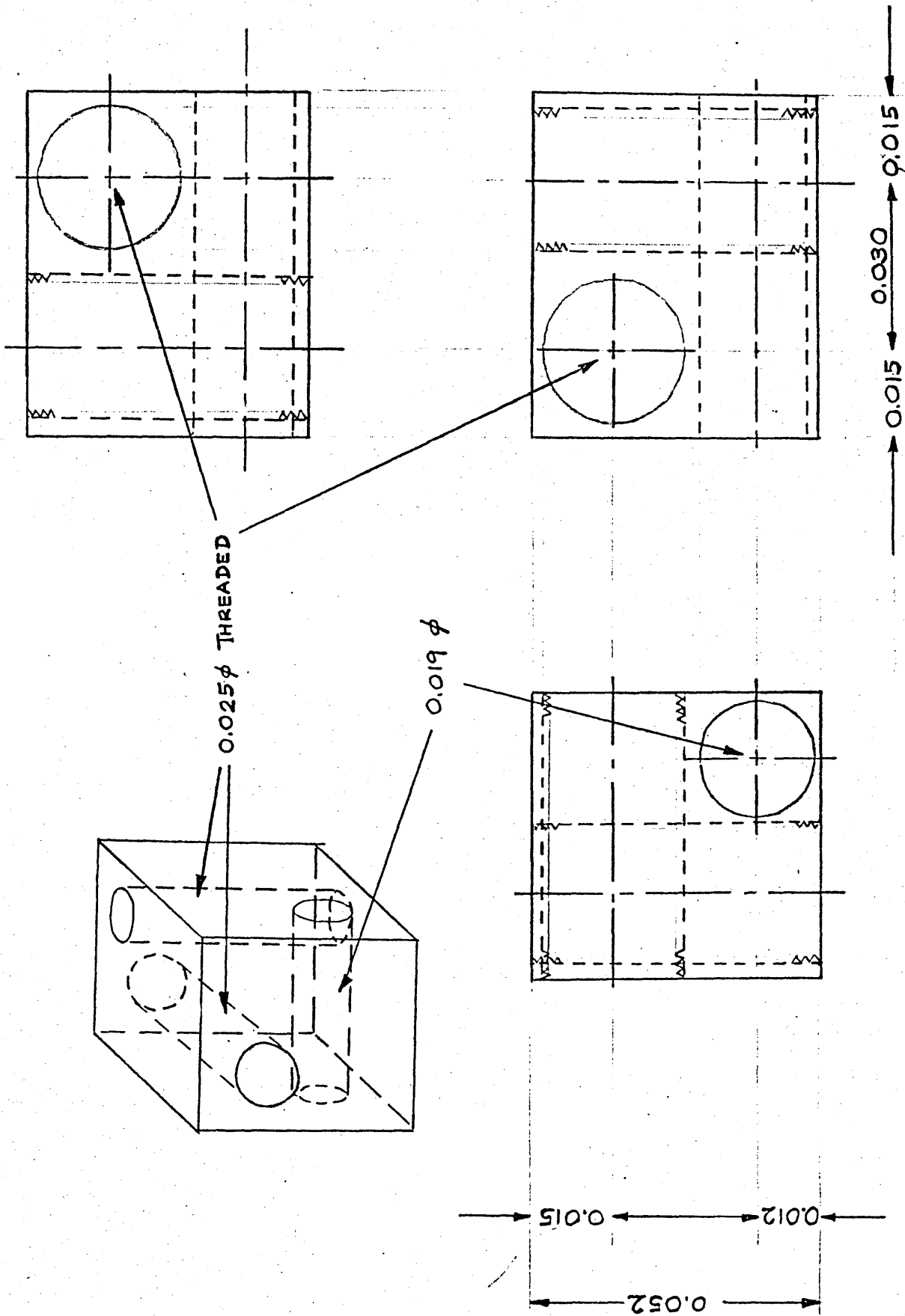


FIG. A.5.7. THE PROBE HOLDER.

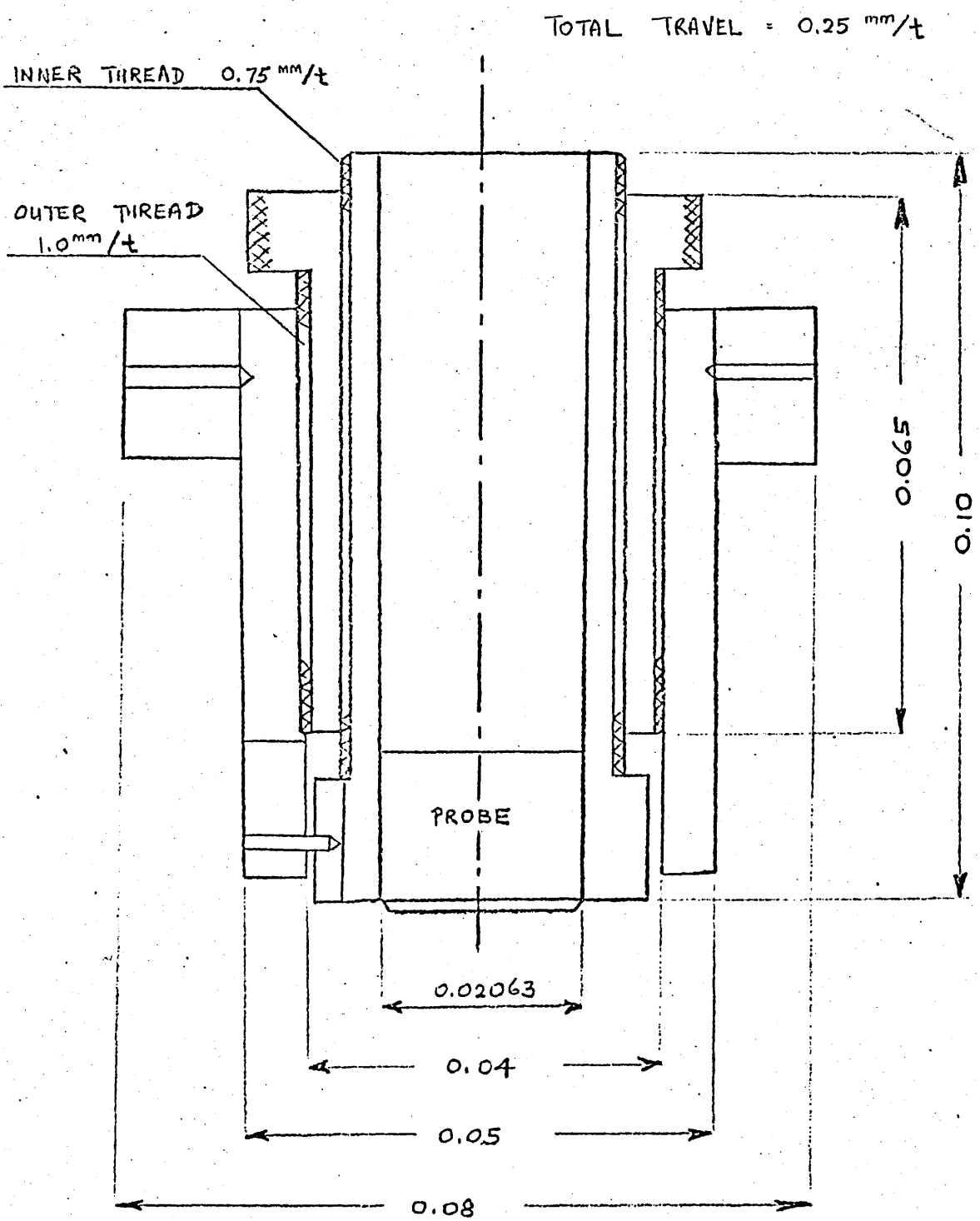
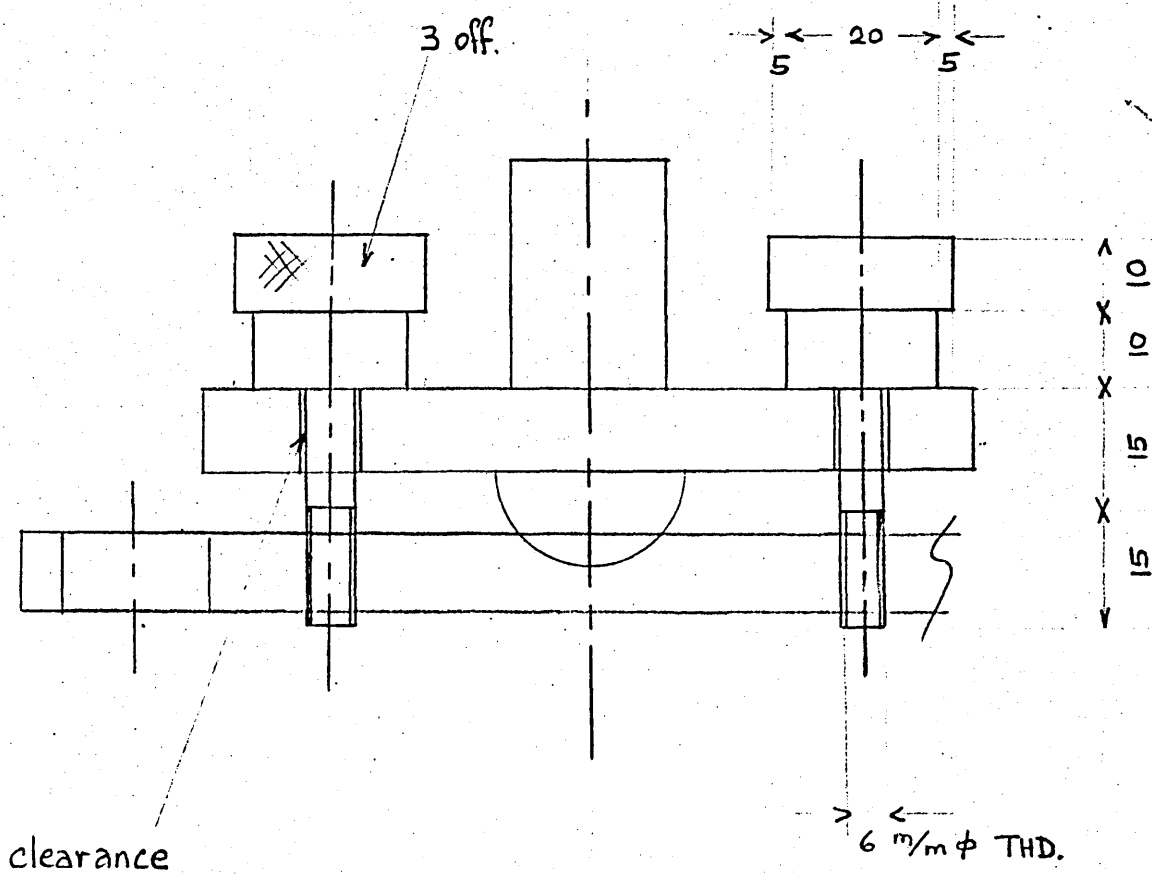


FIG. A.5.8. FINE ADJUSTMENT MECHANISM (GAP SIZE)



all dimensions in mm.

FIG. A.5.9. FINE ADJUSTMENT MECHANISM (TILT)

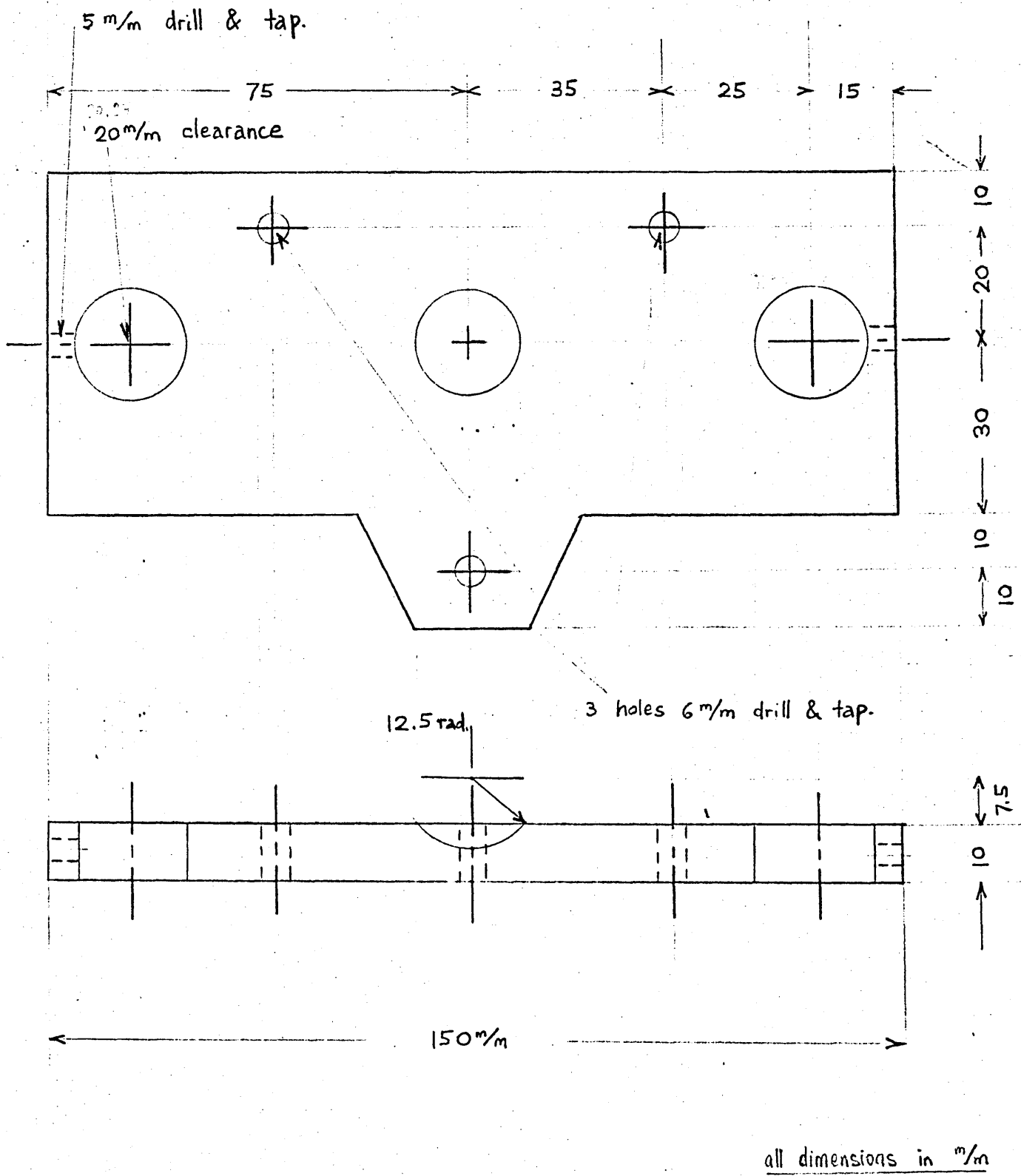


FIG. A.5.10. FINE ADJUSTMENT MECHANISM (BASE PLATE)

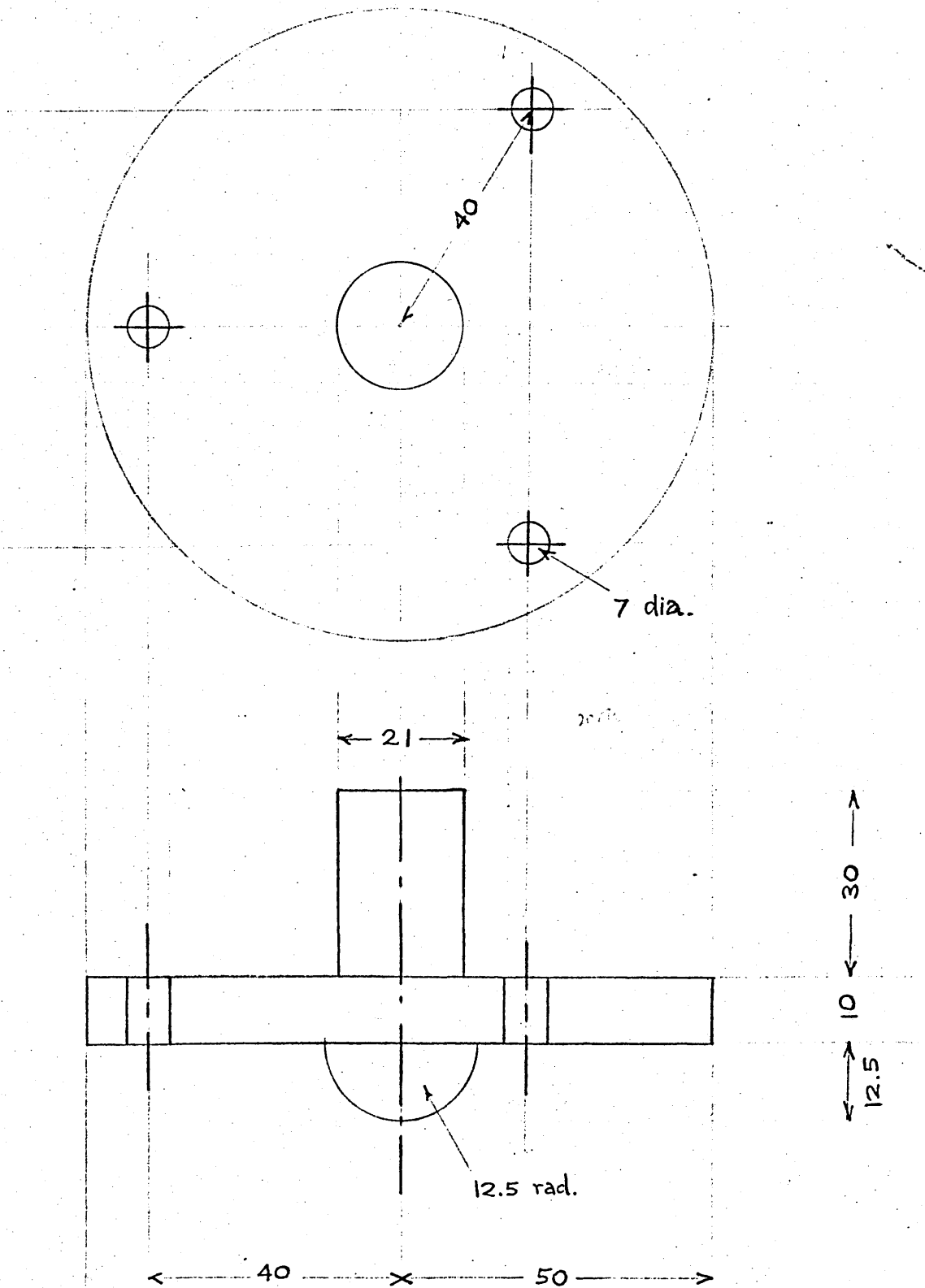


FIG A.5.II. FINE ADJUSTMENT MECHANISM (TOP PLATE)

all dimensions in m/m.

ALL DIMENSIONS IN MM

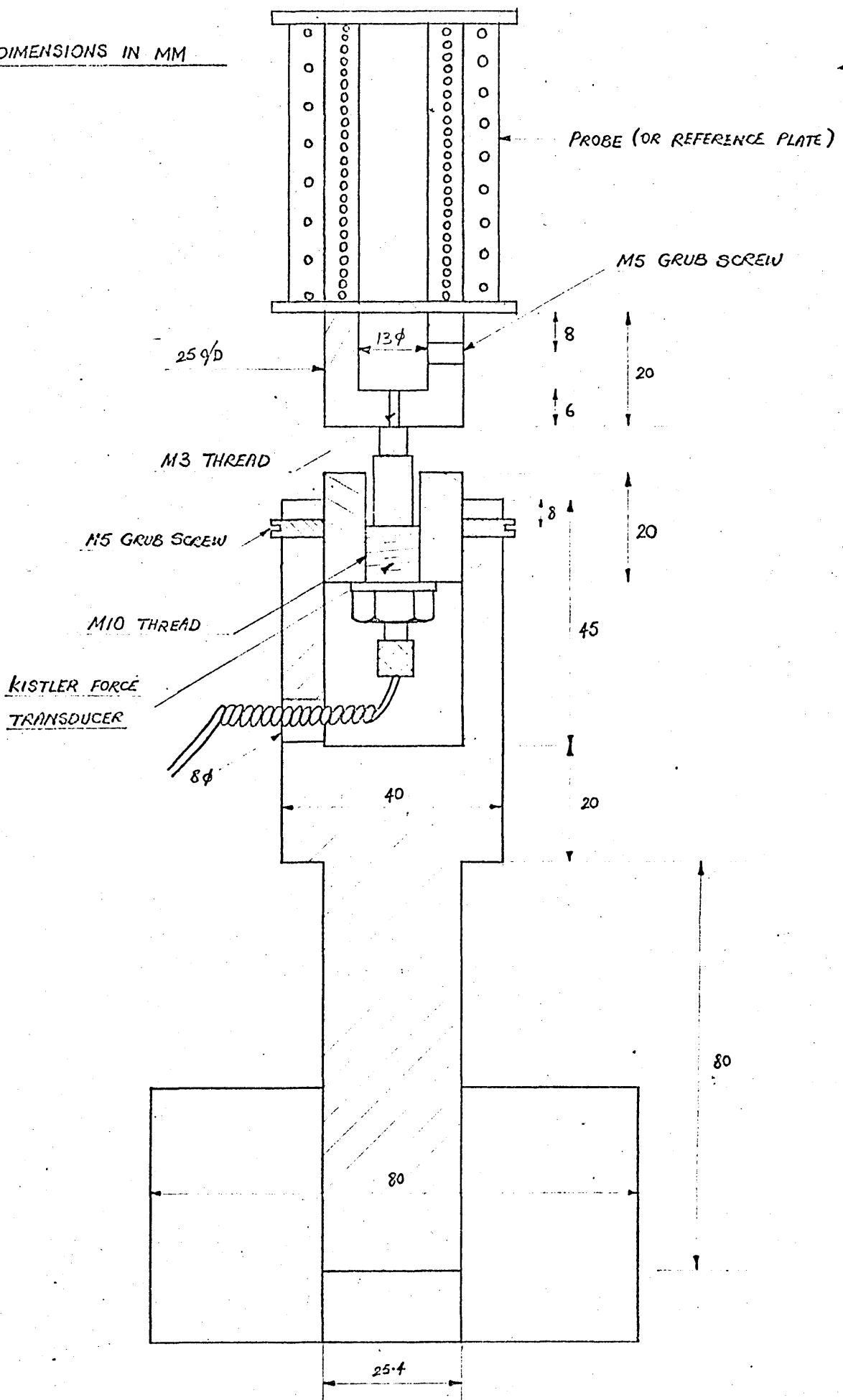


FIG. A. 5-12. FORCE TRANSDUCER HOUSING

Calibration of the vibration pickup transducer

This section describes the method adopted in the calibration of the proximity probe measuring static displacement as well as amplitude of vibration.

The probe used is a Wayne-Kerr type E capacitance probe with its associated TE200 transducer equipment. The probe is part of a large family of non-contacting displacement transducers used in vibration studies to eliminate the possibility of the transducer interfering with the vibration characteristics of the structure tested. This is especially evident in the present case where a transducer of considerable mass, e.g. an accelerometer, used to measure the vibration of a thin plate, would drastically alter its vibration characteristics and render them totally false.

Capacitance probes work on the principle that when a probe is placed near to a conducting surface, a capacitance exists between this surface and the face of the probe. The capacitance so formed is made use of in the feedback loop of a high gain amplifier thereby changing its impedance and causing a voltage output to be formed which is proportional to the gap distance between the probe and the surface. The aim of the calibration is to obtain this relationship between the voltage output of the probe and its amplifier equipment and the amplitude of vibration that it measures.

It was decided not to use Wayne-Kerr vibration meters but actually calibrate the probe in preparation for future work on random vibration since Wayne-Kerr vibration meters are only calibrated for sinusoidal wave excitation and are hence valid only for discrete excitation work. The calibration of the probe in terms of R.M.S. volts and R.M.S. amplitudes of vibration would however be equally valid for random excitation work. A block diagram of the apparatus used in the calibration is shown in figure A.6.1.

The probe was positioned above a reference block (plate 7), on opposite sides of which were mounted two accelerometers, and which was fastened on to a vibrator. Adjustment of the probe-to-vibrating-surface gap was possible using the mechanism described in section 4.2. The voltage output of the accelerometer and amplifier system was recorded with corresponding readings of the probe and amplifier output when vibrating

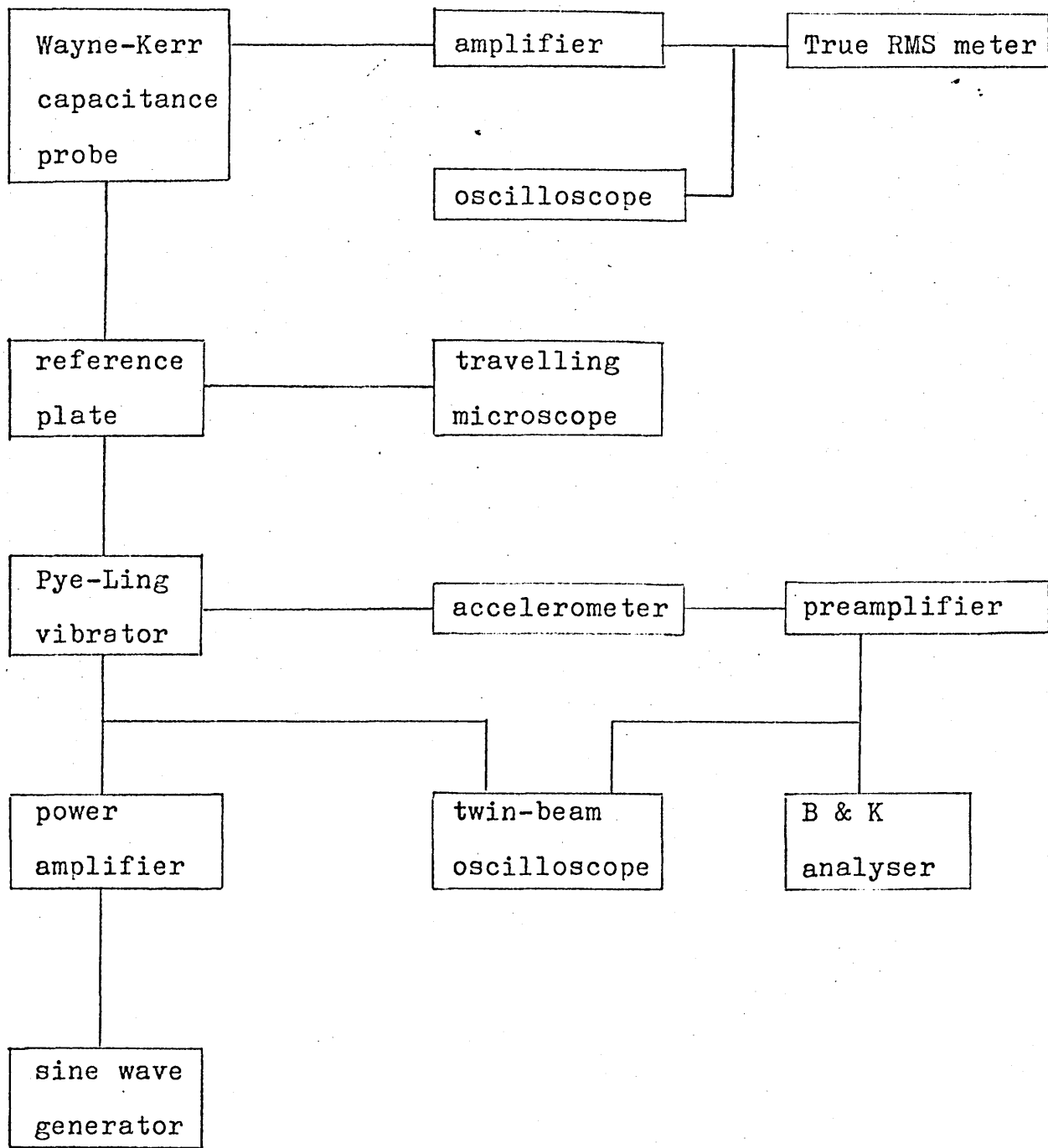


Figure A.6.1

Block diagram of apparatus used for the calibration of the Wayne-Kerr capacitance probe.

at a fixed frequency of 30 Hz but with different amplitudes of vibration. The same procedure was repeated with several different frequencies but keeping the probe-to-surface distance constant. Finally the probe-to-surface distance was varied and the above procedure repeated.

The amplitudes of vibration were calculated from the accelerometer outputs and graphs of amplitude of vibration against probe output were plotted. The gradients of these graphs were calculated for each probe-to-surface distance and a final graph plotted, showing the effects of the probe-to-surface distance on these gradients.

Facility for double integration of acceleration by the Bruel and Kjaer preamplifier to obtain amplitude of vibration was available but limited to specified frequencies of 1, 3, 10, 30, 100 and 300 Hz. As a result this method was only used as a check for the values of amplitudes of vibration which were calculated from actual acceleration figures.

A travelling microscope was used to measure static displacements and low frequency vibrations when a visual measurement of the amplitude of vibration provides a check on the accelerometer readings at low frequencies.

The angular fine adjustment mechanism was used to adjust the gap between the probe and the vibrating surface to ensure that they were parallel. This was to prevent the surfaces otherwise touching when the gap size and the amplitude of vibration approach each other. Apart from this however little effort was necessary since from the manufacturers specification an eight degree angle carried an error of only 1% in the distance measurement and no error at all in the vibration amplitude measurement since only the difference between the alternating peaks were measured.

Calibration of the non-contacting exciter

This section describes the method used to calibrate the non-contacting electromagnetic vibrator developed.

Figure A.7.1 is a block diagram of the instrumentation used in the calibration of the exciter in which the effect of signal amplitude, frequency response and gap distance were investigated.

The exciter was mounted above a reference block supported by a steel column housing a piezoelectric load sensitive transducer (plate 10). The force generated by the exciter would therefore act on the block and be transmitted through the load cell. A sinusoidal signal was applied to the inner coil and a corresponding d.c. bias to the outer coil of the noncontacting exciter which is set at a fixed distance from the reference block. This produces an alternating force onto the block which, acting on the load cell, produces a signal monitoring the force generated by the exciter. This was set to read directly in Newtons of force using a compatible factory calibrated charge amplifier. The output was checked to be of the same sinusoidal waveform as the excitation voltage to the exciter, both traces being displayed on a twin beam oscilloscope.

The excitation signal amplitude was then varied but retaining the same frequency and the variation of force output of the exciter with input voltage obtained. The whole procedure was repeated at various signal frequencies and calibrations corresponding to each obtained. Also by keeping the amplitude of the input signal constant but varying its frequency the frequency response of the exciter was obtained.

Finally the effect of variation of the gap between the exciter and the surface of the structure excited on the force output was obtained, keeping the frequency and amplitude of the input signal fixed.

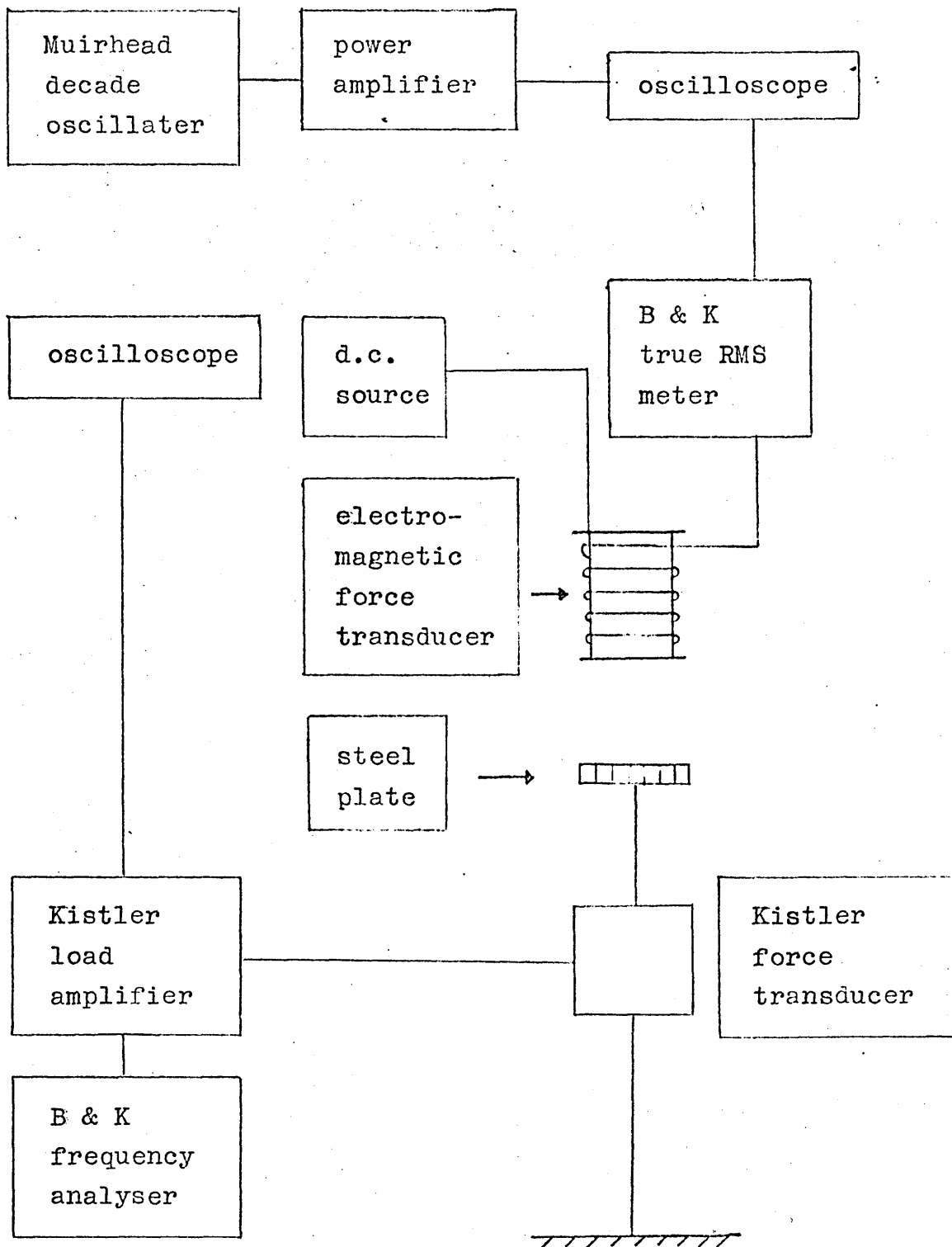


fig. A.7.1 Block diagram of instrumentation used for calibration of non-contacting force transducer.